Stony Brook University

Random Matrix Theories for Lattice QCD Dirac Operators

A Dissertation Presented

by

Savvas Zafeiropoulos

to

The Graduate School

in Partial Fulfillment of the Requirements

for the Degree of

Doctor of Philosophy

in

Physics

Stony Brook University

August 2013

Stony Brook University

The Graduate School

Savvas Zafeiropoulos

We, the dissertation committee for the above candidate for the Doctor of Philosophy degree, hereby recommend acceptance of this dissertation.

Jacobus Verbaarschot – Dissertation Advisor
Professor, Department of Physics and Astronomy

Vladimir Goldman – Chairperson of Defense
Professor, Department of Physics and Astronomy

Michael Creutz
Adjunct Professor, Department of Physics and Astronomy
and Brookhaven National Laboratory

Urs Heller
Editor, Physical Review D
American Physical Society

This dissertation is accepted by the Graduate School.

Charles Taber
Interim Dean of the Graduate School

Abstract of the Dissertation

Random Matrix Theories for Lattice QCD Dirac Operators

by

Savvas Zafeiropoulos

Doctor of Philosophy

in

Physics

Stony Brook University

2013

The main topic of this thesis is the study of the spectral properties of the Dirac operator of Lattice Quantum Chromodynamics (QCD). Lattice QCD is the main regularization for ab initio non-perturbative calculations and despite the fact that it is almost four decades old, the spectral properties of the Dirac operator have not been fully understood. The main effort of this thesis is to study analytically the low lying Dirac eigenvalues with the use of Random Matrix Theory techniques. A full analytical control of this part of the spectrum may be helpful to avoid problems of lattice simulations in the deep chiral regime. The first chapter contains a derivation of the joint probability distribution of the eigenvalues of the Wilson Dirac operator which is the master quantity for the derivation of all spectral correlation functions. Explicit results of the density of the complex eigenvalues, the density of the real eigenvalues as well as the distribution of the chiralities over the real eigenvalues are provided. In this analysis we have included the Low Energy Constants (LECs) that enter in the leading order

of the Symanzik expansion. We describe the effects of the LECs on the spectrum and we provide novel relations which would allow for their determination from lattice data. Next we consider the Hermitian Wilson Dirac operator of QCD-like theories. In particular we consider the case of two color QCD with fundamental quarks as well as any color QCD with adjoint quarks. We derive the partition function of these theories and calculate analytically and numerically the microscopic spectral density and provide bounds for the spectral density of the real eigenvalues of the corresponding Non-Hermitian Wilson Dirac operator. In the last chapter we consider the two-dimensional Dirac operator and different gauge groups as well as number of colors and also even-even, odd-odd and mixed spacetime lattices. We classify these theories in terms of random matrix theories. Analytical results for the microscopic spectral density of each particular case are compared with lattice simulations.

I would lovingly like to dedicate this thesis to:

the memory of my beloved grandfather Savvas for giving us everything that he had...

to my mother Georgia for her endless love and for always being there...

to my father Lucas because he is the reason that me and my sister are able to materialize our dreams for being an ideal example...

to my sister Adamantia because some people are just born from the same mother and some others are born best friends for ever.

Contents

List of Figures

Acknowledgements

It is a great pleasure for me to thank my advisor Jacobus Verbaarschot for all his guidance and support. For the endless discussions about physics, for teaching me how to do research and for always pushing me to perform in the best of my abilities. I deeply appreciate all his help.

I would also like to express my gratitude to Mario Kieburg for our excellent collaboration, for teaching me many mathematical aspects, for his mentorship and patience.

I am truly indebted to both Jac and Mario and without them my education here at Stony Brook would have been far less integrated.

During my years as a graduate student I profited from many discussions in particular with Sasha Abanov, Peter van Nieuwenhuizen, Edward Shuryak and Ismail Zahed.

At this point I would also like to thank the committee of my defense : Michael Creutz, Vladimir Goldman and Urs Heller.

All these years at Stony Brook wouldn't have been so pleasant if I was not surrounded by my good friends: Constantinos Constantinou, Marcos Crichigno, Ozan Erdogan, Panagiotis Gianniotis, Giannis Iatrakis, Pedro Liendo, Frasher Loshaj, Elli Pomoni, Pilar Staig and Chris Winterowd. I will truly miss you all.

Last but not least, I would like to thank Selin for all her support in all the difficult moments, for being next to me...

Chapter 1

Introduction

1.1 Brief Introduction to Lattice Gauge Theory

Quantum Chromodynamics (QCD) is the theory of strong interactions, describing one of the four fundamental forces in nature, the color force. It is a non abelian quantum field theory with gauge group $SU(3)$ of color. The full Lagrangian including fermions ψ, gauge fields A, gauge fixing and the Faddeev-Popov ghosts b, c is

$$\mathcal{L} = -\frac{1}{4}F^2 + \frac{1}{2}(\partial \cdot A)^2 + \bar{\psi}(i\gamma \cdot D - m)\psi + b(-\partial \cdot D)c, \tag{1.1}$$

where D_μ is the covariant derivative defined as $D_\mu = \partial_\mu - igA_\mu$. The Yang-Mills curvature F is given as the commutator of two covariant derivatives. The gauge fixing term supplemented by the kinetic term of the ghosts must be there in order to render the path integral finite, due to over counting because of the gauge symmetry. Moreover only with the inclusion of these terms can one derive the correct set of Feynman rules needed for the calculation of the perturbative expansion of any gauge invariant correlation function. The theory has passed very stringent, high precision experimental tests in very high energy experiments. Perturbative QCD (pQCD) had enormous success, Gross, Politzer and Wilczek were awarded the 2004 Nobel prize in physics for their ground breaking work in the discovery of asymptotic freedom. However, perturbative techniques become futile when the gauge coupling grows large. This is the case that one encounters in the realm of Nuclear Physics. All the very important phenomena of QCD such as color confinement and chiral symmetry breaking are deeply non-perturbative in nature and one has to employ a drastically different approach than the perturbative techniques which

are well known since the birth of Quantum Field Theory. There have been several attempts to make the non-perturbative studies tractable mainly utilizing models and effective theories which resemble some of the main features of QCD. The only ab initio approach is the one of lattice QCD where the path integral is discretized on a space-time lattice yielding a very high dimensional integral that can be directly simulated by a computer using techniques originating from Statistical Mechanics. Due to the fact that the integration over the gauge variables is compact and hence is well defined, one does not necessarily need to gauge fix, contrary to most continuum regularizations [6]. One focuses only on the Dirac and gauge term of the Lagrangian since they yield a correct well behaved functional integral. The formulation of the lattice theory is in Euclidean space, the path integral plays the role of the partition function and the expectation values of operators are given by statistical averages. Discretizing the fermion term of the action the naive approach is to place the spinors on the lattice sites and replace the derivatives by finite differences

$$S_f^{naive}[\psi,\bar{\psi}] = a^4 \sum_n \bar{\psi}_n \left(\sum_\mu \gamma_\mu \frac{\psi_{n+\hat{\mu}} - \psi_{n-\hat{\mu}}}{2a} + m\psi_n \right). \tag{1.2}$$

In the above notation we replace the four vector x by na where a is the lattice spacing and the four vector n has integer valued components labelling the lattice sites. By $\hat{\mu}$ we denote the unit vector in the μ direction. The spacetime integral of the action has been replaced by a double summation over all the lattice sites n and all four spacetime indices μ. At the moment we will set the pathologies of the fermion discretization aside and we will introduce the gauge fields in a gauge invariant fashion. It is exactly the same way one introduces gauge fields in the continuum, by requiring invariance of the action under the local symmetry group. If one focuses on the term $\bar{\psi}_n \psi_{n+\hat{\mu}}$ it is clear that this term is not invariant under a gauge transformation by an element $g_n \in SU(3)$. Under a gauge transformation $\bar{\psi}_n \psi_{n+\hat{\mu}} \to \bar{\psi}_n g_n^\dagger g_{n+\hat{\mu}} \psi_{n+\hat{\mu}}$ and in order to preserve gauge invariance one needs to introduce a link variable $U \in SU(3)$ which transforms as $\widetilde{U}_{\mu;n} \to g_n U_{\mu;n} g_{n+\hat{\mu}}^\dagger$. The link variables play the role of a gauge transporter and they are formally related to the continuum gauge fields as $U_{\mu;n} = e^{iaA_{\mu;n}}$. With the introduction of the gauge degrees of freedom the fermion action coupled to gauge fields takes the form

$$S_f^{naive}[\psi,\bar{\psi},U] = a^4 \sum_n \bar{\psi}_n \left(\sum_\mu \gamma_\mu \frac{U_{\mu;n}\psi_{n+\hat{\mu}} - U_{\mu;n-\hat{\mu}}^\dagger \psi_{n-\hat{\mu}}}{2a} + m\psi_n \right). \tag{1.3}$$

The Yang-Mills (YM) action for the gluons is replaced by the Wilson gauge action for which one can show that it reduces to the YM action in the naive continuum limit ($a \to 0$) . The Wilson gauge action is constructed with the aid of the simplest non-trivial gauge invariant quantity, the trace of the plaquette variable. The plaquette variable is defined as the trace of the product of link variables circulating a unit cell (hypercube) of the space time lattice, while the Wilson gauge action is defined as

$$S_g^W[U] = \frac{2N_c}{g^2} \sum_n \sum_{\mu<\nu} \mathrm{Re}\,\mathrm{tr}\,(1 - U_{\mu\nu;n}), \tag{1.4}$$

where the plaquette variable is defined as

$$U_{\mu\nu;n} = U_{\mu;n} U_{\nu;n+\hat{\mu}} U^\dagger_{\mu;n+\hat{\nu}} U^\dagger_{\nu;n}.$$

This choice for the gauge action is not unique, as long as the gauge invariance and spacetime symmetries are being preserved any closed loop made out of link variables can be used to construct the gauge action. These actions would all yield the YM action in the continuum limit but will differ in $O(a^2)$. This feature can be used for our own benefit since forming appropriate linear combinations of traces of links one can reduce the leading order discretization error. On this ground lies the idea of Symanzik improvement which we will analyze in greater detail later on [7, 8]. Usually, in lattice studies one needs to include only the gauge action and the fermion action, while the gauge fixing term is not needed because of the compactness of the gauge group. Only for particular cases such as monopole studies one would need to fix the gauge in advance [9]. Once the path integral is defined for lattice QCD one can in principle study any Euclidean correlation function of operators since it suffices to evaluate the statistical average defined by

$$\langle O_1 \dots O_k \rangle = \frac{1}{\mathcal{Z}} \int D[U] D[\psi] D[\bar{\psi}] e^{-S_g - S_f} O_1 \dots O_k \ , \tag{1.5}$$

where $D[U]$ is the Haar measure, $D[\psi] = \prod_n d\psi_n$ and $\mathcal{Z}$ is the partition function defined as

$$\mathcal{Z} = \int D[U] D[\psi] D[\bar{\psi}] e^{-S_g - S_f}. \tag{1.6}$$

Fermions and the lattice

1.1.1 Doublers and the Wilson prescription

While the main parts of discretizing the gauge degrees of freedom on a spacetime lattice can be mainly captured by the prescription of the introduction of the link variables, the discretization of the fermionic degrees of freedom is a very complicated process which has been the focus of theoretical studies for over three decades. The reason is the infamous doubling problem. On the lattice with periodic boundary conditions the momentum space for d dimensions is the Brillouin zone $[-\pi/a, \pi/a]^d$. This has a direct impact on the energy-momentum dispersion relation and results to additional particles in the spectrum. While the continuum fermion propagator $\frac{1}{\gamma_\mu p_\mu}$ has for massless fermions, only one pole at

$$p_\mu = (0, 0, 0, 0), \tag{1.7}$$

the lattice propagator

$$S(p) = \frac{m\mathbb{1} - ia^{-1}\sum_\mu \gamma_\mu \sin(p_\mu a)}{m^2 + a^{-2}\sum_\mu \sin^2(p_\mu a)} \tag{1.8}$$

has, in four dimensions for massless fermions, fifteen additional poles whenever one of the momentum components is equal to zero or π/a which comprise the corners of the Brillouin zone. Wilson identified the source of the problem which has to do with the fact that chiral symmetry and the spacetime lattice are not compatible. For the purpose of avoiding the unwanted doublers Wilson added an extra term to the action, a dimension five operator which is the lattice discretization of the Laplacian and acts as a mass term [10]. The Dirac operator with the addition of the Wilson term takes the form

$$D_W = \gamma \cdot D + m\mathbb{1} - \frac{1}{2}aD^2 \tag{1.9}$$

The Wilson term vanishes in the naive continuum limit but at finite lattice spacing it lifts the doublers since it contributes "effectively" to the mass proportionally to $1/a$. Alas, the Wilson term as a mass term is not invariant under chiral symmetry.

1.1.2 Chiral symmetry and the lattice

Chiral symmetry which can be encapsulated as $\{D, \gamma_5\} = 0$ is violated by the Wilson term even in the chiral limit ($m \to 0$). This is not a coincidence.

Nielsen and Ninomiya [11–13] in 1981 proved a no-go theorem according to which it is impossible to construct a lattice fermion action that is

- Local
- Undoubled
- has the correct continuum limit
- is chirally symmetric

The addition of the Wilson term brings another major change which will affect the spectrum of the Dirac operator dramatically. At zero lattice spacing the Dirac operator is antihermitian with purely imaginary eigenvalues. At finite lattice spacing the Wilson-Dirac operator has mixed hermiticity properties with eigenvalues scattered on the complex plane. Actually the Wilson-Dirac operator retains a symmetry called γ_5- hermiticity. According to which $\gamma_5 D_W \gamma_5 = D_W^\dagger$ and therefore the operator $D_5 = \gamma_5 D_W$ is a hermitian operator. This relation has important consequences on the spectrum of the operator and we will study them in great detail in the following chapters. One can easily prove using the γ_5 -hermiticity and the fact that $\gamma_5^2 = 1$ that the characteristic polynomial of D_W

$$\det(D_W - \lambda \mathbb{1}) = (\det(D_W - \lambda^* \mathbb{1}))^*, \tag{1.10}$$

which has as a consequence that the spectrum consists of complex conjugate eigenvalues or real eigenvalues. Moreover there is also information regarding the eigenvectors of D_W, namely only eigenvectors corresponding to real eigenvalues have non zero chirality. Defining the chirality as $\langle k|\gamma_5|k\rangle$ we see that $\lambda\langle k|\gamma_5|k\rangle = \langle k|\gamma_5 D_W|k\rangle = \langle k|D^\dagger\gamma_5|k\rangle = \lambda^*\langle k|\gamma_5|k\rangle$, which means that $(\lambda - \lambda^*)\langle k|\gamma_5|k\rangle = 0$ and as a result only real modes can have non zero chirality.

1.1.3 Staggered Fermions

Giving up chiral symmetry is a heavy price to pay, therefore Susskind and Kogut [14] came up with their approach on how to deal with the irritating doubling problem. Their idea was to redistribute the fermionic degrees of freedom over the lattice in such a way that one goes from an initial lattice with lattice spacing equal to a to a blocked lattice with lattice spacing equal to $2a$. What they actually achieved is that they attack the problem directly to its root which is the size of the Brillouin zone (and it was the denominator of the propagator which was zero at the corners of the BZ). The naive fermionic

action (1.2) which describes the 16 fermionic flavors has a high amount of symmetry because of the degeneracy. One can perform a "spin diagonalization" [15] which is a transformation acting on the fermion fields mixing Dirac and Lorentz indices and eventually get rid of the γ matrices. The "spin diagonalization" reads

$$\begin{aligned} \psi'_n &= \gamma_1^{n_1}\gamma_2^{n_2}\gamma_3^{n_3}\gamma_4^{n_4}\psi_n, \\ \bar{\psi}'_n &= \bar{\psi}_n\gamma_4^{n_4}\gamma_3^{n_3}\gamma_2^{n_2}\gamma_1^{n_1}. \end{aligned} \tag{1.11}$$

After the spin diagonalization the naive fermion action will transform to

$$S_f[\psi', \bar{\psi}'] = a^4 \sum_n \bar{\psi}'_n \left(\sum_\mu \eta_{\mu;n} \frac{\psi'_{n+\hat{\mu}} - \psi'_{n-\hat{\mu}}}{2a} + m\psi'_n \right) \tag{1.12}$$

where the staggered sign functions η are the "remainders" of the gamma matrices and are defined as

$$\begin{aligned} \eta_{1;n} &= 1 \\ \eta_{2;n} &= (-1)^{n_1} \\ \eta_{3;n} &= (-1)^{n_1+n_2} \\ \eta_{4;n} &= (-1)^{n_1+n_2+n_3} \\ \eta_{5;n} &= (-1)^{n_1+n_2+n_3+n_4} \end{aligned} \tag{1.13}$$

This action is trivial (diagonal) in Dirac space so by retaining only one of the four identical components we end up with the staggered action where the one component Grassmann fields χ and $\bar{\chi}$ are coupled to the link variables U.

$$S_f[\chi, \bar{\chi}] = a^4 \sum_n \bar{\chi}_n \left(\sum_\mu \eta_{\mu;n} \frac{U_{\mu;n}\chi_{n+\hat{\mu}} - U_{\mu;n-\hat{\mu}}\chi_{n-\hat{\mu}}}{2a} + m\chi_n \right) \tag{1.14}$$

This action has the advantage that it preserves a U (1) $\times$ U (1) subgroup of the initial chiral symmetry group. In particular the transformation

$$\begin{aligned} \chi_n &\rightarrow e^{i\theta\eta_{5;n}}\chi_n \\ \bar{\chi}_n &\rightarrow \bar{\chi}_n e^{i\theta\eta_{5;n}} \end{aligned} \tag{1.15}$$

leaves the staggered action invariant. In the case of Wilson fermions with the addition of the Wilson term the action lost the chiral symmetry, in the case of staggered fermions the action is still invariant under a subgroup ($U(1) \times$

$U(1)$) of the chiral symmetry group. This is a good feature especially for studies of phenomena such as the spontaneous breaking of chiral symmetry. Unfortunately, staggered fermions still maintain a four-fold degeneracy and one needs to make a decision on how to simulate e.g. two or three dynamical flavors. Several lattice collaborations have adopted the approach of "rooting". This accounts for taking the fourth root of the fermion determinant in order to get rid of the degeneracy. While this strategy is completely justifiable in perturbative studies, an analytical proof in the non-perturbative regime is far from obvious and it has sparked a rather strong controversy [16–19]. To understand in a deeper way the emergence of four flavors (tastes) in the continuum limit we will follow [20] and we will set $U_\mu = \mathbb{1}$ to make the analysis simpler and more clear. We mentioned that in the staggered formulation one distributes the spinor degrees of freedom in the different sites of the hypercube. Here we will follow the reverse construction and we will regroup again all the degrees of freedom from the corners of the hypercube. The lattice sites will carry the label n_μ (we have N_μ sites), the hypercubes will be labelled as h_μ and the corners of the hypercube $s_\mu = 0, 1$. With this notation we achieve to render the sign function $\eta_{\mu;n} = \eta_{\mu;2h+s} = \eta_s$ hypercube independent. If we define new quark fields

$$\begin{aligned} q_{h;ab} &= \frac{1}{8}\sum_s \Gamma^s_{ab}\chi_{2h+s}, \\ \bar{q}_{h;ab} &= \frac{1}{8}\sum_s \bar{\chi}_{2h+s}\Gamma^{s*}_{ba}. \end{aligned} \tag{1.16}$$

The matrix

$$\Gamma^s = \gamma_1^{s_1}\gamma_2^{s_2}\gamma_3^{s_3}\gamma_4^{s_4} \tag{1.17}$$

fulfils orthogonality and completeness relations which will be very useful in the following steps of the derivation. The mass term of (1.14) can be trivially re-expressed in the new variables. If we use the completeness relation

$$\frac{1}{4}\sum_s \Gamma^{s*}_{ba}\Gamma^s_{b'a'} = \delta_{aa'}\delta_{bb'}$$

that the Γ matrices satisfy one can see that

$$a^4\sum_n \bar{\chi}_n\chi_n = (2a)^4\sum_h \mathrm{tr}\,(\bar{q}_h q_h). \tag{1.18}$$

For the transformation of the kinetic term one needs to exercise extra care since the fields $\chi_{2h+s\pm\hat{\mu}}$ do not necessarily belong to the same hypercube.

$$\chi_{2h+s+\hat{\mu}} = \begin{cases} \chi_{2h+s+\hat{\mu}} = 2\mathrm{tr}\,\Gamma^{s+\hat{\mu}\dagger} q_h, & \text{if } s_\mu = 0, \\ \chi_{2(h+\hat{\mu})+s-\hat{\mu}} = 2\mathrm{tr}\,\Gamma^{s-\hat{\mu}\dagger} q_{h+\hat{\mu}}, & \text{if } s_\mu = 1. \end{cases} \tag{1.19}$$

If we use $\Gamma^{s\pm\hat{\mu}} = \eta_{\mu;s}\gamma_\mu\Gamma^s$ then (1.19) transforms to

$$\chi_{2h+s+\hat{\mu}} = 2\eta_{\mu;s}\mathrm{tr}\,(\Gamma^{s\dagger}\gamma_\mu(q_h\delta_{s_\mu,0} + q_{h+\hat{\mu}}\delta_{s_\mu,1})). \tag{1.20}$$

The fermion action after some tedious algebra

$$S^f[q,\bar{q}] = (2a)^4 \sum_h [m\mathrm{tr}\,\bar{q}(h)q(h) + \sum_\mu \mathrm{tr}\,\bar{q}_h\gamma_\mu\nabla_\mu q_h - a\sum_\mu \mathrm{tr}\,\bar{q}_h\gamma_5\Box_\mu q_h\gamma_\mu\gamma_5], \tag{1.21}$$

where ∇_μ and $\Box_\mu$ are the symmetric derivative and the symmetric Laplacian in the blocked lattice with lattice spacing $b = 2a$. We introduce the matrices $\xi_\mu = \gamma_\mu^\top$ which will play the role of the gamma matrices in a particular type of flavor space namely the taste space. As we mentioned earlier the staggered formulation gets rid of the doublers but one ends up with four species of fermions in four dimensions, the so called four tastes. The staggered action in the blocked lattice, in the spin-taste basis, reads

$$S^f[\psi,\bar{\psi}] = b^4 \sum_h [m\mathrm{tr}\,\bar{\psi}_h^t\psi_h^t + \sum_\mu \mathrm{tr}\,\bar{\psi}_h^t\gamma_\mu\nabla_\mu\psi_h^t - a\sum_\mu \mathrm{tr}\,\bar{\psi}_h^t\gamma_5(\xi_5\xi_\mu)_{tt'}\Box_\mu\psi_h^{t'}]. \tag{1.22}$$

1.1.4 Ginsparg-Wilson fermions

In 1982 Ginsparg and Wilson (GW) generalized the continuum relation of chiral symmetry $\{D,\gamma_5\} = 0$ with a term proportional to the lattice spacing a on the RHS [21]. The GW relation

$$\{D,\gamma_5\} = aD\gamma_5 D, \tag{1.23}$$

had initially not attracted a lot of attention because it was only in 1997 that Neuberger [22] constructed a Dirac operator that solves this equation. The overlap operator is constructed by using the hermitian Dirac operator D_5 and takes the form

$$D_{ov} = 1 - \gamma_5\mathrm{sign}\,(D_5), \tag{1.24}$$

where the sign of a hermitian matrix can be defined through the spectral theorem for Hermitian matrices or computationally as $D_5(D_5^2)^{-1/2}$. Another approach with exact chiral symmetry is that of the domain wall fermions where one introduces an auxiliary fifth dimension in order to obtain 4-dim chiral fermions [23]. The five dimensional action is very reminiscent to the Wilson action and this is an important point since there are many high performance algorithms available. The price that one has to pay for the excellent chiral properties of the GW fermions is the actual numerical cost of the simulation. In the case of the overlap operator the construction through the sign function is very costly while in the case of the domain wall fermions the numerical cost of the fifth dimension is large. This is the main reason that many large lattice collaborations still use Wilson and staggered fermions with a lot of success [24].

1.1.5 The continuum limit

One can understand the introduction of the spacetime lattice as a non-perturbative regulator, so in the end of the calculation one needs to calculate the $a \to 0$ limit. The total lattice action, the one that actually has a lattice practitioner in her/his code, does not include the lattice spacing at least not explicitly. In essence, the lattice spacing a is "hidden" in the coupling g. To understand the true continuum limit in a deeper way one has to use the techniques of renormalization group. Since we change the scale of the system we need to do the appropriate changes on the masses m and the coupling g in order to keep physics constant. In a lattice simulation one usually works with bare quantities (e.g. m_{lat}). The requirement that the physical quantities e.g (m_{ph} (which can be the mass of a pion or a ρ meson)), which are the ones that can be measured experimentally, are independent of the lattice spacing is encapsulated by the Callan-Symanzik (CS) equation.

$$a\partial_a m_{ph} = 0. \tag{1.25}$$

The lattice observable is related to the physical one as $m_{lat}(g(a)) = am_{ph}$

$$a\partial_a m_{ph} = -\frac{1}{a} m_{lat} + \frac{dm_{lat}}{dg(a)} \frac{dg(a)}{da} = 0. \tag{1.26}$$

The β function of the theory, which is defined by $-a$ times the derivative of the coupling g with respect to the lattice spacing, can be calculated in perturbation theory. The two-loop result, which is renormalization scheme

independent reads

$$\beta(g) = -\beta_0 g^3 - \beta_1 g^5 + O(g^7), \tag{1.27}$$

where the coefficients are given by

$$\begin{aligned} \beta_0 &= \frac{1}{(4\pi)^2}\left(\frac{11}{3}N_c - \frac{2}{3}N_f\right), \\ \beta_1 &= \frac{1}{(4\pi)^4}\left(\frac{34}{3}N_c^2 - \frac{10}{3}N_c N_f - \frac{N_c^2-1}{N_c}N_f\right), \end{aligned} \tag{1.28}$$

and N_c , N_f is the number of colors and flavors, respectively. Substituting this expression into the definition of the β -function, the solution of the differential equation yields

$$a = \frac{1}{\Lambda} e^{\frac{-1}{2\beta_0 g^2}} g^{-\beta_1/\beta_0^2} e^{-\beta_1/\beta_0^2 \log(\beta_0 + \beta_1 g^2)}. \tag{1.29}$$

It is noteworthy to observe that initially we started with a theory with no dimensionful parameters but after the process of regularization we generated an energy scale Λ. This is the phenomenon of dimensional transmutation. Moreover, another interesting point is that the continuum limit is achieved at $g = 0$. At that point $m_{lat} = a m_{ph} = 0$ and equivalently for the correlation length $\xi = \frac{1}{m_{lat}} \to \infty$. It is therefore mandatory for the correlation length to diverge at criticality so that the system will "forget" its lattice structure. This is always the case for second order phase transitions in Statistical Mechanics and as well as in lattice QCD.

1.2 Chiral Perturbation Theory

Chiral Perturbation Theory (chPT), is the effective field theory for low energy QCD and describes the dynamics of the pseudo Nambu-Goldstone bosons of the spontaneously broken approximate flavor symmetry. Effective field theories are usually non-renormalizable effective descriptions of the low energy regime of the more complicated fundamental theories. They usually comprise an expansion in momenta and masses and due to the fundamental theorem of S. Weinberg one needs to explicitly write down all terms which are compatible with the symmetries of the underlying theory [25]. Clearly, this accounts for an infinite number of terms with unknown couplings and in order to make sense out of this expansion one needs to set up a power counting scheme and to get some information regarding the couplings. We will analyze different power counting schemes in the ensuing paragraphs so we should first clarify how we can obtain the values of the different couplings. If one could solve the fundamental theory then one would be able to calculate these couplings which

are known as Gasser-Leutwyler coefficients or low-energy constants (LECs) [26–28]. This is not the case for QCD and therefore they have to be treated as free parameters and they have to be fitted to experimental data. The non-renormalizabilty of the theory would be a reason by itself to immediately discard it but we have to point out that chPT is renormalizable in an EFT sense, which means that to a given order in the expansion of masses and momenta it can be rendered finite by an inclusion of a finite number of counterterms which would essentially redefine the fields, the masses and the couplings.

At this point the reader would be puzzled since we claimed that lattice QCD is a non-perturbative tool which allows for the calculation of hadronic observables so if this is the case why would we want to a reside to a perturbative expansion instead of computing numerically all the required quantities. The answer is that lattice QCD comes along with its own problems which can be at least partially treated with the aid of chPT. One could pinpoint the main points as [29]

- Because of finite computational resources, lattice studies have to take place at non-physical values of the quark masses which are significantly larger than the physical values. ChPt can be used to extrapolate the obtained results to physical values.

- Lattice simulations can not access scattering amplitudes because one can only evaluate the time evolution operator in imaginary time. This is a requirement for Markovian Monte Carlo methods to be applicable for the computation of expectation values of observables. Once again chPT can be used to analytically continue to Minkowski space. The process that has to be followed is simple. One fits the lattice correlation functions to the expression of chPT at a given order of the momentum and mass expansion. Once this fitting has been performed one can perform an analytic continuation in chPT and obtain information of amplitudes in Minkowski space.

- All the lattice computations are taking place at finite values of the lattice spacing a which induces scaling violations and affects the interactions of the NG bosons, this will be addressed mainly when we will discuss Wilson chPT.

- Green's functions can also be calculated via partial quenching. One can choose the valence quark mass different than the sea quark mass. It is computationally cheaper to vary the valence quark mass and not the sea quark mass of the dynamical fermions. At the end of the calculation one needs to extrapolate in the valence quark mass and this is the step where

chPT plays a crucial role. Moreover, one can use different masses and even different lattice discretizations for the sea and the valence quarks. This makes simulations numerically more affordable since one will choose lattice fermions with almost perfect chiral properties only for the valence quarks which will mainly affect the operator mixing and a numerically cheap method for the sea quarks.

1.2.1 Continuum chPT

The most general effective Lagrangian describing the dynamics of NG bosons for three flavor QCD, in the chiral limit, should be invariant under the global symmetry group

$$SU(3)_L \times SU(3)_R \times U(1)_B, \tag{1.30}$$

where we have gotten rid of the axial symmetry $U(1)_A$ which is violated at the quantum level because of the anomaly. If (1.30) was realized in nature one would observe "parity partners" i.e. hadronic pairs with opposite parity but equal masses. This is clearly not the case and what we actually observe in the hadronic spectrum is eight pseudo-NG bosons, the π's, η and K's. The reason for -pseudo- is because of the fact that u, d, s quarks have finite masses but rather small compared to the typical hadronic scale of Λ_{QCD} and the other hadronic masses. To be more precise the s quark mass is not that small but one can use this approximation with a grain of salt. The expansion parameter is $m_\pi/(4\pi f_\pi)$ and since the mass of the s quark is $\sim 100MeV$ while the pion decay constant is $\sim 93MeV$ and therefore still the expansion parameter is small. This experimental observation which is supported by many lattice simulations leads us to conclude that the flavor symmetry is spontaneously broken to SU $(3)_{\mathrm{V}} \times$ U $(1)_{\mathrm{B}}$ and therefore the ground state of the theory shall be invariant only under SU $(3)_{\mathrm{V}} \times$ U $(1)_{\mathrm{B}}$. Further spontaneous breakdown of the vector subgroup is prohibited in continuum QCD by the Vafa-Witten theorem [30]. If we encapsulate all eight NG bosons in a matrix

$$\phi(x) = \begin{pmatrix} \pi^0 + \frac{1}{\sqrt{3}}\eta & \sqrt{2}\pi^+ & \sqrt{2}K^+ \\ \sqrt{2}\pi^- & -\pi^0 + \frac{1}{\sqrt{3}}\eta & \sqrt{2}K^0 \\ \sqrt{2}K^- & \sqrt{2}\bar{K}^0 & -\frac{2}{\sqrt{3}}\eta \end{pmatrix} \tag{1.31}$$

we obtain the basic degree of freedom of the EFT which is the unitary matrix $U = e^{i\frac{\phi(x)}{F_0}}$,where F_0 is the pion decay constant. To the lowest order in

momenta (derivatives) the most general kinetic term would be

$$\mathcal{L}_{kin} = \frac{F_0^2}{4} \mathrm{tr}\, \partial_\mu U \partial_\mu U^\dagger. \tag{1.32}$$

In order to include the explicit chiral symmetry breaking terms which arise due to the finite non-zero quark masses, we will introduce to lowest order the term

$$\mathcal{L}_m = \frac{F_0^2 B_0}{2} \mathrm{tr}\, (M U^\dagger + U M^\dagger), \tag{1.33}$$

where the relative sign is fixed because of the requirement of parity invariance. The new parameter B_0 has a simple interpretation in terms of known quantities. Computing the mass derivative of the energy state of the ground state $U = \mathbb{1}$ both in QCD and in the EFT we have for the two flavor theory

$$\partial_{m_q} \langle H_{QCD} \rangle_0 |_{m_u = m_d} = \partial_{m_q} \langle H_{EFT} \rangle_0 |_{m_u = m_d}. \tag{1.34}$$

The chiral symmetry violating part of the Hamiltonian of QCD is the mass term,

$$H_{QCD} = -(m_u \bar{u} u + m_d \bar{d} d). \tag{1.35}$$

For the ground state of the EFT we have

$$H_{EFT} = -F_0^2 B_0 (m_u + m_d). \tag{1.36}$$

From (1.34) and (1.35, 1.36) we deduce that

$$B_0 = \frac{\langle q\bar{q} \rangle}{F_0^2}, \tag{1.37}$$

where $\langle q\bar{q} \rangle$ is the chiral condensate which serves as the order parameter of the spontaneous breaking of chiral symmetry and it represents either $\bar{u}u$ or $\bar{d}d$. If we Taylor expand the unitary field (the mass term), the coefficient of the terms quadratic in the pseudoscalar fields will be the squares of their masses. So if we assume $m_u = m_d = m$ then at tree-level we obtain the Gell-Mann, Oakes, Renner relations [31]

$$\begin{aligned} m_\pi^2 &= 2B_0 m, \\ m_K^2 &= B_0 (m + m_s), \\ m_\eta^2 &= \frac{2}{3} B_0 (m + m_s), \end{aligned} \tag{1.38}$$

and by combining the above relations we obtain the Gell-Mann Okubo relation [32]

$$m_\pi^2 = 4m_K^2 - 3m_\eta^2. \tag{1.39}$$

In the next order in derivatives, we have the terms which are of fourth order in momenta and we will simply quote the result of Gasser and Leutwyler [27] for the sake of completeness since we will always be working to $\mathcal{O}(p^2)$ in the rest of this thesis

$$\begin{aligned}\mathcal{L}_4 = & L_1 \left\{\mathrm{Tr}[D_\mu U (D^\mu U)^\dagger]\right\}^2 + L_2 \mathrm{Tr}\left[D_\mu U (D_\nu U)^\dagger\right] \mathrm{Tr}\left[D^\mu U (D^\nu U)^\dagger\right] \\ & + L_3 \mathrm{Tr}\left[D_\mu U (D^\mu U)^\dagger D_\nu U (D^\nu U)^\dagger\right] + L_4 \mathrm{Tr}\left[D_\mu U (D^\mu U)^\dagger\right] \mathrm{Tr}\left(\chi U^\dagger + U \chi^\dagger\right) \\ & + L_5 \mathrm{Tr}\left[D_\mu U (D^\mu U)^\dagger (\chi U^\dagger + U \chi^\dagger)\right] + L_6 \left[\mathrm{Tr}\left(\chi U^\dagger + U \chi^\dagger\right)\right]^2 \\ & + L_7 \left[\mathrm{Tr}\left(\chi U^\dagger - U \chi^\dagger\right)\right]^2 + L_8 \mathrm{Tr}\left(U \chi^\dagger U \chi^\dagger + \chi U^\dagger \chi U^\dagger\right) \\ & - i L_9 \mathrm{Tr}\left[f_{\mu\nu}^R D^\mu U (D^\nu U)^\dagger + f_{\mu\nu}^L (D^\mu U)^\dagger D^\nu U\right] + L_{10} \mathrm{Tr}\left(U f_{\mu\nu}^L U^\dagger f_R^{\mu\nu}\right) \\ & + H_1 \mathrm{Tr}\left(f_{\mu\nu}^R f_R^{\mu\nu} + f_{\mu\nu}^L f_L^{\mu\nu}\right) + H_2 \mathrm{Tr}\left(\chi \chi^\dagger\right). \end{aligned} \tag{1.40}$$

In the above expression we encounter apart from the usual unknown couplings (LECs) which have to be fixed by fits to experimental data some new terms. The source χ which is simply given by $\chi = 2B_0 M$ and notice that we have promoted the global chiral symmetry to a local one. We introduced left l_μ and right r_μ gauge fields promoted the derivatives to covariant derivatives with the minimal coupling prescription

$$\partial_\mu U \to \partial_\mu U - i l_\mu U + i U r_\mu. \tag{1.41}$$

The fourth order term contains also the traceless field strengths

$$\begin{aligned} f_{\mu\nu}^L &= \partial_\mu l_\nu - \partial_\nu l_\mu - i[l_\mu, l_\nu], \\ f_{\mu\nu}^R &= \partial_\mu r_\nu - \partial_\nu r_\mu - i[r_\mu, r_\nu]. \end{aligned} \tag{1.42}$$

Note that the coupling of the effective Lagrangian to external gauge fields does not contribute any new terms at $\mathcal{O}(p^2)$. Because of the gauging of (1.30) one needs also to add the Wess-Zumino term to account for the anomaly[33]. Also, this term is also not going to enter in the analysis of the next chapters.

1.2.2 Finite Volume

One of the main issues of a lattice simulation is that it takes place in a finite volume. In order to eliminate the systematic effects that will arise due to the finite volume one would naively think that it suffices to simulate in larger and

larger volumes. When the lattice volume increases the cost of the simulation increases very fast and this sets stringent limitations on the size of the lattice. Also here, EFT field theory will be of great aid in order to extrapolate to the infinite volume limit and also it will give us an analytical understanding of scales i.e. when the lattice volume can be considered as large enough. So finite volume EFT is based on a double expansion, in momenta and inverse volume. One could calculate the pion mass using finite volume EFT and the result shows how the finite box affects physical observables where e.g. for the pion mass at leading order [1]

$$m_\pi(L) = m_\pi(\infty)(1 + \frac{1}{N_f F_\pi^2}\frac{1}{L^{3/2}}e^{-mL}). \tag{1.43}$$

There are two conditions regarding the lattice volume. The first one is how the typical scale for chiral symmetry breaking, $4\pi F_\pi$ relates to the size of the box. In this case one would require

$$\frac{2\pi}{L} << 4\pi F_\pi \tag{1.44}$$

which is a necessary condition to be satisfied if one expects a finite amount of discrete momenta in the relevant low energy regime. The other condition stems from the relative size of m_π and $1/L$. If $m_\pi L << 1$ then the pion Compton wavelength is much larger than the size of the box that we use to regulate the theory and therefore the pion cannot propagate. This regime is called the "ϵ-regime" and then $m_\pi \propto \frac{1}{L^2} \propto \mathcal{O}(\epsilon^2)$. The opposite limit, $m_\pi L >> 1$ leads to the p-"regime" where $m_\pi \propto \frac{1}{L} \propto \mathcal{O}(p)$. In this regime the pion is free to propagate and experience the fact that the box has boundaries. Physical correlators will behave differently in the two regimes for example the correlator of two axial charges studied by Hansen and Leutwyler [1]

$$\langle Q_i^A(t) Q_i^A(0)\rangle = \delta_{ik} L^3 \Gamma(t) \tag{1.45}$$

where the infinite volume correlator is proportional to $m_\pi e^{-m_\pi t}$ (see Fig.1.1).

One could ask oneself about the use of the rather unphysical ϵ - regime. In a realistic lattice simulation working with masses in the deep chiral regime and with very large volumes is very challenging in terms of the numerical cost. Therefore one can work in the numerically cheaper ϵ - regime in order to extract numerically the values of the LECs. Determination in the two different regimes of the pion decay constant gives very close results. To quote

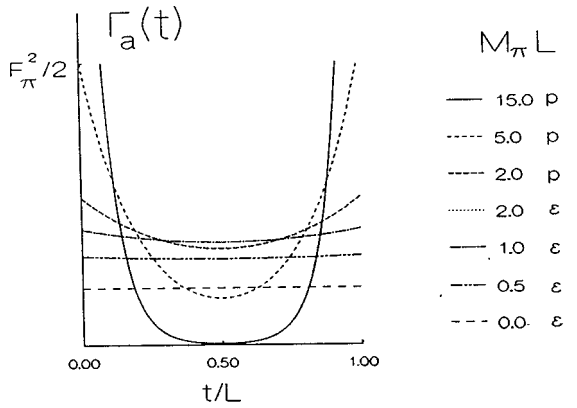

Figure 1.1: The time dependence of the axial charge correlator as a function of $m_\pi L$. One observes that the p-regime yields a result close to the infinite volume result. Note that the two regimes give close results for $m_\pi L = 2$. Courtesy of [1]

some actual numerical values from a quenched simulation [34–36]

$$\begin{aligned} F_{\pi_\epsilon} &= (102 \pm 4) MeV, \\ F_{\pi_p} &= (104 \pm 2) MeV. \end{aligned} \tag{1.46}$$

An important difference between the two different regimes is the contribution of the zero momentum modes versus the contribution of the non-zero momentum modes to the path integral. If we write our dynamical field U as

$$U(x) = U_0 e^{\frac{\sqrt{2}}{F_\pi}\xi(x)}, \tag{1.47}$$

where U_0 is an $N_f \times N_f$ dimensional matrix representing the constant zero momentum modes while the dynamical modes are denoted by $\xi(x)$ where $\int d^4x \xi(x) = 0$. In the p-regime where $m_\pi L \geq 1$ (where L is the linear extent of the box in which we regulate the theory) the constant modes can be treated perturbatively while in the ϵ-regime where $m_\pi L << 1$, the zero momentum modes have to be treated non perturbatively unless $mV\Sigma >> 1$. In the ϵ-regime at leading order the non-zero momentum modes decouple from the partition function and the remainder is a unitary matrix integral

$$\mathcal{Z} \propto \int_{SU(N_f)} dU e^{V\Sigma \mathrm{Re}\,\mathrm{tr}\,(MU^\dagger)} \tag{1.48}$$

which allows for direct connection with Random Matrix Theory (RMT) as

we will see in the following chapters. For the one flavor theory the partition function is

$$Z_{N_f=1} \propto e^{mV\Sigma\cos\theta} \tag{1.49}$$

while the two flavor partition function (in the case of equal quark masses) can be simplified to

$$Z_{N_f=2} \propto \frac{I_1(mV\Sigma)}{mV\Sigma}. \tag{1.50}$$

The partition function at fixed value of the vacuum angle θ reads

$$\mathcal{Z} \propto \int_{SU(N_f)} dU e^{V\Sigma \mathrm{Re}\,\mathrm{tr}\,(\exp(i\theta/N_f)MU^\dagger)}. \tag{1.51}$$

1.2.3 Wilson Chiral Perturbation Theory

The introduction of the Wilson term has a major impact on the physics of the infrared regime of QCD. Even though one could use renormalization group arguments and claim that since the Wilson term is an irrelevant operator it should not have any effect, the fact that it breaks chiral symmetry explicitly has drastic consequences on the physics of the NG bosons. It is therefore mandatory to include discretization errors into the effective description of low energy QCD. Actually, if one fails to include discretization errors, just based on the assumption that they are negligible for small values of the lattice spacing then the use of EFT would induce large systematic uncertainties for the reasons mentioned above. The best way to introduce the discretization effects is by following Symanzik's approach [7, 8], which was originally done for $\lambda\phi^4$ theory, and introduce higher dimensional operators to lattice QCD with Wilson fermions. Therefore we will obtain corrections of the form

$$\mathcal{L} \to \mathcal{L} + a\mathcal{L}^{(5)} + a^2\mathcal{L}^{(6)} + \ldots \tag{1.52}$$

The $\mathcal{L}^{(5)}$ will contain the Pauli term $\bar{\psi} i\sigma_{\mu\nu}F_{\mu\nu}\psi$ and a term with two derivatives i.e. $\bar{\psi}D_\mu D_\mu\psi$ while the $\mathcal{L}^{(6)}$ will in general contain terms with 3 derivatives. If we restrict our analysis to $\mathcal{O}(a^2)$ the most general terms that will contribute in the EFT would be [37–40]

$$\mathcal{L}(a^2) = -a^2W_6[\mathrm{tr}\,(U+U^\dagger)]^2 - a^2W_7[\mathrm{tr}\,(U-U^\dagger)]^2 - a^2W_8\mathrm{tr}\,(U^2+U^{\dagger 2}). \tag{1.53}$$

It is noteworthy that two different terms (Pauli term, two derivative term see above) of the fundamental theory map to the same term of the EFT because

of the fact that they have the same chiral properties. The reason that we are focusing at the NLO terms in the chiral Lagrangian is because the terms $\mathcal{O}(a)$ can be reabsorbed by a redefinition of the mass $m \to m + a$. Note that (1.53) contains three unknown low energy constants, we will provide greater detail on them in the following chapters.

1.3 Random Matrix Theory (RMT)

Random matrices are generalizations of random variables where the random variable itself is matrix valued. RMT is a vast field with applications ranging from the calculation of correlation functions of eigenvalues to the modelling of complex dynamical systems. In physics they were first introduced by Wigner in the literature of Nuclear Physics [41]. Wigner employed RMT techniques to describe the excited energy states of heavy nuclei. His idea was rather simple but had profound implications since it generalized the basic concepts and principles of Statistical Mechanics. Since it is impossible to know analytically each matrix element of the Hamiltonian of a complex nucleus we might as well assume that each matrix element is a random number with the only restriction imposed that this random Hamiltonian has the same global symmetry properties with the Hamiltonian of the nucleus. Then the next step, the difficult one, is to identify universal quantities , i.e. quantities which are not dependent on the particular dynamics and are only dictated by the global symmetries of the physical problem. In this new type of statistical averages one changes the traditional ensemble average of identical physical systems with a new type of average over systems with different Hamiltonians but with common global symmetries.

RMT had large success in very diverse topics ranging from Nuclear Physics, 2 -dim Quantum Gravity [42], Condensed Matter Physics all the way to number theory in the study of the correlation of zeros of the Riemann ζ function [43]. At this point we will refer the reader to some very detailed reviews where all the milestones of RMT are being summarized [44]. RMT also relates all the above mentioned fields with quantum chaos since according to the Bohigas, Giannoni, Schmit conjecture [2] a quantum system whose classical quantum part is chaotic will exhibit eigenvalue correlations dictated by RMT. Typical example of the manifestation of this relation is the spectrum of the Schrödinger Hamiltonian of the Sinai billiard. In this case there is a sharp distinction with respect to the spectral properties of an integrable system where the nearest neighbor distribution of the eigenvalues (energy levels) is given by Poisson statistics, $P(s) = \exp(-s)$, for uncorrelated eigenvalues see Fig. (1.3).

There are two broad categories of Random Matrices, the Hermitian ones

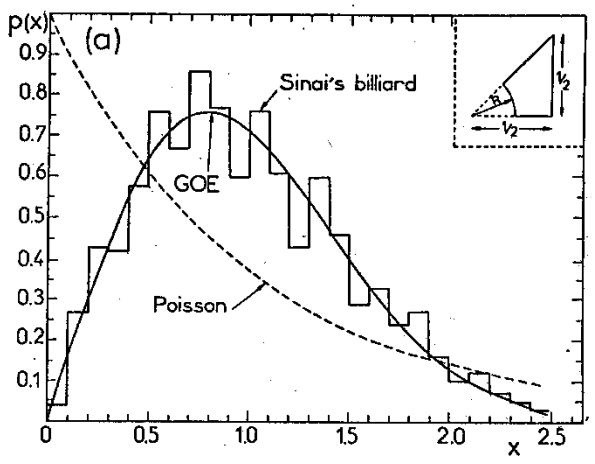

Figure 1.2: The Nearest Neighbor distribution for Sinai's billiard versus the result for correlated eigenvalues (GOE) and uncorrelated eigenvalues (Poisson). Courtesy of [2].

and the non-Hermitian ones. There are ten different ensembles of Hermitian matrices and each one of them is tangent to a corresponding symmetric space [45]. The first three ensembles of RM are the Wigner-Dyson ensembles [43, 46] which are $n \times n$ random Hermitian matrices with either real, complex or quaternion matrix elements distributed according to a Gaussian probability distribution

$$P(H)DH = e^{-\frac{n\beta}{4}\mathrm{tr}\, H^2} DH. \tag{1.54}$$

The measure in the above probability distribution is given by the product over the matrix elements of the Hermitian matrix H. They are classified by the Dyson index β where we can distinguish three cases. The case where H is a real symmetric matrix, this ensemble has Dyson index $\beta = 1$, the case where H is a complex Hermitian matrix, in this case $\beta = 2$ and the case of where the matrix H is quaternion self dual matrix in which case $\beta = 4$. There is a less known case which is very rarely used with $\beta = 8$ and in this case where the matrix elements are octonions. The next category of Random Matrices consists of the chiral ensembles where the matrix H has the chiral structure of the QCD Dirac operator [47]. They are defined as the ensembles of $(2n + \nu) \times (2n + \nu)$ Hermitian matrices where

$$D = \begin{pmatrix} 0 & W \\ -W^\dagger & 0 \end{pmatrix} \tag{1.55}$$

where the matrix elements are distributed according to a probability distribu-

tion which resembles the QCD partition function

$$P(W)DW \propto \det{}^{N_f} \begin{pmatrix} 0 & W \\ -W^\dagger & 0 \end{pmatrix} e^{-\frac{n\beta}{4}\mathrm{tr}\, WW^\dagger} DW. \tag{1.56}$$

The matrix W is a rectangular $n \times (n+\nu)$ matrix again with either real, complex or quaternion matrix elements. As a result of W being rectangular the Dirac operator has ν generic zero modes which is in accordance with the Atiyah-Singer index theorem for the Dirac operator in the background of a gauge field configuration with winding number equal to ν. The last class of Random Matrices consists of the Altland-Zirnbauer ensembles which model the superconducting Hamiltonian of Bogoliubov and de Gennes [48]. In this case the structure of the Hamiltonian is given by

$$H = \begin{pmatrix} A & B \\ B^\dagger & -A^\top \end{pmatrix} \tag{1.57}$$

and the matrix elements are distributed according to

$$P(H)DH \propto e^{-\frac{n\beta}{4}\mathrm{tr}\, HH^\dagger} DH. \tag{1.58}$$

In this Hamiltonian the matrix A is Hermitian and B is either symmetric with complex matrix elements (class C) or real symmetric (class CI). The other possibility is that B is antisymmetric with complex matrix elements (class D) or antisymmetric with quaternion matrix elements (class $DIII$). The key property that categorizes Random Matrices according to the different values of the Dyson index are the antiunitary symmetries. In quantum mechanics after the Hamiltonian has been brought to a block diagonal form with each block sharing different quantum numbers one can consider the antiunitary symmetry of time reversal for which there are three different possibilities which lead to the three classes of Random Matrices. The time reversal operator T can be written as $T = UK$ where U is a unitary matrix and K is the complex conjugation operator. If a system is invariant under time reversal and also rotationally invariant then the Hamiltonian of this system can be represented by a real symmetric matrix ($\beta = 1$). For this one needs to use the fact that for the time reversal operator $T^2 = 1$ and utilizing that one can build a T invariant basis in which H is given by a real symmetric matrix. This basis can be constructed following a simple iterative procedure. Starting from a basis vector $|n_1>$ one constructs the basis vector $|e_1> = |n_1> + T|n_1>$ then chooses the next vector $|n_2>$ orthogonal to $|e_1>$ and follows a similar procedure for the rest of the basis vectors.

The next case is when $T^2 = -1$, this is the case of systems with spin 1/2

and no rotational symmetry. In this case all eigenvalues of the Hamiltonian are doubly degenerate and the matrix elements of the Hamiltonian are quaternions and it has been coined as the $\beta = 4$ ensemble. In this case $T = \mathbb{1}_N \otimes (-i\sigma_2)K$ then since the Hamiltonian is invariant under this operator T i.e. $THT^{-1} = H$ then the block structure of T results in a 2×2 block structure for each matrix element of the Hamiltonian. Each matrix element is of the form $q = q_0 + q_1 i + q_2 j + q_3 k$ with $i^2 = j^2 = k^2 = -1$ and $ijk = -1$.

Finally, we have the case with no antiunitary symmetries, in this case the Hamiltonian is a Hermitian matrix with complex matrix elements and Dyson index $\beta = 2$.

In field theory we have a similar situation. In this case the Dirac operator commutes with an operator T which for the case of $N_c = 2$ and fundamental fermions is given by $= \gamma_2\gamma_4\tau_2 K$ where τ_2 acts in color space and $C = \gamma_2\gamma_4$ is the charge conjugation operator. Using a similar construction as in the case of the Schrödinger Hamiltonian one can show that the Dirac operator is comprised by real matrix elements and this is the case of $\beta = 1$ for the chiral ensembles.

In the case of any number of color adjoint fermions we have again an antiunitary symmetry. Here, $T = \gamma_2\gamma_4 K$ and $T^2 = -1$, this is the case of $\beta = 4$ for the chiral ensembles and the Dirac operator has quaternion matrix elements.

Finally the case of $SU(N_c \geq 3)$ with fundamental fermion possesses no antiunitary symmetries and therefore the Dirac operator has complex matrix elements ($\beta = 2$).

At this point we would like to motivate why the study of the Dirac spectrum has important information concerning non-perturbative aspects of QCD. There is a famous relation derived by Banks and Casher [49] which relates the spectral density of the Dirac operator to the chiral condensate which is the order parameter for the spontaneous breaking of chiral symmetry

$$\Sigma = |\langle \bar{\psi}\psi \rangle| = \frac{\pi \rho(0)}{V}. \tag{1.59}$$

In the above relation $\rho(\lambda)$ is the spectral density of the Dirac operator formally defined as

$$\rho(\lambda) = \langle \Sigma_n \delta(\lambda - \lambda_n) \rangle_{YM}. \tag{1.60}$$

We will now prove this relation [50] . Considering the "spatial" trace of the

Dirac propagator

$$\begin{aligned}\frac{1}{V}\int d^4x S(x,x) &= \frac{1}{V}\int d^4x \langle\bar{\psi}(x)\psi(x)\rangle_{YM} \\ &= \frac{1}{V}\int d^4x \langle\sum_n \frac{v_n(x)v_n^\dagger(x)}{m-i\lambda_n}\rangle_{YM} \\ &= \frac{2m}{V}\langle\sum_{\lambda_n>0}\frac{1}{m^2+\lambda_n^2}\rangle_{YM} \\ &= \frac{2m}{V}\int_0^\infty \frac{\rho(\lambda)}{m^2+\lambda^2}. \end{aligned} \tag{1.61}$$

If we take the double limit $\lim_{m\to 0}\lim_{V\to\infty}$ the above expression simply yields $\pi\rho(0)$.

An immediate consequence of the Banks-Casher relation is that the eigenvalue spacing of the smallest eigenvalues $\Delta\lambda = \frac{1}{\rho(0)} = \frac{\pi}{\Sigma V}$ in sharp contrast to the eigenvalue spacing of the free system where $\Delta\lambda \propto \frac{1}{V^{1/4}}$. We see that the interactions of the Dirac fermions with the gauge fields creates level repulsion on the spectrum and as a result the correlations of the lowest eigenvalues will be given by chiral RMT. The fact that the lowest eigenvalues scale as $1/V\Sigma$ leads us to introduce the concept of microscopic spectral density [47]

$$\rho_s(\hat{\lambda}) = \lim_{V\to\infty}\frac{1}{V\Sigma}\rho\left(\frac{\hat{\lambda}}{V\Sigma}\right). \tag{1.62}$$

The claim is that this is a universal function determined only by global symmetries. Furtherly, since chPT in the ϵ -regime and chiral RMT share the same global symmetries they belong to the same universality class. It only suffices then because of the universality argument to compute the microscopic spectral density of the simplest theory in the universality class namely chiral Random Matrix Theory.

1.3.1 The Microscopic Spectral Density

There are two main techniques that are the most powerful and appropriate in order to solve the Random Matrix Models and to obtain the spectral density. The one is the orthogonal polynomial method [43] and the other is the supersymmetric approach [51, 52].

The method of Orthogonal Polynomials

We will employ both and derive the microscopic spectral density for the chiral Gaussian Unitary ensemble (chGUE) just to illustrate the different aspects of these techniques. We will start from the method of orthogonal polynomials since historically it was the first method employed to access the spectral correlations of chGUE [53]. The partition function reads

$$Z^{\beta=2}_{N_f,\nu}(m_1,\ldots,m_{N_f}) = \int DW \prod_{f=1}^{N_f} \det(\mathcal{D}+m_f) e^{-\frac{N}{2}\mathrm{tr}\, W^\dagger W}\,, \tag{1.63}$$

where

$$\mathcal{D} = \begin{pmatrix} 0 & iW \\ iW^\dagger & 0 \end{pmatrix}. \tag{1.64}$$

In this case as we mentioned $\mathcal{D}$ has complex matrix elements and if we perform a singular value decomposition on W, i.e. $W = U\Lambda V^\dagger$ then the partition function is factorizing in a part depending on the eigenvalues and a part depending on the eigenvectors. The part depending on the eigenvectors drops out. The Jacobian of this transformation is given by

$$\mathcal{J}(\Lambda) = |\Delta(\lambda^2)|^2 \prod_k \lambda_k^{2|\nu|+1} \tag{1.65}$$

and it can be computed either by a brute force differentiation [47], or by a Faddeev-Popov trick [54, 55] or simply by dimensional arguments. The Vandermonde determinant $\Delta(\lambda^2)$ is defined as

$$\Delta(\lambda^2) = \prod_{k<l}(\lambda_k^2 - \lambda_l^2)\,. \tag{1.66}$$

After this transformation the partition function is an integral over the eigenvalues of the Dirac operator

$$Z^{\beta=2}_{N_f,\nu}(m_1,\ldots,m_{N_f}) = \int d\lambda |\Delta(\lambda^2)|^2 \prod_k \lambda_k^{2|\nu|+1} e^{-\frac{N}{2}\lambda_k^2} \prod_f m_f^{|\nu|}(\lambda_k^2+m_f^2). \tag{1.67}$$

The joint probability distribution function (jpdf) is given by the integrand of (1.67). To obtain the spectral density one needs to integrate the joint probability distribution function with respect to $n-1$ eigenvalues (here we consider the massless case)

$$\rho(\lambda_1) = \int \prod_{k=2}^{n} d\lambda_k \rho_n(\lambda_1, \cdots, \lambda_n). \tag{1.68}$$

In the orthogonal polynomial method by performing manipulations that do not alter the determinant one can re-express the Vandermonde determinant in terms of orthogonal polynomials which fulfil an orthogonality relation with the joint probability distribution function as a weight function.

$$\prod_{k<l}(\lambda_k^2 - \lambda_l^2) = \begin{vmatrix} 1 & \cdots & 1 \\ \vdots & \ddots & \vdots \\ \lambda_1^{2(n-1)} & \cdots & \lambda_n^{2(n-1)} \end{vmatrix} \propto \begin{vmatrix} P_0(\lambda_1^2) & \cdots & P_0(\lambda_n^2) \\ \vdots & \ddots & \vdots \\ P_{n-1}(\lambda_1^2) & \cdots & P_{n-1}(\lambda_n^2) \end{vmatrix}. \tag{1.69}$$

For $m_f = 0$ these polynomials are the associated Laguerre polynomials

$$P_k(\lambda^2) = \left(\frac{N}{2}\frac{k!}{\Gamma(N_f + \nu + k + 1)}\right)^{1/2} L_k^{N_f+\nu}\left(\frac{\lambda^2 n}{2}\right). \tag{1.70}$$

If we define $z = \frac{\lambda^2 n}{2}$ then after expanding the determinant and using the orthogonality properties of the associated Laguerre polynomials the spectral density reads

$$\rho(z) \propto \sum_{k=0}^{N-1} \frac{k!}{\Gamma(N_f + \nu + k + 1)} L_k^{N_f+\nu}(z) L_k^{N_f+\nu}(z) z^{N_f+\nu+1/2} e^{-z}. \tag{1.71}$$

In order to perform the sum over the orthogonal polynomials we will utilize the Christoffel-Darboux formula

$$\sum_{j=0}^{n} \frac{P_j(x)P_j(y)}{h_j} = \frac{k_n}{h_n k_{n+1}} \frac{P_n(y)P_{n+1}(x) - P_{n+1}(y)P_n(x)}{x - y}, \tag{1.72}$$

where h_j is the norm of the polynomials and k_j is the leading coefficient (i.e. the one multiplying x^n). After performing the sum one arrives at the finite n spectral density for the chGUE

$$\rho(z) = \frac{N}{2}\frac{N!}{\Gamma(N_f + \nu + N)} \left(L_{N-1}^{N_f+\nu}(z) L_{N-1}^{N_f+\nu+1}(z) - L_N^{N_f+\nu}(z) L_{N-2}^{N_f+\nu+1}(z)\right) z^{N_f+\nu+1/2} e^{-z}. \tag{1.73}$$

At this point we will take the microscopic limit which is defined as the double scaling limit $N \to \infty$ with $\hat{z} = Nz$ kept fixed and of order 1.

$$\lim_{n\to\infty} \frac{1}{n^\alpha} L_n^\alpha(\frac{\hat{z}}{n}) = \hat{z}^{-\frac{\alpha}{2}} J_\alpha(2\sqrt{\hat{z}}), \tag{1.74}$$

where J_α is the Bessel function of the first kind. Finally the microscopic spectral density (in the massless case) reads

$$\rho_S(\hat{z}) = \frac{\hat{z}}{2}(J^2_{N_f+\nu}(\hat{z}) - J_{N_f+\nu+1}(\hat{z})J_{N_f+\nu-1}(\hat{z})). \tag{1.75}$$

From the structure of the jpdf (1.67) it is clear that for massless quarks there is a duality between flavor and topology. A non zero winding number can be introduced by adding ν massless flavors. Since this is a property of the jpdf it will be inherited to all the correlation functions.

The Supersymmetric Method

A key quantity that provides direct access to the spectrum of the Dirac operator is the one-point Green's function also known as the resolvent in RMT literature. The resolvent is given by the averaged (over the ensemble) trace of the inverse Dirac operator. In order to compute it we can utilize the usual field theoretical techniques. We first introduce source terms in the path integral, then differentiate with respect to the sources and finally set the sources to zero at the end of the calculation. If we add an extra species of fermionic and bosonic flavors we obtain the partially quenched partition function [56, 57]

$$Z^{\rm pq}_\nu = \int [dA]_\nu \frac{\det(i\not{D} + m_{v1})}{\det(i\not{D} + m_{v2})} \prod_{f=1}^{N_f} \det(i\not{D} + m_f)\, e^{-S_{YM}}, \tag{1.76}$$

where $m_{v_1} = m_{v_2} + J$. If we set $J = 0$ the partially quenched partition function coincides with the original partition function. To calculate the resolvent we can differentiate

$$\Sigma(m_v; m_1, \cdots, m_{N_f}) = \frac{1}{V} \frac{\partial}{\partial J}\bigg|_{J=0} \log Z^{\rm pq}_\nu. \tag{1.77}$$

The discontinuity of Σ across the imaginary axis [57, 58] yields the spectral density. For $N_f = 0$ we obtain

$$\mathrm{Disc}|_{m_v=i\lambda}\,\Sigma(m_v) = \lim_{\epsilon\to 0}\{\Sigma(i\lambda+\epsilon) - \Sigma(i\lambda-\epsilon)\} = 2\pi\sum_k \langle\delta(\lambda+\lambda_k)\rangle = 2\pi\rho(\lambda). \tag{1.78}$$

This procedure is quite general and in principle one can calculate all higher point correlation functions by the addition of the sufficient number of extra species with opposite statistics.

The next step is to construct the quenched low energy effective theory. For this we need to consider the whole pseudo Nambu-Goldstone spectrum. Because of the extra fermionic and bosonic quarks we have a much richer structure. Apart from the ordinary $q\bar{q}$ mesons which we will denote by ϕ we have ghost mesons $\tilde{q}\bar{\tilde{q}}$ denoted by $\tilde{\phi}$ and also fermionic mesons $\tilde{q}\bar{q}$ and $q\bar{\tilde{q}}$ denoted by χ and $\chi^\dagger$. All these fields are going to be collected in a matrix

$$\Phi = \begin{pmatrix} \phi & \bar{\chi} \\ \chi & i\tilde{\phi} \end{pmatrix}. \tag{1.79}$$

The matrix Φ is a supermatrix since it encapsulates fermions and bosons. A general supermatrix M [51, 52] is written in a boson (B), fermion (F) basis

$$M = \begin{pmatrix} A & C \\ D & B \end{pmatrix}. \tag{1.80}$$

The matrices A, B are comprised of ordinary variables while the matrices C, D are comprised of Grassmann variables. The supermatrix acts on supervectors defined by

$$V = \begin{pmatrix} \eta_1 \\ \vdots \\ \eta_m \\ \phi_1 \\ \vdots \\ \phi_n \end{pmatrix}, \tag{1.81}$$

where η are Grassmann variables while ϕ are commuting variables. The notions of trace and determinant generalize to their corresponding *super* counterparts.

$$\mathrm{Str}\, M = \mathrm{tr}\, A - \mathrm{tr}\, B,$$

$$\mathrm{Sdet}\,(U) = e^{\mathrm{Str}\,\ln U} = \det(A - CB^{-1}D)/\det(B).$$

Note that we are use a different convention in the ensuing chapters but we always warn the reader in such case. The unitary field will be given by

$$U = \exp(i\sqrt{2}\Phi/F_\pi). \tag{1.82}$$

The partially quenched Lagrangian for all masses set to zero is invariant under

$$U_L(N_f + N_v|N_v) \otimes U_R(N_f + N_v|N_v) \tag{1.83}$$

which breaks spontaneously to

$$U_V(N_f + N_v|N_v). \tag{1.84}$$

For our quenched calculation we consider $N_f = 0$ and $N_v = 1$. The partition function of the effective theory for partially quenched QCD at very low energies in the ϵ- regime reduces to a superunitary matrix integral [57, 58]

$$Z^\nu_{N_f}(\hat{\mathcal{M}}) = \int_{U\in U(N_f+1|1)} dU\, \mathrm{Sdet}^{\,\nu} U e^{V\frac{\Sigma}{2}\,\mathrm{Str}\,(\hat{\mathcal{M}}U + \hat{\mathcal{M}}U^{-1})}. \tag{1.85}$$

We will evaluate this partition function for the quenched case $N_f = 0$. We therefore need an explicit parametization of the supergroup $U(1|1)$. This was studied in [59] and we will just quote the parametrization which is basically a graded generalization of the Euler angles parametrization.

$$U = \begin{pmatrix} e^{i\theta} & 0 \\ 0 & e^{s} \end{pmatrix} \exp \begin{pmatrix} 0 & \alpha \\ \beta & 0 \end{pmatrix}. \tag{1.86}$$

For $N_f = 0$ we simply get one for the Jacobian of this parametrization [57]. Therefore the quenched partition function reads

$$\begin{aligned} Z^\nu_{N_f=0}(m_v + J, m_v) &= \int \frac{d\theta}{2\pi}\, ds\, d\beta\, d\alpha\, e^{\nu(i\theta - s)} \\ \times \quad \exp &\left[\Sigma_0 V\, \mathrm{Str} \begin{pmatrix} m_v + J & 0 \\ 0 & m_v \end{pmatrix} \begin{pmatrix} (1 + \frac{1}{2}\alpha\beta)\cos\theta & \alpha(e^{i\theta} - e^{-s})/2 \\ \beta(e^{s} - e^{-i\theta})/2 & (1 - \frac{1}{2}\alpha\beta)\cosh s \end{pmatrix}\right], \end{aligned} \tag{1.87}$$

where the Grassmann integrals can be calculated by brute force after the finite expansion of the exponentials.

To calculate the chiral condensate we differentiate with respect to the

source and after setting the source to zero we obtain

$$\Sigma(m_v) = \frac{\Sigma_0}{2} \int \frac{d\theta}{2\pi}\, ds\; e^{\mu_v(\cos\theta - \cosh s)}\; e^{\nu(i\theta - s)}\; \left[\cosh s(\mu_v \cos\theta + \mu_v \cosh s - 1)\right], \tag{1.88}$$

which after utilizing the Wronskian identity for Bessel functions

$$K_\nu(x) I_{\nu+1}(x) + I_\nu(x) K_{\nu+1}(x) = \frac{1}{x}, \tag{1.89}$$

can be written as

$$\frac{\Sigma(m_v)}{\Sigma_0} = \mu_v \left[I_\nu(\mu_v) K_\nu(\mu_v) + I_{\nu+1}(\mu_v) K_{\nu-1}(\mu_v)\right] + \frac{\nu}{\mu_v}, \tag{1.90}$$

where $\mu_v = m_v V \Sigma_0$. If we now calculate the discontinuity of the chiral condensate across the imaginary axis by employing (1.78) we recover the result of the orthogonal polynomial analysis for the quenched spectral density (1.75) which for arbitrary ν reads

$$\rho_S\left(\hat{z}\right) = \frac{\hat{z}}{2}(J_\nu^2(\hat{z}) - J_{\nu+1}(\hat{z}) J_{\nu-1}(\hat{z})) + \nu\delta(\hat{z}). \tag{1.91}$$

It is really important to mention that we have arrived at exactly the same result which was initially obtained by RMT methods by a different path, using partially quenched chiral perturbation theory. We will continue using this equivalence of chiral RMT and ϵ -regime chiral perturbation theory in the next chapters since both of them even though they are equivalent, they have advantages and disadvantages. Chiral perturbation theory provides universality since according to Weinberg's prescription one simply calculates utilizing an effective theory with all the terms that are contributing to a particular order being present in the Lagrangian. On the other hand RMT has a plethora of very powerful mathematical techniques which allows for results unavailable by other means.

Chapter 2

Spectral Properties of the Wilson Dirac Operator

2.1 Introduction

The drastically increasing computational power as well as algorithmic improvements over the last decades provide us with deep insights in non-perturbative effects of Quantum Chromodynamics (QCD). However, the artifacts of the discretization, i.e. a finite lattice spacing, are not yet completely under control. In particular, in the past few years a large numerical [60–67] and analytical [5, 68–73] effort was undertaken to determine the low energy constants of the terms in the chiral Lagrangian that describe the discretization errors. It is well known that new phase structures arise such as the Aoki phase [74] and the Sharpe-Singleton scenario [37]. A direct analytical understanding of lattice QCD seems to be out of reach. Fortunately, as was already realized two decades ago, the low lying spectrum of the continuum QCD Dirac operator can be described in terms of Random Matrix Theories (RMTs) [47, 75].

Recently, RMTs were formulated to describe discretization effects for staggered [76, 77] as well as Wilson [5, 68–70] fermions. Although these RMTs are more complicated than the chiral Random Matrix Theory formulated in [47, 75], in the case of Wilson fermions a complete analytical solution of the RMT has been achieved [5, 68–73]. Since the Wilson RMT shares the global symmetries of the Wilson Dirac operator it will be equivalent to the corresponding (partially quenched) chiral Lagrangian in the microscopic domain (also known as the ϵ-domain) [39, 78–82].

Joint work with M. Kieburg and J.J.M. Verbaarschot.

Quite recently, there has been a breakthrough in deriving eigenvalue statistics of the infrared spectrum of the Hermitian [83] as well as the non-Hermitian [3, 4, 84, 85] Wilson Dirac operator. These results explain [73] why the Sharpe-Singleton scenario is only observed for the case of dynamical fermions [63, 67, 86–95] and not in the quenched theory [96–99] while the Aoki phase has been seen in both cases. First comparisons of the analytical predictions with lattice data show a promising agreement [64–66]. Good fits of the low energy constants are expected for the distributions of individual eigenvalues [5, 68–70, 100].

Up to now, mostly the effect of W_8 [3–5, 69, 70, 83], and quite recently also of W_6 [71, 73, 101], on the Dirac spectrum were studied in detail. In this article, we will discuss the effect of all three low energy constants. Thereby we start from the Wilson RMT for the non-Hermitian Wilson Dirac operator proposed in Refs. [68]. In Sec. 2.2 we recall this Random Matrix Theory and its properties. Furthermore we derive the joint probability density of the eigenvalues which so far was only stated without proof in Refs. [73, 85]. We also discuss the approach to the continuum limit in terms of the Dirac spectrum.

In Sec. 2.3, we derive the level densities of D_{W} starting from the joint probability density. Note that due to its γ_5-Hermiticity D_{W} has complex eigenvalues as well as exactly real eigenvalues. Moreover, the real modes split into those corresponding to eigenvectors with positive and negative chirality. In Sec. 2.4, we discuss the spectrum of the quenched non-Hermitian Wilson Dirac operator in the microscopic limit in detail. In particular the asymptotics at small and large lattice spacing are studied. The latter limit is equal to a mean field limit for some quantities which can be trivially read off.

In Sec. 2.5 we summarize our results. In particular we present easily measurable quantities which can be used for fitting the three low energy constants $W_{6/7/8}$ and the chiral condensate Σ. Detailed derivations are given in several appendices. The joint probability distribution is derived in A.1. Some useful integral identities are given in B.1 and in C.1 we perform the microscopic limit of the graded partition function that enters in the distribution of the chiralities over the real eigenvalues of D_W. Finally, some asymptotic results are derived in D.1.

2.2 Wilson Random Matrix Theory and its Joint Probability Density

In Sec. 2.2.1 we introduce the Random Matrix Theory for the infrared spectrum of the Wilson Dirac operator and recall its most important properties. Its joint probability density is given in Sec. 2.2.2, and the continuum limit is derived in Sec. 2.2.3.

2.2.1 The random matrix ensemble

We consider the random matrix ensemble [5, 68–70]

$$D_{\rm W} = \begin{pmatrix} A & W \\ -W^\dagger & B \end{pmatrix} \tag{2.1}$$

distributed by the probability density

$$\begin{aligned} P(D_{\rm W}) &= \left(\frac{n}{2\pi a^2}\right)^{[n^2+(n+\nu)^2]/2} \left(-\frac{n}{2\pi}\right)^{n(n+\nu)} \exp\left[-\frac{a^2}{2}\left(\mu_{\rm r}^2 + \frac{n+\nu}{n}\mu_{\rm l}^2\right)\right] \\ &\times \exp\left[-\frac{n}{2a^2}(\mathrm{tr}\, A^2 + \mathrm{tr}\, B^2) - n\mathrm{tr}\, WW^\dagger + \mu_{\rm r}\,\mathrm{tr}\, A + \mu_{\rm l}\,\mathrm{tr}\, B\right]. \end{aligned} \tag{2.2}$$

The Hermitian matrices A and B break chiral symmetry and their dimensions are $n \times n$ and $(n+\nu)\times(n+\nu)$, respectively, where ν is the index of the Dirac operator. Both $\mu_{\rm r}$ and $\mu_{\rm l}$ are one dimensional real variables. The chiral RMT describing continuum QCD [47] is given by the ensemble (2.1) with A and B replaced by zero. The N_f flavor RMT partition function is defined by

$$Z^\nu_{N_f}(m) = \int D[D_W] P(D_W) \mathrm{det}^{N_f}(D_W + m). \tag{2.3}$$

Without loss of generality we can assume $\nu \geq 0$ since the results are symmetric under $\nu \to -\nu$ and $\mu_{\rm r} \leftrightarrow \mu_{\rm l}$.

The Gaussian integrals over the two variables $\mu_{\rm r}$ and $\mu_{\rm l}$ yield the two low energy constants W_6 and W_7 [5, 68–70]. The reason is that the integrated probability distribution

$$\begin{aligned} &P(D_{\rm W}, W_{6/7} \neq 0) \\ &\quad = \int_{-\infty}^{\infty} P(D_{\rm W}) \exp\left[-\frac{a^2(\mu_{\rm r}+\mu_{\rm l})^2}{16V|W_6|} - \frac{a^2(\mu_{\rm r}-\mu_{\rm l})^2}{16V|W_7|}\right] \frac{a^2 d\mu_{\rm r}\, d\mu_{\rm l}}{8\pi V\sqrt{W_6 W_7}} \end{aligned} \tag{2.4}$$

generates the terms $(\mathrm{tr}\, A + \mathrm{tr}\, B)^2$ and $(\mathrm{tr}\, A - \mathrm{tr}\, B)^2$ which correspond to the

squares of traces in the chiral Lagrangian [78–81]. In the microscopic domain the corresponding partition function for $N_{\rm f}$ fermionic flavors is then given by

$$Z^{\nu}_{N_{\rm f}}(\widetilde{m}) = \int\limits_{{\rm U}\,(N_{\rm f})} d\mu(U) \exp\left[\frac{\Sigma V}{2}{\rm tr}\,\widetilde{m}(U+U^{-1}) - \widetilde{a}^2 V W_6 {\rm tr}^{\,2}(U+U^{-1})\right] \times \exp\left[-\widetilde{a}^2 V W_7 {\rm tr}^{\,2}(U-U^{-1}) - \widetilde{a}^2 V W_8 {\rm tr}\,(U^2+U^{-2})\right] \det{}^{\nu} U \quad (2.5)$$

with the physical quark masses $\widetilde{m} = {\rm diag}\,(\widetilde{m}_1, \ldots, \widetilde{m}_{N_{\rm f}})$, the space-time volume V, the physical lattice spacing $\widetilde{a}$ and the chiral condensate Σ. The low energy constant W_8 is generated by the term ${\rm tr}\,A^2 + {\rm tr}\,B^2$ in Eq. (2.2) and is *a priori* positive. We include the lattice spacing a in the standard deviation of A and B, cf. Eq. (2.2), out of convenience for deriving the joint probability density. We employ the sign convention of Refs. [5, 68–70] for the low energy constants.

The microscopic limit ($n \to \infty$) is performed in Sec. 2.3. In this limit the rescaled lattice spacing $\widehat{a}_8^2 = na^2/2 = \widetilde{a}^2 V W_8$, the rescaled parameters $\widehat{m}_6 = a^2(\mu_{\rm r} + \mu_{\rm l})$, $\widehat{\lambda}_7 = a^2(\mu_{\rm r} - \mu_{\rm l})$ and the rescaled eigenvalues $\widehat{Z} = 2nZ = {\rm diag}\,(2nz_1, \ldots, 2nz_{2n+\nu})$ of $D_{\rm W}$ are kept fixed for $n \to \infty$. The mass $\widehat{m}_6$ and axial mass $\widehat{\lambda}_7$ are distributed with respect to Gaussians with variance $8\widehat{a}_6^2 = -8\widetilde{a}^2 V W_6$ and $8\widehat{a}_7^2 = -8\widetilde{a}^2 V W_7$, respectively. Note the minus sign in front of $W_{6/7}$. As was shown in Ref. [73] the opposite sign is inconsistent with the symmetries of the Wilson Dirac operator. The notation is slightly different from what is used in the literature to get rid of the imaginary unit in $\widehat{a}_6$ and $\widehat{a}_7$.

The joint probability density $p(Z)$ of the eigenvalues $Z = {\rm diag}\,(z_1, \ldots, z_{2n+\nu})$ of D_W can be defined by

$$I[f] = \int\limits_{\mathbb{C}^{(2n+\nu)\times(2n+\nu)}} f(D_{\rm W}) P(D_{\rm W}) d[D_{\rm W}] = \int\limits_{\mathbb{C}^{(2n+\nu)}} f(Z) p(Z) d[Z], \quad (2.6)$$

where f is an arbitrary ${\rm U}\,(n, n+\nu)$ invariant function. The random matrix $D_{\rm W}$ is $\gamma_5 = {\rm diag}\,(\mathbb{1}_n, -\mathbb{1}_{n+\nu})$ Hermitian, i.e.

$$D_{\rm W}^{\dagger} = \gamma_5 D_{\rm W} \gamma_5. \quad (2.7)$$

Hence, the eigenvalues z come in complex conjugate pairs or are exactly real. The matrix $D_{\rm W}$ has ν generic real modes and $2(n-l)$ additional real eigenvalues ($0 \leq l \leq n$). The index l decreases by one when a complex conjugate pair enters the real axis.

2.2.2 The joint probability density of D_{W}

Let D_l be D_{W} if it can be quasi-diagonalized by a non-compact unitary rotation $U \in \mathrm{U}(n, n+\nu)$, i.e. $U\gamma_5 U^\dagger = \gamma_5$, to

$$D_l = UZ_lU^{-1} = U \left(\begin{array}{cc|cc} x_1 & 0 & 0 & 0 \\ 0 & x_2 & y_2 & 0 \\ \hline 0 & -y_2 & x_2 & 0 \\ 0 & 0 & 0 & x_3 \end{array}\right) U^{-1}, \tag{2.8}$$

where the real diagonal matrices $x_1 = \mathrm{diag}\,(x_1^{(1)}, \ldots, x_{n-l}^{(1)})$, $x_2 = \mathrm{diag}\,(x_1^{(2)}, \ldots, x_l^{(2)})$, $y_2 = \mathrm{diag}\,(y_1^{(2)}, \ldots, y_l^{(2)})$ and $x_3 = \mathrm{diag}\,(x_1^{(3)}, \ldots, x_{n+\nu-l}^{(3)})$ have the dimension $n-l$, l, l and $n+\nu-l$, respectively. The matrices x_1 and x_3 comprise all real eigenvalues of D_l corresponding to the right handed and left handed modes, respectively. We refer to an eigenvector ψ of D_W as right-handed if the chirality is positive definite, i.e.

$$\langle\psi|\gamma_5|\psi\rangle > 0, \tag{2.9}$$

and as left-handed if the chirality is negative definite. The eigenvectors corresponding to complex eigenvalues have vanishing chirality. The complex conjugate pairs are $(z_2 = x_2 + \imath y_2, z_2^* = x_2 - \imath y_2)$. Note that it is not possible to diagonalize D_W with a $\mathrm{U}(n, n+\nu)$ transformation with complex conjugate eigenvalues.

The quasi-diagonalization $D_l = UZ_lU^{-1}$ determines U up to a $\mathrm{U}^{\,2n+\nu-l}(1) \times \mathrm{O}^{\,l}(1,1)$ transformation while the set of eigenvalues Z_l can be permuted in $l!(n-l)!(n+\nu-l)!2^l$ different ways. The factor 2^l is due to the complex conjugation of a complex pair. The Jacobian of the transformation to eigenvalues and the coset $\mathbb{G}_l = \mathrm{U}(n, n+\nu)/[\mathrm{U}^{\,2n+\nu-l}(1) \times \mathrm{O}^{\,l}(1,1)]$ is given by

$$|\Delta_{2n+\nu}(Z_l)|^2, \tag{2.10}$$

where the Vandermonde determinant is defined as

$$\Delta_{2n+\nu}(Z) = \prod_{1\le i<j\le 2n+\nu} (z_i - z_j) = (-1)^{n+\nu(\nu-1)/2} \det\left[z_i^{j-1}\right]_{1\le i,j\le 2n+\nu}. \tag{2.11}$$

The functional $I[f]$ in Eq. (2.6) is a sum over $n+1$ integrations on disjoint

sets, i.e.

$$I[f] = \sum_{l=0}^{n} \frac{1}{2^l (n-l)!l!(n+\nu-l)!} \times \int\limits_{\mathbb{R}^{\nu+2(n-l)}\times\mathbb{C}^l} f(Z_l) \left[\int\limits_{\mathbb{G}_l} P(U Z_l U^{-1}) d\mu_{\mathbb{G}_l}(U) \right] |\Delta_{2n+\nu}(Z_l)|^2 d[Z_l]. \tag{2.12}$$

where we have normalized the terms with respect to the number of possible permutations of the eigenvalues in Z. Thus we have for the joint probability density over all sectors of eigenvalues

$$\begin{aligned} p(Z)d[Z] &= \sum_{l=0}^{n} p_l(Z_l) d[Z_l] \\ &= \sum_{l=0}^{n} \frac{|\Delta_{2n+\nu}(Z_l)|^2 d[Z_l]}{2^l (n-l)!l!(n+\nu-l)!} \int\limits_{\mathbb{G}_l} P(U Z_l U^{-1}) d\mu_{\mathbb{G}_l}(U). \end{aligned} \tag{2.13}$$

Here $p_l(Z_l)$ is the joint probability density for a fixed number of complex conjugate eigenvalue pairs, namely l. The integration over U is nontrivial and will be worked out in detail in A.1.

In a more mathematical language the normalization factor in Eq. (2.13) can be understood as follows. If the permutation group of N elements is denoted by $\mathbf{S}(N)$ while the group describing the reflection $y \to -y$ is $\mathbb{Z}_2$, the factor $2^l(n-l)!l!(n+\nu-l)!$ is the volume of the finite subgroup $\mathbf{S}(n-l) \times \mathbf{S}(l) \times \mathbf{S}(n+\nu-l) \times \mathbb{Z}_2^l$ of $\mathrm{U}(n, n+\nu)$ which correctly normalizes each summand. Originally we had to divide $\mathrm{U}(n, n+\nu)$ by the set $\mathrm{U}^{2n+\nu-l}(1) \times \mathrm{O}^l(1,1) \times \mathbf{S}(n-l) \times \mathbf{S}(l) \times \mathbf{S}(n+\nu-l) \times \mathbb{Z}_2^l$ because it is the maximal subgroup whose image of the adjoint mapping commutes with Z_l. The reasoning is as follows. Let $\Sigma[Z_l] = \{U Z_l U^{-1} | U \in \mathrm{U}(n, n+\nu)\}$ be the orbit of Z_l and $\Sigma_c[Z_l] = \{\widehat{Z}_l \in \Sigma[Z_l] | [\widehat{Z}_l, Z_l] = 0\}$ a subset of this orbit. Then all orderings in each of the three sets of eigenvalues x_1, (z_2, z_2^*) and x_3 as well as the reflections $y_j^{(2)} \to -y_j^{(2)}$ are in $\Sigma_c[Z_l]$. This subset $\Sigma_c[Z_l] \subset \Sigma[Z_l]$ can be represented by the finite group $\mathbf{S}(n-l) \times \mathbf{S}(l) \times \mathbf{S}(n+\nu-l) \times \mathbb{Z}_2^l$. This group is called the Weyl group in group theory. The Lie group $\mathrm{U}^{2n+\nu-l}(1) \times \mathrm{O}^l(1,1)$ acts on $\Sigma_c[Z_l]$ as the identity since it commutes with Z_l. The group $\mathrm{U}^{2n+\nu-l}(1)$ represents $2n+\nu-l$ complex phases along the diagonal commuting with the set which consists of Z_l with a fixed l. Each non-compact orthogonal group $\mathrm{O}(1,1)$ reflects the invariance of a single complex conjugate eigenvalue pair under a hyperbolic transformation which is equal to a Lorentz-transformation

in a 1+1 dimensional space-time.

There are two ways to deal with the invariance under $\mathrm{U}^{\,2n+\nu-l}(1)\times\mathrm{O}^{\,l}(1,1)\times\mathbf{S}(n-l)\times\mathbf{S}(l)\times\mathbf{S}(n+\nu-l)\times\mathbb{Z}_2^l$ in an integral such that we correctly weigh all points. We have either to divide $\mathrm{U}\,(n,n+\nu)$ by the whole subgroup or we integrate over a larger coset and reweigh the measure by the volume of the subgroups not excluded. The ordering enforced by $\mathbf{S}(n-l)\times\mathbf{S}(l)\times\mathbf{S}(n+\nu-l)\times\mathbb{Z}_2^l$ is difficult to handle in calculations. Therefore, we have decided for a reweighting of the integration measure by $1/[(n-l)!(n+\nu-l)!l!2^l]$. However the Lie group $\mathrm{U}^{\,2n+\nu-l}(1)\times\mathrm{O}^{\,l}(1,1)$, in particular the hyperbolic subgroups, has to be excluded since its volume is infinite.

In this section as well as in A.1, we use the non-normalized Haar-measures induced by the pseudo metric

$$\mathrm{tr}\, dD_{\mathrm{W}}^2 = \mathrm{tr}\, dA^2 + \mathrm{tr}\, dB^2 - 2\mathrm{tr}\, dW dW^\dagger. \tag{2.14}$$

Therefore the measures for D_{W} and Z_l are

$$\begin{aligned} d[D_{\mathrm{W}}] &= \prod_{j=1}^{n} dA_{jj} \prod_{1\le i<j\le n} 2\, d\,\mathrm{Re}\, A_{ij} d\,\mathrm{Im}\, A_{ij} \prod_{j=1}^{n+\nu} dB_{jj} \\ &\times \prod_{1\le i<j\le n+\nu} 2\, d\,\mathrm{Re}\, B_{ij} d\,\mathrm{Im}\, B_{ij} \prod_{\substack{1\le i\le n\\ 1\le j\le n+\nu}} (-2)\, d\,\mathrm{Re}\, W_{ij} d\,\mathrm{Im}\, W_{ij}, \end{aligned} \tag{2.15}$$

$$d[Z_l] = \prod_{j=1}^{n-l} dx_j^{(1)} \prod_{j=1}^{l} 2\imath\, dx_j^{(2)} dy_j^{(2)} \prod_{j=1}^{n+\nu-l} dx_j^{(3)}. \tag{2.16}$$

The Haar measure $d\mu_{\mathbb{G}_l}$ for the coset $\mathbb{G}_l$ is also induced by $d[D_{\mathrm{W}}]$ and results from the pseudo metric, i.e.

$$\mathrm{tr}\, dD_{\mathrm{W}}^2 = \mathrm{tr}\, dZ_l^2 + \mathrm{tr}\, [U^{-1}dU, Z_l]_-^2. \tag{2.17}$$

The reason for this unconventional definition is the non-normalizability of the measure $d\mu_{\mathbb{G}_l}$ because $\mathbb{G}_l$ is non-compact for $l>0$. Hence the normalization resulting from definition (2.17) seems to be the most natural one, and it helps in keeping track of the normalizations.

In A.1 we solve the coset integrals (2.13). The first step is to linearize the quadratic terms in UZ_lU^{-1} by introducing auxiliary Gaussian integrals over additional matrices which is along the idea presented in Ref. [83]. In this way we split the integrand in a part invariant under $\mathrm{U}\,(n,n+\nu)$ and a non-invariant part resulting from an external source. The group integrals appearing in this calculations are reminiscent of the Itsykson-Zuber integral. However they are

over non-compact groups and thus, much more involved than in Ref. [83]. Because of the $\mathrm{U}(n) \times \mathrm{U}(n+\nu)$ invariance of the probability distribution of D_{W}, the joint eigenvalue distribution is a symmetric function of n eigenvalues which we label by "r" and $n+\nu$ eigenvalues labelled by "l". The γ_5-Hermiticity imposes reality constraints on the eigenvalues resulting in δ-functions in the joint probability distribution. Similarly to the usual Itzykson-Zuber integral, the symmetric function of the eigenvalues turns out to be particularly simple (see A.1)

$$p(Z)d[Z] = c(1+a^2)^{-n(n+\nu-1/2)}a^{-n-\nu^2}\exp\left[-\frac{a^4}{4(1+a^2)}(\mu_{\mathrm{r}}-\mu_{\mathrm{l}})^2\right] \tag{2.18}$$
$$\times\Delta_{2n+\nu}(Z)\det\begin{bmatrix} \left\{g_2(z_i^{(\mathrm{r})},z_j^{(\mathrm{l})})dx_i^{(\mathrm{r})}dy_i^{(\mathrm{r})}dx_j^{(\mathrm{l})}dy_j^{(\mathrm{l})}\right\}_{\substack{1\le i\le n\\ 1\le j\le n+\nu}} \\ \left\{\left(x_j^{(\mathrm{l})}\right)^{i-1}g_1(x_j^{(\mathrm{l})})\delta(y_j^{(\mathrm{l})})dx_j^{(\mathrm{l})}dy_j^{(\mathrm{l})}\right\}_{\substack{1\le i\le \nu\\ 1\le j\le n+\nu}} \end{bmatrix}.$$

The last ν rows become zero in the continuum limit resulting in ν exact zero modes (see subsection 2.2.3). At finite a they can be interpreted as broadened "zero modes". The functions in the determinant are given by

$$g_2(z_1,z_2) = g_r(x_1,x_2)\delta(y_1)\delta(y_2)+g_{\mathrm{c}}(z_1)\delta(x_1-x_2)\delta(y_1+y_2), \tag{2.19}$$
$$g_{\mathrm{r}}(x_1,x_2) = \exp\left[-\frac{n}{4a^2}\left(x_1+x_2-\frac{a^2(\mu_{\mathrm{r}}+\mu_{\mathrm{l}})}{n}\right)^2+\frac{n}{4}(x_1-x_2)^2\right] \tag{2.20}$$
$$\times\left[\mathrm{sign}\,(x_1-x_2)-\mathrm{erf}\left[\sqrt{\frac{n(1+a^2)}{4a^2}}(x_1-x_2)-\sqrt{\frac{a^2}{4n(1+a^2)}}(\mu_{\mathrm{r}}-\mu_{\mathrm{l}})\right]\right],$$
$$g_{\mathrm{c}}(z) = -2\imath\,\mathrm{sign}\,(y)\exp\left[-\frac{n}{a^2}\left(x-\frac{a^2(\mu_{\mathrm{r}}+\mu_{\mathrm{l}})}{2n}\right)^2-ny^2\right], \tag{2.21}$$
$$g_1(x) = \exp\left[-\frac{n}{2a^2}\left(x-\frac{a^2\mu_{\mathrm{l}}}{n}\right)^2\right]. \tag{2.22}$$

We employ the error function "erf" and the function "sign" which yields the sign of the argument. The constant is equal to

$$\frac{1}{c} = (-1)^{\nu(\nu-1)/2+n(n-1)/2}\left(\frac{16\pi}{n}\right)^{n/2}(2\pi)^{\nu/2}n^{-\nu^2/2-n(n+\nu)}\prod_{j=0}^{n}j!\prod_{j=0}^{n+\nu}j!, \tag{2.23}$$

and is essentially the volume of the group $\mathrm{U}(n)\times\mathrm{U}(n+\nu)\times\mathbf{S}(n)\times\mathbf{S}(n+\nu)$.

The two-point weight g_2 consists of two parts. The first term, g_r, represents a pair of real modes where one eigenvalue corresponds to a right-handed eigenvector and the other one to a left-handed one. The second term, g_c, enforces that a complex eigenvalue comes with its complex conjugate only. The function g_1 is purely Gaussian. As we will see in the next subsection, in the small a limit this will result in a distribution of the former zero modes that is broadened to the Gaussian Unitary Ensemble (GUE) [3–5, 64–66, 69, 70, 83].

For N_f dynamical quarks with quark mass m_f the joint probability distribution is simply given by [73]

$$p^{(N_\mathrm{f})}(z) = \prod_{f=1}^{N_\mathrm{f}} \prod_{k=1}^{2n+\nu} (z_k + m_f) p(Z). \tag{2.24}$$

The expansion in g_c yields the joint probability density for a fixed number of complex conjugate pairs,

$$\begin{aligned} p_l(Z_l)d[Z_l] = {} & \frac{(-1)^{(n-l)l} c (1+a^2)^{-n(n+\nu-1/2)} a^{-n-\nu^2} n!(n+\nu)!}{(n-l)!l!(n+\nu-l)!} \\ & \times \exp\left[-\frac{a^4}{4(1+a^2)}(\mu_\mathrm{r} - \mu_\mathrm{l})^2\right] \Delta_{2n+\nu}(Z) \\ & \times \det \begin{bmatrix} \{g_r(x_i^{(1)}, x_j^{(3)}) dx_i^{(1)} dx_j^{(3)}\}_{\substack{1\le i\le n-l \\ 1\le j\le n+\nu-l}} \\ \{(x_j^{(3)})^{i-1} g_1(x_j^{(3)}) dx_j^{(3)}\}_{\substack{1\le i\le \nu \\ 1\le j\le n+\nu-l}} \end{bmatrix} \prod_{j=1}^{l} g_c(z_j^{(2)}) dx_j^{(2)} dy_j^{(2)}. \end{aligned} \tag{2.25}$$

The factorials in the prefactor are the combinatorial factor which results from the expansion of the determinant in co-factors with l columns and l rows less. Note that they correspond to the coset of finite groups, $[\mathbf{S}(n)\times\mathbf{S}(n+\nu)]/[\mathbf{S}(n-l)\times\mathbf{S}(l)\times\mathbf{S}(n+\nu-l)]$, which naturally occurs when diagonalizing D_W in a fixed sector, see the discussion after Eq. (2.13).

2.2.3 The continuum limit

In this section, we take the continuum limit of the joint probability density p, i.e. $a \to 0$ at fixed z, μ_r and μ_l. In this limit the probability density (2.2) of D_W trivially becomes the one of chiral RMT which is equivalent to continuum QCD in the ϵ-regime [47]. We expect that this is also the case for the joint probability density.

The small a limit of the two point weight (2.18) is given by

$$g_2(z_1,z_2) \overset{a\ll 1}{=} -2\imath\,\mathrm{sign}\,(y_1)\sqrt{\frac{a^2\pi}{n}}\exp\left[-ny_1^2\right]\delta(x_1)\delta(x_2)\delta(y_1+y_2) \tag{2.26}$$

The function g_{r} vanishes due to the error function which cancels with the sign function. The expansion of the determinant (2.18) yields $(n+\nu)!/\nu!$ terms which are all the same. Thus, we have

$$\begin{aligned}\lim_{a\to 0} p(Z)d[Z] = c(-1)^{\nu(\nu-1)/2}\frac{(n+\nu)!}{\nu!}\left(-2\imath\sqrt{\frac{\pi}{n}}\right)^n \\ \times\lim_{a\to 0} a^{-\nu^2}\Delta_{2n+\nu}(\imath y,-\imath y,x)\Delta_\nu(x) \\ \times\prod_{j=1}^{n}\mathrm{sign}\,(y_j)\exp\left[-ny_j^2\right]dy_j\prod_{j=1}^{\nu}\exp\left[-\frac{n}{2a^2}x_j^2\right]dx_j.\end{aligned} \tag{2.27}$$

Thereby we have already evaluated the Dirac delta-functions. The real part of the complex eigenvalues $z_j^{(\mathrm{r}/\mathrm{l})}$, $1\le j\le n$, and $z_j^{(\mathrm{l})}$, $n+1\le j\le n+\nu$, vanishes and they become the variables $\pm\imath y_j$, $1\le j\le n$, and x_j, $1\le j\le\nu$, respectively. Note, that the random variables x scale with a while y is of order 1. Therefore the distribution of the two sets of eigenvalues factorizes into a product that can be identified as the joint probability density of a $\nu\times\nu$ dimensional GUE on the scale of a and the chiral Unitary Ensemble on the scale 1,

$$\begin{aligned}\lim_{a\to 0} p(Z)d[Z] &= \frac{1}{(2\pi)^{\nu/2}}\left(\frac{n}{a^2}\right)^{\nu^2/2}\prod_{j=0}^{\nu}\frac{1}{j!}\Delta_\nu^2(x)\prod_{j=1}^{\nu}\exp\left[-\frac{n}{2a^2}x_j^2\right]dx_j \\ &\times\frac{n^{n^2+\nu n}}{n!}\prod_{j=0}^{n-1}\frac{1}{(j+\nu)!j!}\Delta_n^2(y^2)\prod_{j=1}^{n}2\Theta(y_j)y_j^{2\nu+1}\exp\left[-ny_j^2\right]dy_j,\end{aligned} \tag{2.28}$$

where Θ is the Heaviside distribution.

2.3 From the joint probability density function to the level densities

The level density is obtained by integrating the joint probability density (2.18) over all eigenvalues of D_{W} except one. We can choose to exclude an eigenvalue of $z^{(\mathrm{r})}$ or one of the $z^{(\mathrm{l})}$'s. When we exclude $z_1^{(\mathrm{r})}$ we have to expand the

determinant (2.18) with respect to the first row. All resulting terms are the same and consist of a term for which $z_1^{(\mathrm{r})}$ is complex and a term for which $z_1^{(\mathrm{r})}$ is real. We thus have [3, 4]

$$\int p(Z) \prod_{z_j \neq z_1^{(\mathrm{r})}} d[z_j] \;=\; \rho_{\mathrm{r}}\,(x_1^{(\mathrm{r})})\delta(y_1^{(\mathrm{r})}) + \frac{1}{2}\rho_{\mathrm{c}}(z_1^{(\mathrm{r})}). \tag{2.29}$$

When excluding $z_1^{(\mathrm{l})}$ and expanding the determinant (2.18) with respect to the first column we notice that the first n terms are the same while the remaining ν terms have to be treated separately. Again the spectral density is the sum of the density of the real modes, which are left-handed in this case, and the density of the complex modes [3, 4]

$$\int p(Z) \prod_{z_j \neq z_1^{(\mathrm{l})}} d[z_j] \;=\; \rho_{\mathrm{l}}\,(x_1^{(\mathrm{l})})\delta(y_1^{(\mathrm{l})}) + \frac{1}{2}\rho_{\mathrm{c}}(z_1^{(\mathrm{l})}). \tag{2.30}$$

The level densities ρ_{r} and ρ_{l} are the densities of the real right- and left-handed modes, respectively. Interestingly the level density of the complex modes appears symmetrically in both equations. The reason is the vanishing chirality of eigenvectors corresponding to the complex eigenvalues.

Let us consider the case when excluding $z_1^{(\mathrm{r})}$. The Vandermonde determinant without a factor $(z_1^{(\mathrm{r})} - z_1^{(\mathrm{l})}) \prod_{k=2}^{n}(z_1^{(\mathrm{r})} - z_k)(z_1^{(\mathrm{l})} - z_k)$ and the cofactor from expanding the first row of the determinant can be identified as the joint probability distribution with one pair $(z^{(\mathrm{r})}, z^{(\mathrm{l})})$ less. The $z_1^{(\mathrm{l})}$-integral over this distribution together with the factor $\prod_{k=2}^{n}(z_1^{(\mathrm{r})} - z_k)(z_1^{(\mathrm{l})} - z_k)$ can be identified as the partition function with two additional flavors. We thus find

$$\rho_{\mathrm{r}}\,(x) \;\propto\; \int_{-\infty}^{\infty} g_{\mathrm{r}}(x,x')(x-x')Z_{N_f+2}^{n-1,\nu}(x,x',m_k)dx', \tag{2.31}$$

$$\rho_{\mathrm{c}}(z) \;\propto\; g_{\mathrm{c}}(z)(z-z^*)Z_{N_f+2}^{n-1,\nu}(z,z^*,m_k). \tag{2.32}$$

The fermionic partition function is given by

$$\begin{aligned} Z_{N_f+2}^{n-1,\nu}(z_1,z_2,m_k) \;=\; & \int \det(D_{\mathrm{W}} - z_1 \mathbb{1}_{n-1}) \det(D_{\mathrm{W}} - z_2 \mathbb{1}_{n-1}) \\ & \times \prod_{k=1}^{N_{\mathrm{f}}} (D_{\mathrm{W}} + m_k \mathbb{1}_{n-1}) P(D_{\mathrm{W}}) d[D_{\mathrm{W}}]. \end{aligned} \tag{2.33}$$

In the microscopic limit this is simply a unitary matrix integral which can be easily evaluated numerically. Note that the integral over the variables $\mu_{\mathrm{r}\,/\mathrm{l}}$ which introduces the low energy constants $W_{6/7}$ can already be performed at this step.

Considering the exclusion of $z_{1\mathrm{l}}$ we have to expand the determinant in the joint probability density with respect to the first column resulting in a much more complicated expression

$$\begin{aligned}\rho_{\mathrm{l}}(z) &\sim n\int\limits_{\mathbb{C}} d[\widetilde{z}](z-\widetilde{z})g_2(z,z_{\mathrm{tr}})Z^{n-1,\nu}_{N_f=2}(z,\widetilde{z})+\alpha\delta(y)\sum_{p=1}^{\nu}(-1)^{\nu-p}\\ &\times\left(\begin{array}{c} n+\nu-1 \\ \nu-p \end{array}\right)x^{p-1}g_1(x)\int\limits_{\mathbb{R}^{\nu-p}}\prod_{j=1}^{\nu-p}dx_j x_j^p g_1(x_j)\Delta_{\nu-p}(x_1,\cdots,x_{\nu-p})\\ &\times\Delta_{\nu-p+1}(x,x_1,\cdots,x_{\nu-p})Z^{n,p}_{N_f=\nu-p+1}(x,x_1,\cdots,x_{\nu-p}) \qquad (2.34)\end{aligned}$$

with a certain constant α which we will specify in the microscopic limit. Again $g_2(z,z_{\mathrm{r}})$ is the sum of a term comprising the distribution of the complex eigenvalue density and a term giving the real eigenvalue density. For the complex eigenvalue density we find the same expression as obtained by integration over $z_{1\mathrm{l}}$.

For $\nu=1$, the density of the real eigenvalues simplifies to

$$\rho_{\mathrm{l}}(x)|_{\nu=1}\sim n\int\limits_{-\infty}^{\infty}dx_{\mathrm{r}}\,(x_{\mathrm{r}}-x)g_r(x_{\mathrm{r}},x)Z^{n-1,\nu}_{N_f=2}(x_{\mathrm{r}},x)+\alpha g_1(x)Z^{n,0}_{N_f=1}(x). \qquad (2.35)$$

The distribution of chirality over the real modes is the difference

$$\rho_\chi(x) = \rho_{\mathrm{l}}(x)-\rho_{\mathrm{r}}(x), \qquad (2.36)$$

resulting in

$$\rho_\chi|_{\nu=1}\sim\alpha g_1(x)Z^{n,0}_{N_f=1}(x)+n\int\limits_{-\infty}^{\infty}dx'(x'-x)(g_r(x',x)+g_r(x,x'))Z^{n-1,1}_{N_f=2}(x',x), \qquad (2.37)$$

where we used that the $N_f=0$ partition function is symmetric in x and x'. For $\mu_r=\mu_l$, the last two terms cancel resulting in a very simple expression for $\rho_\chi(x)$. Notice that the integral over the second term vanishes such that it does not contribute to the normalization of the distribution of chirality over

the real modes

$$\int dx \rho_\chi(x) = \nu. \tag{2.38}$$

For $\nu = 2$ we find

$$\begin{aligned}\rho_\chi(x)|_{\nu=2} \quad \sim \quad & \alpha x g_1(x) Z^{n,1}_{N_f=1}(x) - \alpha(n+1) g_1(x) \int_{-\infty}^{\infty} dx' x'(x-x') g_1(x') Z^{n,0}_{N_f=2}(x,x') \\ & + n \int_{-\infty}^{\infty} dx'(x'-x)(g_r(x',x) + g_r(x,x')) Z^{n-1,2}_{N_f=2}(x',x). \end{aligned} \tag{2.39}$$

In the microscopic limit the two flavor partition functions can be replaced by a unitary matrix integral which still can be easily evaluated numerically including the integrals over $\widehat{m}_6$ and $\widehat{\lambda}_7$.

For large values of ν the expression of the distribution of chirality over the real modes obtained from expanding the determinant gets increasingly complicated. However, there is an alternative expression in terms of a supersymmetric partition function [3, 4, 102],

$$\rho_\chi(x) \quad \propto \quad \lim_{\varepsilon \to 0} \mathrm{Im} \left. \frac{\partial}{\partial J} \right|_{J=0} \int \frac{\det(D_{\mathrm{W}} - (x+J)\mathbb{1})}{\det(D_{\mathrm{W}} - x\mathbb{1} - \imath\varepsilon\gamma_5)} P(D_{\mathrm{W}}) d[D_{\mathrm{W}}]. \tag{2.40}$$

In the ensuing sections we will use this expression to calculate the microscopic limit of the distribution of chirality over the real modes.

2.3.1 Microscopic Limit of the Eigenvalue Densities

The goal of this chapter is to derive and analyze the microscopic limit of ρ_{r}, ρ_χ, and ρ_{c} including those terms involving non-zero values of W_6 and W_7 in the chiral Lagrangian. We only give results for the quenched case. It is straightforward to include dynamical quarks but this will be worked out in a forthcoming publication. The result for the distribution of chirality over the real modes with dynamical quarks for $W_6 = W_7 = 0$ was already given in [102], and an explicit expression for the distribution of the complex eigenvalues in the presence of dynamical quarks and non-zero values W_6, W_7 and W_8 was derived in [73].

The microscopic limit of the spectral densities is obtained from the microscopic limit of the partition functions and the functions appearing in the joint probability distribution. The microscopic parameters that are kept fixed for

$V \to \infty$, are defined by

$$\begin{aligned} \widehat{a}_6^2 &= -\widetilde{a}^2 V W_6, \qquad \widehat{a}_7^2 = -\widetilde{a}^2 V W_7, \qquad \widehat{a}_8^2 = na^2/2 = \widetilde{a}^2 V W_8, \quad (2.41) \\ \widehat{m}_6 &= a^2(\mu_r + \mu_l), \qquad \widehat{\lambda}_7 = a^2(\mu_r - \mu_l), \qquad \widehat{x} = 2nx. \quad (2.42) \end{aligned}$$

The microscopic limit of the probability distribution of $\widehat{m}_6$ and $\widehat{\lambda}_7$ is given by

$$p(\widehat{m}_6, \widehat{\lambda}_7) = \frac{1}{16\pi \widehat{a}_6 \widehat{a}_7} \exp\left[-\frac{\widehat{m}_6^2}{16\widehat{a}_6^2} - \frac{\widehat{\lambda}_7^2}{16\widehat{a}_7^2} \right], \quad (2.43)$$

and the functions that appear in the joint probability distribution simplify to

$$\begin{aligned} \widehat{g}_{\rm r}(\widehat{x}, \widehat{x}', \widehat{m}_6, \widehat{\lambda}_7) &= \exp\left[-\frac{(\widehat{x} + \widehat{x}' - 2\widehat{m}_6)^2}{32\widehat{a}_8^2} \right] \\ &\quad \times \left[\mathrm{sign}\,(\widehat{x} - \widehat{x}') - \mathrm{erf}\left[\frac{(\widehat{x} - \widehat{x}')/2 - \widehat{\lambda}_7}{\sqrt{8\widehat{a}_8}} \right] \right], \quad (2.44) \\ \widehat{g}_{\rm c}(\widehat{z}) &= -2\imath\, \mathrm{sign}\,(\widehat{y}) \exp\left[-\frac{(\widehat{x} - \widehat{m}_6)^2}{8\widehat{a}_8^2} \right], \quad (2.45) \\ \widehat{g}_1(\widehat{x}) &= \exp\left[-\frac{(\widehat{x} - \widehat{m}_6 + \widehat{\lambda}_7)^2}{16\widehat{a}_8^2} \right]. \quad (2.46) \end{aligned}$$

The microscopic limit of the spectral densities obtained in Eqs. (2.31), (2.32) and (2.40) is given by

$$\begin{aligned} \rho_{\rm r}(\widehat{x}) &= \frac{1}{32\sqrt{2\pi}\widehat{a}_8} \int_{\mathbb{R}^3} d\widehat{m}_6 d\widehat{\lambda}_7 d\widehat{x}' p(\widehat{m}_6, \widehat{\lambda}_7)(\widehat{x} - \widehat{x}') \widehat{g}_{\rm r}(\widehat{x}, \widehat{x}', \widehat{m}_6, \widehat{\lambda}_7) \\ &\quad \times Z_{2/0}^{\nu}(\widehat{x} + \widehat{m}_6, \widehat{x}' + \widehat{m}_6, \widehat{\lambda}_7, \widehat{a}_8), \quad (2.47) \\ \rho_{\rm c}(\widehat{z}) &= \frac{\imath\widehat{y}}{32\sqrt{2\pi}\widehat{a}_8} \int_{\mathbb{R}^2} d\widehat{m}_6 d\widehat{\lambda}_7 p(\widehat{m}_6, \widehat{\lambda}_7) \widehat{g}_c(\widehat{z}, \widehat{z}^*, \widehat{m}_6) \\ &\quad \times Z_{2/0}^{\nu}(\widehat{z} + \widehat{m}_6, \widehat{z}^* + \widehat{m}_6, \widehat{\lambda}_7, \widehat{a}_8), \quad (2.48) \\ \rho_{\chi}(\widehat{x}) &= \frac{1}{\pi} \lim_{\varepsilon \to 0} \mathrm{Im} \int d\widehat{m}_6 d\widehat{\lambda}_7 p(\widehat{m}_6, \widehat{\lambda}_7) G_{1/1}(\widehat{x} + \widehat{m}_6, \widehat{\lambda}_7 + \imath\varepsilon, \widehat{a}_8). \quad (2.49) \end{aligned}$$

The resolvent $G_{1/1}$ follows from the graded partition function

$$\begin{aligned} G_{1/1}(\widehat{x}+\widehat{m}_6,\widehat{\lambda}_7+\imath\varepsilon,\widehat{a}_8) &= \frac{d}{d\widehat{x}'}Z^{\nu}_{1/1}(\widehat{x}+\widehat{m}_6,\widehat{x}'+\widehat{m}_6,\widehat{\lambda}_7+\imath\varepsilon,\widehat{a}_8)\Big|_{\widehat{x}'=\widehat{x}} \\ &= \lim_{n\to\infty}\frac{1}{2n}\int \mathrm{tr}\,\frac{1}{D_{\mathrm{W}}-2n\widehat{x}\mathbb{1}_{2n+\nu}-\imath\varepsilon\gamma_5}P(D_{\mathrm{W}})d[D_{\mathrm{W}}]. \end{aligned} \tag{2.50}$$

The microscopic limit of the two flavor partition function follows from the chiral Lagrangian. In the diagonal representation of the unitary 2×2 matrix, it can be simplified by means of an Itzykson-Zuber integral and is given by

$$\begin{aligned} Z^{\nu}_{2/0}(\widehat{z}_1,\widehat{z}_2,\widehat{\lambda}_7,\widehat{a}_8) &= \frac{1}{2\pi^2}\int d\varphi_1 d\varphi_2 \sin^2((\varphi_1-\varphi_2)/2)e^{\imath\nu(\varphi_1+\varphi_2)} \\ &\quad\times\exp\left[\imath\widehat{\lambda}_7(\sin\varphi_1+\sin\varphi_2)-4\widehat{a}_8^2(\cos^2\varphi_1+\cos^2\varphi_2)\right] \\ &\quad\times\frac{\exp\left[\widehat{z}_1\cos\varphi_1+\widehat{z}_2\cos\varphi_2\right]-\exp\left[\widehat{z}_2\cos\varphi_1+\widehat{z}_1\cos\varphi_2\right]}{(\cos\varphi_1-\cos\varphi_2)(\widehat{z}_1-\widehat{z}_2)}. \end{aligned} \tag{2.51}$$

The normalization is chosen such that we find

$$Z^{\nu}_{2/0}(\widehat{z}_1,\widehat{z}_2,\widehat{\lambda}_7=0,\widehat{a}_8=0) = \frac{\widehat{z}_1 I_{\nu+1}(\widehat{z}_1)I_{\nu}(\widehat{z}_2)-\widehat{z}_2 I_{\nu+1}(\widehat{z}_2)I_{\nu}(\widehat{z}_1)}{\widehat{z}_1^2-\widehat{z}_2^2} \tag{2.52}$$

the well known result [103] at vanishing lattice spacing, where I_ν is the modified Bessel function of the first kind.

The microscopic limit of the graded partition function follows from the chiral Lagrangian [68] which can be written as an integral over a $(1/1)\times(1/1)$ supermatrix [102]

$$U=\begin{bmatrix} e^{\vartheta} & \eta^* \\ \eta & e^{\imath\varphi}\end{bmatrix},\ \vartheta\in\mathbb{R},\ \varphi\in[0,2\pi], \tag{2.53}$$

with η and η^* two independent Grassmann variables. Let the normalization of the integration over the Grassmann variables be

$$\int \eta^*\eta d\eta d\eta^* = \frac{1}{2\pi}. \tag{2.54}$$

Then the graded partition function is

$$Z^{\nu}_{1/1}(\widehat{z}_1,\widehat{z}_2,\widehat{\lambda}_7\pm\imath\varepsilon,\widehat{a}_8)=\int\frac{\imath de^{\imath\varphi}}{2\pi}de^{\vartheta}d\eta d\eta^{*}\mathrm{Sdet}^{\nu}U\exp[-\widehat{a}_8^2\mathrm{Str}\,(U^2+U^{-2})] \tag{2.55}$$
$$\times\exp\left[\pm\frac{\imath}{2}\mathrm{Str}\,\widehat{Z}(U-U^{-1})-\left(\varepsilon\pm\frac{\imath\widehat{\lambda}_7}{2}\right)\mathrm{Str}\,(U+U^{-1})\right],$$

where $\widehat{Z}=\mathrm{diag}(\widehat{z}_1,\widehat{z}_2)$ with the normalization adjusted by the continuum limit

$$Z^{\nu}_{1/1}(\widehat{z}_1,\widehat{z}_2,\widehat{\lambda}_7=0,\widehat{a}_8=0)=\widehat{z}_1K_{\nu+1}(\widehat{z}_1)I_{\nu}(\widehat{z}_2)-\widehat{z}_2I_{\nu+1}(\widehat{z}_2)K_{\nu}(\widehat{z}_1). \tag{2.56}$$

The function K_ν is the modified Bessel function of the second kind.

There are various ways to calculate this integral. One possibility is a brute force evaluation of the Grassmann integrals as in [68, 101]. Then the Gaussian integrals over $\widehat{m}_6$ and $\widehat{\lambda}_7$ can be performed analytically leaving us with a non-singular two-dimensional integral. A second possibility would be to rewrite the integrals as in [102]. Then we end up with a two dimensional singular integral (see C.1) which can be evaluated numerically with some effort. The third way to evaluate the integral, is a variation of the method in [102] and results in a one dimensional integral and a sum over Bessel functions that can be easily numerically evaluated (see section 2.4.3).

2.4 The eigenvalue densities and their properties

To illustrate the effect of non-zero $\widehat{a}_6$ and $\widehat{a}_7$ we first discuss the case $\widehat{a}_8=0$. For the general case, with $\widehat{a}_8$ also non-zero, we will discuss the distribution of the additional real eigenvalues, the distribution of the complex eigenvalues, and finally the distribution of chirality over the real eigenvalues of D_W.

2.4.1 Spectrum of D_W for $\widehat{a}_8=0$

.

The low-energy constants $\widehat{a}_6$ and $\widehat{a}_7$ are introduced through the addition of the Gaussian stochastic variable $\widehat{m}_6+\widehat{\lambda}_7\gamma_5$ to D_{W} resulting in the Dirac operator

$$D=D_{\mathrm{W}}+(m+\widehat{m}_6)\mathbb{1}+\widehat{\lambda}_7\gamma_5. \tag{2.57}$$

For $\widehat{a}_8=0$ the Dirac operator D_{W} is anti-Hermitian, and the eigenvalues of

$D_{\rm W}\,(\widehat{\lambda}_7, \widehat{m}_6) = D - m$ are given by

$$\widehat{z}_\pm = \widehat{m}_6 \pm \imath\sqrt{\lambda_{\rm W}^2 - \widehat{\lambda}_7^2}, \tag{2.58}$$

where $\imath\lambda_{\rm W}$ is an eigenvalue of $D_{\rm W}$. The distribution of the eigenvalues of D is obtained after integrating over the Gaussian distribution of $\widehat{m}_6$ and $\widehat{\lambda}_7$.

As can be seen from Eq. (2.58), in case $\widehat{a}_6 = \widehat{a}_8 = 0$ and $\widehat{a}_7 \neq 0$, the eigenvalues of D are either purely imaginary or purely real depending on whether $\widehat{\lambda}_7$ is smaller or larger than λ_W, respectively. Paired imaginary eigenvalues penetrate the real axis only through the origin when varying $\widehat{\lambda}_7$. Introducing a non-zero W_6, broadens the spectrum by a Gaussian parallel to the real axis but since $\widehat{m}_6$ is just an additive constant to the eigenvalues nothing crucial happens.

In the continuum the low lying spectral density of the quenched Dirac operator is given by [47]

$$\begin{aligned} \rho_{\rm cont.}(\widehat{z}) &= \delta(\widehat{x})\left[\nu\delta(\widehat{y}) + \frac{|\widehat{y}|}{2}(J_\nu^2(\widehat{y}) - J_{\nu-1}(\widehat{y})J_{\nu+1}(\widehat{y}))\right] \\ &= \delta(\widehat{x})\left[\nu\delta(\widehat{y}) + \rho_{\rm NZ}(\widehat{y})\right]. \end{aligned} \tag{2.59}$$

The function J_ν is the Bessel function of the first kind. The level density $\rho_{\rm NZ}$ describes the distribution of the generic non-zero eigenvalues, only.

For non-zero $W_{6/7}$ the distribution of the zero modes represented by the Dirac delta-functions in Eq. (2.59) is broadened by a Gaussian, i.e.

$$\rho_\chi(\widehat{z}, \widehat{a}_8 = 0) = \frac{\nu}{\sqrt{16\pi(\widehat{a}_6^2 + \widehat{a}_7^2)}} \exp\left[-\frac{\widehat{x}^2}{16(\widehat{a}_6^2 + \widehat{a}_7^2)}\right]. \tag{2.60}$$

Complex modes have vanishing chirality and do not contribute to the distribution of chirality over the real modes. Additional pairs of real modes also do not contribute to ρ_χ. The reason is the symmetric integration of $\widehat{\lambda}_7$ over the real axis. The eigenvalues remain the same under the change $\widehat{\lambda}_7 \to -\widehat{\lambda}_7$, see Eq. (2.58). However the corresponding eigenvectors interchange the sign of the chirality which can be seen by the symmetry relation

$$D_{\rm W}\,(\widehat{\lambda}_7, \widehat{m}_6) = -\gamma_5 D_{\rm W}\,(-\widehat{\lambda}_7, -\widehat{m}_6)\gamma_5. \tag{2.61}$$

Thus the normalized eigenfunctions ($\langle\psi_\pm|\psi_\pm\rangle = 1$) corresponding to the eigenvalues $\widehat{z}_\pm$, i.e.

$$D_{\rm W}\,(\widehat{\lambda}_7, \widehat{m}_6)|\psi_\pm\rangle = \widehat{z}_\pm|\psi_\pm\rangle, \tag{2.62}$$

also fulfills the identity

$$D_{\rm W}\,(-\widehat{\lambda}_7,-\widehat{m}_6)\gamma_5|\psi_\pm\rangle = -\widehat{z}_\pm\gamma_5|\psi_\pm\rangle. \tag{2.63}$$

Since the quark mass $\widehat{m}_6$ enters with unity we have also

$$D_{\rm W}\,(-\widehat{\lambda}_7,\widehat{m}_6)\gamma_5|\psi_\pm\rangle = \widehat{z}_\mp\gamma_5|\psi_\pm\rangle. \tag{2.64}$$

The wavefunctions $\gamma_5|\psi_\pm\rangle$ shares the same chirality with $|\psi_\pm\rangle$. Moreover $|\psi_+\rangle$ and $|\psi_-\rangle$ have opposite chirality because the pair of eigenvalues $\widehat{z}_\pm$ is assumed to be real and their difference $|\widehat{z}_+ - \widehat{z}_-|$ non-zero. This can be seen by the eigenvalue equations

$$\begin{aligned} D_{\rm W}\,(\widehat{\lambda}_7,\widehat{m}_6=0)|\psi_\pm\rangle &= \pm\sqrt{\widehat{\lambda}_7^2-\lambda_{\rm W}^2}\,|\psi_\pm\rangle, \\ \langle\psi_\pm|D_{\rm W}\,(-\widehat{\lambda}_7,\widehat{m}_6=0) &= \langle\gamma_5 D_{\rm W}\,(-\widehat{\lambda}_7,\widehat{m}_6=0)\gamma_5\psi_\pm| = \mp\sqrt{\widehat{\lambda}_7^2-\lambda_{\rm W}^2}\,\langle\psi_\pm|. \end{aligned} \tag{2.65}$$

In the second equation we used the γ_5-Hermiticity of $D_{\rm W}$. We multiply the first equation with $\langle\psi_\pm|$ and the second with $|\psi_\pm\rangle$ and employ the normalization of the eigenmodes such that we find

$$\begin{aligned} \langle\psi_\pm|D_{\rm W}\,(\widehat{\lambda}_7,\widehat{m}_6=0)|\psi_\pm\rangle &= \pm\sqrt{\widehat{\lambda}_7^2-\lambda_{\rm W}^2}\,, \\ \langle\psi_\pm|D_{\rm W}\,(-\widehat{\lambda}_7,\widehat{m}_6=0)|\psi_\pm\rangle &= \mp\sqrt{\widehat{\lambda}_7^2-\lambda_{\rm W}^2}\,. \end{aligned} \tag{2.66}$$

We subtract the second line from the first and use the identity $D_{\rm W}\,(\widehat{\lambda}_7,\widehat{m}_6 = 0) - D_{\rm W}\,(-\widehat{\lambda}_7,\widehat{m}_6=0) = 2\widehat{\lambda}_7\gamma_5$, i.e.

$$\widehat{\lambda}_7\langle\psi_\pm|\gamma_5|\psi_\pm\rangle = \pm\sqrt{\widehat{\lambda}_7^2-\lambda_{\rm W}^2}\,, \tag{2.67}$$

which indeed shows the opposite chirality of $|\psi_+\rangle$ and $|\psi_-\rangle$. Thus $|\psi_+\rangle$ and $\gamma_5|\psi_-\rangle$ have opposite sign of chirality but their corresponding eigenvalues are the same. Therefore the average of their chiralities at a specific eigenvalue vanishes.

The distribution of the complex eigenvalues can be obtained by integrating over those $\lambda_{\rm W}$ fulfilling the condition $|\lambda_{\rm W}| > |\widehat{\lambda}_7|$. After averaging over $\widehat{m}_6$

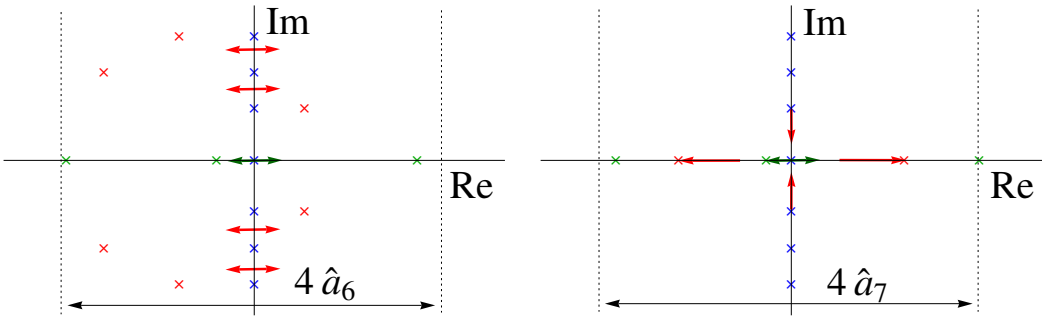

Figure 2.1: Schematic plots of the effects of W_6 (left plot) and of W_7 (right plot). The low energy constant W_6 broadens the spectrum parallel to the real axis according to a Gaussian with width $4\widehat{a}_6 = 4\sqrt{-VW_6\tilde{a}^2}$, but does not change the continuum spectrum in a significant way. When W_7 is switched on and $W_6 = 0$ the purely imaginary eigenvalues invade the real axis through the origin and only the real (green crosses) are broadened by a Gaussian with width $4\widehat{a}_7 = 4\sqrt{-VW_7\widetilde{a}^2}$.

and $\widehat{\lambda}_7$ we find

$$\begin{aligned}\rho_{\rm c}(\widehat{z}=\widehat{x}+i\widehat{y},\widehat{a}_8=0) &= \frac{\exp\left[-\widehat{x}^2/(16\widehat{a}_6^2)\right]}{16\pi|\widehat{a}_6\widehat{a}_7|}\int\limits_{\mathbb{R}^2}\rho_{\rm NZ}(\lambda_{\rm W})\exp\left[-\frac{\widehat{\lambda}_7^2}{16\widehat{a}_7^2}\right] \\ &\quad\times\delta\left(\sqrt{\lambda_{\rm W}^2-\widehat{\lambda}_7^2}-|\widehat{y}|\right)\Theta(|\lambda_{\rm W}|-|\widehat{\lambda}_7|)d\lambda_{\rm W}\,d\widehat{\lambda}_7 \\ &= \frac{\exp\left[-\widehat{x}^2/(16\widehat{a}_6^2)\right]}{4\pi|\widehat{a}_6\widehat{a}_7|}\int\limits_{|\widehat{y}|}^{\infty}\frac{|\widehat{y}|\rho_{\rm NZ}(\lambda_{\rm W})d\lambda_{\rm W}}{\sqrt{\lambda_{\rm W}^2-\widehat{y}^2}}\exp\left[\frac{\lambda_{\rm W}^2-\widehat{y}^2}{16\widehat{a}_7^2}\right].\end{aligned} \tag{2.68}$$

The original continuum result is smoothed by a distribution with a Gaussian tail. The oscillations in the microscopic spectral density dampen due to a non-zero W_7 similar to the effect of a non-zero value W_8, cf. Ref. [3, 4]. We also expect a loss of the height of the first eigenvalue distributions around the origin. Pairs of eigenvalues are moving from the imaginary axis to the real axis and thus lowering their probability density on the imaginary axis. The distribution $\rho_{\rm c}$ for non-zero $\widehat{a}_8$ will be discussed in full detail in Sec. 2.4.2.

The distribution of the additional real modes can be obtained by integrating the continuum distribution, $\rho_{\rm NZ}$ over $|\lambda_{\rm W}| < |\lambda_7|$ analogous to the complex

case. We find

$$\rho_{\mathrm{r}}(\widehat{x}, W_8 = 0) = \frac{1}{16\pi|\widehat{a}_6\widehat{a}_7|}\int\limits_{\mathbb{R}^3} \rho_{\mathrm{NZ}}(\lambda_{\mathrm{W}})\exp\left[-\frac{\widehat{m}_6^2}{16\widehat{a}_6^2} - \frac{\widehat{\lambda}_7^2}{16\widehat{a}_7^2}\right] \tag{2.69}$$
$$\times\delta\left(\sqrt{\widehat{\lambda}_7^2 - \lambda_{\mathrm{W}}^2} - |\widehat{m}_6 - \widehat{x}|\right)\Theta(|\widehat{\lambda}_7| - |\lambda_{\mathrm{W}}|)d\lambda_{\mathrm{W}}\, d\widehat{\lambda}_7 d\widehat{m}_6$$
$$= \int\limits_{\mathbb{R}^2} \frac{|\widehat{m}_6| d\widehat{m}_6 d\lambda_{\mathrm{W}}}{8\pi|\widehat{a}_6\widehat{a}_7|\sqrt{\lambda_{\mathrm{W}}^2 + \widehat{m}_6^2}}\rho_{\mathrm{NZ}}(\lambda_{\mathrm{W}})\exp\left[-\frac{\lambda_{\mathrm{W}}^2 + \widehat{m}_6^2}{16\widehat{a}_7^2} - \frac{(\widehat{m}_6 + \widehat{x})^2}{16\widehat{a}_6^2}\right].$$

The number of additional real modes given by the integral of $\rho_{\mathrm{r}}(\widehat{x})$ over $\widehat{x}$ only depends on $\widehat{a}_7$, as it should be since $\widehat{m}_6$ is just an additive constant to the eigenvalues. Moreover ρ_{r} will inherit the oscillatory behavior of ρ_{NZ} although most of it will be damped by the Gaussian cut-off. The mixture of this effect with the effect of a non-zero W_8 is highly non-trivial, but we expect that, at small lattice spacings, we can separate both contributions. For a sufficiently small value of $\widehat{a}_6$ the behavior of $\rho_{\mathrm{r}}(\widehat{x})$ for $\widehat{x} \to 0$ is given by $\rho_{\mathrm{r}}(\widehat{x}) = \widetilde{c}|x| + \ldots$ with $\widetilde{c} > 0$ for vanishing W_8 and thus, $\rho_{\mathrm{r}}(\widehat{x}) = c_0 + c_1\widehat{x}^2 + \ldots$ with $c_0, c_1 > 0$ for non-zero W_8. Hence, we will see a soft repulsion of the additional real eigenvalues from the origin which still allows real eigenvalues to be zero.

The discussion of the real modes for non-zero $\widehat{a}_8$ as well is given in Sec. 2.4.2.

2.4.2 Eigenvalue distributions for non-zero values of W_6, W_7 and W_8

In this subsection all three low-energy constants are non-zero. As in the previous subsection, we will consider the distribution of the real eigenvalues of D_{W}, the distribution of the complex eigenvalues of D_{W}, and the distribution of the chiralities over the real eigenvalues of D_{W}. The expressions for these distributions were already given in section 2.3, but in this section we further simplify them and calculate the asymptotic expressions for large and small values of $\widehat{a}$.

Distribution of the additional real modes

The quenched eigenvalue density of the right handed modes is given by Eq. (2.47). The Gaussian average over the variables $\widehat{m}_6$ and $\widehat{\lambda}_7$ can be worked out analytically. The result is given by (see B.1 for integrals that were used to obtain

this result)

$$\rho_{\mathrm{r}}(\widehat{x}) = \frac{1}{16\pi^2} \int\limits_{[0,2\pi]^2} d\varphi_1 d\varphi_2 \sin^2\left[\frac{\varphi_1-\varphi_2}{2}\right] e^{\imath\nu(\varphi_1+\varphi_2)} \frac{\widetilde{k}(\widehat{x},\varphi_1,\varphi_2)-\widetilde{k}(\widehat{x},\varphi_2,\varphi_1)}{\cos\varphi_2-\cos\varphi_1} \tag{2.70}$$

with

$$\begin{aligned}\widetilde{k}(\widehat{x},\varphi_1,\varphi_2) &= \exp\left[4\widehat{a}_6^2(\cos\varphi_1-\cos\varphi_2)^2 - 4\widehat{a}_7^2(\sin\varphi_1+\sin\varphi_2)^2\right] \\ &\times \exp\left[4\widehat{a}_8^2\left(\cos\varphi_1-\frac{\widehat{x}}{8\widehat{a}_8^2}\right)^2 - 4\widehat{a}_8^2\left(\cos\varphi_2-\frac{\widehat{x}}{8\widehat{a}_8^2}\right)^2\right] \\ &\times\left[\mathrm{erf}\left[\frac{\widehat{x}-8(\widehat{a}_6^2+\widehat{a}_8^2)\cos\varphi_1+8\widehat{a}_6^2\cos\varphi_2}{\sqrt{8(\widehat{a}_8^2+2\widehat{a}_6^2)}}\right]\right. \\ &\left.+\,\mathrm{erf}\left[\frac{8(\widehat{a}_6^2+\widehat{a}_8^2)\cos\varphi_1-8\widehat{a}_6^2\cos\varphi_2-8\imath\widehat{a}_7^2\sin\varphi_1-8\imath\widehat{a}_7^2\sin\varphi_2-\widehat{x}}{\sqrt{16(\widehat{a}_8^2+\widehat{a}_6^2+\widehat{a}_7^2)}}\right]\right].\end{aligned} \tag{2.71}$$

The effect of each low energy constant on ρ_{r} is shown in Fig. 2.2.

At small lattice spacing, $\widehat{a} \ll 1$, the distribution ρ_{r} has support on the scale of $\widehat{a}$. In particular it is given by derivatives of a specific function, i.e.

$$\begin{aligned}\rho_{\mathrm{r}}(\widehat{x}) &\overset{\widehat{a}\ll 1}{=} \frac{1}{4}\left(\frac{1}{(\nu!)^2}\frac{\partial^{2\nu}}{\partial t_1^\nu \partial t_2^\nu} - \frac{1}{(\nu-1)!(\nu+1)!}\frac{\partial^{2\nu}}{\partial t_1^{\nu-1}\partial t_2^{\nu+1}}\right)\Bigg|_{t_1=t_2=0} \\ &\times\frac{\widehat{k}(\widehat{x},t_1,t_2)-\widehat{k}(\widehat{x},t_2,t_1)}{t_2-t_1},\end{aligned} \tag{2.72}$$

where

$$\begin{aligned}\widehat{k}(\widehat{x},t_1,t_2) = &\exp\left[\widehat{a}_6^2(t_1-t_2)^2+\widehat{a}_7^2(t_1+t_2)^2+\widehat{a}_8^2\left(t_1-\frac{\widehat{x}}{4\widehat{a}_8^2}\right)^2-\widehat{a}_8^2\left(t_2-\frac{\widehat{x}}{4\widehat{a}_8^2}\right)^2\right] \\ \times&\left[\mathrm{erf}\left[\frac{\widehat{x}-4(\widehat{a}_6^2+\widehat{a}_8^2)t_1+4\widehat{a}_6^2 t_2}{\sqrt{8(\widehat{a}_8^2+2\widehat{a}_6^2)}}\right]+\mathrm{erf}\left[\frac{4(\widehat{a}_6^2+\widehat{a}_7^2+\widehat{a}_8^2)t_1-4(\widehat{a}_6^2-\widehat{a}_7^2)t_2-\widehat{x}}{\sqrt{16(\widehat{a}_8^2+\widehat{a}_6^2+\widehat{a}_7^2)}}\right]\right].\end{aligned} \tag{2.73}$$

The error functions guarantee a Gaussian tail on the scale of $\widehat{a}$. Furthermore, the height of the distribution is of order $\widehat{a}^{2\nu+1}$. Hence, additional real modes are strongly suppressed for $\nu > 0$ and the important contributions only result from $\nu = 0$. This behavior becomes clearer for the expression of the average

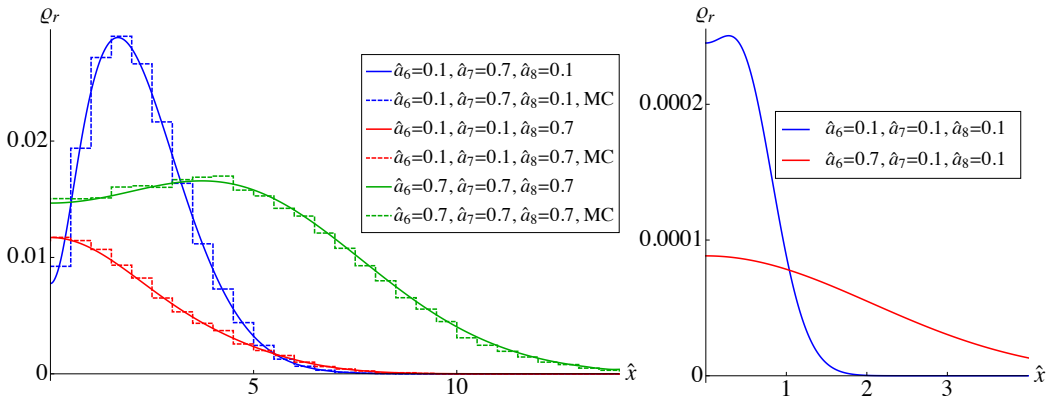

Figure 2.2: The distribution of additional real modes is shown for various parameters $\widehat{a}_{6/7/8}$. The analytical results (solid curves) agree with the Monte Carlo simulations of the Random Matrix Theory (histogram [MC] with bin size 0.5 and with different ensemble and matrix sizes) for $\nu = 1$. We plot only the positive real axis since ρ_{r} is symmetric. Notice that the two curves for $\widehat{a}_7 = \widehat{a}_8 = 0.1$ (right plot) are two orders smaller than the other curves (left plot) and because of bad statistics we have not performed simulations for this case. Notice the soft repulsion of the additional real modes from the origin at large $\widehat{a}_7 = \sqrt{-VW_7}\widetilde{a}$ as discussed in the introductory section. The parameter $\widehat{a}_6 = \sqrt{-VW_6}\widetilde{a}$ smoothes the distribution.

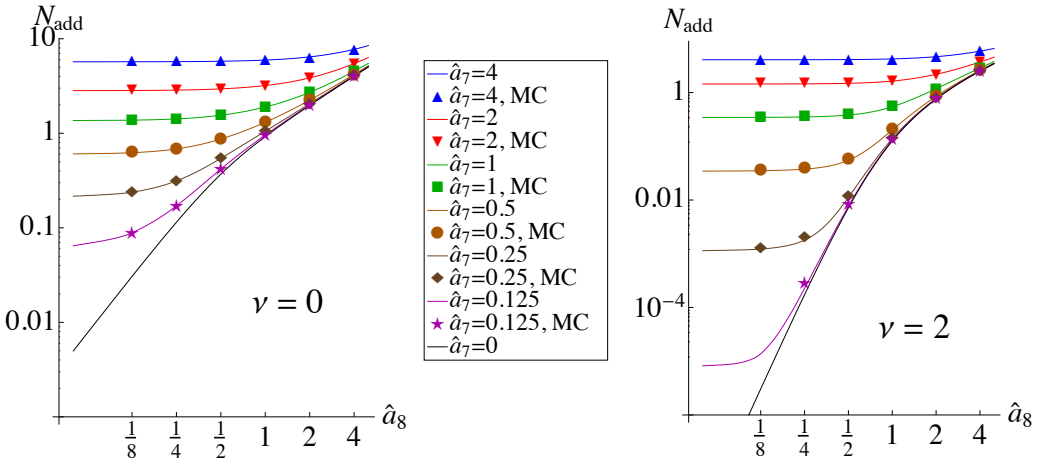

Figure 2.3: Log-log plots of $N_{\rm add}$ as a function of $\widehat{a}_8 = \sqrt{VW_8\widetilde{a}^2}$ for $\nu = 0$ (left plot) and $\nu = 2$ (right plot). The analytical results (solid curves) are compared to Monte Carlo simulations of RMT (symbols; ensemble and matrix size varies). Notice that W_6 has no effect on $N_{\rm add}$. The saturation around zero is due to a non-zero value of $\widehat{a}_7 = \sqrt{-VW_7\widetilde{a}^2}$. For $\widehat{a}_7 = 0$ (lowest curves) the average number of additional real modes behaves like $\widehat{a}_8^{2\nu+2}$, see Ref. [3, 4].

number of the additional real modes. This quantity directly follows from the result (2.71),

$$
\begin{aligned}
N_{\rm add} &= 2\int_{-\infty}^{\infty} \rho_{\rm r}(\widehat{x})d\widehat{x} \qquad (2.74)\\
&= \int_0^{2\pi} \frac{d\Phi}{4\pi}\cos[2\nu\Phi]\frac{1-\exp\left[-(4\widehat{a}_8^2+8\widehat{a}_7^2)\sin^2\Phi\right] I_0\left[(4\widehat{a}_8^2-8\widehat{a}_7^2)\sin^2\Phi\right]}{\sin^2\Phi}\\
&= \sum_{n=\nu+1}^{\infty}\sum_{j=0}^{\lfloor n/2\rfloor}(-1)^{\nu-1+n}\frac{(2n-2)!\,(\widehat{a}_8^2-2\widehat{a}_7^2)^{2j}\,(\widehat{a}_8^2+2\widehat{a}_7^2)^{n-2j}}{2^{2j-1}\Gamma(n-\nu)\Gamma(n+\nu)\Gamma(n-2j+1)(j!)^2},
\end{aligned}
$$

where the symbol $\lfloor n/2\rfloor$ denotes the largest integer smaller than or equal to $n/2$.

The average number of the real modes does not depend on the low energy constant $W_6 = -\widehat{a}_6^2/(\widetilde{a}^2V)$ because this constant induces overall fluctuations of the Dirac spectrum parallel to the $\widehat{x}$-axis.

The asymptotics of $N_{\rm add}$ at large and small lattice spacing is given by

$$N_{\rm add} = \begin{cases} \sum_{j=0}^{\lfloor \nu/2 \rfloor} \frac{(\widehat{a}_8^2 - 2\widehat{a}_7^2)^{2j} \, (\widehat{a}_8^2 + 2\widehat{a}_7^2)^{\nu-2j+1}}{2^{2j-1}\Gamma(\nu-2j+2)(j!)^2} \propto \widehat{a}^{2\nu+2}, & \widetilde{a} \ll 1, \\ \sqrt{\frac{64\widehat{a}_7^2}{\pi^3}} E\left(\sqrt{1 - \frac{\widehat{a}_8^2}{2\widehat{a}_7^2}}\right) \propto \widehat{a}, & \widetilde{a} \gg 1, \end{cases} \tag{2.75}$$

see D.1.1 for a derivation. The function E is the elliptic integral of the second kind, i.e

$$E(x) = \int_0^{\pi/2} \sqrt{1 - x^2 \sin^2 \varphi} d\varphi. \tag{2.76}$$

In Ref. [3, 4] this result was derived for $\widehat{a}_6 = \widehat{a}_7 = 0$. Notice that for large lattice spacings the number of additional real modes increases linearly with $\widehat{a}$ and is independent of ν.

The average number of additional real modes can be used to fix the low energy constants from lattice simulations. For $\nu = 0$, a sufficient number of eigenvalues can be generated to keep the statistical error small. For $\nu = 0$ and $\nu = 1$ the average number of additional real modes is given by

$$\begin{aligned} N_{\rm add}^{\nu=0} &\overset{\widetilde{a}\ll 1}{=} 2(\widehat{a}_8^2 + 2\widehat{a}_7^2) \\ &= 2V\widetilde{a}^2(W_8 - 2W_7), \end{aligned} \tag{2.77}$$

$$\begin{aligned} N_{\rm add}^{\nu=1} &\overset{\widetilde{a}\ll 1}{=} (\widehat{a}_8^2 + 2\widehat{a}_7^2)^2 + \frac{1}{2}(\widehat{a}_8^2 - 2\widehat{a}_7^2)^2 \\ &= V^2\widetilde{a}^4 \left[(W_8 - 2W_7)^2 + \frac{1}{2}(W_8 + 2W_7)^2\right]. \end{aligned} \tag{2.78}$$

These simple relations can be used to fit lattice data at small lattice spacing. In Fig. 2.3 we illustrate the behavior of $N_{\rm add}$ by a log-log plot.

The distribution $\rho_{\rm r}$ takes a much simpler form at large lattice spacing. Then, the integrals can be evaluated by a saddle point approximation resulting

The authors of Ref. [66] obtained $\widehat{a}_{6/7/8} \approx 0.1$. The number of their configurations with $\nu = 0$ was about 1000 so that the average number of additional real modes for the full ensemble would be $N_{\rm add}^{\nu=0} \approx 10$ with a statistical error of about thirty percent.

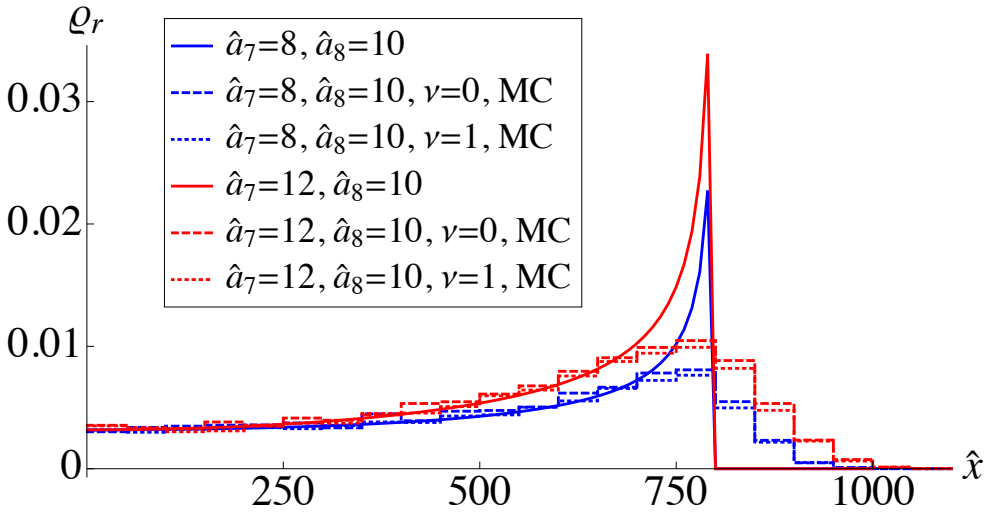

Figure 2.4: At large lattice spacing the distribution of additional real modes develops square root singularities at the boundaries. The analytical results at $\widehat{a} \to \infty$ (solid curves) are compared to Monte Carlo simulations at non-zero, but large lattice spacing (histogram [MC], with bin size 50, $\widehat{a}_6 = \sqrt{-VW_6\widetilde{a}^2} = 0.01$ and $n = 2000$ for an ensemble of 1000 matrices). Due to the finite matrix size and the finite lattice spacing, $\rho_{\rm r}$ has a tail which drops off much faster than the size of the support. The low energy constant $\widehat{a}_8 = \sqrt{VW_8\widetilde{a}^2}$ is chosen equal to 10. Therefore the boundary is at $\widehat{x} = 800$ which is confirmed by the Monte Carlo simulations. The dependence on W_6 and ν is completely lost.

in the expression (see D.1.2)

$$\rho_{\rm r}(\widehat{x}) \overset{\widetilde{a}\gg 1}{=} \begin{cases} \dfrac{1}{8\pi^2\widehat{a}_7\widehat{a}_6}\displaystyle\int_0^\infty d\widetilde{x}\cosh\left(\frac{\widetilde{x}\widehat{x}}{8\widehat{a}_6^2}\right)K_0\left(\frac{\widetilde{x}^2}{32\widehat{a}_7^2}\right)\widetilde{x} \\ \qquad\qquad \times\exp\left[-\dfrac{\widetilde{x}^2}{32\widehat{a}_7^2}-\dfrac{\widetilde{x}^2+\widehat{x}^2}{16\widehat{a}_6^2}\right], & \widehat{a}_8=0, \\ \dfrac{\Theta(8\widehat{a}_8^2-|\widehat{x}|)}{2(2\pi)^{3/2}\widehat{a}_8^2}\sqrt{\widehat{a}_8^2+2\widehat{a}_7^2\dfrac{\widehat{x}^2}{(8\widehat{a}_8^2)^2-\widehat{x}^2}}, & \widehat{a}_8\neq 0. \end{cases} \tag{2.79}$$

Notice that we have square root singularities at the two edges of the support if both $\widehat{a}_7 \neq 0$ and $\widehat{a}_8 \neq 0$, cf. Fig. 2.4. So the effect of the low energy constant W_7 is different than what we would have expected naively.

Distribution of the complex eigenvalues

The expression for the distribution of the complex eigenvalues given in Eq. (2.48) can be simplified by performing the integral of $\widehat{m}_6$ and $\widehat{\lambda}_7$ resulting in

$$\begin{aligned}\rho_{\rm c}(\widehat{z}) \;=\; & \frac{|\widehat{y}|}{2(2\pi)^{5/2}\sqrt{\widehat{a}_8^2+2\widehat{a}_6^2}}\int_{[0,2\pi]^2} d\varphi_1 d\varphi_2 \sin^2\left[\frac{\varphi_1-\varphi_2}{2}\right]\cos[\nu(\varphi_1+\varphi_2)] \\ & \times\mathrm{sinc}\left[\widehat{y}(\cos\varphi_1-\cos\varphi_2)\right]\exp\left[-4\widehat{a}_8^2\left(\left(\cos\varphi_1-\frac{\widehat{x}}{8\widehat{a}_8^2}\right)^2+\left(\cos\varphi_2-\frac{\widehat{x}}{8\widehat{a}_8^2}\right)^2\right)\right] \\ & \times\exp\left[\frac{4\widehat{a}_6^2\widehat{a}_8^2}{\widehat{a}_8^2+2\widehat{a}_6^2}\left(\cos\varphi_1+\cos\varphi_2-\frac{\widehat{x}}{4\widehat{a}_8^2}\right)^2-4\widehat{a}_7^2(\sin\varphi_1+\sin\varphi_2)^2\right].\end{aligned} \tag{2.80}$$

The function $\mathrm{sinc}(x) = \sin x/x$ is the *sinus cardinalis*. This result reduces to the expressions obtained in Ref. [3, 4] for $\widehat{a}_6 = \widehat{a}_7 = 0$.

To compare to numerical simulations it is useful to consider the projection of the complex modes onto the imaginary axis. The result for the projected

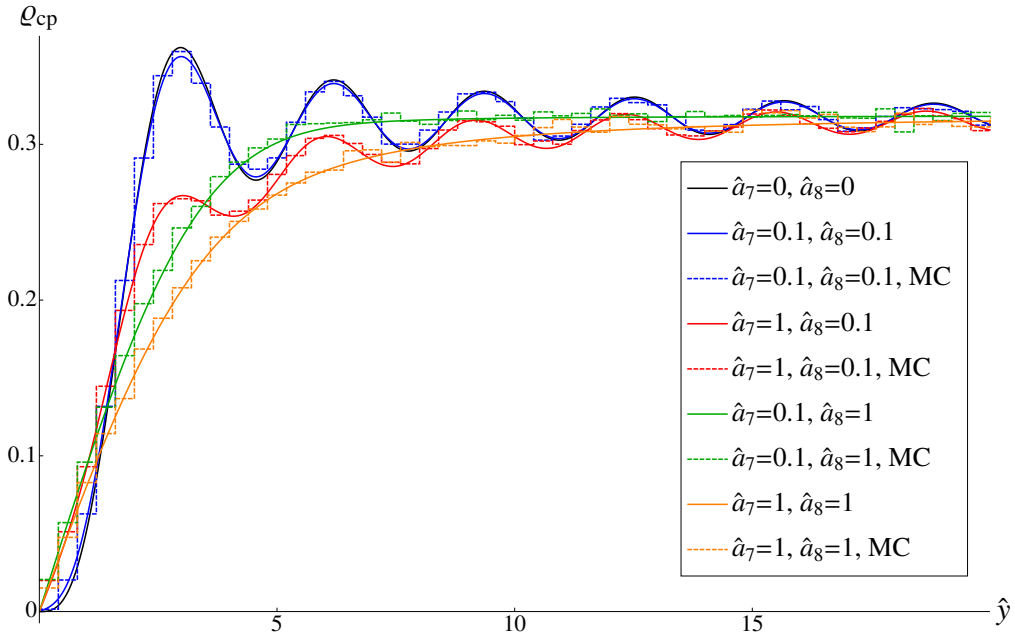

Figure 2.5: Comparison of the analytical result (solid curves) and Monte Carlo simulations of the Random Matrix Theory (histogram [MC] with bin size equal to 0.4 and varying ensemble size and matrix size) for the distribution of the complex eigenvalues projected onto the imaginary axis. The index of the Wilson Dirac operator is $\nu = 1$ for all curves. Notice that $\widehat{a}_6 = \sqrt{-VW_6}\widetilde{a}$ does not affect this distribution. The comparison of $\widehat{a}_7 = \widehat{a}_8 = 0.1$ with the continuum result (black curve) shows that $\rho_{\rm cp}$ is still a good quantity to extract the chiral condensate Σ at small lattice spacing.

eigenvalue density can be simplified to

$$\begin{aligned}\rho_{\rm cp}(\widehat{y}) &= \int_{-\infty}^{\infty} \rho_{\rm c}(\widehat{x}+\imath\widehat{y})d\widehat{x} \qquad (2.81)\\ &= \frac{|\widehat{y}|}{(2\pi)^2}\int_{[0,2\pi]^2} d\varphi_1 d\varphi_2 \sin^2\left[\frac{\varphi_1-\varphi_2}{2}\right]\mathrm{sinc}\left[\widehat{y}(\cos\varphi_1-\cos\varphi_2)\right]\\ &\times\cos[\nu(\varphi_1+\varphi_2)]\exp\left[-2\widehat{a}_8^2(\cos\varphi_1-\cos\varphi_2)^2-4\widehat{a}_7^2(\sin\varphi_1+\sin\varphi_2)^2\right].\end{aligned}$$

Again this function is independent of W_6 as was the case for $N_{\rm add}$. The reason is that the Gaussian broadening with respect to the mass $\widehat{m}_6$ is absorbed by the integral over the real axis. At small lattice spacing $\rho_{\rm cp}$ approaches the continuum result $\rho_{\rm NZ}$ given in Eq. (2.59) (see Fig. 2.5). Therefore it is still a good quantity to determine the chiral condensate Σ from lattice simulations. In Fig. 2.5, we compare the projected spectral density (solid curves) with numerical results from an ensemble of random matrices (histograms). The spectral density at a couple of eigenvalue spacings away from the origin can be used to determine the chiral condensate according to the Banks-Casher formula.

At small lattice spacing, $\rho_{\rm c}$ factorizes into a Gaussian distribution of the real part of the eigenvalues and of the level density of the continuum limit,

$$\begin{aligned}\rho_{\rm c}(\widehat{z}) &\overset{\widetilde{a}\ll 1}{=} \frac{|\widehat{y}|}{2(2\pi)^{5/2}\sqrt{\widehat{a}_8^2+2\widehat{a}_6^2}}\exp\left[-\frac{\widehat{x}^2}{8(\widehat{a}_8^2+2\widehat{a}_6^2)}\right]\int_{[0,2\pi]^2} d\varphi_1 d\varphi_2\\ &\times\sin^2\left[\frac{\varphi_1-\varphi_2}{2}\right]\cos[\nu(\varphi_1+\varphi_2)]\mathrm{sinc}\left[\widehat{y}(\cos\varphi_1-\cos\varphi_2)\right]\\ &= \frac{1}{\sqrt{8\pi(\widehat{a}_8^2+2\widehat{a}_6^2)}}\exp\left[-\frac{\widehat{x}^2}{8(\widehat{a}_8^2+2\widehat{a}_6^2)}\right]\rho_{\rm NZ}(\widehat{y}). \qquad (2.82)\end{aligned}$$

Therefore the support of $\rho_{\rm c}$ along the real axis is on the scale $\widehat{a}$ while it is of order 1 along the imaginary axis. It also follows from perturbation theory in the non-Hermitian part of the Dirac operator that the first order correction to the continuum result is a Gaussian broadening perpendicular to the imaginary axis. The width of the Gaussian can be used to determine the combination $\widehat{a}_8^2+2\widehat{a}_6^2 = V\widetilde{a}^2(W_8-2W_6)$ from fitting the results to lattice simulations. Since most of the eigenvalues of $D_{\rm W}$ occur in complex conjugate pairs at small lattice spacing, it is expected to have a relatively small statistical error in this limit. A further reduction of the statistical error can be achieved by integrating the spectral density over $\widehat{y}$ up to the Thouless energy (see Ref. [104] for a definition

of the Thouless energy in QCD).

The behavior drastically changes in the limit of large lattice spacing. Then the distribution reads (see D.1.3)

$$\rho_{\rm c}(\widehat{z}) \;=\; \begin{cases} \dfrac{\Theta(8\widehat{a}_8^2-|x|)}{16\pi\widehat{a}_8^2}\mathrm{erf}\left[\dfrac{|y|}{\sqrt{8\widehat{a}_8^2}}\sqrt{\dfrac{(8\widehat{a}_8^2)^2-\widehat{x}^2}{(8\widehat{a}_8^2)^2-(1-2\widehat{a}_7^2/\widehat{a}_8^2)\widehat{x}^2}}\right], & \widehat{a}_8>0, \\ \dfrac{|\widehat{y}|}{16\pi^2|\widehat{a}_6\widehat{a}_7|}\exp\left[-\dfrac{\widehat{x}^2}{16\widehat{a}_6^2}+\dfrac{\widehat{y}^2}{32\widehat{a}_7^2}\right]K_0\left(\dfrac{\widehat{y}^2}{32\widehat{a}_7^2}\right), & \widehat{a}_8=0. \end{cases} \tag{2.83}$$

There is no dependence on ν, and in the case of $\widehat{a}_8>0$, the result does not depend on $\widehat{a}_6$ and becomes a strip of width $16\widehat{a}_8^2$ along the imaginary axis. To have any structure, the imaginary part of the eigenvalues has to be of order $\widehat{a}$. In the mean field limit, where $|\widehat{y}|/\sqrt{8\widehat{a}_8^2}\gg 1$, $\rho_{\rm c}$ is equal to $1/(16\pi\widehat{a}_8^2)$ on a strip of width $16\widehat{a}_8^2$. Hence, the low energy constants $W_{6/7}$, do not alter the mean field limit of $\rho_{\rm c}$ cf. Ref. [3, 4]. This was already observed in Ref. [73].

The effect of $\widehat{a}_6$ is an overall Gaussian fluctuation perpendicular to the strip of the eigenvalues, and for $\widehat{a}_8=0$, when there is no strip, only the Gaussian fluctuations remain. The second case of Eq. (2.83) can also be obtained from Eq. (2.68) since for large $\widehat{y}$, $\rho_{\rm NZ}$ is equal to $1/\pi$.

2.4.3 The distribution of chirality over the real eigenvalues

The distribution of chirality over the real eigenvalues given in Eq. (2.49) is an expression in terms of the graded partition function $Z^{\nu}_{1/1}$ and the partition function of two fermionic flavors, $Z^{\nu}_{2/0}$, which is evaluated in C.1. Including

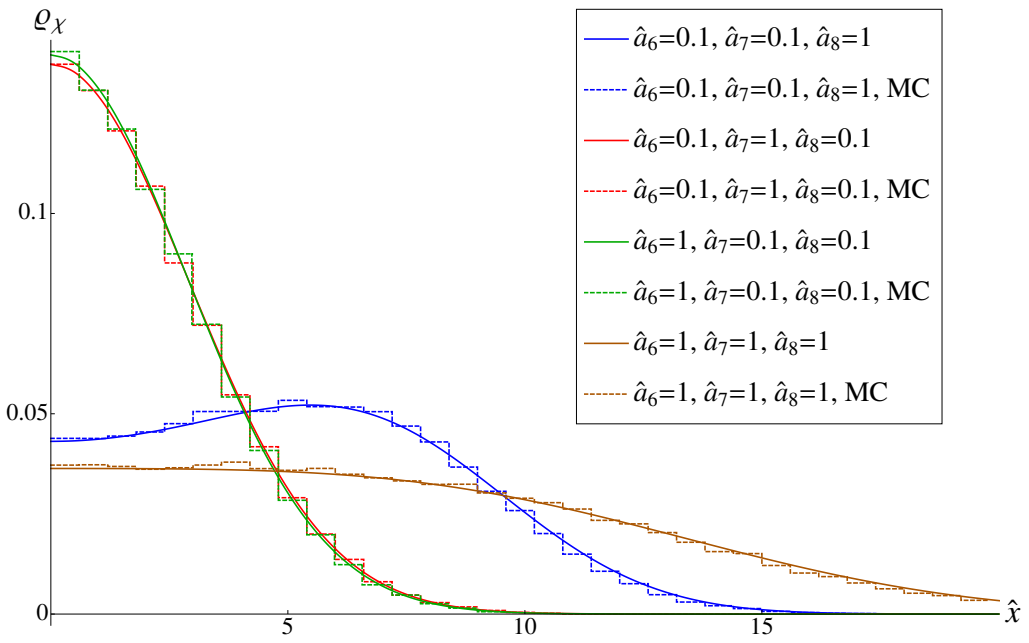

Figure 2.6: The analytical result (solid curves) for ρ_χ is compared to Monte Carlo simulations of RMT (histogram [MC] with bin size 0.6 and varying ensemble and matrix size) for $\nu = 1$. We plotted only the positive real axis since the distribution is symmetric around the origin. At small $\widehat{a}_8 = \sqrt{VW_8\widetilde{a}^2}$ the distributions for $(\widehat{a}_6, \widehat{a}_7) = (\sqrt{-VW_6\widetilde{a}^2}, \sqrt{-VW_7\widetilde{a}^2}) = (1, 0.1), (0.1, 1)$ are almost the same Gaussian as the analytical result predicts. At large $\widetilde{a}_8$ the maximum reflects the predicted square root singularity which starts to build up. We have not included the case $\widehat{a}_{6/7/8} = 0.1$ since it exceeds the other curves by a factor of 10 to 100.

the integrals over $\widehat{m}_6$ and $\widehat{\lambda}_7$ we obtain from Eq. (C.8)

$$\begin{aligned}\rho_\chi(\widehat{x}) &= \frac{(-1)^\nu}{(16\pi)^{3/2}\widehat{a}_8^2|\widehat{a}_7|}\int_{-\infty}^{\infty} d\widehat{\lambda}_7 \int_{\mathbb{R}^2}\frac{ds_1 ds_2}{s_1-\imath s_2}(\imath s_2+\widehat{\lambda}_7)^\nu (s_1-\widehat{\lambda}_7)^\nu \\ &\times \exp\left[-\frac{1}{16\widehat{a}_8^2}\left((s_1-\widehat{x})^2+(s_2+\imath\widehat{x})^2\right)+\frac{\widehat{a}_6^2}{16\widehat{a}_8^4}(s_1-\imath s_2)^2-\frac{\widehat{\lambda}_7^2}{16\widehat{a}_7^2}\right] \\ &\times\left[\frac{\delta^{(\nu-1)}(s_1+\widehat{\lambda}_7)}{(\nu-1)!(s_1-\widehat{\lambda}_7)^\nu}\left(\frac{s_1^2-\widehat{\lambda}_7^2}{s_2^2+\widehat{\lambda}_7^2}\right)^{\nu/2} Z^\nu_{1/1}\left(\sqrt{s_1^2-\widehat{\lambda}_7^2},\imath\sqrt{s_2^2+\widehat{\lambda}_7^2};\widehat{a}=0\right)\right. \\ &\left.-\mathrm{sign}(\widehat{\lambda}_7)\Theta(|\widehat{\lambda}_7|-|s_1|)\left(s_1^2+s_2^2\right)\frac{Z^\nu_{2/0}\left(\sqrt{s_1^2-\widehat{\lambda}_7^2},\imath\sqrt{s_2^2+\widehat{\lambda}_7^2};\widehat{a}=0\right)}{[(s_1^2-\widehat{\lambda}_7^2)(s_2^2+\widehat{\lambda}_7^2)]^{\nu/2}}\right].\end{aligned} \tag{2.84}$$

We recognize the two terms that were obtained in Eqs. (2.37) and (2.39) from the expansion in the first column of the determinant in the joint probability distribution.

Equation (2.84) is a complicated expression which is quite hard to evaluate numerically. However, it is possible to derive an alternative expression in terms of an integral over the supersymmetric coset manifold $U \in \mathrm{Gl}(1/1)/\mathrm{U}(1/1)$. We start from the equality

$$\begin{aligned}&\int \exp\left[-\frac{\widehat{\lambda}_7^2}{16\widehat{a}_7^2}-\frac{\imath\widehat{\lambda}_7}{2}\mathrm{Str}(U+U^{-1})\right]d\widehat{\lambda}_7 \\ &= 4\sqrt{\pi}\widehat{a}_7\exp\left[-\widehat{a}_7^2\mathrm{Str}^{\,2}(U+U^{-1})\right] \\ &= \exp\left[4\widehat{a}_7^2(\mathrm{Sdet}U+\mathrm{Sdet}U^{-1}-2)\right]\int\exp\left[-\frac{\widehat{\lambda}_7^2}{16\widehat{a}_7^2}-\frac{\imath\widehat{\lambda}_7}{2}\mathrm{Str}(U-U^{-1})\right]d\widehat{\lambda}_7 \\ &= \sum_{j=-\infty}^{\infty} I_j(8\widehat{a}_7^2)\mathrm{Sdet}^j U e^{-8\widehat{a}_7^2}\int\exp\left[-\frac{\widehat{\lambda}_7^2}{16\widehat{a}_7^2}-\frac{\imath\widehat{\lambda}_7}{2}\mathrm{Str}(U-U^{-1})\right]d\widehat{\lambda}_7,\end{aligned} \tag{2.85}$$

based on the identity for the $\mathrm{Gl}(1/1)/\mathrm{U}(1/1)$ graded unitary matrices

$$\mathrm{Str}^2(U+U^{-1}) = 8-4(\mathrm{Sdet}U+\mathrm{Sdet}U^{-1})+\mathrm{Str}^2(U-U^{-1}), \tag{2.86}$$

and the expansion

$$\exp\left[x\left(t+\frac{1}{t}\right)\right]=\sum_{j=-\infty}^{\infty}I_j(2x)t^j. \tag{2.87}$$

This allows us to absorb $\widehat{m}_6$ and $\widehat{\lambda}_7$ by a shift of the eigenvalues of the auxiliary supermatrix σ introduced to linearize the terms quadratic in U. The integral over U can now be identified as a graded $1/1$ partition function at $\widehat{a}=0$ and we obtain the result

$$\begin{aligned}\rho_\chi(\widehat{x}) &= \frac{\exp(-8\widehat{a}_7^2)}{16\pi\widehat{a}_8^2}\sum_{j=1}^{\infty}\left(I_{j-\nu}(8\widehat{a}_7^2)-I_{j+\nu}(8\widehat{a}_7^2)\right)\\ &\times\int_{\mathbb{R}^2}\exp\left[-\frac{1}{16\widehat{a}_8^2}\left((s_1-\widehat{x})^2+(s_2+\imath\widehat{x})^2\right)+\frac{\widehat{a}_6^2+\widehat{a}_7^2}{16\widehat{a}_8^4}(s_1-\imath s_2)^2\right]\\ &\times\frac{(-|s_1|)^j\delta^{(j-1)}(s_1)}{(j-1)!}Z^j_{1/1}\left(|s_1|,\imath s_2;\widehat{a}=0\right)\frac{ds_1ds_2}{s_1-\imath s_2}.\end{aligned} \tag{2.88}$$

Notice that the $j=0$ term does not contribute to the distribution of chirality over the real modes because of the symmetry of the Bessel function $I_\nu=I_{-\nu}$. The derivatives of Dirac delta-function originate from the $\mathrm{Im}[1/(s_1-i\epsilon)^j]$-term.

The representation (2.88) is effectively a one-dimensional integral due to the Dirac delta-function. Please notice that Eq. (2.88) reduces to Eq. (2.60) for $\widehat{a}_8=0$. Two plots, Fig. 2.6 ($\nu=1$) and Fig. 2.7, ($\nu=2$) illustrate the effect of each low-energy constant $\widehat{a}_{6/7/8}$ on the distribution ρ_χ.

The expression for $\nu=1$ given by Eq. (2.37) simplifies for $\widehat{a}_7=0$ when the term involving $Z^1_{2/0}$ is absent. After performing the integral over $\widehat{m}_6$ it can be expressed as

$$\rho_\chi(\widehat{x})|_{\nu=1} = \frac{1}{\sqrt{16\pi(\widehat{a}_8^2+\widehat{a}_6^2)}}\int_{-\pi}^{\pi}\frac{d\theta}{2\pi}\exp\left[\frac{(\widehat{x}+8\widehat{a}_8^2\sin\theta)^2}{\widehat{a}_8^2+\widehat{a}_6^2}\right]. \tag{2.89}$$

At small lattice spacing, $0<\widehat{a}\ll 1$, the distribution ρ_χ as well as the integration variables $s_{1/2}$ are of order $\widehat{a}$. Since $I_j(8\widehat{a}_7^2)\propto\widehat{a}_7^{2j}$, the leading order term is given by $j=\nu$ in the sum over j. Thus we have

$$\begin{aligned}\rho_\chi(\widehat{x})\overset{\widehat{a}\ll 1}{=}\frac{1}{16\pi\widehat{a}_8^2}&\int_{\mathbb{R}^2}\exp\left[-\frac{1}{16\widehat{a}_8^2}\left((s_1-\widehat{x})^2+(s_2+\imath\widehat{x})^2\right)+\frac{\widehat{a}_6^2+\widehat{a}_7^2}{16\widehat{a}_8^4}(s_1-\imath s_2)^2\right]\\ &\times\frac{(-|s_1|)^\nu\delta^{(\nu-1)}(s_1)}{(\nu-1)!}Z^\nu_{1/1}\left(s_1,\imath s_2;\widehat{a}=0\right)\frac{ds_1ds_2}{s_1-\imath s_2}.\end{aligned} \tag{2.90}$$

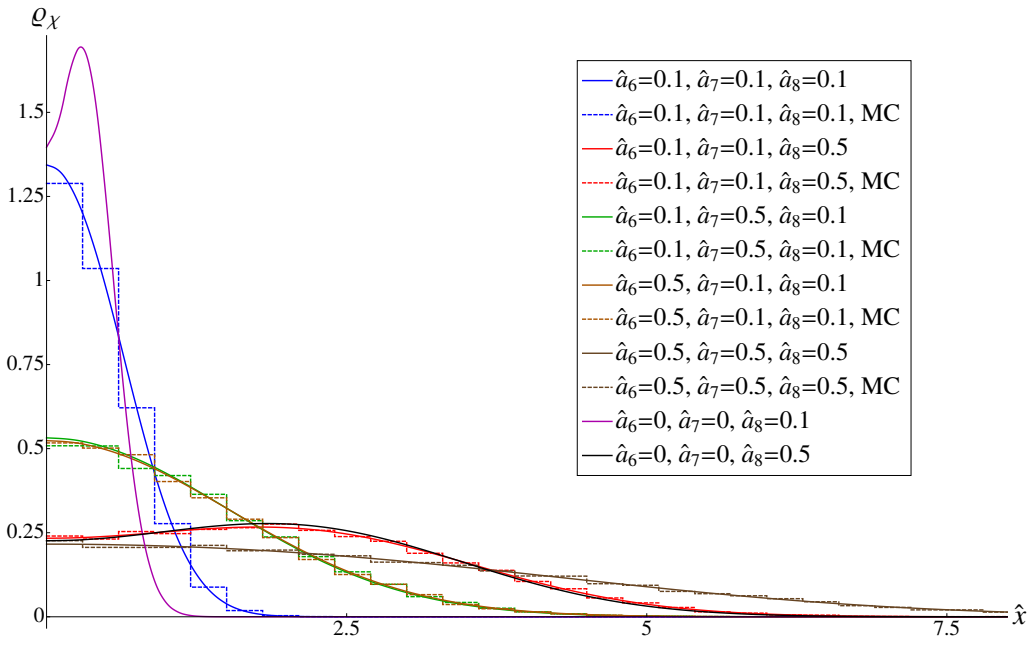

Figure 2.7: We compare the analytical result (solid curves) with Monte Carlo simulations of RMT (histogram [MC] with bin size 0.6 and with varying ensemble and matrix size) for $\nu = 2$. Again we only plotted the positive real-axis because ρ_χ is symmetric in the quenched theory. The two curves with $W_{6/7} = 0$ and $W_8 = 0.1, 0.5$ (purple and black curve) are also added to emphasize that the two peaks (ρ_χ has to be reflected at the origin) can be strongly suppressed by non-zero $W_{6/7}$ although they are only of the same order as W_8. Recall that the two peaks are relics of a 2×2 GUE which is formed by W_8.

In the small $\widehat{a}$ limit we can replace $Z^{\nu}_{1/1}\left(s_1, \imath s_2; \widehat{a}=0\right) \to (\imath s_2/|s_1|)^{\nu}$. The result becomes a polynomial in $\widehat{x}$ times a Gaussian of width $\sqrt{32(\widehat{a}_8^2+\widehat{a}_6^2+\widehat{a}_7^2)}$. Notice that the polynomial is not the one of a GUE anymore as in the case of $a_6 = a_7 = 0$ [5, 69, 70]. For $\nu = 1$, ρ_χ is a pure Gaussian,

$$\rho_\chi^{\nu=1}(\widehat{x}) \overset{\widetilde{a}\ll 1}{=} \frac{1}{\sqrt{16\pi(\widehat{a}_8^2+\widehat{a}_6^2+\widehat{a}_7^2)}} \exp\left[-\frac{\widehat{x}^2}{16(\widehat{a}_8^2+\widehat{a}_6^2+\widehat{a}_7^2)}\right], \quad (2.91)$$

and for $\nu = 2$ it is given by

$$\rho_\chi^{\nu=2}(\widehat{x}) \overset{\widetilde{a}\ll 1}{=} \frac{1}{\sqrt{16\pi(\widehat{a}_8^2+\widehat{a}_6^2+\widehat{a}_7^2)^3}} \left[\widehat{a}_8^2 + 2(\widehat{a}_6^2+\widehat{a}_7^2) + \frac{\widehat{a}_8^2}{8(\widehat{a}_8^2+\widehat{a}_6^2+\widehat{a}_7^2)}\widehat{x}^2\right] \times \exp\left[-\frac{\widehat{x}^2}{16(\widehat{a}_8^2+\widehat{a}_6^2+\widehat{a}_7^2)}\right]. \quad (2.92)$$

At small lattice spacing, ρ_χ only depends on the combinations $\widehat{a}_8^2$ and $(\widehat{a}_6^2+\widehat{a}_7^2)$. Therefore it is in principle possible to determine these two quantities by fitting ρ_χ to lattice results. For example the second moment (variance) of ρ_χ given by

$$\frac{1}{\nu}\int_{-\infty}^{\infty} \rho_\chi(\widehat{x})\widehat{x}^2 d\widehat{x} \overset{\widetilde{a}\ll 1}{=} 8(\nu\widehat{a}_8^2+\widehat{a}_6^2+\widehat{a}_7^2) = 8V\widetilde{a}^2(\nu W_8 - W_6 - W_7),\ \nu > 0, \quad (2.93)$$

at small lattice spacing can be used to fit the combinations $\nu\widehat{a}_8^2+\widehat{a}_6^2+\widehat{a}_7^2$. The statistical error in this quantity scales with the inverse square root of the number of configurations with the index ν. The ensemble of configurations generated in Ref. [66] yields a statistical error of about two to three percent. The statistics can be drastically increased by performing a fit of the variance of ρ_χ to a linear function in the index ν, cf. Eq. (2.93). The slope is then determined by W_8 and the off-set by W_6+W_7 yielding two important quantities.

In D.1.4 we calculate ρ_χ in the limit of large lattice spacing. Then the distribution of chirality over the real eigenvalues has a support on the scale of $\widetilde{a}^2$. The function ρ_χ reads

$$\rho_\chi(\widehat{x}) \overset{\widetilde{a}\gg 1}{=} \begin{cases} \dfrac{\nu}{\pi}\dfrac{\Theta(8\widehat{a}_8^2-|\widehat{x}|)}{\sqrt{(8\widehat{a}_8^2)^2-\widehat{x}^2}}, & \widehat{a}_8 > 0, \\ \dfrac{\nu}{\sqrt{16\pi(\widehat{a}_6^2+\widehat{a}_7^2)}} \exp\left[-\dfrac{\widehat{x}^2}{16(\widehat{a}_6^2+\widehat{a}_7^2)}\right], & \widehat{a}_8 = 0. \end{cases} \quad (2.94)$$

Interestingly, the low energy constants $W_{6/7}$ have no effect on the behavior

of ρ_χ in this limit if $\widehat{a}_8 \neq 0$ which is completely different in comparison to $\rho_{\rm r}$ and $\rho_{\rm c}$. The square root singularities at the boundary of the support are unexpected and were already mentioned in Ref. [3, 4].

2.5 Conclusions

Starting from RMT for the Wilson Dirac operator, we have derived the microscopic limit of the spectral density and the distribution of the chiralities over the Dirac spectrum. We have focused on the quenched theory, but all arguments can be simply extended to dynamical Wilson fermions. Wilson RMT is equivalent to the ϵ-limit of the Wilson chiral Lagrangian and describes the Wilson QCD partition function and Dirac spectra in this limit. The starting point of our analytical calculations is the joint probability density of the random matrix ensemble for the non-Hermitian Wilson-Dirac operator $D_{\rm W}$. This distribution was first obtained in Ref. [3, 4], but a detailed derivation is given in this paper, see A.1.

More importantly, we studied in detail the effect of the three low energy constants, $W_{6/7/8}$, on the quenched microscopic level density of the complex eigenvalues, the additional real eigenvalues and the distribution of chirality over the real eigenvalues. In terms of the effect on the spectrum of $D_{\rm W}$, the low energy constants W_6 and W_7 are structurally different from W_8. The first two can be interpreted in terms of "collective" fluctuations of the eigenvalues, whereas a non-zero W_8 induces interactions between all modes, particularly those with different chiralities. Therefore, the effect of a non-zero W_6 and W_7 at $W_8 = 0$ is just a Gaussian broadening of the Dirac spectrum on the scale of $\widehat{a}$. When $a^2 V W_8 \gg 1$ the interactions between the modes result in a strip of Dirac eigenvalues in the complex plane with real part inside the interval $[-8VW_8\widetilde{a}_8^2, 8VW_8\widetilde{a}_8^2]$. The structure along the imaginary axis is on the scale $\widehat{a}$. As was already discussed in Ref. [73], in the mean field limit, the lattice spacing $\widetilde{a}^2 V$ and the eigenvalues $V\widetilde{z}$ fixed, this structure becomes a box-like strip with hard edges at the boundary of the support and with height $1/(16\pi V W_8 \widetilde{a}^2)$.

We also discussed the limit of small lattice spacing, i.e. the limit $|VW_{6/7/8}|\widetilde{a}^2 \ll 1$. In practice, this limit is already reached when $|VW_{6/7/8}|\widetilde{a}^2 \leq 0.1$. Such values can be indeed achieved via clover improvement as discussed in Ref. [66]. In the small $\widehat{a}$ limit we have identified several quantities that are suitable to fit the four low energy constants, $W_{6/7/8}$ and Σ, to lattice simulations and our analytical results.

Several promising quantities are (applicable **only** at small lattice spacing):

- According to the Banks-Casher formula we have

$$\Delta = \frac{\pi}{\Sigma V}. \tag{2.95}$$

  for the average spacing of the imaginary part of the eigenvalues several eigenvalue spacings from the origin.

- The average number of the additional real modes for $\nu = 0$:

$$N_{\rm add}^{\nu=0} \overset{\widetilde{a}\ll 1}{=} 2V\widetilde{a}^2(W_8 - 2W_7). \tag{2.96}$$

- The width of the Gaussian shaped strip of complex eigenvalues:

$$\frac{\sigma^2}{\Delta^2} \overset{\widetilde{a}\ll 1}{=} \frac{4}{\pi^2}\widetilde{a}^2 V(W_8 - 2W_6). \tag{2.97}$$

- The variance of the distribution of chirality over the real eigenvalues:

$$\frac{\langle \widetilde{x}^2\rangle_{\rho_\chi}}{\Delta^2} \overset{\widetilde{a}\ll 1}{=} \frac{8}{\pi^2}V\widetilde{a}^2(\nu W_8 - W_6 - W_7),\ \nu > 0. \tag{2.98}$$

These quantities are easily accessible in lattice simulations. We believe they will lead to an improvement of the fits performed in Refs. [64–66]. Note that ρ_χ is close to the density of the real eigenvalues in the limit of small lattice spacing (again we mean by this $|VW_{6/7/8}|\widetilde{a} \approx 0.1$ and smaller). This statement is not true in the limit of large lattice spacing where the distribution of the additional real modes dominates the distribution of the real eigenvalues.

The relations (2.96-2.98) is an over-determined set for the low energy constants $W_{6/7/8}$ and Σ^2 and are only consistent if we have relations between these quantities. This can be seen by writing the relations as

$$\widetilde{a}^2 V \begin{bmatrix} 0 & -2 & 1 \\ -2 & 0 & 1 \\ -1 & -1 & 1 \\ -1 & -1 & 2 \end{bmatrix} \begin{bmatrix} W_6 \\ W_7 \\ W_8 \end{bmatrix} = \frac{\pi^2}{8} \begin{bmatrix} 4N_{\rm add}^{\nu=0}/\pi^2 \\ 2\sigma^2/\Delta^2 \\ \langle \widetilde{x}^2\rangle_{\rho_\chi}^{\nu=1}/\Delta^2 \\ \langle \widetilde{x}^2\rangle_{\rho_\chi}^{\nu=2}/\Delta^2 \end{bmatrix}. \tag{2.99}$$

The first three relations are linearly dependent, but none of the other triplets are. We thus have the consistency relation

$$\frac{\langle \widetilde{x}^2\rangle_{\rho_\chi}^{\nu=1}}{\Delta^2} = \frac{\sigma^2}{\Delta^2} + \frac{2}{\pi^2}N_{\rm add}^{\nu=0}. \tag{2.100}$$

There are more relations like Eqs. (2.96-2.98) which can be derived from our analytical results. The only assumption is a sufficiently small lattice spacing.

The value of W_8 follows immediately from the ν dependence of $\langle \widetilde{x}^2 \rangle_{\rho_\chi}$. If there are additional real modes, it cannot be that W_7 and W_8 are both equal to zero. In Ref. [66] it was found $W_8 = 0$ (with clover improvement) and results were fitted as a function of W_6 with $W_7 = 0$. Our prediction is that the number of additional real modes is zero and it would be interesting if the authors of Ref. [66] could confirm that.

The non-trivial effect of W_7 on the quenched spectrum was a surprise for us. In Ref. [73] it was argued that W_7 does not affect the phase structure of the Dirac spectrum. Indeed, we found that the complex eigenvalue density only shows a weak dependence on W_7, and actually becomes W_7 indpendent in the small $\widetilde{a}$-limit. Since, in the thermodynamic limit the number of real eigenvalues is suppressed as $1/\sqrt{V}$ with respect to the number of complex eigenvalues, W_7 will not affect the phase structure of the partition function. However, a non-zero value of W_7 significantly changes the distribution of the real eigenvalues. In particular, in the large $\widehat{a}$-limit, we find a square root singularity at the boundary of the support of the additional real eigenvalues if $W_7 \neq 0$, while it is a uniform distribution for $W_7 = 0$, see Ref. [3, 4]. Nevertheless, we expect in the case of dynamical fermions that the discussion of Ref. [73] also applies to the real spectrum of $D_{\rm W}$.

Chapter 3

Random Matrix Models for the Hermitian Wilson-Dirac operator of QCD-like theories

3.1 Introduction

Chiral Random Matrix Theories [47, 75] have been successful in describing lattice QCD Dirac spectra on the scale of the eigenvalue spacing. It was shown that they are equivalent to the ϵ-limit of QCD which is given by the ϵ-limit of chiral perturbation theory [58]. Recently, Random Matrix Theory was extended to include discretization effects of both the Wilson [68] and the staggered Dirac operator [76]. They are equivalent to the ϵ-limit of Wilson chiral perturbation theory [37, 78] and staggered chiral perturbation theory, respectively [105].

Starting from the chiral Lagrangian of Wilson chiral perturbation theory in the microscopic domain, exact results were obtained for the spectral density of the Hermitian Dirac operator both for the quenched case [68] and the case of dynamical quarks [102]. The spectral density of the non-Hermitian Wilson Dirac operator, could only be accessed by means of powerful random matrix techniques. The results for dynamical quarks show that depending on the value of the low-energy constants either an Aoki phase or a first order scenario is possible [73]. Lattice results for the eigenvalue density [64–66] have been compared successfully to the exact results [3, 70, 73, 83, 102] for the spectral density in the microscopic limit.

Joint work with M. Kieburg and J.J.M. Verbaarschot.

Recently, a great deal of attention has been focused on the conformal limit of QCD and QCD-like theories. Both the two-color theory and the any color adjoint theory are relevant for technicolor theories [106]. The advantage of SU(2) theories is that they require less fermions for achieving conformality than SU(3) theories. Furthermore, the SU(2) theory with two adjoint fermions is relevant for minimal walking technicolor theories [107]. Studies of this theory have been performed for unimproved Wilson fermions [108] and for the analysis of the conformal window, it would be useful to have a better understanding of the discretization errors.

As is the case in the continuum theory, also at non-zero lattice spacing, there is a one to one correspondence between patterns of chiral symmetry breaking and the anti-unitary symmetries of the Dirac operator [75]. We therefore can distinguish three distinct classes. QCD in the fundamental representation with three or more colors is the case without anti-unitary symmetry. When we have an anti-unitary symmetry, $[T, D] = 0$ for the Dirac operator D, then there are two different possibilities. Either $T^2 = 1$ or $T^2 = -1$. In the first case it is always possible to find a gauge field independent basis for which the Dirac operator is real. This is the case for QCD with two colors in the fundamental representation where the chiral symmetry breaking pattern is $\mathrm{SU}(2\mathrm{N_f}) \to \mathrm{USp}(2\mathrm{N_f})$. In the second case it is possible to find a gauge field independent basis in which the matrix elements are expressed as self-dual quaternions. This is the situation for QCD in the adjoint representation where the pattern of chiral symmetry breaking is $\mathrm{SU}(2\mathrm{N_f}) \to \mathrm{SO}(2\mathrm{N_f})$.

The goal of this chapter is to study the effect of a finite lattice spacing on the low lying Dirac eigenvalues and to understand the behavior of the spectral gap of $D_5 + m\gamma_5 = \gamma_5(D_\mathrm{W} + m)$ at finite quark mass as a function of the lattice spacing. In mean field theory, closure of the spectral gap will serve as an order parameter for the onset of the Aoki phase [68].

This chapter is organized as follows. In section 2 we introduce a Wilson Random Matrix Model for SU(2) with fundamental quarks and QCD with adjoint fermions. In particular, we consider the N_f flavor partition function as well as the partially quenched partition function. In section 3, we compare analytical results with Monte Carlo data of the Random Matrix Model. Note that in this chapter we employ a different convention from the one in the introduction for the definition of the Str . In what follows the convention used is $\mathrm{Str}\, M = \mathrm{tr}\, M_{BB} - \mathrm{tr}\, M_{FF}$.

3.2 Spectral Observables for the Wilson Dirac operator

For $a = 0$, the Wilson-Dirac operator has ν generic zero modes in accordance with the Atiyah-Singer index theorem. At finite a, one can define the index of the Dirac operator for a fixed gauge field configuration through spectral flow lines or equivalently by [109]

$$\nu = \sum_{\lambda_k^W \in \mathbb{R}} \text{sign}(\langle k|\gamma_5|k\rangle), \tag{3.1}$$

where the above sum is restricted to the real modes since the eigenfunctions corresponding to complex modes have zero chirality. In addition to that the sum needs to be restricted in the region near $\lambda = 0$ so we do no consider the contribution of the doublers. The partition function of D_5 with N_f flavors is given by

$$Z_{N_f}^{\text{RMT},\nu} = \int dD_5 \det{}^{N_f}(D_5 + m\gamma_5 + z)P(D_5), \tag{3.2}$$

where $P(D_5)$ is the probability distribution of the matrix elements of D_5. In the next section (3.3) we explicitly derive this partition function starting from a RMT with the same global symmetries as QCD and QCD-like theories respectively. In the microscopic limit where the combinations $\widehat{m} = 2mn$, $\widehat{z} = 2zn$ and $\widehat{a}^2 = a^2 n/2$ are kept fixed as $n \to \infty$, the Random Matrix Theory reduces to the ϵ-limit of Wilson chiral perturbation theory,

$$Z_{N_\text{f}}^{\nu} = \int d\mu(U) det^{\kappa} U \exp\left[\text{tr}\,\frac{\widehat{m}}{2}(U + U^{-1}) - \text{tr}\,\frac{\widehat{z}}{2}(U - U^{-1}) - \widehat{a}^2 \text{tr}\,(U^2 + U^{-2})\right] \tag{3.3}$$

with $U \in \text{U}(2N_f)/\text{USp}(2N_f)$ and $\kappa = \nu/2$ for $\beta = 1$ while $U \in \text{U}(2N_f)/\text{O}(2N_f)$ and $\kappa = \nu$ for $\beta = 4$ as is the case for $a = 0$ [110].

The full partition function at fixed vacuum angle θ is given by a sum over the Fourier components Z_ν,

$$Z(\theta) = \sum_{\nu=-\infty}^{\infty} e^{i\nu\theta} Z_\nu. \tag{3.4}$$

In order to access the spectral properties of the Dirac operator we employ the supersymmetric method of RMT. The generating function for the resolvent of D_5 is the partially quenched partition function obtained by adding an

additional fermionic and bosonic quark to the N_f flavor partition function

$$\mathcal{Z}^{\nu}_{N_f+1|1}(\widehat{m},\widehat{m'},\widehat{z},\widehat{z'};\widehat{a}) = \left\langle \det{}^{N_f}(\gamma_5(D_{\rm W}+\widehat{m'}))\frac{\det(\gamma_5(D_{\rm W}+\widehat{m})+\widehat{z})}{\det(\gamma_5(D_{\rm W}+\widehat{m'})+\widehat{z'})}\right\rangle_{\nu}. \tag{3.5}$$

The resolvent of D_5 is given by

$$G^{\nu}(\widehat{z},\widehat{m};\widehat{a}) = \lim_{z'\to z}\partial_z \mathcal{Z}^{\nu}_{1|1} = \left\langle \mathrm{tr}\,\frac{1}{D_5+\widehat{z}}\right\rangle. \tag{3.6}$$

Its discontinuity across the real axis gives the spectral density

$$\rho^{\nu}_5(\widehat{\lambda}^5,\widehat{m};\widehat{a}) = \frac{1}{\pi}\mathrm{Im}\,[G^{\nu}(\widehat{z}=\widehat{\lambda}^5,\widehat{m};\widehat{a})]. \tag{3.7}$$

See Fig. 3.1 for the spectral density of the $\beta = 2$ ensemble and section (3.4) for the results of $\beta = 1, 4$. There is another spectral resolvent if we consider

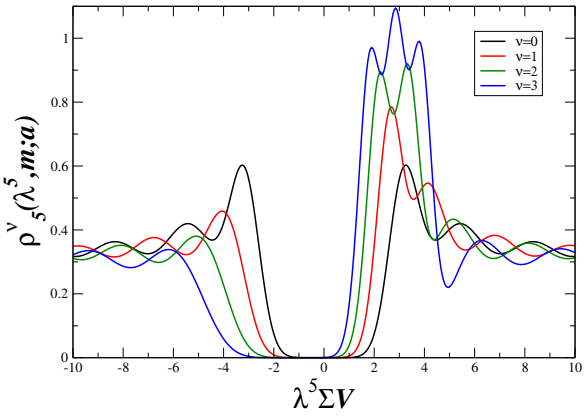

Figure 3.1: The microscopic spectral density of D_5 for $\beta = 2$, $\nu = 0, 1, 2$ and 3 with $\hat{m} = 3$, $\hat{a}_8 = 0.2$ and $\hat{a}_6 = \hat{a}_7 = 0$. At non zero value of the lattice spacing the zero modes spread out into a region around $\hat{\lambda}^5 = \hat{m}$. For negative values of ν the spectral density is reflected at the origin. Courtesy of [5].

the other source, namely the mass [5]

$$\Sigma^{\nu}(m;a) = -\lim_{m'\to m}\frac{d}{dm'}\mathcal{Z}^{\nu}_{N_f+1|1}(m,m',z=0,z'=0;a), \tag{3.8}$$

The discontinuity across the real axis of (3.8) provides the distribution of the

chiralities over the real eigenvalues

$$\rho_\chi^\nu(\hat{\lambda}) = \sum_{\lambda_k \in \mathcal{R}} \delta(\hat{\lambda} - \hat{\lambda_k}) \ \mathrm{sign}(\langle k|\gamma_5|k\rangle) \ = \ \frac{1}{\pi}\mathrm{Im}[\Sigma^\nu(\hat{m_f}, \hat{\lambda})]. \tag{3.9}$$

See Fig. 3.2 for the result for the case of $\beta = 2$ and section (3.4) for the case of $\beta = 1$. The integral of ρ_χ^ν along the real axis is equal to the index ν of the Dirac operator

$$\int_{-\infty}^{\infty} d\hat{\lambda} \ \rho_\chi^\nu(\hat{\lambda}) \ = \ \nu. \tag{3.10}$$

Since $|\langle k|\gamma_5|k\rangle| \leq 1$ we can provide an upper and lower bound for the ρ_{real} which is a difficult quantity to calculate [5]

$$\rho_\chi(\lambda^W) \leq \rho_{\mathrm{real}}(\lambda^W) \leq \rho_{1/\chi}(\lambda^W), \tag{3.11}$$

where

$$\rho_{1/\chi}(\lambda^W) = \rho_5(\lambda^5 = 0, m = \lambda^W; a) = \left\langle \sum_{\lambda_k^W \in \mathbb{R}} \frac{\delta(\lambda_k^W + m)}{|\langle k|\gamma_5|k\rangle|} \right\rangle, \tag{3.12}$$

and the density of real eigenvalues of D_W is defined

$$\rho_{\mathrm{real}}(\lambda^W) \equiv \left\langle \sum_{\lambda_k^W \in \mathbb{R}} \delta(\lambda_k^W + \lambda^W) \right\rangle. \tag{3.13}$$

In the microscopic limit the generating function reduces to a supersymmetric extension of the partition function (3.3). However the integrals over the non-compact part of U are only convergent for imaginary a. To obtain an analytical continuation to real a we have to rotate $U \to iU$. This results in the partition function

$$\begin{aligned} \mathcal{Z}^\nu_{N_{\mathrm{f}}+1|1} \ &= \ \int d\mu(U) \mathrm{Sdet}^{-\kappa} U \exp\left[\frac{-i}{2}\mathrm{Str}\,\widehat{M}(U - U^{-1})\right] \\ &\times \ \exp\left[\frac{i}{2}\mathrm{Str}\,\widehat{Z}(U + U^{-1}) - \widehat{a}^2\mathrm{Str}\,(U^2 + U^{-2})\right]. \end{aligned} \tag{3.14}$$

The integration manifold $U \in \mathrm{U}\,(2\mathrm{N_f} + 2|2)/\mathrm{UOSp}\,(2\mathrm{N_f} + 2|2)$ is the same as for $a = 0$. The mass matrix is given by $\widehat{M} = \mathrm{diag}(\widehat{m}, \widehat{m}, \widehat{m}, \widehat{m})$ whereas the axial mass is given by $\widehat{Z} = \mathrm{diag}(\widehat{z}, \widehat{z}, \widehat{z'}, \widehat{z'})$.
Note that for $z' \to z$ we recover the N_{f} flavor partition function.

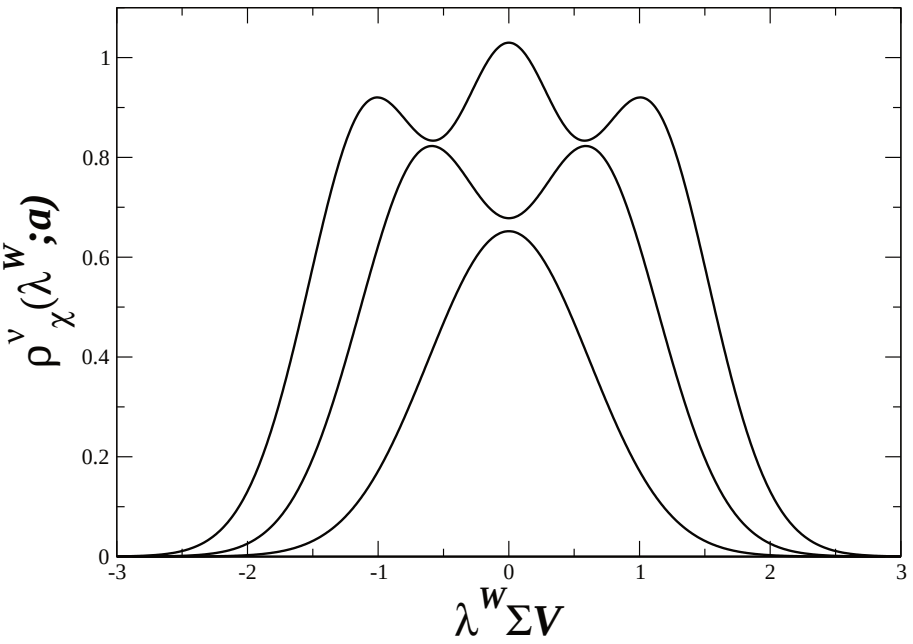

Figure 3.2: The quenched distribution of the chirality over the real modes of D_W for $\beta = 2$ plotted for $\nu = 1, 2$ and 3 with $\hat{a}_8 = 0.2$ and $\hat{a}_6 = \hat{a}_7 = 0$. Courtesy of [5]

To evaluate this integral we need an explicit parametrization of U. Since it involves only four Grassmann variables, it can easily be evaluated by brute force.

3.3 Random Matrix Theory for the Wilson Dirac Operator

The pertinent Random Matrix Theory for Wilson fermions was first introduced in Refs. [5, 68] and has the following structure

$$D_W = \begin{pmatrix} aA & W \\ -W^{\dagger} & aB \end{pmatrix}. \tag{3.15}$$

This is the most general structure for a γ_5- Hermitian matrix. In the off diagonal we have the typical structure for a system with chiral symmetry with W being a $n \times (n + \nu)$ complex matrix. While in the diagonal we have the Hermitian matrices A and B which comprise the explicit chiral symmetry breaking induced by the Wilson term. The probability distribution of the

matrix elements of A, B, W is taken to be Gaussian. We will begin our analysis with the Hermitian Dirac operator D_5 for which the partition function for $N_f + N_v$ fermionic and N_v bosonic flavors takes the form

$$\begin{aligned} Z &\sim \int d[A,B,W] \exp\left[-\frac{n}{2}\left(\mathrm{tr}\, A^2 + \mathrm{tr}\, B^2\right) - n\mathrm{tr}\, WW^\dagger\right] \\ &\times \mathrm{Sdet}^{-1}\left[\begin{pmatrix} aA & W \\ W^\dagger & aB \end{pmatrix} \otimes \mathbb{1}_{N_f+N_v/N_v} + \gamma_5 \otimes m + \mathbb{1}_{2n+\nu} \otimes \lambda^{(L)}\right]. \end{aligned} \tag{3.16}$$

In the partition function we have a superdeterminant which is the combined effect of the determinant of the fermionic flavors with the inverse determinant of the bosonic flavors. The matrices A and B are $n \times n$ and $(n+\nu) \times (n+\nu)$ Hermitian matrices, respectively, and W is a complex $n \times (n+\nu)$ matrix.

In order to write the superdeterminant as a Gaussian integral we must take care of the signs of the imaginary parts in the bosonic components of Z. Therefore we introduce $\lambda^{(L)}$ to render the bosonic integrals convergent.
We also have to mention that for the Grassmann variables we are employing the complex conjugation of the second type which means $\theta^{**} = -\theta$ and $(\theta_1\theta_2)^* = \theta_1^*\theta_2^*$ such that the invariant length element behaves like a real variable, $(\theta\theta^*)^* = \theta\theta^*$. We define

$$\lambda^{(L)} \equiv \mathrm{diag}\,(\lambda_{1f}, \ldots, \lambda_{N_f+N_vf}, \lambda_{1b}, \ldots, \lambda_{N_vb}) + i\mathrm{diag}\,(\mathbb{1}_{N_f+N_v,L})\varepsilon \tag{3.17}$$

with

$$L \equiv \mathrm{diag}\,(L_1, \ldots, L_{N_v}) \tag{3.18}$$

and

$$\widehat{L} = \begin{cases} \mathrm{diag}\,(\mathbb{1}_{N_f+N_v}, L) & \text{if } \beta = 2 \\ \mathrm{diag}\,(\mathbb{1}_{2N_f+2N_v}, L, L) & \text{if } \beta = 1, 4. \end{cases}$$

Let n_- be the number of diagonal matrix elements in L equal to -1 and $n_+ = N_v - n_-$ is the number of diagonal matrix elements equal to $+1$. These quantities take care of the convergence of the bosonic integrals.

$$\begin{aligned} Z &\sim \int d[A,B,W,V] \exp\left[-\frac{n}{2}\left(\mathrm{tr}\, A^2 + \mathrm{tr}\, B^2\right) - n\mathrm{tr}\, WW^\dagger\right] \\ &\times \exp\left[-\varepsilon(\mathrm{Str}\, V_R^\dagger V_R + \mathrm{Str}\, V_L^\dagger V_L)\right] \\ &\times \exp\left[i\mathrm{Str}\, \widehat{L} m V_R^\dagger V_R - i\mathrm{Str}\, \widehat{L} m V_L^\dagger V_L + i\mathrm{Str}\, \widehat{L}\lambda V_R^\dagger V_R + i\mathrm{Str}\, \widehat{L}\lambda V_L^\dagger V_L\right] \\ &\times \exp\left[ia\mathrm{Str}\, \widehat{L} V_R^\dagger A V_R + ia\mathrm{Str}\, \widehat{L} V_L^\dagger B V_L + i\mathrm{Str}\, \widehat{L} V_R^\dagger W V_L + i\mathrm{Str}\, \widehat{L} V_L^\dagger W^\dagger V_R\right] \end{aligned} \tag{3.19}$$

We have rewritten the partition function as a Gaussian integral over superfields where we have N_f physical flavors of sea quarks, N_v additional flavors of valence quarks and N_v bosonic valence quarks in order to obtain the partially quenched partition function. So the dimensions of W and V are

$$\begin{aligned} W &: n \times (n+\nu), \\ V_R &: n \times (\widetilde{\gamma}(N_f+N_v)|\widetilde{\gamma}N_v), \\ V_L &: (n+\nu) \times (\widetilde{\gamma}(N_f+N_v)|\widetilde{\gamma}N_v). \end{aligned} \tag{3.20}$$

The parameter m corresponds to the quark mass and λ is the axial quark mass.

$$m = \begin{cases} m & \text{if } \beta = 2, \\ m \otimes \mathbb{1}_2 & \text{if } \beta = 1, 4. \end{cases} \tag{3.21}$$

$$\lambda = \begin{cases} \lambda & \text{if } \beta = 2, \\ \lambda \otimes \mathbb{1}_2 & \text{if } \beta = 1, 4. \end{cases} \tag{3.22}$$

The term with ε in the exponent ensures the convergence of the integrals, finally

$$\tilde{\gamma} = \begin{cases} 1 & \text{if } \beta = 2, \\ 2 & \text{if } \beta = 1, 4. \end{cases} \tag{3.23}$$

3.3.1 The $\beta = 1$ case

Now we will carry out the A, B, W integrations. In the $\beta = 1$ case, $A^\top = A, B^\top = B, W^\dagger = W^\top$ and the superfields V can be written as follows with ψ being Grassmann valued fields and ϕ real scalar fields :

$$V_{R/L} = \left(\psi_{1;R/L}, \ldots, \psi_{N_f+N_v;R/L}, \psi^*_{1;R/L}, \ldots, \psi^*_{N_f+N_v;R/L}, \phi_{1;R/L}, \ldots, \phi_{2N_v;R/L}\right), \tag{3.24}$$

and

$$V_{R/L}^{\dagger} = \begin{pmatrix} -\psi_{1;R(L)}^{\dagger} \\ \vdots \\ -\psi_{N_f+N_v;R/L}^{\dagger} \\ \psi_{1;R/L}^{\top} \\ \vdots \\ \psi_{N_f+N_v;R/L}^{\top} \\ \phi_{1;R/L}^{\top} \\ \vdots \\ \phi_{2N_v;R/L}^{\top} \end{pmatrix}. \tag{3.25}$$

For our conventions regarding the signs in transposition and for a general review of the Supersymmetric Method in RMT we refer the reader to [111]. The integration over the random matrices A, B, W

$$\begin{aligned} I &= \int d[A,B,W] \exp\left[-n\left(\mathrm{tr}\, A^2 + \mathrm{tr}\, B^2\right) - 2n\mathrm{tr}\, WW^{\top}\right] \\ &\times \exp\left[ia\mathrm{Str}\, \widehat{L}V_R^{\dagger}AV_R + ia\mathrm{Str}\, \widehat{L}V_L^{\dagger}BV_L + i\mathrm{Str}\, \widehat{L}V_R^{\dagger}WV_L + i\mathrm{Str}\, \widehat{L}V_L^{\dagger}W^{\top}V_R\right] \end{aligned} \tag{3.26}$$

can be performed by completing squares resulting in

$$I = \exp\left[-\frac{a^2}{4n}\mathrm{Str}\, \left(\sigma_R^2 + \sigma_L^2\right) - \frac{1}{2n}\mathrm{Str}\, \left(\sigma_R\sigma_L\right)\right],$$

where $\sigma_{R,L} \equiv \widehat{L}V_{R/L}^{\dagger}V_{R,L}$.
Then the partition function reads

$$\begin{aligned} Z &\sim \int d[V] \exp\left[-\varepsilon\mathrm{Str}\, \widehat{L}(\sigma_R + \sigma_L) + i\mathrm{Str}\, m \otimes \mathbb{1}_2(\sigma_R - \sigma_L)\right] \\ &\times \exp\left[i\mathrm{Str}\, \lambda \otimes \mathbb{1}_2(\sigma_R + \sigma_L) - \frac{1}{2n}\mathrm{Str}\, (\sigma_R\sigma_L)\right] \\ &\times \exp[-\frac{a^2}{4n}\mathrm{Str}\, (\sigma_R^2 + \sigma_L^2)]. \end{aligned} \tag{3.27}$$

Under complex conjugation,

$$\sigma_{R/L}^{*} = \mathbf{I_1}\sigma_{R/L}\mathbf{I_1}^{\top} \tag{3.28}$$

where

$$\mathbf{I_1} = \left(\begin{array}{cc|c} 0 & \mathbb{1}_{N_f+N_v} & 0 \\ -\mathbb{1}_{N_f+N_v} & 0 & \\ \hline 0 & & \mathbb{1}_{2N_v} \end{array} \right), \tag{3.29}$$

and

$$\sigma^{\dagger}_{R,L} = \widehat{L}\sigma_{R,L}\widehat{L}, \tag{3.30}$$

which reveals the quaternionic structure of the Fermion-Fermion (FF) and the real structure of the Boson-Boson (BB) block.
At this point we will employ the superbosonization formula [112, 113], see E.1 for details,

$$\sigma_{R/L} \to n\rho_{R/L} \in U(2N_f + 2N_v/2n_+, 2n_-)/\mathrm{UOSp}^{(+)}(2N_f + 2N_v/2n_+, 2n_-). \tag{3.31}$$

The FF block corresponds to CSE while the BB block is not unitary but has n_+ positive definite eigenvalues and n_- negative definite eigenvalues, it is thus real symmetric with signature $(2n_+,2n_-)$. We denote this particular representation of the supergroup by a + [114]. The superbosonized field

$$\rho_{R/L} = \left(\begin{array}{cc} U_{FF,R/L} & \eta^{\dagger} \\ \eta & U_{BB,R,L} \end{array} \right), \tag{3.32}$$

where $U_{BB,R/L} = \Omega_{R/L}\mathrm{diag}\,(L_1, \ldots, L_{N_v}) \otimes \mathbb{1}_2 \exp[\mathrm{diag}\,(\phi_{1,R/L}, \ldots, \phi_{N_v,R/L})]\Omega^{-1}_{R/L}$ with $\phi_{i,R/L} \in (-\infty, \infty)$ and

$$\begin{aligned} U_{FF,R/L} &\in \mathrm{CSE}\,(2N_f + 2N_v), \\ \Omega^{R/L}_{BB} &\in \mathrm{O}\,(2n_+, 2n_-). \end{aligned} \tag{3.33}$$

If we define the rescaled variables $\widehat{\lambda} = 2n\lambda$, $\widehat{m} = 2nm$ and $\widehat{a}^2 = na^2/4$ with ε being infinitesimal such that $n\varepsilon \approx \varepsilon$ as $n \to \infty$. The superbosonization formula gives

$$\begin{aligned} Z &= \int d\mu(\rho_R) d\mu(\rho_L) \mathrm{Sdet}^{\,\kappa_R}\rho_R \mathrm{Sdet}^{\,\kappa_L}\rho_L \\ &\times \exp\left[-\varepsilon \mathrm{Str}\,\widehat{L} \otimes \mathbb{1}_2(\rho_R + \rho_L) + \frac{i}{2}\mathrm{Str}\,\widehat{m} \otimes \mathbb{1}_2(\rho_R - \rho_L)\right] \\ &\times \exp\left[-\frac{i}{2}\mathrm{Str}\,\widehat{\lambda} \otimes \mathbb{1}_2(\rho_R + \rho_L) - \frac{n}{2}\mathrm{Str}\,\rho_R\rho_L - \widehat{a}^2\mathrm{Str}\,(\rho_R^2 + \rho_L^2)\right] \end{aligned} \tag{3.34}$$

with

$$\begin{aligned}\kappa_R &= n/2 + N_f - 1/2, \\ \kappa_L &= (n+\nu)/2 + N_f - 1/2.\end{aligned} \tag{3.35}$$

see Ref. [113] for the conventions for $\kappa_{R/L}$.

The saddlepoint equations read

$$\begin{aligned}\rho_R^{-1} &= \rho_L, \\ \rho_L^{-1} &= \rho_R,\end{aligned} \tag{3.36}$$

which imply that $\rho_L = \rho_R^{-1} = U$. After the saddlepoint approximation the partition function takes the form

$$\begin{aligned}Z &= \int d\mu(U) \mathrm{Sdet}^{\,\nu/2} U \\ &\times \exp\left[-\varepsilon \mathrm{Str}\, \widehat{L}(U + U^{-1}) + \frac{i}{2}\mathrm{Str}\, \hat{m} \otimes \mathbb{1}_2 (U - U^{-1})\right] \\ &\times \exp\left[-\frac{i}{2}\mathrm{Str}\, \hat{\lambda} \otimes \mathbb{1}_2 (U + U^{-1}) - \widehat{a}^2 \mathrm{Str}\, (U^2 + U^{-2})\right].\end{aligned} \tag{3.37}$$

In the continuum limit the above partition function with fermionic flavors and by making use of the parametrization $U = \widehat{U}\mathbf{I}\widehat{U}^\top$ with $\widehat{U} \in U(2N_f + 2N_v)$ where $\mathbf{I}$ denotes the antisymmetric unity, gives the well known partition function for chGOE [110].

3.3.2 The $\beta = 2$ case

In this case the non-existence of anti-unitary symmetries leads to a Dirac operator with complex matrix elements. We will start by integrating out the random matrices A, B, W. In the $\beta = 2$ case $A^\dagger = A, B^\dagger = B$ and the superfields V can be written as follows with ψ being Grassmann valued fields and ϕ being complex scalar fields,

$$V_{R/L} = \left(\psi_{1;R/L}, \ldots, \psi_{N_f+N_v;R/L}, \phi_{1;R/L}, \ldots, \phi_{N_v;R/L}\right) \tag{3.38}$$

and

$$V_{R/L}^{\dagger} = \begin{pmatrix} -\psi_{1;R(L)}^{\dagger} \\ \vdots \\ -\psi_{N_f+N_v;R/L}^{\dagger} \\ \phi_{1;R/L}^{\dagger} \\ \vdots \\ \phi_{N_v;R/L}^{\dagger} \end{pmatrix}. \tag{3.39}$$

The integration over the random matrices A, B, W yields

$$\begin{aligned} I &= \int d[A,B,W] \exp\left[-\frac{n}{2}\left(\mathrm{tr}\, A^2 + \mathrm{tr}\, B^2\right) - n\mathrm{tr}\, WW^{\dagger}\right] \\ &\times \exp\left[ia\mathrm{Str}\, \widehat{L}V_R^{\dagger}AV_R + ia\mathrm{Str}\, \widehat{L}V_L^{\dagger}BV_L + i\mathrm{Str}\, \widehat{L}V_R^{\dagger}WV_L + i\mathrm{Str}\, \widehat{L}V_L^{\dagger}W^{\dagger}V_R\right], \end{aligned} \tag{3.40}$$

where by completion of the squares we get

$$I = \exp\left[-\frac{a^2}{2n}\mathrm{Str}\, \left(\sigma_R^2 + \sigma_L^2\right) - \frac{1}{n}\mathrm{Str}\, \left(\sigma_R\sigma_L\right)\right] \tag{3.41}$$

with $\sigma_{R,L} \equiv \widehat{L}V_{R/L}^{\dagger}V_{R,L}$. Then the partition function reads

$$\begin{aligned} Z &\sim \int d[V] \exp\left[-\varepsilon\mathrm{Str}\, \widehat{L}(\sigma_R + \sigma_L) + i\mathrm{Str}\, m(\sigma_R - \sigma_L)\right] \\ &\times \exp\left[i\mathrm{Str}\, \lambda(\sigma_R + \sigma_L) - \frac{1}{n}\mathrm{Str}\, (\sigma_R\sigma_L) - \frac{a^2}{2n}\mathrm{Str}\, (\sigma_R^2 + \sigma_L^2)\right] \end{aligned} \tag{3.42}$$

At this point we will employ the superbosonization formula [112, 113] and E.1 for details,

$$\sigma_{R/L} \to n\rho_{R/L} \in \mathrm{U}\left(N_f + N_v | n_+, n_-\right), \tag{3.43}$$

where the FF block corresponds to CUE $(N_f + N_v)$ and the BB block to Hermitian matrices with n_+ positive definite eigenvalues and n_- negative eigenvalues. The superbosonized field

$$\rho_{R/L} = \begin{pmatrix} U_{FF,R/L} & \eta^{\dagger} \\ \eta & U_{BB,R,L} \end{pmatrix} \tag{3.44}$$

where $U_{BB,R/L} = \Omega_{R/L}\mathrm{diag}\,(L_1,\ldots,L_{N_v})\exp[\mathrm{diag}\,(\phi_{1,R/L},\ldots,\phi_{N_v,R/L})]\Omega^{-1}_{R/L}$ with $\phi_{i,R/L} \in (-\infty,\infty)$ where

$$\begin{aligned} U_{FF,R/L} &\in \mathrm{CUE}\,(N_f+N_v), \\ \Omega^{R/L}_{BB} &\in \mathrm{U}\,(n_+,n_-). \end{aligned} \tag{3.45}$$

If we define the rescaled variables $\widehat{\lambda} = 2n\lambda$, $\widehat{m} = 2nm$ and $\widehat{a}^2 = na^2/2$ with ε being infinitesimal such that $n\varepsilon \approx \varepsilon$ as $n \to \infty$. Note the slight difference in the definition of the rescaled variables (there is a multiplication by 2 with respect to $\beta = 1$) and also not that no approximation has been employed. The purpose is to obtain a universal microscopic chiral Lagrangian where the only difference among the three symmetry class will be the integration supermanifold. The superbosonization formula yields

$$\begin{aligned} Z &= \int d\mu(\rho_R)d\mu(\rho_L)\mathrm{Sdet}^{\,\kappa_R}\rho_R\mathrm{Sdet}^{\,\kappa_L}\rho_L \\ &\times \exp\left[-\varepsilon\mathrm{Str}\,\widehat{L}\otimes\mathbb{1}_2(\rho_R+\rho_L)+\frac{i}{2}\mathrm{Str}\,\widehat{m}(\rho_R-\rho_L)\right] \\ &\times \exp\left[-\frac{i}{2}\mathrm{Str}\,\widehat{\lambda}(\rho_R+\rho_L)-n\mathrm{Str}\,\rho_R\rho_L-\widehat{a}^2\mathrm{Str}\,(\rho_R^2+\rho_L^2)\right] \end{aligned} \tag{3.46}$$

with

$$\begin{aligned} \kappa_R &= n+N_f, \\ \kappa_L &= n+\nu+N_f, \end{aligned} \tag{3.47}$$

see Ref. [113] for our conventions.
The saddlepoint equations read

$$\begin{aligned} \rho_R^{-1} &= \rho_L, \\ \rho_L^{-1} &= \rho_R, \end{aligned} \tag{3.48}$$

which imply that $\rho_L = \rho_R^{-1} = U$ After the saddlepoint approximation the partition function takes the form

$$\begin{aligned} Z &= \int d\mu(U) \mathrm{Sdet}^{\nu} U \\ &\times \exp\left[-\varepsilon \mathrm{Str}\, \widehat{L}(U+U^{-1}) + \frac{i}{2}\mathrm{Str}\, \widehat{m}(U-U^{-1})\right] \\ &\times \exp\left[-\frac{i}{2}\mathrm{Str}\, \widehat{\lambda}(U+U^{-1}) + \widehat{a}^2 \mathrm{Str}\,(U^2+U^{-2})\right]. \end{aligned} \tag{3.49}$$

If one restricts oneself only to fermionic flavors and performs an analytic continuation $U \to iU$ and also takes the continuum limit $\hat{a} \to 0$ then one ends up with the fermionic partition function of chGUE [110].

3.3.3 The $\beta = 4$ case

In this case the existence of the antiunitary symmetry dictates that the Dirac operator can be cast in a form with quaternion matrix elements. We will first carry out the A, B, W integrations. In the $\beta = 4$ case $A^d = A, B^d = B, W^\dagger = W^d$ with the quaternion dual defined as $X^d = \mathbf{I} X^\top \mathbf{I}$, where $\mathbf{I}$ is the symplectic unity.

In this case the superfields V will be of the form

$$\begin{aligned} V_{R/L} \quad &= \left(\begin{pmatrix} \psi_{1;R/L} \\ \psi^*_{1;R/L} \end{pmatrix}, \ldots, \begin{pmatrix} \psi_{2N_f+2N_v;R/L} \\ \psi^*_{2N_f+2N_v;R/L} \end{pmatrix}, \begin{pmatrix} \phi_{1,1;R/L} & -\phi^*_{1,2;R/L} \\ \phi_{1,2;R/L} & \phi^*_{1,1;R/L} \end{pmatrix} \right) \\ &, \ldots, \begin{pmatrix} \phi_{N_v,1;R,L} & -\phi^*_{N_v,2;R/L} \\ \phi_{N_v,2;R/L} & \phi^*_{N_v,1;R/L} \end{pmatrix} \Bigg), \end{aligned}$$

$$V^\dagger_{R/L} = \begin{pmatrix} \left(-\psi^\dagger_{1;R/L}, \psi^\top_{1;R/L}\right) \\ \vdots \\ \left(-\psi^\dagger_{2N_f+2N_v;R/L}, \psi^\top_{2N_f+2N_v;R/L}\right) \\ \begin{pmatrix} \phi^\dagger_{1,1;R/L} & \phi^\dagger_{1,2;R/L} \\ -\phi^\top_{1,2;R/L} & \phi^\top_{1,1;R/L} \end{pmatrix} \\ \vdots \\ \begin{pmatrix} \phi^\dagger_{N_v,1;R/L} & \phi^\dagger_{N_v,2;R/L} \\ -\phi^\top_{N_v,2;R/L} & \phi^\top_{N_v,1;R/L} \end{pmatrix} \end{pmatrix}. \tag{3.50}$$

Our convention for a quaternion $q = q_0 \mathbb{1} + i a_k \sigma_k$ where σ_k are the three Pauli

matrices. It is reflected by the choice of signs for the bosonic fields of (3.50). We will first perform the integrals over the random matrices A, B, W

$$\begin{aligned} I &= \int d[A,B,W] \exp\left[-\frac{n}{2}\left(\mathrm{tr}\, A^2 + \mathrm{tr}\, B^2\right) - n\mathrm{tr}\, WW^\dagger\right] \\ &\times \exp\left[ia\mathrm{Str}\, LV_R^\dagger AV_R + ia\mathrm{Str}\, LV_L^\dagger BV_L + i\mathrm{Str}\, LV_R^\dagger WV_L + i\mathrm{Str}\, LV_L^\dagger W^\dagger V_R\right] \end{aligned} \tag{3.51}$$

where by completion of the squares we get

$$I = \exp\left[-\frac{a^2}{2n}\mathrm{Str}\,\left(\sigma_R^2 + \sigma_L^2\right) - \frac{1}{n}\mathrm{Str}\,\left(\sigma_R\sigma_L\right)\right], \tag{3.52}$$

where $\sigma_{R/L} \equiv \widehat{L}V_{R/L}^\dagger V_{R,L}$. Then the partition function reads

$$\begin{aligned} Z &\sim \int d[V] \exp\left[-\varepsilon\mathrm{Str}\,\widehat{L}(\sigma_R + \sigma_L) + i\mathrm{Str}\, m \otimes \mathbb{1}_2(\sigma_R - \sigma_L)\right] \\ &\times \exp\left[i\mathrm{Str}\,\lambda \otimes \mathbb{1}_2(\sigma_R + \sigma_L) - \frac{1}{n}\mathrm{Str}\,(\sigma_R\sigma_L)\right] \\ &\times \exp[-\frac{a^2}{2n}\mathrm{Str}\,(\sigma_R^2 + \sigma_L^2)], \end{aligned} \tag{3.53}$$

where

$$\sigma_{R/L}^* = \mathbf{I_4}\sigma_{R/L}\mathbf{I_4}^\top \tag{3.54}$$

with

$$\mathbf{I_4} = \left(\begin{array}{c|cc} \mathbb{1}_{2N_f+2N_v} & \multicolumn{2}{c}{0} \\ \hline 0 & 0 & \mathbb{1}_{N_v} \\ & -\mathbb{1}_{N_v} & 0 \end{array}\right) \tag{3.55}$$

and

$$\sigma_{R/L}^\dagger = \widehat{L}\sigma_{R,L}\widehat{L}. \tag{3.56}$$

The above two equations describe the real structure of the FF block, the quaternionic structure of the BB block and the L-Hermiticity.
At this point we will employ the superbosonization formula [112, 113]

$$\sigma_{R/L} \to n\rho_{R/L} \in U(2N_f + 2N_v/2n_+, 2n_-)/\mathrm{UOSp}^{(-)}(2N_f + 2N_v/2n_+, 2n_-), \tag{3.57}$$

Where the FF block corresponds to COE $(N_f + N_v)$ and the BB block corresponds to self-dual Hermitian matrices with n_+ positive definite eigenvalues and n_- negative definite ones, we denote this particular representation of the

supergroup by a $-$ [114]. The superbosonized field

$$\rho_{R/L} = \begin{pmatrix} U_{FF,R/L} & \eta^\dagger \\ \eta & U_{BB,R/L} \end{pmatrix}, \tag{3.58}$$

where

$$U_{BB,R/L} = \Omega_{BB,R/L}\mathrm{diag}\,(L_1,\ldots,L_{N_v})\otimes\mathbb{1}_2\exp[\mathrm{diag}\,(\phi_{1,R,L},\ldots,\phi_{N_v,R,L})]\Omega_{BB}^{(R/L)^{-1}}$$

with

$$\begin{aligned} U_{FF,R/L} &\in \mathrm{COE}\,(2N_f+2N_v), \\ \Omega_{BB,R/L} &\in \mathrm{USp}\,(2n_+,2n_-). \end{aligned} \tag{3.59}$$

The Circular Orthogonal Ensemble (COE) corresponds to unitary matrices from the coset $U(n)/O(n)$. If we define the rescaled variables $\hat{\lambda}=2n\lambda$, $\hat{m}=2nm$ and $\hat{a}^2=na^2/2$ the superbosonization formula yields

$$\begin{aligned} Z &= \int d\mu(\rho_R)d\mu(\rho_L)\mathrm{Sdet}^{\,\kappa_R}\rho_R\mathrm{Sdet}^{\,\kappa_L}\rho_L \\ &\times \exp\left[-\varepsilon\mathrm{Str}\,\widehat{L}(\rho_R+\rho_L)+i\mathrm{Str}\,\widehat{m}\otimes\mathbb{1}_2(\rho_R-\rho_L)\right] \\ &\times \exp\left[-i\mathrm{Str}\,\widehat{\lambda}\otimes\mathbb{1}_2(\rho_R+\rho_L)-n\mathrm{Str}\,\rho_R\rho_L-\widehat{a}^2\mathrm{Str}\,(\rho_R^2+\rho_L^2)\right] \end{aligned} \tag{3.60}$$

with [113]

$$\begin{aligned} \kappa_R &= n+N_f+1/2, \\ \kappa_L &= n+\nu+N_f+1/2. \end{aligned} \tag{3.61}$$

The saddlepoint equations read

$$\begin{aligned} \rho_R^{-1} &= \rho_L, \\ \rho_L^{-1} &= \rho_R. \end{aligned} \tag{3.62}$$

Which imply that $\rho_L=-\rho_R^{-1}=U$.

After the saddlepoint approximation the partition function takes the form

$$\begin{aligned} Z &= \int d\mu(U)\mathrm{Sdet}^{\nu}U \\ &\times \exp\left[-\varepsilon\mathrm{Str}\,\widehat{L}\otimes \mathbb{1}_2(U+U^{-1}) + \frac{i}{2}\mathrm{Str}\,\widehat{m}\otimes\mathbb{1}_2(U-U^{-1})\right] \\ &\times \exp\left[-\frac{i}{2}\mathrm{Str}\,\widehat{\lambda}\otimes\mathbb{1}_2(U+U^{-1}) - \widehat{a}^2\mathrm{Str}\,(U^2+U^{-2})\right]. \end{aligned} \tag{3.63}$$

In the continuum limit the above partition function with fermionic flavors and by making use of the parametrization $U = \widehat{U}\widehat{U}^{\top}$ with $\widehat{U} \in U(2N_f+2N_v)$ gives the well known partition function for chGSE [110].
It is interesting to note that the form of the partition function is universal for all values of the Dyson index β. It is only the integration manifold that discriminates the three different classes. This is sometimes called orbifold equivalence in the literature [115].

3.3.4 Explicit parametrizations

$\beta = 1$

We will now use an explicit parametrization of the U field in order to evaluate the partition function analytically. Because of the above mentioned symmetries the parametrization should reflect the quaternionic nature of the FF block with the Kramers degeneracy and the real symmetric nature of the BB block. A parametrization satisfying these constraints is

$$U = \begin{pmatrix} e^{i\theta} & 0 & \eta_1 & \eta_2 \\ 0 & e^{i\theta} & \eta_1^* & \eta_2^* \\ \eta_1^* & -\eta_1 & e^{s_1} & 0 \\ \eta_2^* & -\eta_2 & 0 & e^{s_2} \end{pmatrix}. \tag{3.64}$$

Note that the BB block has been diagonalized and the diagonalization matrix has been absorbed by a redefinition of the Grassmann variables. It is important to point out that the Jacobian of this transformation has to be included in the measure.

$\beta = 2$

For the case of $\beta = 2$ we can either use (1.86) or rewritten in a way unifying all three classes

$$U = \begin{pmatrix} e^{i\theta} & \eta \\ -\eta^* & e^s \end{pmatrix}. \tag{3.65}$$

$\beta = 4$

Based on the previous analysis the parametrization should reflect the quaternionic nature of the BB block with the Kramers degeneracy and the real symmetric nature of the FF block. A parametrization fulfilling these requirements

$$U = \begin{pmatrix} e^{i\theta_1} & 0 & \eta_1^* & -\eta_1 \\ 0 & e^{i\theta_2} & \eta_2^* & -\eta_2 \\ -\eta_1 & -\eta_2 & e^s & 0 \\ -\eta_1^* & -\eta_2^* & 0 & e^s \end{pmatrix}. \tag{3.66}$$

Note that in this parametrization the FF block has been diagonalized. It is important to point out that the Jacobian of this transformation has to be included in the measure.

3.4 Analytical and Numerical results

To illustrate our analytical results we compare in Fig. 3.3 the results obtained from (3.14) for $\nu = 0$ and $m = 0$ with numerical ones obtained by calculating the eigenvalues of an ensemble of random matrices. Surprisingly, the spectral density at zero decreases by a factor $\sqrt{2}$ for any nonzero value of a which is confirmed both by the analytical and the numerical calculation. The reason for the non-uniformity of the $a \to 0$ limit is that for $a \neq 0$ the convergence of the integral is achieved through the U^2-term while for $a = 0$ the convergence comes from the U-term. In Fig. 3.5 we see how this dip in the spectral density develops for arbitrarily small values of the lattice spacing. The effect of diagonal blocks that comprise the Wilson term in the Random Matrix Model can thus be seen for arbitrarily small values of a.

In Fig. 3.4 we study the distribution of the first positive eigenvalue. Apparently, the diagonal blocks of the Wilson Dirac operator lead to a weak repulsion of the two eigenvalues closest to zero, but for larger values of a, there is no repulsion away from zero. The average position of the first eigenvalue increases as is shown by the corresponding vertical bar perpendicular to the real axis.

For $N_f = 1$ there is no spontaneous symmetry breaking but only explicit breaking due to the anomaly and the QCD partition function for QCD with

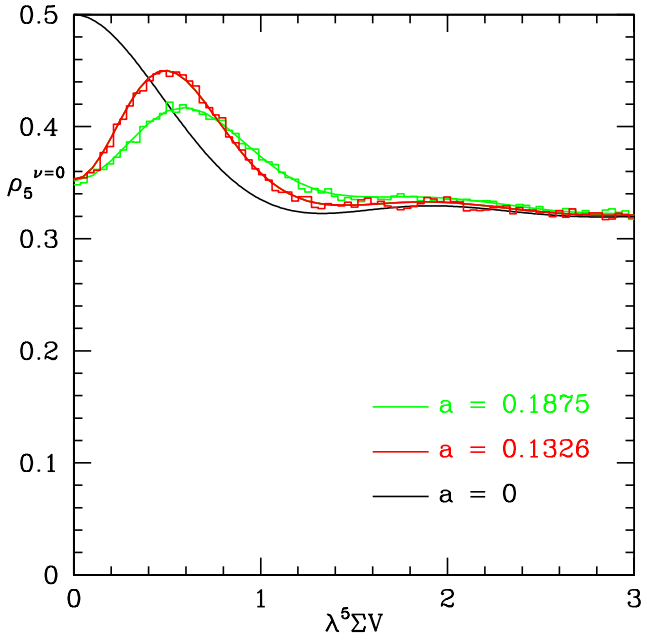

Figure 3.3: The analytical results (solid curves) compared to the results of the Monte Carlo simulation (histograms).

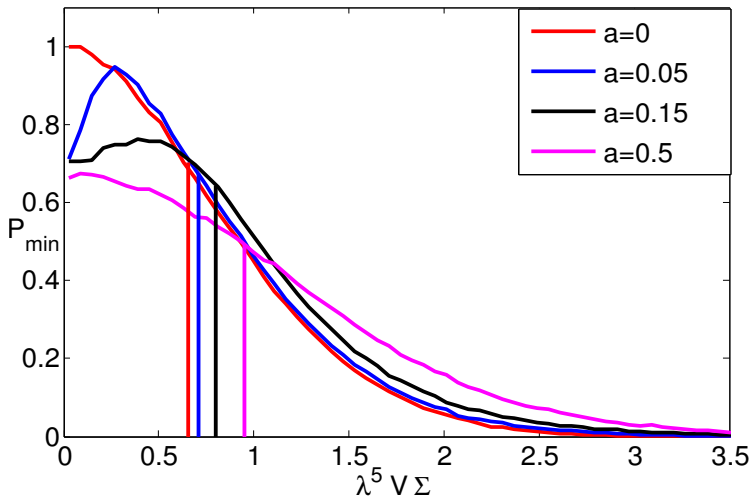

Figure 3.4: The distribution of the first positive eigenvalue, with $\widehat{m} = 0$, $\nu = 0$. The average position of this eigenvalue (denoted by the vertical bar) shifts away from the origin for increasing a.

two colors is the same as for QCD with three or more colors. Indeed for $N_f = 1$

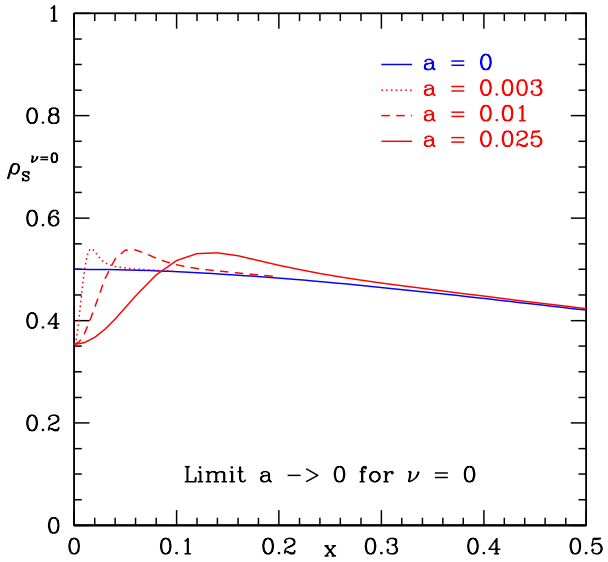

Figure 3.5: The spectral density of D_5 for $\nu = 0$ and values of a as in the legend of the figure.

the partition function can be written as

$$Z^{\nu}_{N_f=1} \propto \int_{-\pi}^{\pi} d\phi e^{i\nu\phi} e^{2m\cos\phi - 4a^2\cos 2\phi}, \tag{3.67}$$

which coincides with the one-flavor partition function for $\beta = 2$ (see [68]). Notice that this partition function is not necessarily positive definite. In general the partition function can be cast into a Pfaffian (see [116] and appendix B thereof for a detailed derivation of this result). The result is given by

$$Z_\nu(m) \sim \frac{1}{(2N_f-1)!!}\mathrm{Pf}[A] \tag{3.68}$$

with

$$A_{pq} = (q-p)\int_{-\pi}^{\pi}\frac{d\theta}{2\pi}e^{i(q+p)\theta + i\nu\theta + 2m\cos\theta - 4a^2\cos 2\theta}. \tag{3.69}$$

The indices q and p run between $-(N_f - \frac{1}{2})$ and $N_f - \frac{1}{2}$. Next we would like to look at the chiral condensate $\Sigma(m)$ given by the logarithmic derivative of the partition function of D_W with respect to the mass. In Fig. 3.6 we show the chiral condensate as a function of the mass m for $\nu = 2$ and two values of the lattice spacing. For $\nu \neq 0$, the distribution of the zero modes is a Dirac

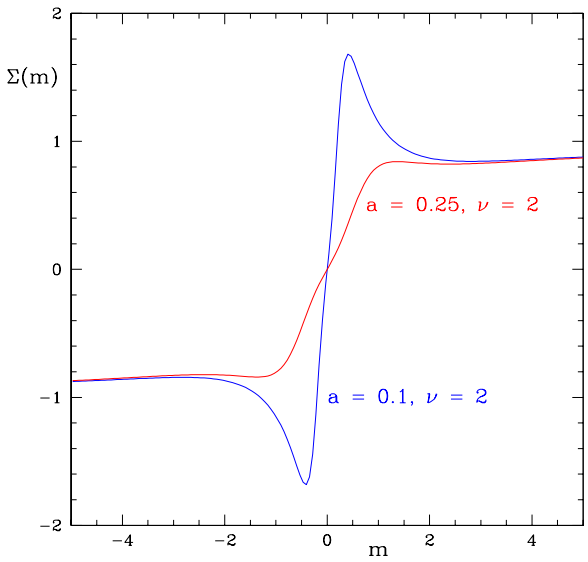

Figure 3.6: The chiral condensate for $N_f = 2$ with $\nu = 2$ and values of a as in the legend of the figure.

delta function for $a = 0$. As we increase the value of a their distribution gets broadened with a width proportional to a. This is similar to what happens in QCD with three or more colors in the fundamental representation. As can be seen from Figs. 3.7 and 3.8, at about $\widehat{a} = 0.5$ the peak due to the would be zero modes has disappeared almost completely.

For $a = 0$ the spectrum of D_5 has a gap $[-m, m]$, but at finite lattice spacing eigenvalues of tail states penetrate the gap [68]. Our results provide an explicit analytical handle on these states and allow us to identify the point where eigenvalues approach the center of the spectral gap and inversion of the Dirac operator becomes very difficult.

For $a = 0$, the spectral density of the two-color theory develops a square root type of singularity at the edge of the gap, $\rho_5(\widehat{\lambda}^5) \sim 1/\sqrt{(\lambda^5)^2 - m^2} + \nu\delta(\lambda^5 - m)$ (see Fig. 4). For $\beta = 2$, on the other hand, the spectral density approaches a finite limit at $\lambda^5 = m$. Next, we would like to address the real eigenvalues of the non-Hermitian Wilson Dirac operator. The Wilson Dirac operator has as least ν real eigenvalues if one does not take into account the doublers. Because the eigenvalues of the Wilson Dirac operator occur in complex conjugate pairs, additional real eigenvalues may be produced when a pair collides with the real axis. Depending on the expectation value of γ_5 the

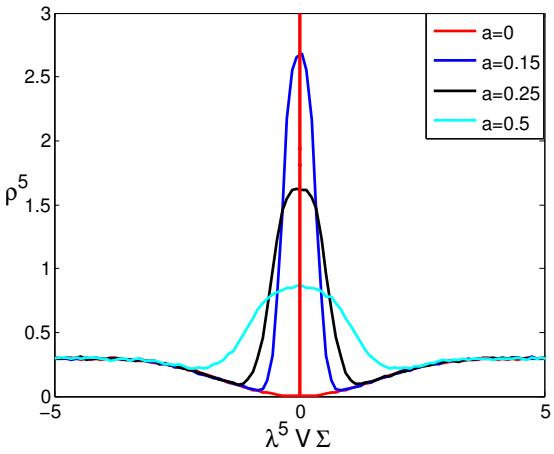

Figure 3.7: Spectral density ρ_5 at $\nu = 2$ and $\widehat{m} = 0$. Note the presence of zero modes for $a = 0$ and the widening of the peak as we increase a.

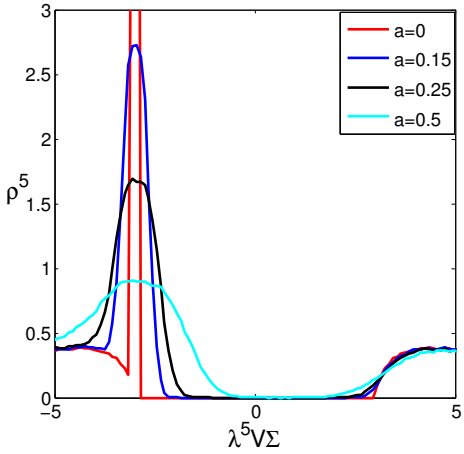

Figure 3.8: Spectral density ρ_5 at $\nu = 2$ and $\widehat{m} = -3$. For $a = 0$ the spectrum has a gap of width $2m$ which closes for increasing a.

density of the real eigenvalues may be decomposed as [3]

$$\rho^{\nu}_{\text{real}}(\lambda^W) = \rho^{\nu}_r(\lambda^W) + \rho^{\nu}_l(\lambda^W). \tag{3.70}$$

Even though we have not calculated analytically the eigenvalue density of the real eigenvalues we have obtained analytically and numerically ρ_χ the distribution of the chiralities over the real eigenvalues as well as the distribution of the inverse chiralities over the real eigenvalues $\rho_{1/\chi}$ see Figs. 3.9 and 3.10. These quantities, as we already explained, will serve as an upper and lower bound for the density of the real eigenvalues, see Fig. 3.11. The distribution of the chiralities over the real part of the spectrum of D_W [5, 72]

$$\rho^{\nu}_{\chi}(\lambda^W) = \left\langle \sum_{\lambda^W_k \in \mathbb{R}} \delta(\lambda^W + \lambda^W_k) \text{sign}(\langle k|\gamma_5|k\rangle) \right\rangle_{\nu} = \rho^{\nu}_l(\lambda^W) - \rho^{\nu}_r(\lambda^W), \tag{3.71}$$

was derived in the case of the $\beta = 2$ ensemble in [5, 68] and for dynamical quarks in [69, 102]. We have that

$$\rho^{\nu}_{\chi}(\lambda^W) \leq \rho^{\nu}_{\text{real}}(\lambda^W) \quad \text{and} \quad \int d\lambda^W \rho^{\nu}_{\chi}(\lambda^W) = \left\langle \sum_{\lambda^W_k \in \mathbb{R}} \text{sign}(\langle k|\gamma_5|k\rangle) \right\rangle_{\nu} = \nu. \tag{3.72}$$

In the limit of small lattice spacing the two distributions will merge towards

each other and one can impose very strict limits on the distribution of the real modes. In Figs. 3.12 and 3.13 we show scatter plots of the eigenvalues of D_{W}.

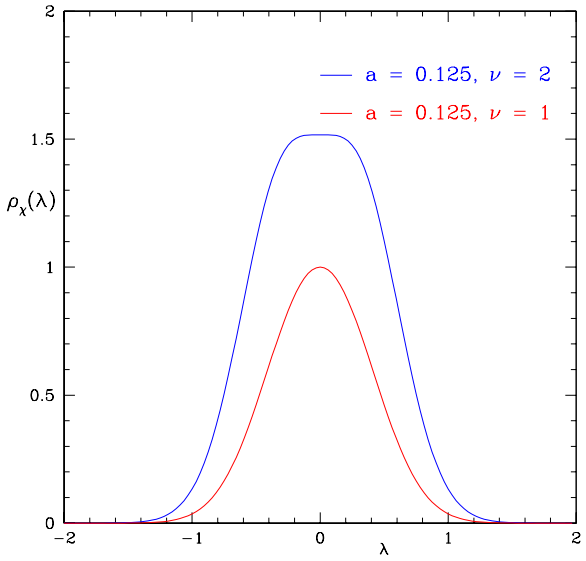

Figure 3.9: The chirality distribution for a=0.125 and $\nu = 1$ and $\nu = 2$.

For $a = 0$ the Wilson Dirac operator D_{W} is anti-Hermitian and the eigenvalues lie on the imaginary axis (see Fig. 3.12). In contrast to this behavior, D_{W} is non-Hermitian at finite a. Hence, it has a complex spectrum. Because D_{W} is still γ_5-Hermitian its complex eigenvalues occur in complex conjugate pairs, and at least $|\nu|$ eigenvalues are real (see Fig. 3.13). The additional real modes always appear in an even number. In Fig. 3.13 we show a spectrum of D_{W} for $\nu = 5$ with seven real modes.

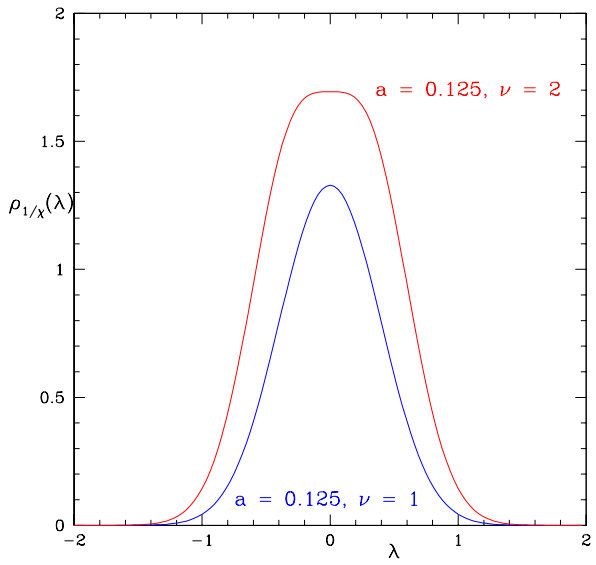

Figure 3.10: The inverse chirality distribution for a=0.125 and $\nu = 1$ and $\nu = 2$.

3.4.1 Constraints on the sign of W_8

The γ_5-Hermiticity imposes constraints on the signs of the LECs of Wilson chiral Perturbation Theory. The best way to see this is through Random Matrix Theory. Up to this point throughout this thesis we have postulated that $W_8 > 0$. If one would like to model Wilson fermions with $W_8 < 0$ then one has to study the Wilson Dirac operator at imaginary lattice spacing. This was first shown in [5, 70] for the case of $N_c > 3$ and fundamental quarks. In [5] it was proven that the following inequalities hold for a γ_5- Hermitian and an anti-Hermitian Wilson Dirac operator

$$Z^{\nu}_{N_f=2}(m,z) = \langle \det{}^2(\gamma_5(D_W+m)+z)\rangle > 0 \qquad \text{for} \quad m,z \quad \text{real.} \tag{3.73}$$

For an anti-Hermitian Dirac operator we have that

$$i^{-2\dim(D)} Z^{\nu}_{N_f=2}(m,z) = i^{-2\dim(D)} \langle \det{}^2((D_W+im)+iz\gamma_5)\rangle > 0 \qquad \text{for} \quad m,z \quad \text{real,} \tag{3.74}$$

where $\dim(D)$ is the total dimension of the Dirac matrix. Regarding the dimension of the Dirac matrix we need to clarify that we are considering a lattice Dirac operator which has a finite dimension. In the continuum limit, $i^{2\dim(D)} = (-1)^{\nu}$. Notice that in lattice QCD the dimension of D is always

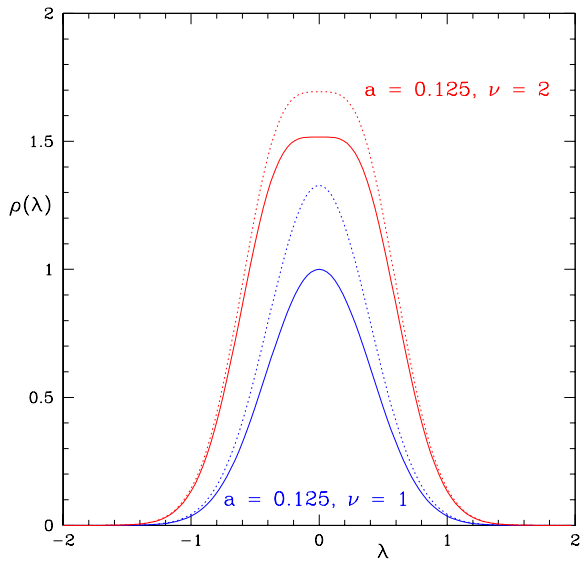

Figure 3.11: Comparison of the the chirality distribution (solid curves) and the inverse chirality distribution (dotted curve) with the density of real eigenvalues obtained from a numerical simulation of the corresponding random matrix ensemble. Results are given for $a = 0.125$ and $\nu = 1$ (blue) and $\nu = 2$ (red)

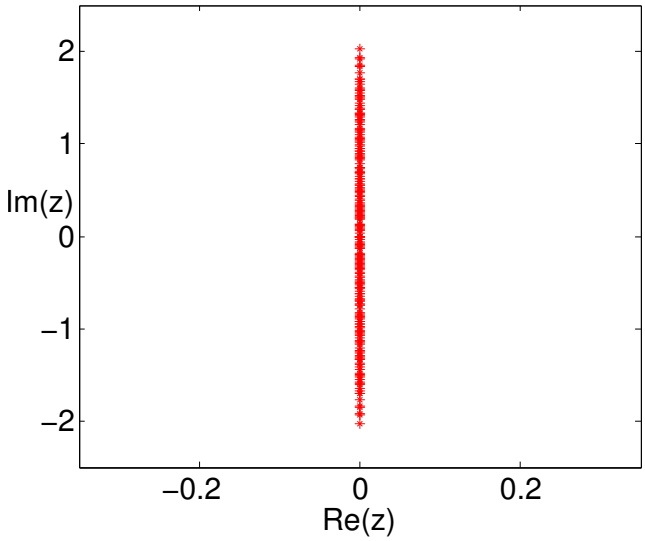

Figure 3.12: Spectrum of a randomly generated matrix D_{W} with $\nu = 5$ and $m = 0$ at vanishing lattice spacing, i.e. $\widehat{a} = 0$.

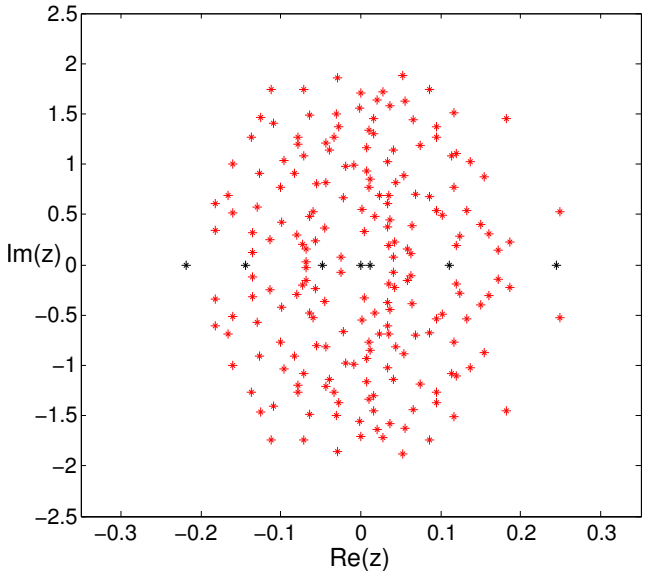

Figure 3.13: Spectrum of a randomly generated matrix $D_{\rm W}$ with $\nu = 5$ and $m = 0$ for a finite lattice spacing ($\widehat{a} = 1$).

even. By changing variables $U \to iU$ in the partition function (3.14) it follows that

$$Z_\nu^{\chi,\,N_f}(0,0,W_8) = (i)^{N_f\nu} Z_\nu^{\chi,\,N_f}(0,0,-W_8).$$

For large values of the mass the partition functions for $+W_8$ and $-W_8$ have the same sign, thus, one of them must change sign as a function of m, and not both signs of W_8 can be allowed by the QCD inequalities. In Fig. 3.14 we show the $N_f = 2$ partition function of $\beta = 1$ for $\nu = 1$ as a function of m . The blue curve corresponds to $W_8 > 0$, whereas the red curve to $W_8 < 0$.

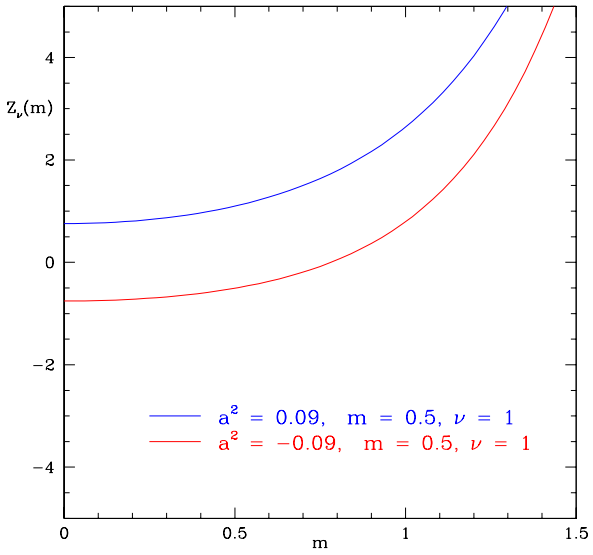

Figure 3.14: The mass dependence of the two-flavor partition function for $a^2 = \pm 0.09$ and $\nu = 1$.

3.5 The case of adjoint fermions

For the case of fermions in the adjoint representation and any number of colors we have performed numerical simulations of the microscopic spectral density for the case of $\nu = 0, 2$. In this case the Vandermonde determinant raised to the fourth power in the measure leads to increased repulsion from the origin. The microscopic spectrum exhibits strong oscillations which are persistent with the increase of the lattice spacing. While for the cases of $\beta = 1, 2$ the microscopic structure would be completely lost for values of $\hat{a} = 0.5$ and above this is clearly not the case for $\beta = 4$ as we can see in Figs. 3.15 and 3.16.

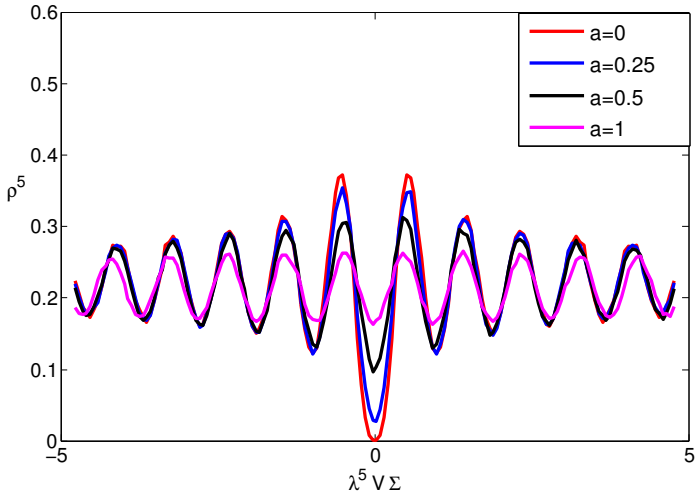

Figure 3.15: Spectral density of D_5 at $\nu = 0$ and $\widehat{m} = 0$ for the case of adjoint quarks ($\beta = 4$). Notice the presence of strong oscillations for the adjoint case.

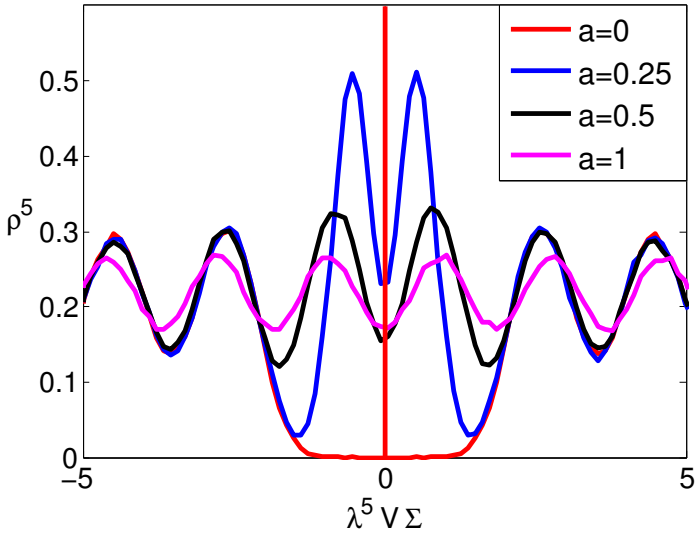

Figure 3.16: Spectral density of D_5 at $\nu = 2$ and $\widehat{m} = 0$ for the case of adjoint quarks ($\beta = 4$).The zero modes are given by two delta functions at $a = 0$ which eventually broadens as in the case of the other two ensembles.

3.6 Conclusions

We have introduced Random Matrix Theories for the Wilson Dirac operator of QCD like theories and have obtained explicit analytical results for the spectral density of two-color QCD. The analytical results have been compared to

Monte Carlo simulations of the proposed random matrix ensemble. Furthermore, numerical results for the spectral density for non-zero quark mass and index ν have been presented. We stress that although the increase of computational power has allowed for lattice simulations in the deep chiral regime it is not possible to invert the Wilson Dirac operator when eigenvalues are sufficiently close to zero. Our results identify the parameter domain where such eigenvalues appear and can be potentially useful for identifying the parameter domain for simulations with dynamical quarks. Actually, the probability to obtain small eigenvalues is higher for the two-color theory than for QCD with more colors because of the lack of repulsion from the origin. Our analytical results can be extended to the case of adjoint QCD.

Chapter 4

The Spectral Properties of the Naive and Staggered Dirac operator close to the continuum limit

4.1 Introduction

In QCD depending on the fermion representation and on the number of colors there is a classification based on the global symmetries as well as the existence of anti-unitary symmetries.

For $N_c = 2$ and fermions in the fundamental representation there is an anti-unitary symmetry (T) which commutes with the Dirac operator and with the property $T^2 = 1$. We can make use of this symmetry to cast the Dirac operator in a basis with real matrix elements. The anti-unitary symmetry is given by $T = \tau_2 C K$. Here τ_2 acts in color space, C is the charge conjugation operator while K is the complex conjugation operator. The corresponding ensemble is the chiral Gaussian Orthogonal ensemble (chGOE) and has Dyson index $\beta = 1$ [75]. For $N_c > 2$ and fermions in the fundamental representation there is no anti-unitary symmetry which commutes with the Dirac operator therefore the Dirac operator has complex matrix elements. The corresponding ensemble is the chiral Gaussian Unitary ensemble (chGUE) and has Dyson index $\beta = 2$ [75]. For adjoint fermions there is an anti-unitary symmetry (T)

Joint work with M. Kieburg and J.J.M. Verbaarschot.

which commutes with the Dirac operator and with the property $T^2 = -1$. We can make use of this symmetry to cast the Dirac operator in a basis with quaternion matrix elements or equivalently in terms of Pauli matrices. The anti-unitary symmetry is given by $T = CK$. The corresponding ensemble is the chiral Gaussian Symplectic ensemble (chGSE) and has Dyson index $\beta = 4$ [75]. The analytical predictions of RMT where immediately confirmed through semiclassical simulations in the instanton liquid model [117] as well as through lattice simulations [118]. One of the most widely used lattice discretizations is the one of staggered fermions. Studying the spectral properties of the staggered Dirac operator one is surprised by the striking property that at finite lattice spacing the staggered Dirac operator has reversed spectral statistics with respect to the continuum one for the case of $SU(2)$ fundamental as well as for the case of adjoint quarks [118]. In particular the two color theory for $a \neq 0$ has eigenvalue statistics given by the chiral Gaussian Symplectic ensemble while at $a = 0$ it follows the chiral Gaussian Orthogonal ensemble. In other dimensions there is also such a reversal but not necessarily involving the chiral ensembles. This is an effect of the spin-diagonalization which replaces the γ-matrices with the Kawamoto-Smit phases. There have been several studies [119–123] on this topic but still a clean interpretation has not been suggested.

In this analysis we consider a more general setup studying naive fermions in all fermion representations and also even-even, odd-odd and even-odd spacetime lattices. The conclusions for naive fermions in an even-even lattice apply directly to staggered fermions. In RMT there exist ten hermitian random matrix ensembles which are the three Wigner-Dyson ensembles (GOE, GUE, GSE), the three chiral ensembles (chGOE, chGUE, chGSE) and the four Altland-Zirnbauer ensembles (CI, D, C, DIII). These ensembles are the tangent spaces of a corresponding symmetric space and therefore bear the name of the Cartan classification [45]. It is surprising that almost the complete classification manifests itself in a rather "unrelated" context of the two-dimensional naive (staggered) QCD. A careful reader will notice that we will encounter eight out of the ten classes of Hermitian Random Matrices the only ones absent are AI and AII which correspond to the GOE and the GSE.

The Dirac spectrum is described by chRMT only for virtualities below the Thouless energy. Below the energy scale of the Thouless energy the chiral Lagrangian is dominated by the static modes and essentially the QCD partition function factorizes and one ends up with a zero dimensional unitary matrix integral. For four spacetime dimensions the $E_T \sim \frac{1}{\sqrt{V}}$ while for two dimensions it behaves as $E_T \sim 1/V$ [104, 124]. From the two dimensional spectra that we will present below, one can easily deduce that the scale of the Thouless energy is of the order of the eigenvalue spacing. In our simulation we find

that the Thouless energy is less in the even-odd case for $SU(2)$ QCD with fundamental quarks. Another important issue which needs to be addressed is that the whole analysis is based on the spontaneous symmetry breaking of chiral symmetry. The fact that we are focusing on the two-dimensional theory seems to upset the Coleman-Mermin-Wagner (CMW) theorem which prohibits the spontaneous breaking of continuous symmetries for systems with $d \leq 2$ with short range interactions. Our numerical simulations suggest that our results are consistent with a finite value of the chiral condensate and spontaneously broken chiral symmetry. It is part of ongoing investigation to clarify the apparent disagreement with the CMW theorem.

4.2 The theoretical background of the Euclidean Dirac operator and its analogue in RMT

Let us consider the Euclidean Dirac operator of QCD-like theories,

$$\mathcal{D} = \gamma^{\mu}(\partial_{\mu} + \imath A^{a}_{\mu} T_{a}), \tag{4.1}$$

where A^{a}_{μ} are real valued functions and T_a are the generators of the color representation. Hence we are able to write the Dirac operator in a 2-dim matrix block structure depending on another operator, i.e.

$$\mathcal{D} = \begin{bmatrix} 0 & \mathcal{W} \\ -\mathcal{W}^{\dagger} & 0 \end{bmatrix}, \tag{4.2}$$

where

$$\mathcal{W} = \partial_1 + \imath\partial_2 + (\imath A^{a}_{1} - A^{a}_{2}) T_{a} \tag{4.3}$$

in two dimensions and

$$\mathcal{W} = -i\sigma^{j}\partial_{j} + \partial_4 + (\sigma^{j} A^{a}_{j} + i A^{a}_{4}) T_{a} \tag{4.4}$$

in four dimensions using the standard chiral representation of Euclidean Dirac matrices.

The matrix-valued generators T_a have crucial influence on the level statistics. If we consider two color QCD with fermions in the fundamental representation T_a are the three Pauli matrices τ_a in color space. Then the covariant derivative

$$\mathcal{D}_{\mu} = \partial_{\mu} + \imath A^{a}_{\mu} T_{a} \tag{4.5}$$

is τ_2-real and anti-Hermitian, i.e.

$$\mathcal{D}_\mu^\top = -\tau_2 \mathcal{D}_\mu \tau_2. \tag{4.6}$$

For a larger number of colors with the fermions in the fundamental representation the symmetry under complex conjugation like in Eq. (4.6) is lost, only the anti-Hermiticity of $\mathcal{D}$ survives. However, the covariant derivative is real and anti-Hermitian for the fermions in the adjoint representation for any number of colors $N_c \geq 2$, i.e.

$$\mathcal{D}_\mu^\dagger = -\mathcal{D}_\mu \text{ and } \mathcal{D}_\mu^* = \mathcal{D}_\mu. \tag{4.7}$$

The reason for this is that the generators T_a are imaginary anti-symmetric in the adjoint representation.

This symmetry analysis has some crucial consequences for the operator $\mathcal{W}$. For $\beta = 2$, $\mathcal{W}$ fulfils no further symmetries in both dimensions ($d = 2, 4$). Hence it can be modelled by the random matrix $W \in \mathbb{C}^{(n+\nu)\times n}$ which is the model proposed by Shuryak and Verbaarschot [47]. The variable ν is the index of the Dirac operator.

The situation is different for $\beta = 1, 4$. Consider the case of $\beta = 1$. Then for $d = 2$, the symmetry discussion above, see Eq. (4.6), tells us that

$$\mathcal{W}^\dagger = -\tau_2 \mathcal{W}^* \tau_2. \tag{4.8}$$

The Dirac operator with $\mathcal{W}$ replaced by $\tau_2 \mathcal{W} \equiv \widetilde{W}$ has the same eigenvalues and $\widetilde{\mathcal{W}} = \widetilde{\mathcal{W}}^\top$. The corresponding random matrix model is obtained by replacing

$$\widetilde{\mathcal{W}} \to W \in \mathbb{C}^{2n\times 2n} \tag{4.9}$$

with $W = W^\top$. This model is different from the one for $d = 4$ where we have the symmetry relation

$$T\mathcal{W} = \mathcal{W}T, \tag{4.10}$$

where $T = K\sigma_2 \otimes \tau_2$ with σ_2 and τ_2 the Pauli-matrices in Dirac space and color space, respectively, and K the complex conjugation. The square of the anti-unitary operator T is $T^2 = 1$. Hence there is a real basis where $\mathcal{W}$ is real which indeed agrees with Verbaarschot's result [125]. This QCD-like theory is modelled by $W \in \mathbb{R}^{(n+\nu)\times n}$. In this analysis which is based on the fact that the coupling is strong we have $\nu = 0$.

Also for $\beta = 4$ we have two different situations when considering the two

dimensions $d = 2$ and $d = 4$. For $d = 2$ the operator $\mathcal{W}$ fulfils the symmetry

$$\mathcal{W}^\top = -\mathcal{W}. \tag{4.11}$$

which results into the random matrix model

$$\mathcal{W} \to W = -W^T \in \mathbb{C}^{(2n+\nu)\times(2n+\nu)}. \tag{4.12}$$

The index ν only takes the values $\nu = 0, 1$. This symmetry changes in four dimensions. Then we have

$$T\mathcal{W} = \mathcal{W}T \tag{4.13}$$

with $T = K\sigma_2$ which yields the square $T^2 = -1$. Thus it can be modelled by the random matrix $W \in \mathbb{H}^{(n+\nu)\times n}$, where $\mathbb{H}$ is the algebra of quaternions. The latter result again agrees with Ref. [75, 126].

4.3 Chiral Lagrangians of 2d continuous QCD

In the ensuing subsections we derive the joint probability density of the eigenvalues of the random matrix

$$D = \begin{bmatrix} 0 & W \\ -W^\dagger & 0 \end{bmatrix} \text{ distributed by } P(D) \propto \exp[-n\mathrm{tr}\, WW^\dagger] \tag{4.14}$$

fulfilling the symmetries discussed in Sec. 4.2. We can already read off some important properties of the level repulsion from these densities which will be summarized together with the lattice models of naive fermions in Sec. 4.4.

Moreover we show that the QCD-like theory indeed agrees with RMT in the ϵ-regime, namely they share the same chiral Lagrangian in the lowest order and the same symmetry breaking pattern.

4.3.1 $SU(2)$ fundamental, $d = 2$

The QCD-like theory

In two dimensions and two colors the Dirac operator for fermions in the fundamental representation is

$$\mathcal{D} = \begin{bmatrix} 0 & \mathcal{W} \\ -\mathcal{W}^\dagger & 0 \end{bmatrix} \text{ with } \mathcal{W}^\dagger = -\tau_2 \mathcal{W}^* \tau_2. \tag{4.15}$$

Then the fermionic part of the Lagrangian is given by

$$\mathcal{L} = \mathrm{tr}\,\bar{\psi}\mathcal{D}\psi = \mathrm{tr}\,\psi_{\mathrm{L}}^{\dagger}\,\mathcal{W}\psi_{\mathrm{L}} - \mathrm{tr}\,\psi_{\mathrm{R}}^{\dagger}\,\mathcal{W}^{\dagger}\psi_{\mathrm{R}}\,, \tag{4.16}$$

where we arranged the quarks in the matrix $\psi = (\psi_1, \psi_2, \ldots, \psi_{N_{\mathrm{f}}})$ (N_{f} is the number of quark flavors) with

$$\psi = \begin{bmatrix} \psi_{\mathrm{R}} \\ \psi_{\mathrm{L}} \end{bmatrix} \text{ and } \bar{\psi} = \psi^{\dagger}\gamma_0 = \begin{bmatrix} \psi_{\mathrm{L}}^{\dagger} & \psi_{\mathrm{R}}^{\dagger} \end{bmatrix}. \tag{4.17}$$

Note that in the analysis of the symmetries we use the γ_0 in the definition of the Dirac conjugate. The reason we employ this notation is in order to support the immediate recognizability of the flavor symmetries. Of course within the path integral ψ and $\bar{\psi}$ have to be understood as independent integration variables. Notice that ψ_{R} and ψ_{R}^{*} are real independent and the same is true for ψ_{L} and ψ_{L}^{*}. Due to the symmetry (4.15) the Langrangian can be rewritten into a symmetrized form

$$\begin{aligned} \mathcal{L} \;=\; & \frac{1}{2}\mathrm{tr}\left(\begin{bmatrix} \psi_{\mathrm{L}}^{T} \\ -\psi_{\mathrm{L}}^{\dagger}\tau_2 \end{bmatrix}\tau_2\mathcal{W}\begin{bmatrix} \psi_{\mathrm{L}} & \tau_2\psi_{\mathrm{L}}^{*} \end{bmatrix} - \begin{bmatrix} \psi_{\mathrm{R}}^{\dagger} \\ -\psi_{\mathrm{R}}^{T}\tau_2 \end{bmatrix}\mathcal{W}^{\dagger}\tau_2\begin{bmatrix} \psi_{\mathrm{R}}^{*} & \tau_2\psi_{\mathrm{R}} \end{bmatrix}\right) \\ & \times \begin{bmatrix} 0 & -\mathbb{1}_{N_{\mathrm{f}}} \\ \mathbb{1}_{N_{\mathrm{f}}} & 0 \end{bmatrix}. \end{aligned} \tag{4.18}$$

The terms depending on ψ_L and ψ_R are independent in flavor space. This Lagrangian is invariant under the transformation

$$\begin{bmatrix} \psi_{\mathrm{L}} & \tau_2\psi_{\mathrm{L}}^{*} \end{bmatrix} \to \begin{bmatrix} \psi_{\mathrm{L}} & \tau_2\psi_{\mathrm{L}}^{*} \end{bmatrix} U_{\mathrm{L}}\,, \quad \begin{bmatrix} \psi_{\mathrm{R}}^{*} & \tau_2\psi_{\mathrm{R}} \end{bmatrix} \to \begin{bmatrix} \psi_{\mathrm{R}}^{*} & \tau_2\psi_{\mathrm{R}} \end{bmatrix} U_{\mathrm{R}} \tag{4.19}$$

with $U_{\mathrm{R}}\,, U_{\mathrm{L}} \in \mathrm{USp}\,(2N_{\mathrm{f}})$. Hence the Lagrangian is invariant under the global flavor symmetry group $\mathrm{USp}\,(2N_{\mathrm{f}}) \times \mathrm{USp}\,(2N_{\mathrm{f}})$. We denote the compact symplectic group by USp . The chiral condensate describes the onset of the spontaneous symmetry breaking of chirality and is defined by

$$\begin{aligned} \Sigma \;&=\; \left\langle \mathrm{tr}\,\bar{\psi}\psi \right\rangle = \left\langle \mathrm{tr}\,\psi_{\mathrm{L}}^{\dagger}\,\psi_{\mathrm{R}} + \mathrm{tr}\,\psi_{\mathrm{R}}^{\dagger}\,\psi_{\mathrm{L}} \right\rangle \\ &=\; -\frac{1}{2}\left\langle \mathrm{tr}\left(\begin{bmatrix} \psi_{\mathrm{L}}^{T} \\ -\psi_{\mathrm{L}}^{\dagger}\tau_2 \end{bmatrix}\begin{bmatrix} \psi_{\mathrm{R}}^{*} & \tau_2\psi_{\mathrm{R}} \end{bmatrix} - \begin{bmatrix} \psi_{\mathrm{R}}^{\dagger} \\ -\psi_{\mathrm{R}}^{T}\tau_2 \end{bmatrix}\begin{bmatrix} \psi_{\mathrm{L}} & \tau_2\psi_{\mathrm{L}}^{*} \end{bmatrix}\right)\right\rangle, \end{aligned} \tag{4.20}$$

where $\langle . \rangle$ denotes the average over the configurations. The maximal subgroup that leaves the chiral condensate constant under the transformation (4.19)

yields the condition

$$U_{\mathrm{R}}^{-1} = U_{\mathrm{L}}^{T} \tag{4.21}$$

on the transformation matrices. Thus the symmetry breaking pattern is $\mathrm{USp}\,(2N_{\mathrm{f}}) \times \mathrm{USp}\,(2N_{\mathrm{f}}) \to \mathrm{USp}\,(2N_{\mathrm{f}})$. The corresponding effective chiral Lagrangian in the lowest order is then

$$\mathcal{L}_{\chi} = \Sigma V \mathrm{tr} \begin{bmatrix} M & 0 \\ 0 & M \end{bmatrix} U \quad \text{with } U \in \mathrm{USp}\,(2N_{\mathrm{f}}). \tag{4.22}$$

The physical quark masses are denoted by the diagonal matrix M and V is the space-time volume which is two-dimensional here.

RMT

Let us look at the corresponding RMT model. We consider the probability distribution

$$P(W)d[W] = \exp\left[-n\mathrm{tr}\, WW^{\dagger}\right] \prod_{1\le i<j\le 2n} \frac{2n}{\pi} d\,\mathrm{Re}\; W_{ij} d\,\mathrm{Im}\; W_{ij} \prod_{l=1}^{n} \frac{n}{\pi} d\,\mathrm{Re}\; W_{ll} d\,\mathrm{Im}\; W_{ll} \tag{4.23}$$

with $W = W^{T} \in \mathbb{C}^{2n\times 2n}$. The joint probability density of the eigenvalues of the chiral random matrix

$$D = \begin{bmatrix} 0 & W \\ -W^{\dagger} & 0 \end{bmatrix} \tag{4.24}$$

modelling the Dirac operator is defined by

$$\int\limits_{\mathbb{C}^{2n\times 2n}} f(D)P(W)d[W] = \int\limits_{\mathbb{R}_{+}^{2n}} f(\pm\imath\Lambda)p(\Lambda) \prod_{1\le j\le 2n} d\lambda_j \tag{4.25}$$

for any function f invariant under $\mathrm{Gl}\,(2n) \times \mathrm{Gl}\,(2n)$.

The characteristic polynomial of D fulfills the relation

$$\det(D - \imath\lambda \mathbb{1}_{4n}) = \det(WW^{\dagger} - \lambda^2 \mathbb{1}_{2n}) = \det(W^{\dagger}W - \lambda^2 \mathbb{1}_{2n}). \tag{4.26}$$

Let $U \in \mathrm{U}\,(2n)/\mathrm{U}^{\,2n}(1)$ be the matrix diagonalizing $WW^{\dagger}$, i.e.

$$WW^{\dagger} = U\Lambda^2 U^{\dagger} \tag{4.27}$$

with the positive definite, diagonal matrix $\Lambda^2 \in \mathbb{R}_+^{2n}$. Then we can relate the eigenvectors of $WW^\dagger$ with those of $W^\dagger W$ (by employing the fact that W is a complex symmetric matrix), i.e.

$$U^*\Lambda^2 = (U\Lambda^2)^* = (WW^\dagger U)^* = W^*W^TU^* = W^\dagger WU^*. \tag{4.28}$$

Thus, we have

$$W^\dagger W \;=\; U^*\Lambda^2 U^T, \tag{4.29}$$

and the combination of Eqs. (4.27) and (4.29) yields

$$W \;=\; UZU^T, \tag{4.30}$$

with the complex, diagonal matrix $Z \in \mathbb{C}^{2n}$ and $U \in \mathrm{U}(2n)/\mathrm{U}^{2n}(1)$. The right hand side of Eq. (4.30) can be used as a parametrization of W since after absorbing the phases of Z the number of degrees of freedom are $2n(2n+1)$ on both sides of Eq. (4.30). The phases of Z can be absorbed in U such that we consider the parametrization

$$W \;=\; U\Lambda U^T, \tag{4.31}$$

with the positive definite, diagonal matrix $\Lambda \in \mathbb{R}_+^{2n}$ and $U \in \mathrm{U}(2n)$.

In the next step we calculate the invariant length element which directly yields the Haar measure of W in the coordinates (4.30),

$$\begin{aligned}
\mathrm{tr}\, dW dW^\dagger \;&=\; \mathrm{tr}\, d\Lambda^2 + \mathrm{tr}\, \left(U^\dagger dU\Lambda + \Lambda(U^\dagger dU)^T\right)\left(U^\dagger dU\Lambda + \Lambda(U^\dagger dU)^T\right)^\dagger \\
&=\; \sum_{1\le i\le 2n} (d\lambda_i^2 + 4\lambda_i^2 (U^\dagger dU)_{ii}^2) \\
&\quad + \sum_{1\le i<j\le 2n} \left[\; (U^\dagger dU)_{ij},\;\; (U^\dagger dU)_{ij}^*\;\right] \begin{bmatrix} \lambda_i\lambda_j & -\dfrac{\lambda_i^2+\lambda_j^2}{2} \\ -\dfrac{\lambda_i^2+\lambda_j^2}{2} & \lambda_i\lambda_j \end{bmatrix} \begin{bmatrix} (U^\dagger dU)_{ij}, \\ (U^\dagger dU)_{ij}^* \end{bmatrix}.
\end{aligned} \tag{4.32}$$

Here, we have used the anti-Hermiticity of $U^\dagger dU$ and the fact that the diagonal elements are purely imaginary. Reading off the metric from the invariant length element (4.32) we find the joint probability density

$$p(\Lambda) \prod_{1\le j\le 2n} d\lambda_j \propto |\Delta_{2n}(\Lambda^2)| \prod_{1\le j\le 2n} \exp\left[-n\lambda_j^2\right] \lambda_j d\lambda_j \tag{4.33}$$

for the eigenvalues of D. This is the joint probability density for chiral GOE with $\nu = 1$. Hence the microscopic spectral density will have a linear slope at the origin and the level repulsion will be linear at small distances.

Although everything seems to look like chiral GOE with $\nu = 1$ there is a crucial difference in the joint probability distribution function and in the mass dependence of the partition function. The chGOE joint probability distribution function has one exactly zero mode while the present ensemble does not. Let us consider the partition function with $N_{\rm f}$ dynamical fermions, i.e.

$$Z(M) = \int \prod_{j=1}^{N_{\rm f}} \det(D + m_j) P(W) d[W]. \tag{4.34}$$

In combination with Eq. (4.26) we immediately see that $Z(0) \neq 0$ while the partition function vanishes in the case for chiral GOE with $\nu = 1$. In the next few paragraphs we are going to show that this property will go through to the microscopic limit and will yield the chiral Lagrangian (4.22).

To derive the partition function, we rewrite the determinants as Gaussians over Grassmann variables

$$Z(M) \propto \int \exp\left[-n\mathrm{tr}\, WW^\dagger + \mathrm{tr}\, V_R^\dagger W V_L - \mathrm{tr}\, V_L^\dagger W^\dagger V_R + \mathrm{tr}\, M(V_R^\dagger V_R + V_L^\dagger V_L)\right] d[W, V]. \tag{4.35}$$

The matrix τ_2 was absorbed in the V_R. The matrices V_R and V_L are both $2n \times N_{\rm f}$ rectangular matrices only consisting of independent Grassmann variables as matrix elements. Because W is symmetric we have to symmetrize the matrices $V_L V_R^\dagger$ and $V_R V_L^\dagger$. Afterwards we integrate over W and obtain

$$\begin{aligned} Z(M) &\propto \int \exp\left[-\frac{1}{4n}\mathrm{tr}\,(V_L V_R^\dagger - V_R^* V_L^T)(V_R V_L^\dagger - V_L^* V_R^T) + \mathrm{tr}\, M(V_R^\dagger V_R + V_L^\dagger V_L)\right] d[V] \\ &\propto \int \exp\left[\frac{1}{4n}\mathrm{tr}\,(\tau_2 \otimes \mathbb{1}_{N_{\rm f}})\sigma(\tau_2 \otimes \mathbb{1}_{N_{\rm f}})\sigma^T + \mathrm{tr}\,(\mathbb{1}_2 \otimes M)\sigma\right] d[V], \end{aligned} \tag{4.36}$$

where

$$\sigma = \begin{bmatrix} V_R^\dagger \\ -V_L^T \end{bmatrix} \begin{bmatrix} V_R, & V_L^* \end{bmatrix}. \tag{4.37}$$

The dyadic, nilpotent matrix σ can be replaced by a unitary matrix $U \in \mathrm{U}(2N_{\rm f})$ via the superbosonization formula [127] and see E.1 for details. We

rescale $U \to 2nU$, introduce the rescaled mass $\widehat{M} = 2nM$ and arrive at

$$Z(\widehat{M}) \;\propto \int\limits_{\mathrm{U}\,(2N_{\mathrm{f}})} \exp\left[n\mathrm{tr}\,(\tau_2 \otimes \mathbb{1}_{N_{\mathrm{f}}})U(\tau_2 \otimes \mathbb{1}_{N_{\mathrm{f}}})U^T + \mathrm{tr}\,(\mathbb{1}_2 \otimes \widehat{M})U\right] \det{}^{-2n} U d\mu(U), \tag{4.38}$$

where $d\mu$ is the normalized Haar-measure.

In the microscopic limit ($n \to \infty$ and $\widehat{M}$ fixed) we apply the saddlepoint approximation. The saddlepoint equation is given by

$$U^{-1} = (\tau_2 \otimes \mathbb{1}_{N_{\mathrm{f}}})U^T(\tau_2 \otimes \mathbb{1}_{N_{\mathrm{f}}}). \tag{4.39}$$

Since $U \in \mathrm{U}\,(2N_{\mathrm{f}})$ Eq. (4.39) implies $U \in \mathrm{USp}\,(2N_{\mathrm{f}})$ or equivalently the saddlepoint manifold is the set of unitary symplectic matrices. We find the final result

$$\begin{aligned} Z(\widehat{M}) &= \int\limits_{\mathrm{USp}\,(2N_{\mathrm{f}})} \exp\left[\mathrm{tr}\,(\mathbb{1}_2 \otimes \widehat{M})U\right] d\mu(U), \\ &= \int\limits_{\mathrm{USp}\,(2N_{\mathrm{f}})} \exp\left[\frac{1}{2}\mathrm{tr}\,(\mathbb{1}_2 \otimes \widehat{M})(U + U^{-1})\right] d\mu(U), \end{aligned} \tag{4.40}$$

which proves the equivalence among RMT in the microscopic limit for the 2-dim model and two color QCD in the ϵ-regime for fundamental fermions. Compare with the chiral Lagrangian (4.22). From this result it is immediate that $Z(0) \neq 0$. Moreover the chiral symmetry breaking pattern agrees with 2-dim SU (2)-gauge theory in the fundamental representation but is different from the one known for chiral GOE.

4.3.2 $SU(N_c)$ adjoint, $d = 2$

The QCD-like theory

Let us recall the symmetries of the Dirac operator of adjoint fermions with an arbitrary number of colors. The lattice Dirac operator has the usual chiral structure,

$$\mathcal{D} = \begin{bmatrix} 0 & \mathcal{W} \\ -\mathcal{W}^\dagger & 0 \end{bmatrix} \text{ with } \mathcal{W}^\dagger = -\mathcal{W}^*, \tag{4.41}$$

and $\mathcal{W}$ is odd dimensional (denoted by $\nu = 1$) for even N_c and even dimensional (denoted by $\nu = 0$) for odd N_c. Then the "kinetic" part of the Dirac Lagrangian describing the $N_{\rm f}$ quarks $\psi = (\psi_1, \ldots, \psi_{N_{\rm f}})$ can be rewritten in the eigenbasis of the flavor symmetries as

$$\begin{aligned}
\mathcal{L} &= \mathrm{tr}\,\bar{\psi}\mathcal{D}\psi = \mathrm{tr}\,\psi_{\rm L}^\dagger \mathcal{W}\psi_{\rm L} - \mathrm{tr}\,\psi_{\rm R}^\dagger \mathcal{W}^\dagger \psi_{\rm R}\,, \qquad (4.42)\\
&= \frac{1}{2}\mathrm{tr}\left[\begin{array}{c} \frac{1}{\sqrt{2}}(\psi_{\rm L}^T + \psi_{\rm L}^\dagger) \\ \frac{\imath}{\sqrt{2}}(\psi_{\rm L}^T - \psi_{\rm L}^\dagger)\end{array}\right]\mathcal{W}\left[\begin{array}{cc} \frac{1}{\sqrt{2}}(\psi_{\rm L} + \psi_{\rm L}^*), & \frac{\imath}{\sqrt{2}}(\psi_{\rm L} - \psi_{\rm L}^*)\end{array}\right]\\
&\quad + \frac{1}{2}\mathrm{tr}\left[\begin{array}{c} \frac{1}{\sqrt{2}}(\psi_{\rm R}^T - \psi_{\rm R}^\dagger) \\ \frac{\imath}{\sqrt{2}}(\psi_{\rm R}^T + \psi_{\rm R}^\dagger)\end{array}\right]\mathcal{W}^\dagger\left[\begin{array}{cc} \frac{1}{\sqrt{2}}(\psi_{\rm R} - \psi_{\rm R}^*), & \frac{\imath}{\sqrt{2}}(\psi_{\rm R} + \psi_{\rm R}^*)\end{array}\right],
\end{aligned}$$

which is invariant under the transformation

$$\begin{aligned}
\left[\begin{array}{cc} \frac{1}{\sqrt{2}}(\psi_{\rm L} + \psi_{\rm L}^*), & \frac{\imath}{\sqrt{2}}(\psi_{\rm L} - \psi_{\rm L}^*)\end{array}\right] &\to \left[\begin{array}{cc} \frac{1}{\sqrt{2}}(\psi_{\rm L} + \psi_{\rm L}^*), & \frac{\imath}{\sqrt{2}}(\psi_{\rm L} - \psi_{\rm L}^*)\end{array}\right] O_{\rm L}\,,\\
\left[\begin{array}{cc} \frac{1}{\sqrt{2}}(\psi_{\rm R} - \psi_{\rm R}^*), & \frac{\imath}{\sqrt{2}}(\psi_{\rm R} + \psi_{\rm R}^*)\end{array}\right] &\to \left[\begin{array}{cc} \frac{1}{\sqrt{2}}(\psi_{\rm R} - \psi_{\rm R}^*), & \frac{\imath}{\sqrt{2}}(\psi_{\rm R} + \psi_{\rm R}^*)\end{array}\right] O_{\rm R} \qquad (4.43)
\end{aligned}$$

with $O_{\rm R}\,, O_{\rm L} \in \mathrm{O}\,(2N_{\rm f})$. However the axial anomaly, the Jacobian of the transformation is given by $\det{}^\nu(O_{\rm R}\,O_{\rm L}\,)$. Thus the theory is covariant under the global symmetry group $O(2N_{\rm f}) \times O(2N_{\rm f})$. In this basis the chiral condensate reads

$$\begin{aligned}
\Sigma &= \left\langle \mathrm{tr}\,\bar{\psi}\psi \right\rangle = \left\langle \mathrm{tr}\,\psi_{\rm L}^\dagger \psi_{\rm R} + \mathrm{tr}\,\psi_{\rm R}^\dagger \psi_{\rm L} \right\rangle \qquad (4.44)\\
&= \frac{1}{2}\left\langle \mathrm{tr}\left[\begin{array}{c} \frac{1}{\sqrt{2}}(\psi_{\rm L}^T + \psi_{\rm L}^\dagger) \\ \frac{\imath}{\sqrt{2}}(\psi_{\rm L}^T - \psi_{\rm L}^\dagger)\end{array}\right]\left[\begin{array}{cc} \frac{1}{\sqrt{2}}(\psi_{\rm R} - \psi_{\rm R}^*), & \frac{\imath}{\sqrt{2}}(\psi_{\rm R} + \psi_{\rm R}^*)\end{array}\right]\right\rangle,\\
&\quad - \frac{1}{2}\left\langle \mathrm{tr}\left[\begin{array}{c} \frac{1}{\sqrt{2}}(\psi_{\rm R}^T - \psi_{\rm R}^\dagger) \\ \frac{\imath}{\sqrt{2}}(\psi_{\rm R}^T + \psi_{\rm R}^\dagger)\end{array}\right]\left[\begin{array}{cc} \frac{1}{\sqrt{2}}(\psi_{\rm L} + \psi_{\rm L}^*), & \frac{\imath}{\sqrt{2}}(\psi_{\rm L} - \psi_{\rm L}^*)\end{array}\right]\right\rangle.
\end{aligned}$$

Thus we find again the condition

$$O_{\rm R}^{-1} = O_{\rm L}^T \qquad (4.45)$$

which is equivalent to the symmetry breaking pattern is $O(2N_{\rm f}) \times O(2N_{\rm f}) \to O(2N_{\rm f})$. The corresponding effective chiral partition function in the lowest order is

$$Z = \int_{U \in O(2N_{\rm f})} d\mu(U) \det{}^{\nu} U e^{-\mathcal{L}_\chi} \tag{4.46}$$

where $\mathcal{L}_\chi$ is given by

$$\Sigma V \mathrm{tr} \begin{bmatrix} M & 0 \\ 0 & M \end{bmatrix} U. \tag{4.47}$$

The variables M and V have still the same meaning as the diagonal mass matrix and the space-time volume, respectively.

RMT

Because of the existence of the zero mode we need to treat odd and even size matrices differently we will discriminate the two cases by $\nu = 0, 1$. Then we consider the RMT model

$$P(W) d[W] = \exp\left[-n \mathrm{tr}\, W W^\dagger\right] \prod_{1 \le i < j \le 2n+\nu} \frac{2n}{\pi} d\,\mathrm{Re}\; W_{ij}\, d\,\mathrm{Im}\; W_{ij} \tag{4.48}$$

with an anti-symmetric complex matrix $W = -W^T \in \mathbb{C}^{(2n+\nu)\times(2n+\nu)}$ and the Dirac random matrix

$$D = \begin{bmatrix} 0 & W \\ -W^\dagger & 0 \end{bmatrix}. \tag{4.49}$$

Analogously to the discussion in the subsection 4.3.1 we can quasi-diagonalize W, i.e.

$$W \;=\; \begin{cases} U(\tau_2 \otimes \Lambda) U^T, & \text{for } \nu = 0, \\ U \mathrm{diag}\,[\tau_2 \otimes \Lambda, 0] U^T, & \text{for } \nu = 1 \end{cases} \tag{4.50}$$

with a positive definite, diagonal matrix $\Lambda \in \mathbb{R}_+^n$ and the unitary matrix $U \in \mathrm{U}\,(2n+\nu)/[\mathrm{SU}^n(2) \times \mathrm{U}^{\,\nu}(1)]$. The division with respect to the subgroup $\mathrm{SU}^n(2)$ is a result of the identity $\widetilde{U} \tau_2 \widetilde{U}^T = \tau_2$ for all $\widetilde{U} \in \mathrm{SU}(2)$. Moreover we have to divide by $\mathrm{U}\,(1)$ if $\nu = 1$ since the matrix W has a generic zero mode in this case.

The matrix $\tau_2 \otimes \Lambda$ has as eigenvalues $\pm\lambda_j$. The calculation of the Haar

measure is very similar to the one for the ($\beta = 1,\ d = 2$) case,

$$\begin{aligned}\mathrm{tr}\, dW dW^\dagger &= 2\mathrm{tr}\, d\Lambda^2 \\ &+\mathrm{tr}\, \left(U^\dagger dU(\tau_2\otimes\Lambda) + (\tau_2\otimes\Lambda)(U^\dagger dU)^T\right)\left(U^\dagger dU(\tau_2\otimes\Lambda) + (\tau_2\otimes\Lambda)(U^\dagger dU)^T\right)^\dagger \\ &= \sum_{1\le i\le n}(2d\lambda_i^2 + 8\lambda_i^2(U^\dagger dU)_{ii}^2)\end{aligned} \tag{4.51}$$

$$+\sum_{1\le i<j\le n}\left[\ (U^\dagger dU)_{ij},\quad (U^\dagger dU)_{ij}^*\ \right]\begin{bmatrix} \lambda_i\lambda_j \mathbb{1}_2\otimes\mathbb{1}_2 & -\dfrac{\lambda_i^2+\lambda_j^2}{2}\tau_2\otimes\tau_2 \\ -\dfrac{\lambda_i^2+\lambda_j^2}{2}\tau_2\otimes\tau_2 & \lambda_i\lambda_j\mathbb{1}_2\otimes\mathbb{1}_2\end{bmatrix}\begin{bmatrix}(U^\dagger dU)_{ij}, \\ (U^\dagger dU)_{ij}^*\end{bmatrix}$$

for $\nu = 0$ and

$$\begin{aligned}\mathrm{tr}\, dW dW^\dagger &= 2\mathrm{tr}\, d\Lambda^2 \\ &+\mathrm{tr}\, \left(U^\dagger dU\,\mathrm{diag}\,[\tau_2\otimes\Lambda, 0] + \mathrm{diag}\,[\tau_2\otimes\Lambda, 0](U^\dagger dU)^T\right) \\ &\times\left(U^\dagger dU\,\mathrm{diag}\,[\tau_2\otimes\Lambda, 0] + \mathrm{diag}\,[\tau_2\otimes\Lambda, 0](U^\dagger dU)^T\right)^\dagger \\ &= \sum_{1\le i\le n}(2d\lambda_i^2 + 2\lambda_i^2\left[4(U^\dagger dU)_{ii}^2 + |U^\dagger dU|_{i,2n+1}^2 + |U^\dagger dU|_{i+n,2n+1}^2\right])\end{aligned} \tag{4.52}$$

$$+\sum_{1\le i<j\le n}\left[\ (U^\dagger dU)_{ij},\quad (U^\dagger dU)_{ij}^*\ \right]\begin{bmatrix} \lambda_i\lambda_j \mathbb{1}_2\otimes\mathbb{1}_2 & -\dfrac{\lambda_i^2+\lambda_j^2}{2}\tau_2\otimes\tau_2 \\ -\dfrac{\lambda_i^2+\lambda_j^2}{2}\tau_2\otimes\tau_2 & \lambda_i\lambda_j\mathbb{1}_2\otimes\mathbb{1}_2\end{bmatrix}\begin{bmatrix}(U^\dagger dU)_{ij}, \\ (U^\dagger dU)_{ij}^*\end{bmatrix}$$

for $\nu = 1$. The elements $(U^\dagger dU)_{ii}$ correspond to the remaining degrees of the subgroup $\mathrm{U}^n(2)$ which are located on the block-diagonal of U and the 4-dim complex vectors $(U^\dagger dU)_{ij}$ $(1 \le i < j \le n)$ collectively denote the four independent complex matrix elements of the 2×2-block connecting λ_i and λ_j. Hence, the joint probability density is

$$p(\Lambda)\prod_{1\le j\le 2n} d\lambda_j \propto \Delta_n^4(\Lambda^2)\prod_{1\le j\le n}\exp\left[-n\lambda_j^2\right]\lambda_j d\lambda_j \tag{4.53}$$

for $\nu = 0$. For $\nu = 1$ there is an additional zero eigenvalue, thus the distribution of the non-zero eigenvalues is

$$p(\Lambda)\prod_{1\le j\le 2n} d\lambda_j \propto \Delta_n^4(\Lambda^2)\prod_{1\le j\le n}\exp\left[-n\lambda_j^2\right]\lambda_j^5 d\lambda_j. \tag{4.54}$$

Notice that the densities (4.53) and (4.54) are the same as for chiral GSE with the index, $\nu = \pm 1/2$.

The partition function with $N_{\rm f}$ fermionic flavors,

$$Z(M) = \int \prod_{j=1}^{N_{\rm f}} \det(D + m_j) P(W) d[W], \tag{4.55}$$

can be again mapped to flavor space via the rectangular $(2n+\nu) \times N_{\rm f}$ matrices V_R and V_L comprising only Grassmann variables. Integrating over W we find the analogue of Eq. (4.36),

$$\begin{aligned} Z(M) &\propto \int \exp\left[-\frac{1}{4n}\mathrm{tr}\,(V_L V_R^\dagger + V_R^* V_L^T)(V_R V_L^\dagger + V_L^* V_R^T) + \mathrm{tr}\, M(V_R^\dagger V_R + V_L^\dagger V_L)\right] d[V] \\ &\propto \int \exp\left[\frac{1}{4n}\mathrm{tr}\,(\tau_1 \otimes \mathbb{1}_{N_{\rm f}})\sigma(\tau_1 \otimes \mathbb{1}_{N_{\rm f}})\sigma^T + \mathrm{tr}\,(\mathbb{1}_2 \otimes M)\sigma\right] d[V] \end{aligned} \tag{4.56}$$

with

$$\sigma = \begin{bmatrix} -V_L^T \\ V_R^\dagger \end{bmatrix} \begin{bmatrix} V_R, & V_L^* \end{bmatrix}. \tag{4.57}$$

The superbosonization formula [127], as well as E.1 for details, replaces σ by a unitary matrix in $\mathrm{U}\,(2N_{\rm f})$ which yields

$$Z(\widehat{M}) \propto \int\limits_{\mathrm{U}\,(2N_{\rm f})} \exp\left[n\mathrm{tr}\,(\tau_1 \otimes \mathbb{1}_{N_{\rm f}})U(\tau_1 \otimes \mathbb{1}_{N_{\rm f}})U^T + \mathrm{tr}\,(\mathbb{1}_2 \otimes \widehat{M})U\right] \det{}^{-2n-\nu} U d\mu(U). \tag{4.58}$$

We obtain the microscopic limit by taking n to infinity which gives the saddlepoint equation

$$U^{-1} = (\tau_1 \otimes \mathbb{1}_{N_{\rm f}})U^T(\tau_1 \otimes \mathbb{1}_{N_{\rm f}}). \tag{4.59}$$

and is equivalent to the restriction on the group $\mathrm{O}(2N_{\rm f})$, i.e.

$$\begin{aligned} Z(\widehat{M}) &= \int\limits_{\mathrm{O}(2N_{\rm f})} \exp\left[\mathrm{tr}\,(\mathbb{1}_2 \otimes \widehat{M})U\right] \det{}^{-\nu} U d\mu(U) \\ &= \int\limits_{\mathrm{O}(2N_{\rm f})} \exp\left[\frac{1}{2}\mathrm{tr}\,(\mathbb{1}_2 \otimes \widehat{M})(U + U^{-1})\right] \det{}^{-\nu} U d\mu(U). \end{aligned} \tag{4.60}$$

It is important to point out that the partition function for $\nu = 0$ remains finite in the limit $\widehat{M} \to 0$ but vanishes for $\nu = 1$ as $M \to 0$). When summing over

the index ν we project the integral (4.60) to an integral over $\mathrm{SO}(2N_\mathrm{f})$ since the determinant of U takes only the values ± 1.

4.4 Lattice models of 2d QCD of naive fermions and $g \to \infty$

In this section we consider the microscopic limit of naive fermions in the strong coupling limit and their corresponding RMT. This means that the Wilson gauge action and any modification of it vanishes. Thus the gauge group elements on the lattice links are distributed by the Haar-measure of the gauge group, only. We compare our predictions via RMT with 2-dim lattice simulations in the strong coupling limit.

4.4.1 General lattice model

The covariant derivatives can be readily constructed via the translation operators. Before we are doing so we introduce the lattice. Let $|j\rangle$ be the j'th site in one direction of a lattice written in Dirac's bra-ket notation. Then the dual vector is $\langle j|$. The translation operator of a $L_1 \times L_2$ lattice in direction μ is given by

$$T_\mu = \begin{cases} \sum\limits_{\substack{1\le i\le L_1\\ 1\le j\le L_2}} U_{1ij} \otimes |i\rangle\langle i+1| \otimes |j\rangle\langle j|, & \mu = 1, \\ \sum\limits_{\substack{1\le i\le L_1\\ 1\le j\le L_2}} U_{2ij} \otimes |i\rangle\langle i| \otimes |j\rangle\langle j+1|, & \mu = 2. \end{cases} \tag{4.61}$$

The matrices $U_{\mu ij}$ are given in some representation of the special unitary group $\mathrm{SU}(N_\mathrm{c})$ and weighted with the Haar-measure on $\mathrm{SU}(N_\mathrm{c})$. Hence, the translation operators T_μ are unitary.

The naive Dirac operator on the lattice is

$$\mathcal{D} = \begin{bmatrix} 0 & \mathcal{W} \\ -\mathcal{W}^\dagger & 0 \end{bmatrix} = \begin{bmatrix} 0 & T_x - T_x^\dagger + \imath(T_y - T_y^\dagger) \\ T_x - T_x^\dagger - \imath(T_y - T_y^\dagger) & 0 \end{bmatrix} \tag{4.62}$$

Due to the lattice structure an additional symmetry can exist in each direction if the number of the sites in this direction is even. Thereby we distinguish three cases of a two dimensional lattice. Each of these cases will show a different universal behavior as we will see in the ensuing sections. Hence we expect three universality cases for each of the two Dyson indices $\beta = 1, 4$. For $\beta = 2$

we will find that the odd-odd and the even-even case give the same result resulting into two universality classes. We will see that the mixed case with one odd and one even number of lattice sites yields an additional symmetry. Moreover we assume that both lengths L_1 and L_2 are larger than 2 because only then the lattice theory exhibits generic behavior in the low lying Dirac spectrum.

Consider L_μ is even. Then the operator

$$\Gamma_5^{(\mu)} = \begin{cases} \sum\limits_{\substack{1\le i\le L_1\\ 1\le j\le L_2}} (-1)^i \mathbb{1}_{N_c} \otimes |i\rangle\langle i| \otimes |j\rangle\langle j|, & \mu = 1, \\ \sum\limits_{\substack{1\le i\le L_1\\ 1\le j\le L_2}} (-1)^j \mathbb{1}_{N_c} \otimes |i\rangle\langle i| \otimes |j\rangle\langle j|, & \mu = 2 \end{cases} \tag{4.63}$$

fulfils the following relation

$$\Gamma_5^{(\mu)} T_\omega \Gamma_5^{(\mu)} = (-1)^{\delta_{\mu\omega}} T_\omega. \tag{4.64}$$

This operator incorporates the color structure in the first part of the tensor product as well as two projectors in the x and y directions. Note we need an even number of sites in the direction μ for (4.64) to hold. $\Gamma_5^{(\mu)}$ should not be confused with the spinorial γ_5. In the case that we are considering a direction with an even number of lattice sites it just assign a $+$ sign to an even site and respectively a $-$ sign to an odd site. In the case of an even-even lattice the product $\Gamma_5^{(1)}\Gamma_5^{(2)} = \eta_5$ where η_5 is the staggered version of γ_5.

Assuming L_1 and L_2 to be odd, $\mathcal{W}$ is simply given by

$$\mathcal{W} = T_1 - T_1^\dagger + \imath(T_2 - T_2^\dagger) \tag{4.65}$$

with no additional symmetries.

If only one direction has an even number of sites (e.g. L_1 without loss of generality) and the other one an odd number W has a block structure

$$\mathcal{W} = \begin{bmatrix} \imath S_2^{(\mathrm{e}|\mathrm{e})} & S_1^{(\mathrm{e}|\mathrm{o})} \\ -(S_1^{(\mathrm{e}|\mathrm{o})})^\dagger & \imath S_2^{(\mathrm{o}|\mathrm{o})} \end{bmatrix}. \tag{4.66}$$

The operators $S_2^{(\mathrm{e}|\mathrm{e})}, S_2^{(\mathrm{o}|\mathrm{o})}$ are submatrices of $T_2 - T_2^\dagger$ and accordingly the operator $S_1^{(\mathrm{e}|\mathrm{o})}$ is a submatrix of $T_1 - T_1^\dagger$ and should not be confused with the individual matrices T_1, T_2 of (4.65). The operators $S_2^{(\mathrm{e}|\mathrm{e})}$ and $S_2^{(\mathrm{o}|\mathrm{o})}$ are anti-Hermitian while $S_1^{(\mathrm{e}|\mathrm{o})}$ has no Hermiticity condition. The labels "e" and "o"

refer to even and odd sites in the 1-direction.

In the case that we have in both directions an even number of sites we additionally get a chiral structure

$$\mathcal{W} = \left[\begin{array}{cc|cc} & & \imath S_2^{(\mathrm{ee|eo})} & S_1^{(\mathrm{ee|oe})} \\ \multicolumn{2}{c|}{0} & S_1^{(\mathrm{oo|eo})} & \imath S_2^{(\mathrm{oo|oe})} \\ \hline \imath (S_2^{(\mathrm{ee|eo})})^\dagger & -(S_1^{(\mathrm{oo|eo})})^\dagger & \multicolumn{2}{c}{} \\ -(S_1^{(\mathrm{ee|oe})})^\dagger & \imath (S_2^{(\mathrm{oo|oe})})^\dagger & \multicolumn{2}{c}{0} \end{array}\right], \tag{4.67}$$

where $S_2^{(\mathrm{ee|eo})}$, $S_1^{(\mathrm{ee|oe})}$, $S_1^{(\mathrm{oo|eo})}$ and $S_2^{(\mathrm{oo|oe})}$ fulfil no Hermiticity conditions. The double labels like "(ee|eo)" refer to the even-odd structure of each lattice direction. This label should be understood as in the x-direction an even site is connected to an even site while in the y-direction an odd site is connected to an even site. This means that there is a shift in the y-direction by $T_2 - T_2^\dagger$.

In the ensuing sections we will consider the combination of the symmetries of the continuous Dirac operator, i.e. the choice of the gauge group and its representation (see Sec. 4.2), and one of the three structures (4.65), (4.66) and (4.67) resulting from the kind of discretization.

4.4.2 SU(2) and fermions in the fundamental representation

The translation operators are quaternion for two-color fermions in the fundamental representation, i.e.

$$T_\mu^* = (\tau_2 \otimes \mathbb{1}_{L_1 L_2}) T_\mu (\tau_2 \otimes \mathbb{1}_{L_1 L_2}). \tag{4.68}$$

This symmetry carries over to all matrices in the three cases (4.65), (4.66) and (4.67).

Odd-odd

Let L_1 and L_2 be odd. Then the operator $(\tau_2 \otimes \mathbb{1}_{L_1 L_2})\mathcal{W}$ is complex symmetric and $2L_1L_2 \times 2L_1L_2$ dimensional as we can deduce from (4.65) and (4.68). Hence we expect a behaviour like the random matrix model discussed in Sec. 4.3.1. This includes:

- The chiral symmetry breaking pattern for N_f dynamical fermions is $\mathrm{USp}(2N_\mathrm{f}) \times \mathrm{USp}(2N_\mathrm{f}) \to \mathrm{USp}(2N_\mathrm{f})$.

While the following statements hold for the Dirac spectrum of the quenched theory:

- It corresponds to the symmetry CI in the Cartan classification [45, 48] and is thus, one of the Bogoliubov-deGennes ensembles.
- The level repulsion goes with $|\lambda_i^2 - \lambda_j^2|$.
- The repulsion of the levels from the origin goes with $|\lambda_i|$.
- There is no degeneracy of the levels of $\mathcal{D}$.
- There are no generic zero modes.

In particular we can easily say what the microscopic level density is, namely

$$\rho(x) = \frac{x}{2}\left[J_1^2(x) - J_0(x)J_2(x)\right] + \frac{1}{2}J_0(x)J_1(x). \tag{4.69}$$

We only have to make use of the known result for the chiral ensemble [125] with $\beta = 1$ and $\nu = 1$ see (4.89). The comparison of this density with 2-dim lattice simulations of naive-fermions is shown in Fig. 4.1. The agreement is for the lowest eigenvalue perfect but gets worse beyond the second one. This means the Thouless energy is of the order of the eigenvalue spacing. The Thouless energy, in units of the eigenvalue spacing, does not increase when increasing the lattice size since we consider a 2-dim theory where this energy is independent of the system size.

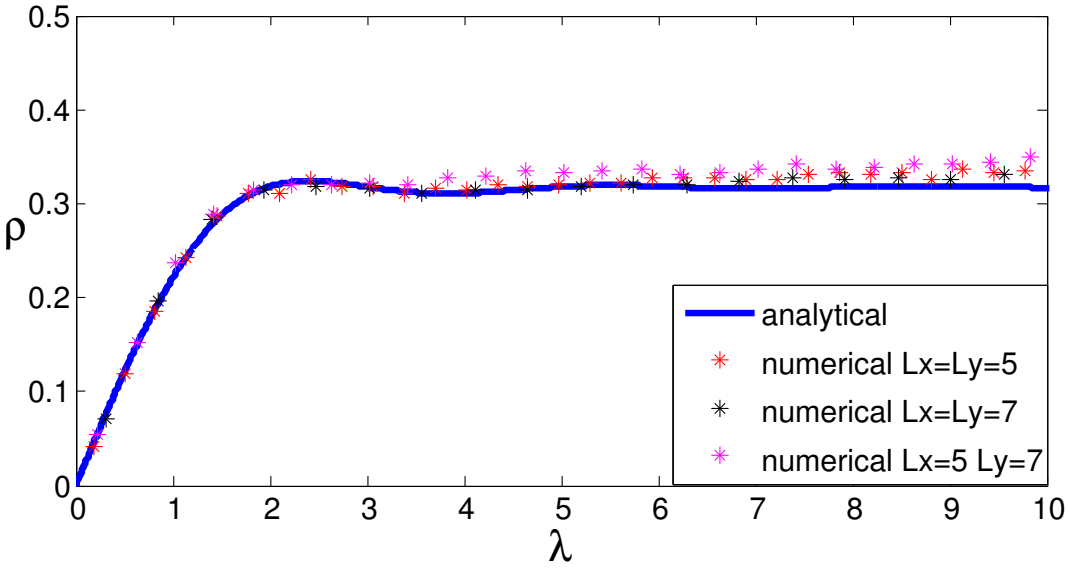

Figure 4.1: Spectral density for L_1, L_2 odd, SU (2) fundamental

Odd-even

Assuming L_1 to be even and L_2 to be odd, to simplify the symmetry relations we introduce the operator $\widetilde{\mathcal{W}}$ defined by

$$(\mathrm{diag}\,(-\imath,1)\otimes \mathbb{1}_{L_1L_2})\mathcal{W}(\mathrm{diag}\,(1,\imath)\otimes \mathbb{1}_{L_1L_2}) = \begin{bmatrix} T_2^{(\mathrm{e}|\mathrm{e})} & T_1^{(\mathrm{e}|\mathrm{o})} \\ -(T_1^{(\mathrm{e}|\mathrm{o})})^\dagger & -T_2^{(\mathrm{o}|\mathrm{o})} \end{bmatrix} = \widetilde{\mathcal{W}}. \tag{4.70}$$

This operator is in the Lie algebra $\mathrm{usp}(2L_1L_2)$ (because of (4.66) and (4.68)), i.e.

$$\widetilde{\mathcal{W}}^\dagger = -\widetilde{\mathcal{W}} \text{ and } \widetilde{\mathcal{W}}^* = (\tau_2\otimes \mathbb{1}_{L_1L_2})\widetilde{\mathcal{W}}(\tau_2\otimes \mathbb{1}_{L_1L_2}). \tag{4.71}$$

We introduced $\widetilde{\mathcal{W}}$ since $\mathcal{W}\in \imath\mathrm{usp}(2L_1L_2)$. usp is the Lie algebra of the compact symplectic group. Note that the minus sign of $T_2^{(\mathrm{o}|\mathrm{o})}$ can be absorbed but since our starting point is (4.66) we will keep it in order not to introduce new notation. The reason we introduce the diagonal matrices is because they make the symmetries more easily read off. The diagonal unitary matrices in Eq. (4.70) do not change the global symmetries since we have still the chiral structure for D. Therefore the transformation (4.70) is only a unitary transformation for $\mathcal{D}\to(\mathrm{diag}\,(-\imath,1,1,-\imath)\otimes \mathbb{1}_{L_1L_2})\mathcal{D}(\mathrm{diag}\,(\imath,1,1,\imath)\otimes \mathbb{1}_{L_1L_2})$.

We expect a universal behavior of the low lying spectrum of the Dirac operator $\mathcal{D}$ such that the operator $\mathcal{W}$ can be replaced by a Gaussian distributed random matrix W in the Lie algebra $\mathrm{usp}(2L_1L_2)$. This symmetry class has the following properties

- The chiral symmetry breaking pattern for N_f dynamical flavors is $\mathrm{USp}\,(4N_\mathrm{f})\to \mathrm{USp}\,(2N_\mathrm{f})\times \mathrm{USp}\,(2N_\mathrm{f})$.

While the following holds for the quenched theory:

- It corresponds to the symmetry class C in the Cartan classification [45] and coincides with the Lie-algebra $\mathrm{usp}(2N)$. Notice that in our conventions we differ by an overall factor of i with respect to [128]. The Lie-algebra $\mathrm{usp}(2N)$ is comprised by the anti-self dual, anti-hermitian matrices.
- The level repulsion goes with $|\lambda_i^2-\lambda_j^2|^2$.
- The repulsion of the levels from the origin goes with $|\lambda_i|^2$.
- There is a double degeneracy of the levels of D due to the interplay of the chirality of D and the fact that $\widetilde{\mathcal{W}}$ is quaternion anti-Hermitian.

- There are no generic zero modes.

The symmetry breaking pattern can be proven in the same way as in the continuum. Because of the anti-Hermiticity of $\widetilde{\mathcal{W}}$ and the complex conjugation properties (4.71) the Dirac kinetic part of the Lagrangian is

$$\begin{aligned}\mathcal{L} &= \operatorname{tr}\bar{\psi}\mathcal{D}\psi = \operatorname{tr}\psi_{\mathrm{L}}^{\dagger}\widetilde{\mathcal{W}}\psi_{\mathrm{L}} - \operatorname{tr}\psi_{\mathrm{R}}^{\dagger}\widetilde{\mathcal{W}}^{\dagger}\psi_{\mathrm{R}}\,, \qquad (4.72)\\ &= \frac{1}{2}\mathrm{tr}\begin{bmatrix}\psi_{\mathrm{R}}^{T}\\ \psi_{\mathrm{L}}^{T}\\ -\psi_{\mathrm{R}}^{\dagger}\tau_2\\ -\psi_{\mathrm{L}}^{\dagger}\tau_2\end{bmatrix}\tau_2\mathcal{W}\begin{bmatrix}\psi_{\mathrm{R}} & \psi_{\mathrm{L}} & \tau_2\psi_{\mathrm{R}}^{*} & \tau_2\psi_{\mathrm{L}}^{*}\end{bmatrix}\begin{bmatrix}0 & -\mathbb{1}_{2N_{\mathrm{f}}}\\ \mathbb{1}_{2N_{\mathrm{f}}} & 0\end{bmatrix},\end{aligned}$$

which has $\mathrm{USp}\,(4N_{\mathrm{f}})$ invariance. The chiral condensate

$$\begin{aligned}\Sigma &= \left\langle\operatorname{tr}\bar{\psi}\psi\right\rangle = \left\langle\operatorname{tr}\psi_{\mathrm{L}}^{\dagger}\psi_{\mathrm{R}} + \operatorname{tr}\psi_{\mathrm{R}}^{\dagger}\psi_{\mathrm{L}}\right\rangle, \qquad (4.73)\\ &= -\frac{1}{2}\mathrm{tr}\begin{bmatrix}\psi_{\mathrm{R}}^{T}\\ \psi_{\mathrm{L}}^{T}\\ -\psi_{\mathrm{R}}^{\dagger}\tau_2\\ -\psi_{\mathrm{L}}^{\dagger}\tau_2\end{bmatrix}\tau_2\begin{bmatrix}\psi_{\mathrm{R}} & \psi_{\mathrm{L}} & \tau_2\psi_{\mathrm{R}}^{*} & \tau_2\psi_{\mathrm{L}}^{*}\end{bmatrix}\underbrace{\begin{bmatrix}0 & 0 & 0 & \mathbb{1}_{N_{\mathrm{f}}}\\ 0 & 0 & \mathbb{1}_{N_{\mathrm{f}}} & 0\\ 0 & \mathbb{1}_{N_{\mathrm{f}}} & 0 & 0\\ \mathbb{1}_{N_{\mathrm{f}}} & 0 & 0 & 0\end{bmatrix}}_{\mathrm{A}}\end{aligned}$$

breaks chiral symmetry down to $\mathrm{USp}\,(4N_{\mathrm{f}}) \to \mathrm{USp}\,(2N_{\mathrm{f}}) \times \mathrm{USp}\,(2N_{\mathrm{f}})$. Diagonalizing the matrix A by a $\mathrm{USp}\,(4N_{\mathrm{f}})$ matrix which can be absorbed in the fields we see that diagonal matrix is $\mathrm{diag}\,(1,1,-1,-1)$ which makes obvious the pattern of chiral symmetry breaking. This symmetry breaking pattern is equal to the one of 3-dim continuum QCD with two colors and fundamental fermions [129]. Notice that chiral symmetry is broken in three dimensions while we still have in our two dimensional case chiral symmetry. A trivial one though due to block structure (degeneracy) of the Dirac operator.

In RMT we replace $\widetilde{\mathcal{W}}$ by an anti-Hermitian quaternion matrix $\widetilde{W} \in \mathrm{usp}(2N)$. The microscopic level density can be easily deduced from the well-known joint probability density of the eigenvalues values of $\widetilde{W}$ [48],

$$p(\Lambda)\prod_{1\le j\le N} d\lambda_j \propto \Delta_N^2(\Lambda^2)\prod_{1\le j\le N}\exp\left[-N\lambda_j^2\right]\lambda_j^2 d\lambda_j. \qquad (4.74)$$

Since the joint probability density looks like the one for chiral GUE with index $\nu = 1/2$ we can use the well known result for the level density [53], which is

$$\rho(x) = \frac{1}{\pi} - \frac{\sin(2x)}{2\pi x}. \qquad (4.75)$$

We compare this level density with lattice simulations in Fig. 4.2. The agreement is only good below the average position of the first eigenvalue. The very small value of the Thouless energy may be the result of the small matrix size of the representation of the gauge group elements, namely SU (2), we are considering. Indeed the Thouless energy increases with an increasing number of colors, as we have seen from the simulations for the other universality classes.

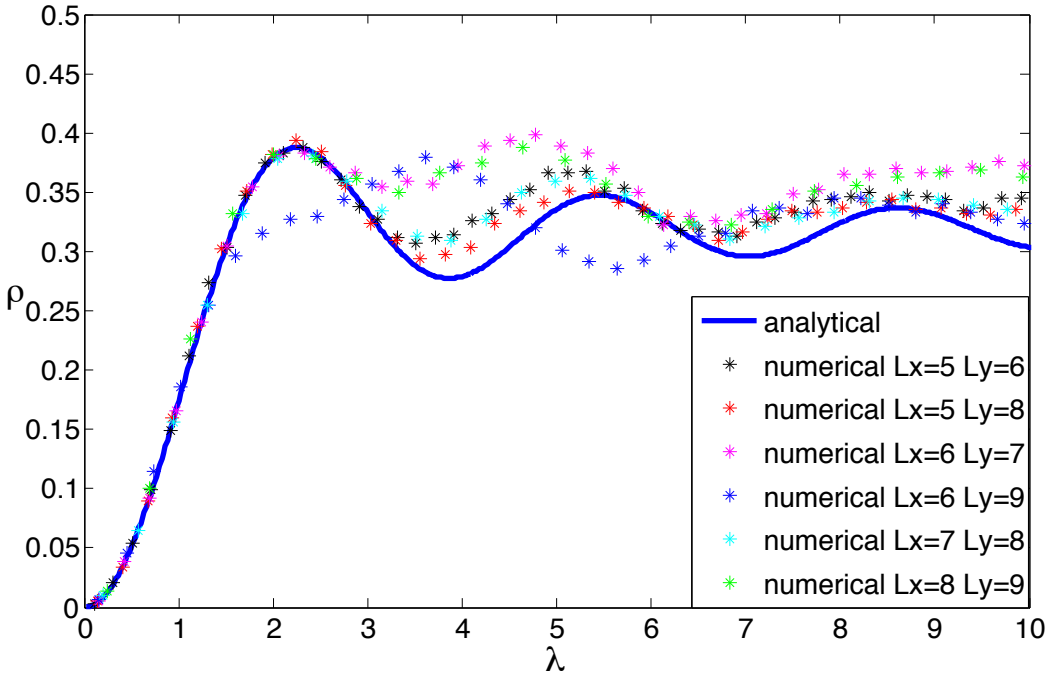

Figure 4.2: Spectral density for L_1 odd L_2 even, SU (2) fundamental. Apparently the Thouless energy (E_T) is $\leq \langle\lambda_1\rangle$ and consequently the agreement is poor ($E_T \propto N_c$).

Even-even

Finally we consider L_1 and L_2 even. The matrix

$$
\begin{aligned}
&(\mathrm{diag}\,(-\imath,1,\imath,1)\otimes \mathbb{1}_{L_1L_2/2})\mathcal{W}(\mathrm{diag}\,(1,-\imath,1,\imath)\otimes \mathbb{1}_{L_1L_2/2}) \\
&= \left[\begin{array}{cc|cc} & & T_2^{(\mathrm{ee|eo})} & T_1^{(\mathrm{ee|oe})} \\ & 0 & T_1^{(\mathrm{oo|eo})} & -T_2^{(\mathrm{oo|oe})} \\ \hline -(T_2^{(\mathrm{ee|eo})})^\dagger & -(T_1^{(\mathrm{oo|eo})})^\dagger & & \\ -(T_1^{(\mathrm{ee|oe})})^\dagger & (T_2^{(\mathrm{oo|oe})})^\dagger & & 0 \end{array}\right] = \left[\begin{array}{cc} 0 & \widetilde{\mathcal{W}} \\ -\widetilde{\mathcal{W}}^\dagger & 0 \end{array}\right]
\end{aligned}
\tag{4.76}
$$

has first of all an additional chiral structure. Once again we introduce the diagonal matrix in order to make the symmetries manifest. Note that the matrices $T_\mu^{(\mathrm{xx|xx})}$ are submatrices of the covariant derivatives $T_\mu - T_\mu^\dagger$. Second the operator $\widetilde{\mathcal{W}}$ is quaternion, i.e.

$$
\widetilde{\mathcal{W}}^* = (\tau_2 \otimes \mathbb{1}_{L_1L_2/2})\widetilde{\mathcal{W}}(\tau_2 \otimes \mathbb{1}_{L_1L_2/2}) \tag{4.77}
$$

with no further symmetries. This means we are in the universality class of chiral GSE, in particular:

- The chiral symmetry breaking pattern for N_f dynamical fermions is $\mathrm{SU}\,(2N_\mathrm{f}) \to \mathrm{SO}\,(2N_\mathrm{f})$

For the quenched theory:

- The level repulsion goes with $|\lambda_i^2 - \lambda_j^2|^4$.
- This ensemble is in the symmetry class of chiral GSE and is denoted by CII in the Cartan classification [45]. In the continuum limit we will have a doubling of flavors.
- The repulsion of the levels from the origin goes with $|\lambda_i|^3$. limit [130].)
- The levels of D are four times degenerate due to the Hermitian quaternion symmetry and the additional chiral structure.
- There are no generic zero modes.

Apart from the degeneracy this is exactly what we would expect for 4-dim continuum QCD with adjoint fermions [110].

The microscopic level density was derived in Ref. [126] and is

$$\rho(x) = x\left[J_0^2(2x) - J_{-1}(2x)J_1(2x)\right] - \frac{1}{2}J_0(2x)\int_0^{2x} J_0(\widetilde{x})d\widetilde{x}. \tag{4.78}$$

This density is compared to lattice simulations in Fig. 4.3. The agreement carries over to the second eigenvalue. Therefore the Thouless energy, as an energy scale, is equal to several eigenvalue spacings.

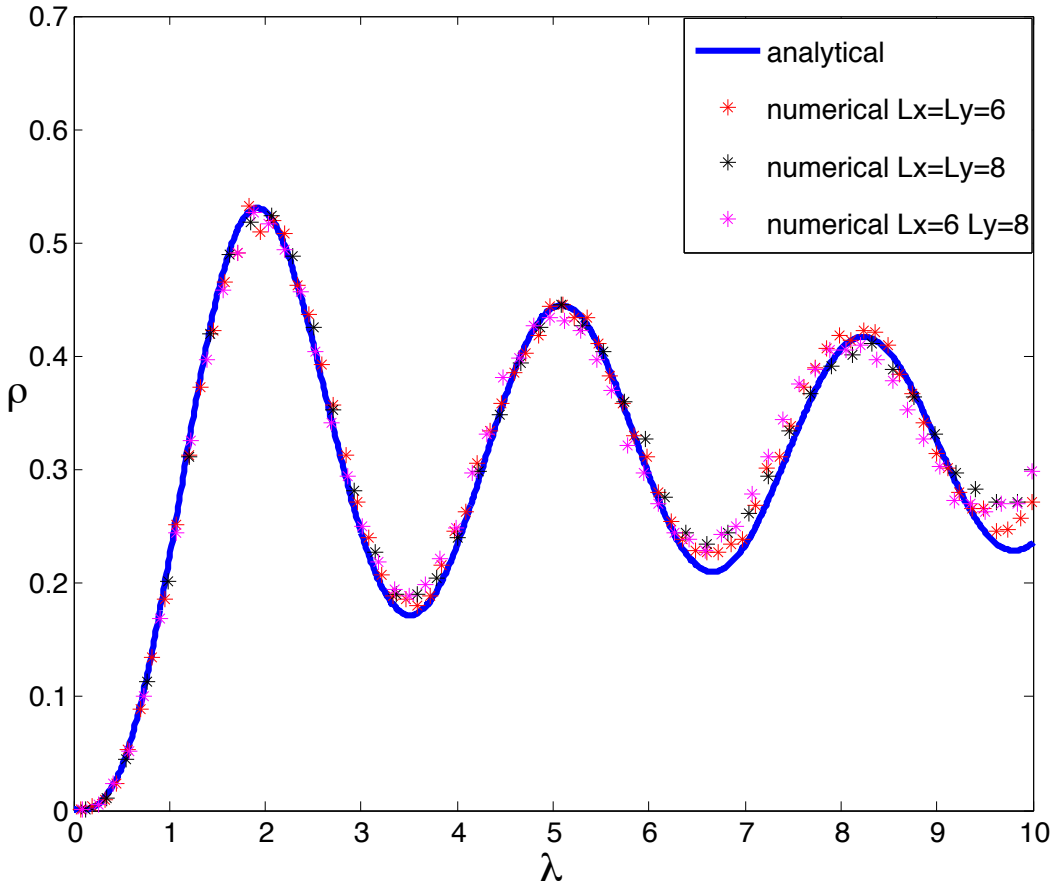

Figure 4.3: Spectral density for L_1, L_2 even, SU (2) fundamental

4.4.3 $\mathrm{SU}(N_\mathrm{c})$ and fermions in the adjoint representation

The translation operators are real for adjoint fermions,

$$T_\mu^* = T_\mu \tag{4.79}$$

and therefore build a subgroup of $\mathrm{O}((N_\mathrm{c}^2-1)L_1L_2)$. Again all matrices in the three cases (4.65), (4.66) and (4.67) inherit this symmetry.

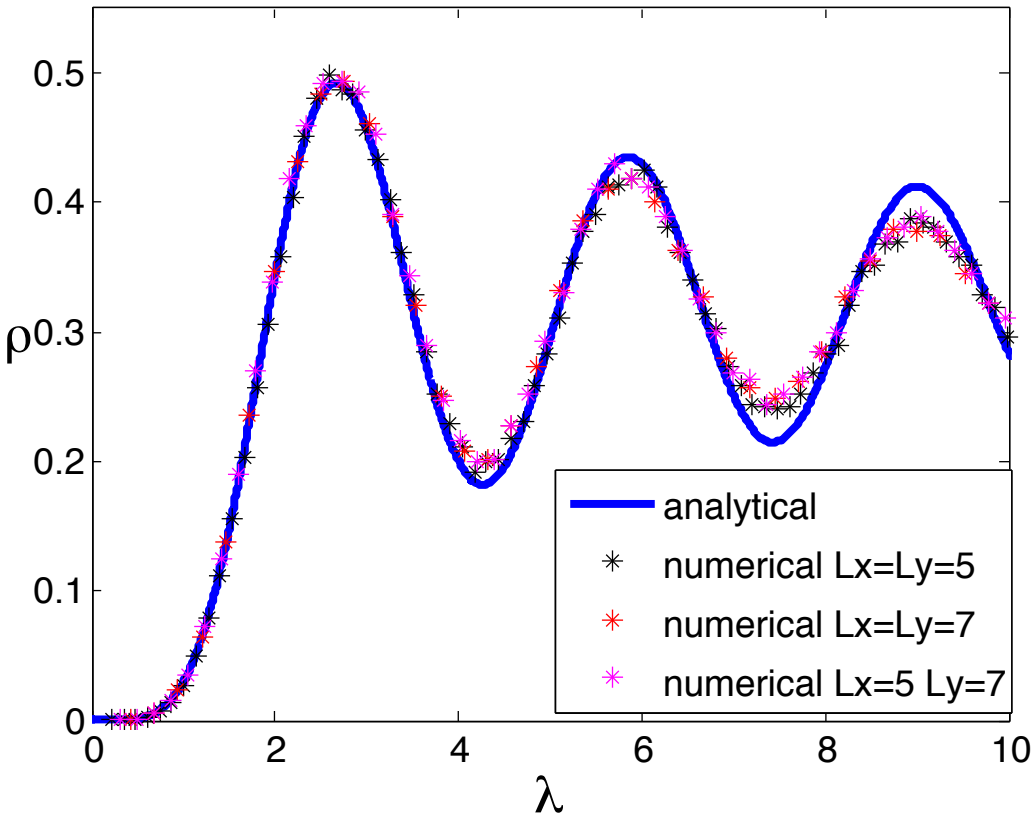

Figure 4.4: Spectral density for L_1, L_2 odd, SU (2) adjoint

Odd-odd

Let us consider first the case of odd L_1 and L_2. Then the operator $\mathcal{W}$ because of (4.65) and (4.79) is complex antisymmetric and we have to distinguish between an even and odd number of colors due to the generic zero modes. The resulting two random matrix ensembles are discussed in Sec. 4.3.2. We derived the following properties:

- The chiral symmetry breaking pattern for N_f dynamical fermions is both for even and odd N_c $\mathrm{SO}(2N_\mathrm{f}) \times \mathrm{SO}(2N_\mathrm{f}) \times \mathbb{Z}_2 \to \mathrm{SO}(2N_\mathrm{f}) \times \mathbb{Z}_2$.

While for the quenched theory:

- The symmetry class is $DIII$ in the Cartan classification [45, 48] and is also one of the Bogoliubov-de Gennes ensembles.
- The level repulsion goes with $|\lambda_i^2 - \lambda_j^2|^4$.
- The repulsion of the levels from the origin goes with $|\lambda_i|^5$ for N_c even and $|\lambda_i|$ for N_c odd.
- All levels of $\mathcal{D}$ are doubly degenerate due to the interplay of the anti-symmetry of $\mathcal{W}$ and of the chiral symmetry of $\mathcal{D}$.
- There are no generic zero modes for N_c odd and two generic zero modes of $\mathcal{D}$ for N_c even. For N_c even, one of the zero modes has positive chirality and the other one negative because $\mathcal{W}$ is an odd-dimensional anti-symmetric matrix which has always one generic zero mode.

The microscopic level density can be easily computed by the known result for chiral GSE [126], see also Eq. (4.78). Employing Eq. (4.78) for $\nu = \pm 1/2$ we have the level densities

$$\rho(x) = \frac{x}{2}\left[2J_1^2(2x) + J_0^2(2x) - J_0(2x)J_2(2x)\right] + \frac{1}{2}J_1(2x) \tag{4.80}$$

for N_c odd and

$$\rho(x) = \frac{x}{2}\left[2J_1^2(2x) + J_0^2(2x) - J_0(2x)J_2(2x)\right] - \frac{1}{2}J_1(2x) \tag{4.81}$$

for N_c even. These analytical results are compared with lattice simulations in Figs. 4.4 and 4.5 for even and odd color, respectively. There is good agreement between RMT predictions and lattice data up to the second and third eigenvalues. In particular the agreement becomes better when increasing the number of colors which confirms our expectation at the end of subsection 4.4.2 that the Thouless energy increases with an increasing matrix size of the chosen gauge group.

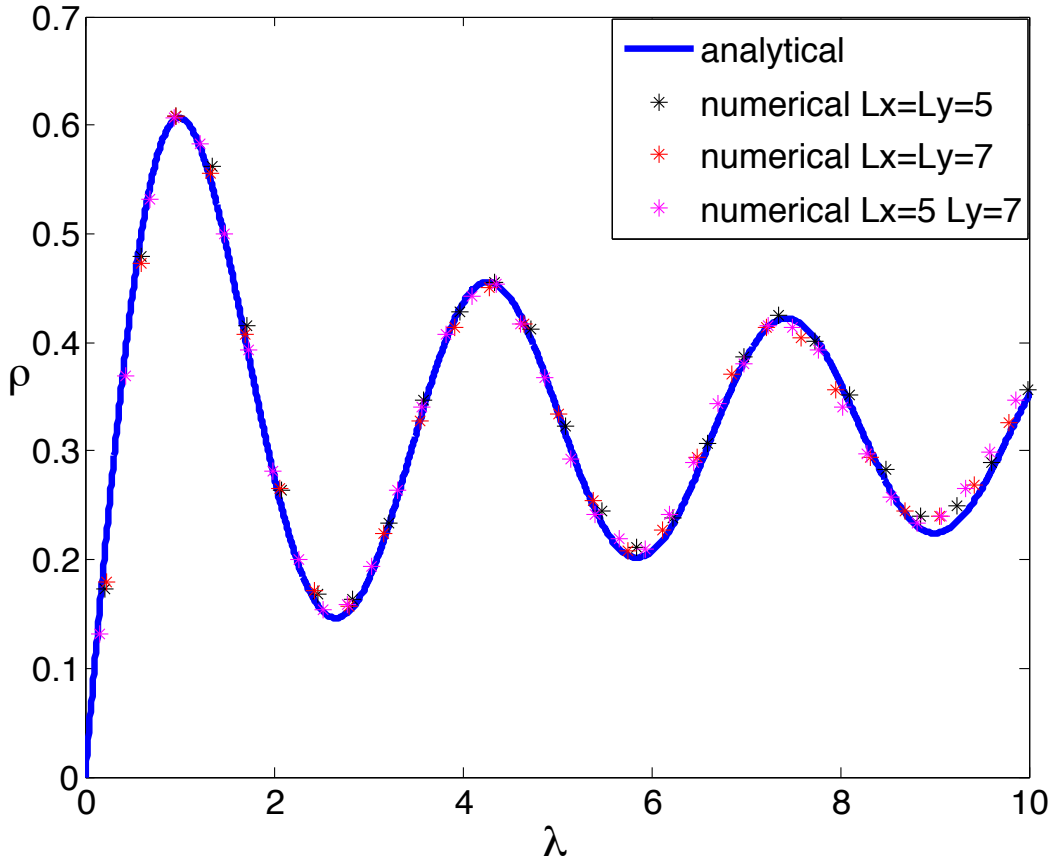

Figure 4.5: Spectral density for L_1, L_2 odd, SU (3) adjoint

Odd-even

Next we consider even L_1 and odd L_2. The introduction of the diagonal matrix makes the symmetries manifest. Then the operator

$$(\mathrm{diag}\,(-\imath,1)\otimes \mathbb{1}_{L_1L_2})\mathcal{W}(\mathrm{diag}\,(1,\imath)\otimes \mathbb{1}_{L_1L_2}) = \begin{bmatrix} T_2^{(\mathrm{e}|\mathrm{e})} & T_1^{(\mathrm{e}|\mathrm{o})} \\ -(T_1^{(\mathrm{e}|\mathrm{o})})^T & -T_2^{(\mathrm{o}|\mathrm{o})} \end{bmatrix} = \widetilde{\mathcal{W}} \tag{4.82}$$

because of (4.66) and (4.79) is real antisymmetric and thus, in the Lie algebra $\mathrm{o}\,(2(N_\mathrm{c}^2-1)L_1L_2)$, i.e.

$$\widetilde{\mathcal{W}}^T = -\widetilde{\mathcal{W}} \text{ and } \widetilde{\mathcal{W}}^* = \widetilde{\mathcal{W}}. \tag{4.83}$$

As will be discussed below the spectrum of $\mathcal{D}$:

- The chiral symmetry breaking pattern of the dynamical theory is $\mathrm{SO}\,(4N_{\mathrm{f}}) \to \mathrm{SO}\,(2N_{\mathrm{f}}) \times \mathrm{SO}\,(2N_{\mathrm{f}})$.

While for the quenched theory:

- The symmetry class is D in the Cartan classification [131] and is equal to the Lie algebra $\mathrm{o}(2N)$. Note that our matrix structure looks different than the one from [128] but the two matrices are equivalent up to a unitary transformation. The matrix of the unitary transformation is

$$\frac{1}{\sqrt{2}} \begin{pmatrix} 1 & 1 \\ i & -i \end{pmatrix}. \tag{4.84}$$

- The level repulsion goes with $|\lambda_i^2 - \lambda_j^2|^2$.
- There is no repulsion of the levels from the origin.
- There is a double degeneracy of the levels of $\mathcal{D}$ due to the combination of the antisymmetry of $\widetilde{\mathcal{W}}$ and the chiral structure of $\mathcal{D}$.
- There are no generic zero modes because in this case the matrix is always even dimensional.

Note that we have not distinguished between even and odd N_{c} because the size of $\mathcal{W}$ of the lattice theory is $2(N_{\mathrm{c}}^2 - 1)L_1L_2$ is always even and, thus we never have a generic zero mode of $\mathcal{W}$.

We observe that the symmetry breaking pattern is identical with the one obtained from 3-dim continuum QCD with adjoint fermions. It can be seen by considering the Lagrangian

$$\begin{aligned} \mathcal{L} &= \mathrm{tr}\,\bar{\psi}\mathcal{D}\psi = \mathrm{tr}\,\psi_{\mathrm{L}}^\dagger \widetilde{\mathcal{W}}\psi_{\mathrm{L}} - \mathrm{tr}\,\psi_{\mathrm{R}}^\dagger \widetilde{\mathcal{W}}^\dagger \psi_{\mathrm{R}} \\ &= \frac{1}{2}\mathrm{tr} \begin{bmatrix} \frac{1}{\sqrt{2}}(\psi_{\mathrm{R}}^T + \psi_{\mathrm{R}}^\dagger) \\ \frac{i}{\sqrt{2}}(\psi_{\mathrm{R}}^T - \psi_{\mathrm{R}}^\dagger) \\ \frac{1}{\sqrt{2}}(\psi_{\mathrm{L}}^T + \psi_{\mathrm{L}}^\dagger) \\ \frac{i}{\sqrt{2}}(\psi_{\mathrm{L}}^T - \psi_{\mathrm{L}}^\dagger) \end{bmatrix} \mathcal{W} \\ &\quad \times \begin{bmatrix} \frac{1}{\sqrt{2}}(\psi_{\mathrm{R}} + \psi_{\mathrm{R}}^*), & \frac{i}{\sqrt{2}}(\psi_{\mathrm{R}} - \psi_{\mathrm{R}}^*), & \frac{1}{\sqrt{2}}(\psi_{\mathrm{L}} + \psi_{\mathrm{L}}^*), & \frac{i}{\sqrt{2}}(\psi_{\mathrm{L}} - \psi_{\mathrm{L}}^*) \end{bmatrix} \end{aligned} \tag{4.85}$$

and the chiral condensate

$$\Sigma = \left\langle \mathrm{tr}\,\bar{\psi}\psi \right\rangle = \left\langle \mathrm{tr}\,\psi_{\mathrm{L}}^{\dagger}\psi_{\mathrm{R}} + \mathrm{tr}\,\psi_{\mathrm{R}}^{\dagger}\psi_{\mathrm{L}} \right\rangle \tag{4.86}$$

$$= \frac{1}{2\imath}\mathrm{tr}\begin{bmatrix} 0 & 0 & 0 & -\mathbb{1}_{N_{\mathrm{f}}} \\ 0 & 0 & \mathbb{1}_{N_{\mathrm{f}}} & 0 \\ 0 & -\mathbb{1}_{N_{\mathrm{f}}} & 0 & 0 \\ \mathbb{1}_{N_{\mathrm{f}}} & 0 & 0 & 0 \end{bmatrix} \begin{bmatrix} \frac{1}{\sqrt{2}}(\psi_{\mathrm{R}}^{T} + \psi_{\mathrm{R}}^{\dagger}) \\ \frac{\imath}{\sqrt{2}}(\psi_{\mathrm{R}}^{T} - \psi_{\mathrm{R}}^{\dagger}) \\ \frac{1}{\sqrt{2}}(\psi_{\mathrm{L}}^{T} + \psi_{\mathrm{L}}^{\dagger}) \\ \frac{\imath}{\sqrt{2}}(\psi_{\mathrm{L}}^{T} - \psi_{\mathrm{L}}^{\dagger}) \end{bmatrix}$$

$$\times \begin{bmatrix} \frac{1}{\sqrt{2}}(\psi_{\mathrm{R}} + \psi_{\mathrm{R}}^{*}), & \frac{\imath}{\sqrt{2}}(\psi_{\mathrm{R}} - \psi_{\mathrm{R}}^{*}), & \frac{1}{\sqrt{2}}(\psi_{\mathrm{L}} + \psi_{\mathrm{L}}^{*}), & \frac{\imath}{\sqrt{2}}(\psi_{\mathrm{L}} - \psi_{\mathrm{L}}^{*}) \end{bmatrix}.$$

Both relations imply the pattern of spontaneous breaking of chiral symmetry $\mathrm{SO}\,(4N_{\mathrm{f}}) \to \mathrm{SO}\,(2N_{\mathrm{f}}) \times \mathrm{SO}\,(2N_{\mathrm{f}})$. Again we emphasize that despite the fact that 3-dim continuum QCD has no chiral symmetry the naive Dirac operator $\mathcal{D}$ has in the 2-dim lattice discretization still a chiral structure though it is a trivial one due to the degeneracy of $\mathcal{D}$. For this particular case the joint probability distribution function of the class D is the same as of the one of the chGUE if we analytically continue to index $\nu = -1/2$. Therefore we can directly obtain the microscopic level density from the one of chiral GUE with index $\nu = -1/2$ [53], and thus

$$\rho(x) = \frac{1}{\pi} + \frac{\sin(2x)}{2\pi x}. \tag{4.87}$$

The agreement of the RMT predictions with lattice simulations, see Fig. 4.6, is so good that the Thouless energy must lie above the fourth eigenvalue. A possible reason for this good agreement could be the matrix size of the gauge group elements which is for $N_{\mathrm{c}} = 3$ equal to eight and is already large.

Even-even

Let L_1 and L_2 be even. The matrix

$$(\mathrm{diag}\,(-\imath, 1, \imath, 1) \otimes \mathbb{1}_{L_1L_2/2})\mathcal{W}(\mathrm{diag}\,(1, -\imath, 1, \imath) \otimes \mathbb{1}_{L_1L_2/2})$$

$$= \left[\begin{array}{cc|cc} & & T_2^{(\mathrm{ee|eo})} & T_1^{(\mathrm{ee|oe})} \\ & 0 & T_1^{(\mathrm{oo|eo})} & -T_2^{(\mathrm{oo|oe})} \\ \hline -(T_2^{(\mathrm{ee|eo})})^T & -(T_1^{(\mathrm{oo|eo})})^T & & \\ -(T_1^{(\mathrm{ee|oe})})^T & (T_2^{(\mathrm{oo|oe})})^T & & 0 \end{array}\right] \tag{4.88}$$

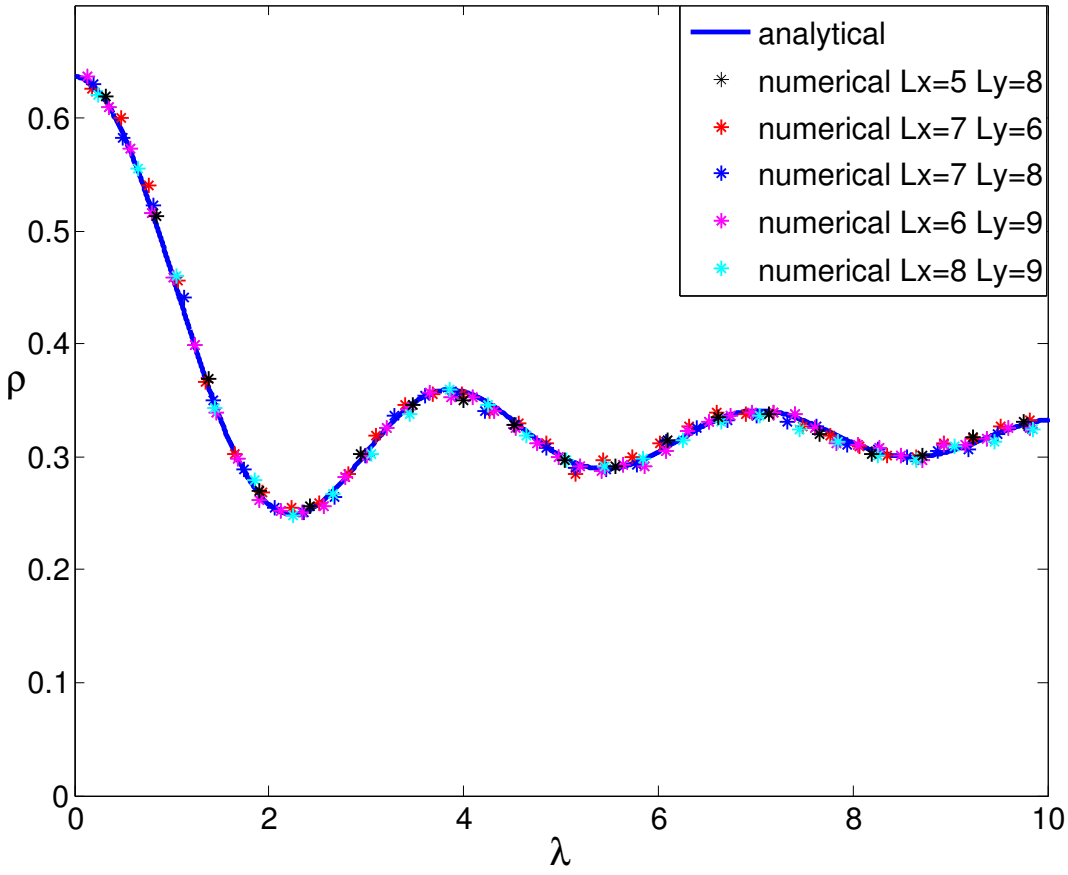

Figure 4.6: Spectral density for L_1 odd L_2 even SU (3) adjoint

is real and has a chiral structure as a consequence of (4.67) and (4.79). We introduced the diagonal matrix in order to make the symmetries manifest. Because the matrix (4.88) is square $\nu = 0$. Therefore we are in the universality class of chiral GOE, in particular:

- The chiral symmetry breaking pattern for N_f dynamical flavors is $\mathrm{SU}(2N_\mathrm{f}) \to \mathrm{SO}(2N_\mathrm{f})$. We expect a doubling of flavors in the continuum limit.

While for the quenched theory:

- This is the chGOE ensemble and is denoted as BDI in the Altland-Zirnbauer classification [45].
- The level repulsion goes with $|\lambda_i^2 - \lambda_j^2|$.
- The repulsion of the levels from the origin goes with $|\lambda_i|^0$.

- The levels of D are doubly degenerate due to the additional chiral structure.
- There are no generic zero modes of D.

The microscopic level density was derived in Ref. [125] and is

$$\rho(x) = \frac{x}{2}\left[J_0^2(x) - J_{-1}(x)J_1(x)\right] + \frac{1}{2}J_0(x)\left[1 - \int_0^x J_0(\widetilde{x})d\widetilde{x}\right]. \qquad (4.89)$$

The comparison of this result with lattice simulations is shown in Fig. 4.7. As in the previous subsection the agreement is astoundingly good such that the Thouless energy lies above the third eigenvalue.

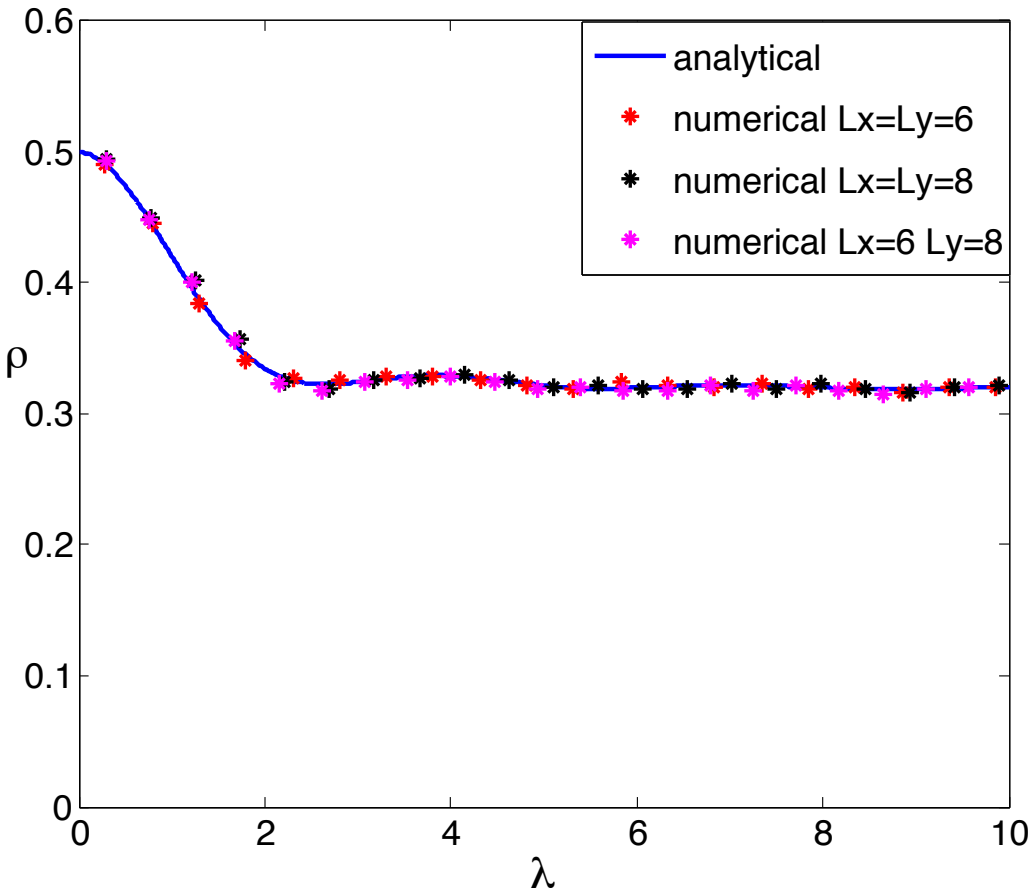

Figure 4.7: Spectral density for L_1, L_2 even, SU (3) adjoint

4.4.4 SU($N_c > 2$) and fermions in the fundamental representation

For QCD with more than two colors and the fermions in the fundamental representation there are only two universality classes. We will see below that the odd-odd case and the even-even case are in the same universality class. Accidentally we encounter the same pattern of chiral symmetry breaking as for 3 - dimensional QCD when $L_1 + L_2$ is odd.

Odd-Odd & Even-even

For $L_1 + L_2$ even we expect the universality case of chiral GUE since we have no symmetry at all for W apart from the artificial chiral symmetry if L_1 and L_2 are even. Hence, we have

- The chiral symmetry breaking pattern for N_f dynamical flavors is

  $$\mathrm{SU}\left(N_\mathrm{f}\right) \times \mathrm{SU}\left(N_\mathrm{f}\right) \to \mathrm{SU}\left(N_\mathrm{f}\right)$$

  for the odd-odd theory and

  $$\mathrm{SU}\left(2N_\mathrm{f}\right) \times \mathrm{SU}\left(2N_\mathrm{f}\right) \to \mathrm{SU}\left(2N_\mathrm{f}\right)$$

  for the even-even theory. We expect a doubling of flavors in the continuum limit.

While for the quenched theory:

- It is in the universality class of chiral GUE which is known as the class $AIII$ in the Altland-Zirnbauer classification [45].
- The level repulsion goes with $|\lambda_i^2 - \lambda_j^2|^2$.
- The repulsion of the levels from the origin goes with $|\lambda_i|^1$.
- The levels of D exhibit a double degeneracy for L_1, L_2 even and show no degeneracy for L_1, L_2 odd.
- There are no generic zero modes.

The microscopic level density is well known [53] and is given by

$$\rho(x) = \frac{x}{2}\left[J_0^2(x) - J_{-1}(x)J_1(x)\right]. \tag{4.90}$$

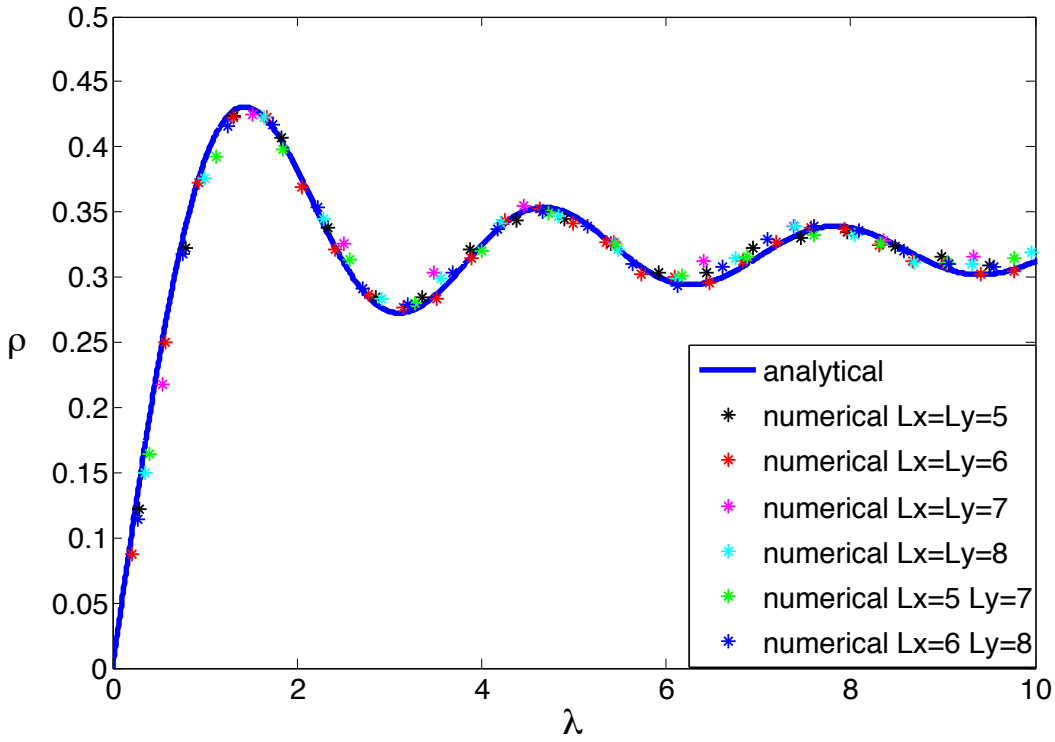

Figure 4.8: Spectral density for $L_1 + L_2 =$ even, SU (3) fundamental

The analytical RMT predictions are again quite good when comparing it with lattice data, see Fig. 4.8. In particular it shows that the odd-odd lattice structure and the even-even one indeed show the same universal behavior and hence, share the same global symmetries apart from the degeneracy.

Even-odd

We have a different situation if $L_1 + L_2$ is odd. Then the operator

$$(\mathrm{diag}\,(-\imath, 1) \otimes \mathbb{1}_{L_1 L_2}) \mathcal{W} (\mathrm{diag}\,(1, \imath) \otimes \mathbb{1}_{L_1 L_2}) = \begin{bmatrix} T_2^{(\mathrm{e}|\mathrm{e})} & T_1^{(\mathrm{e}|\mathrm{o})} \\ -(T_1^{(\mathrm{e}|\mathrm{o})})^\dagger & -T_2^{(\mathrm{o}|\mathrm{o})} \end{bmatrix} = \widetilde{\mathcal{W}} \tag{4.91}$$

is anti-Hermitian as a result of the unitarity of T and (4.66), i.e.

$$\widetilde{\mathcal{W}}^\dagger = -\widetilde{\mathcal{W}}. \tag{4.92}$$

Once again we introduced the diagonal matrix in order to make the symmetries obvious. Since Hermitian and anti-Hermitian matrices only differ by the imaginary unit, we expect the following behavior:

- The chiral symmetry breaking pattern for N_f dynamical flavors is $\mathrm{SU}\,(2N_\mathrm{f}) \to \mathrm{SU}\,(N_\mathrm{f}) \times \mathrm{SU}\,(N_\mathrm{f})$.

While for the quenched theory:

- The corresponding RMT ensemble is GUE which coincides with the class A in the Altland Zirnbauer classification [45].
- The level repulsion goes with $|\lambda_i - \lambda_j|^2$.
- There is no repulsion of the levels from the origin.
- The levels of D are not degenerate.
- There are no generic zero modes of D.

The microscopic level density with the lowest $1/n$ correction (n is the size of the random matrix W) is derived below. Including the $1/n$ corrections we find

$$\rho(x) = \frac{1}{\pi} + \frac{b_1}{n} + \frac{b_2 \cos x}{n}, \tag{4.93}$$

where b_1 and b_2 are computed explicitly below. We compare our analytical result to the numerical of the lattice simulation where b_1 and b_2 are fitting parameters. In the large n-limit both corrections vanish and the only component of lattice data which has to be fitted is the constant height. However the first correction was surprisingly strong when we compared the level density gained

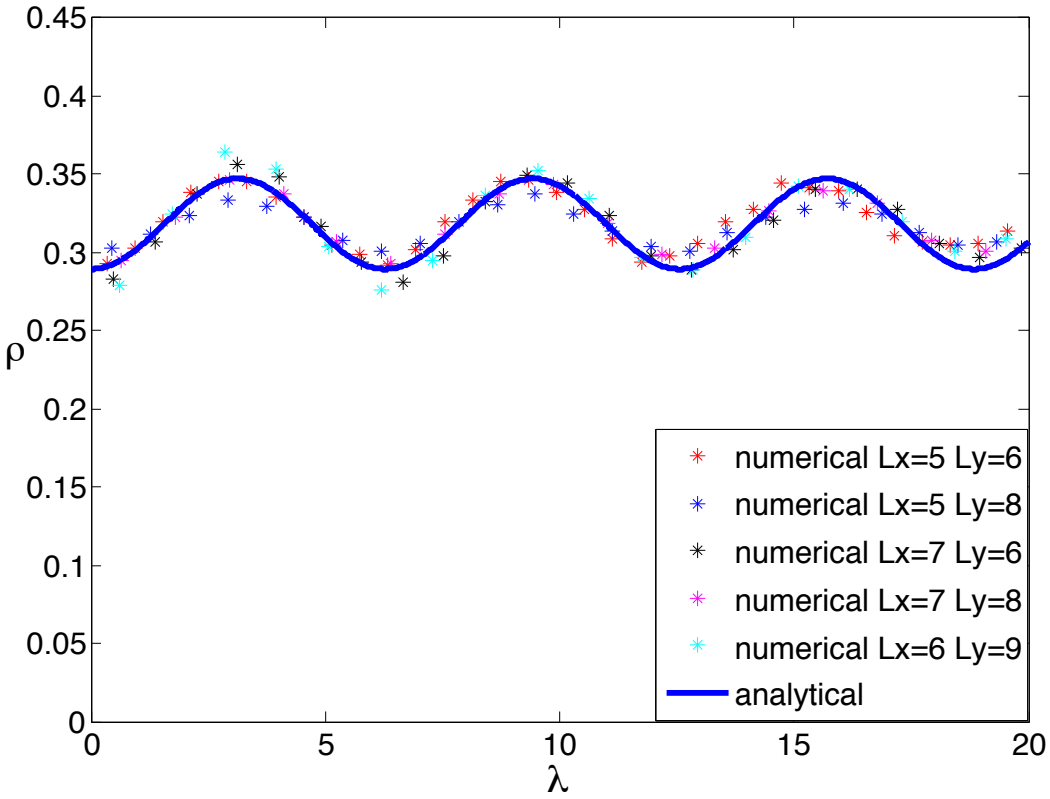

Figure 4.9: Spectral density for $L_1 + L_2 = \text{odd}$, SU (3) fundamental

by RMT with lattice simulations, see Fig. 4.9. As we see below the reason is the additional condition on the operator $\widetilde{\mathcal{W}}$, namely

$$\operatorname{tr} \widetilde{\mathcal{W}} = \operatorname{tr} \mathcal{W} = 0. \tag{4.94}$$

The reason for this identity is the fact that all translation operators T_μ have vanishing diagonal elements and, therefore, $\mathcal{W}$ and $\widetilde{\mathcal{W}}$, too. Note that in this chapter we employ a different convention from the one in the introduction for the definition of the Str . In what follows the convention used is $\operatorname{Str} M = \operatorname{tr} M_{BB} - \operatorname{tr} M_{FF}$. In RMT we can easily calculate the effect of the traceless condition. The level density is given as a random matrix integral,

$$\begin{aligned} \rho_t(x) \;=\; & \frac{1}{\pi} \lim_{\varepsilon \to 0} \operatorname{Im} \left. \frac{\partial}{\partial J} \right|_{J=0} \log \Bigg(\int_{\text{Herm}\,(n)} d[W] \exp \left[-\frac{\operatorname{tr} W^2}{2n} - \frac{t}{2n^2} (\operatorname{tr} W)^2 \right] \\ & \times \operatorname{Sdet}^{-1} (W \otimes \mathbb{1}_{1/1} - \mathbb{1}_n \otimes X) \Bigg), \end{aligned} \tag{4.95}$$

where

$$\mathrm{Sdet}\,(W\otimes \mathbb{1}_{1/1}-\mathbb{1}_n\otimes X)=\frac{\det(W-(x+\imath\varepsilon)\mathbb{1}_n)}{\det(W-(x+J)\mathbb{1}_n)} \tag{4.96}$$

is the super determinant and $X=\mathrm{diag}\,(x+\imath\varepsilon,x+J)$ a diagonal supermatrix. The parameter t generates the traceless condition ($t\to\infty$) as well as the ordinary chiral GUE ($t\to 0$). The square of the trace can be linearized by a Gaussian integral over an auxiliary scalar variable λ. The super determinant is written as a Gaussian integral over a $n\times(1/1)$ rectangular supermatrix V,

$$\begin{aligned}\rho_t(x) &= \frac{-1}{\pi}\lim_{\varepsilon\to 0}\mathrm{Im}\;\frac{\partial}{\partial J}\bigg|_{J=0}\ln\bigg(\int_{\mathrm{Herm}\,(n)}d[W]\int_{\mathbb{R}}d\lambda\int d[V]\exp\left[-\frac{\mathrm{tr}\,W^2}{2n}\right]\\ &\quad\times\exp\left[-\imath\mathrm{tr}\,W\left(VV^\dagger+\frac{\lambda}{n}\mathbb{1}_n\right)-\frac{\lambda^2}{2t}+\imath\mathrm{Str}\,V^\dagger VX\right]\bigg),\end{aligned} \tag{4.97}$$

After integrating over W we recognize that the remaining integrand only depends on invariants of the $(1/1)\times(1/1)$ supermatrix $V^\dagger V$. Hence we apply the superbosonization formula [127] and E.1 and replace $V^\dagger V$ by the unitary supermatrix $U\in\mathrm{U}\,(1/1)$. The parametrization of U is

$$U=\begin{bmatrix} e^{\vartheta} & -\eta^* \\ \eta & e^{\imath\varphi}\end{bmatrix}, \tag{4.98}$$

where η and η^* are two Grassmann variables, $\vartheta\in\mathbb{R}$ and $\varphi\in[0,2\pi[$. Therefore the level density reads

$$\begin{aligned}\rho_t(x) &= \frac{-1}{\pi}\lim_{\varepsilon\to 0}\mathrm{Im}\;\frac{\partial}{\partial J}\bigg|_{J=0}\ln\bigg(\int_{-\infty}^{\infty}d\vartheta\int_0^{2\pi}d\varphi\int d\eta^*d\eta\int_{-\infty}^{\infty}d\lambda\mathrm{Sdet}^{\,n}U\exp\left[-\frac{n}{2}\mathrm{Str}\,U^2\right]\\ &\quad\times\exp\left[-\frac{(1+t)\lambda^2}{2t}+\mathrm{Str}\,U(\imath X-\lambda\mathbb{1}_{1/1})\right]\bigg),\end{aligned} \tag{4.99}$$

The integration over λ and over the Grassmann variables yields

$$\begin{aligned}\rho_t(x) &= \frac{-1}{\pi}\lim_{\varepsilon\to 0}\mathrm{Im}\;\frac{\partial}{\partial J}\bigg|_{J=0}\ln\bigg(\int_{-\infty}^{\infty}d\vartheta\int_0^{2\pi}d\varphi\exp\left[n\vartheta-n\imath\varphi-\frac{n}{2}(e^{2\vartheta}-e^{2\imath\varphi})\right]\\ &\quad\times\exp\left[\frac{t}{2(1+t)}(e^{\vartheta}-e^{\imath\varphi})^2+\imath((x+\imath\varepsilon)e^{\vartheta}-(x+J)e^{\imath\varphi})\right](1+e^{-\vartheta-\imath\varphi})\bigg).\end{aligned} \tag{4.100}$$

In the large n-limit we have to expand ϑ and φ at the two saddlepoints $(\vartheta_0, \varphi_0) = (0,0), (0,\pi)$ by the fluctuations $\delta\vartheta/\sqrt{n}$ and $\delta\varphi/\sqrt{n}$. The saddlepoint $(0,\pi)$ is algebraically suppressed and yields an oscillatory $1/n$ correction. Differentiating with respect to J we obtain

$$\begin{aligned} \rho_t(x) &= \frac{1}{\pi}\mathrm{Im}\,\imath\left(1+\frac{\imath x}{2n}+\frac{(-1)^n}{4n}\exp\left[\frac{2t}{t+1}+2\imath x\right]\right) \\ &= \frac{1}{\pi}\left(1+\frac{(-1)^n}{4n}\exp\left[\frac{2t}{t+1}\right]\cos\left[2x\right]\right). \end{aligned} \tag{4.101}$$

Here we immediately see that the amplitude of the oscillation is enhanced by a factor of $e^2 \approx 7.4$ for a traceless random matrix ($t \to \infty$) in comparison to the original GUE ($t = 0$). Thus we can expect that such a mechanism also influences the level density of the lattice Dirac operator. Surprisingly the next to leading order correction of lattice QCD is also described by RMT although these terms are not universal anymore.

4.5 Conclusions

In this chapter we presented an extension of the general chRMT classification of four dimensions [75]. We identified an artificial chiral structure that the translational operators fulfil (4.64) which as a result yields a very rich structure and we encountered eight out of the ten symmetry classes of the Zirnbauer classification [45]. There has been a similar classification in the context of condensed matter physics in the study of topological insulators [132]. The comparison with direct numerical lattice simulations nicely confirms our analytical predictions. There is an excellent agreement up to the Thouless energy which is of the order of the eigenvalue spacing. Recently, [133] carried out a similar study for continuum QCD. Our results agree with theirs.

Chapter 5

Discussion and Future Work

In this thesis we focused on the development and solution of Random Matrix Theories for lattice Dirac operators. In chapters 2,3 we studied Wilson fermions which is a very popular discretization widely used while in chapter 4 we explored the properties of naive and staggered fermions which are also used extensively by an abundance of lattice practitioners. We will summarize our conclusions separately in order to point out our results in a concrete manner.

Since the introduction of the Wilson term breaks chiral symmetry explicitly the lattice artifacts lead to new terms in chiral Perturbation Theory (chPT). The additional terms in the Symanzik expansion are reminiscent of mass terms, since the Wilson term effectively makes the doublers infinitely heavy in the continuum limit. The low energy effective theory which incorporates the lattice effects is known as Wilson chPT. To leading order in lattice spacing (namely a^2) three new low energy constants are introduced ($W_{6/7/8}$). We studied in detail the effect of each low energy constant on the spectrum of the Dirac operator and identified their effects on the eigenvalues. W_6 and W_7 can be interpreted in terms of "collective" fluctuations of the eigenvalues while W_8 induces interactions among all modes. We calculated explicitly the joint probability distribution function and we integrated all eigenvalues apart from one in order to obtain single eigenvalue distributions. We calculated the quenched microscopic spectral densities of complex eigenvalues, real eigenvalues as well as the distribution of chiralities over the real eigenvalues. We analyzed the limit of small and large lattice spacing which is very closely related to the mean field limit. We presented an explicit unambiguous prescription applicable for lattice simulations close to the continuum limit to derive the numerical values of the low energy constants. We expect to confront these analytical relations with lattice data in the near future. It is important to stress once again that the relations for the extraction of the low energy constants are only applicable at sufficiently small values of lattice spacing. Our results are of

direct phenomenological interest since in studies of QCD with a larger number of flavors in the mean field approach the coefficient in front of W_6, W_7 scales with N_f^2 compared to the coefficient of W_8 which scales with N_f.

Moreover we explored the spectral properties of the Hermitian Wilson Dirac operator of QCD-like theories. Particularly we studied two-color QCD with fundamental quarks as well as QCD with quarks in the adjoint representation and arbitrary number of colors. QCD like theories are very interesting theories with a range of applications extending from physics beyond the Standard Model to finite density studies since they are not hindered by the notorious sign problem. We presented analytical and numerical results for the microscopic spectral density, the chirality distribution, the inverse chirality distribution, the chiral condensate as well as of the spectrum of the non-Hermitian Wilson Dirac operator. Once again, it is important to point out that although lattice simulations currently are carried out in the deep chiral regime it is not possible to invert the Wilson Dirac operator when eigenvalues are sufficiently close to zero. We identified the parameter domain where such eigenvalues appear and our results can be potentially useful for the identification of the parameter domain of simulations with dynamical quarks. We explained that the probability to obtain small eigenvalues is higher for the two-color theory than for QCD with more colors because of the lack of repulsion from the origin. There is undergoing work on the analytical calculations of the adjoint theory since all the results presented for this theory were numerical.

In the last chapter motivated by the peculiar symmetry properties of the staggered Dirac operator close to the continuum limit we studied two dimensional naive fermions on even-even, even-odd, odd-odd lattices. We identified an additional, "artificial", chiral symmetry which eventually leads to a very rich structure of the two dimensional theory. We were able to identify eight out the ten symmetry classes of Hermitian Random Matrix Theory. The initial question, posed in the introduction, why do we encounter different antiunitary symmetry properties at finite lattice spacing in contrast to the continuum was not answered in a clean way and it is part of our ongoing work we expect to be more conclusive in the near future.

Appendix A

Derivation of the joint probability density

In this appendix, we derive the joint probability density in three steps. In A.1.1, following the derivation for the joint probability density of the Hermitian Dirac operator [83] we introduce an auxiliary Gaussian integral such that we obtain a Harish-Chandra like integral that mixes two different types of variables. In A.1.2 this problem is reduced to an Harish-Chandra like integral considered in a bigger framework. We derive an educated guess which fulfils a set of differential equations and a boundary value problem. The asymptotics of the integral for large arguments serve as the boundary. In A.1.2 we perform a stationary phase approximation which already yields the full solution meaning that the semiclassical approach is exact and the Duistermaat-Heckman [134] localization applies. In the last step we plug the result of A.1.2 into the original problem, see A.1.2, and integrate over the remaining variables to arrive at the result for the joint probability density given in the main text.

A.1 Derivation of the joint probability density

A.1.1 Introducing auxiliary Gaussian integrals

We consider the functional $I[f]$, see Eq. (2.12), with an integrable test function f invariant under $\mathrm{U}(n, n+\nu)$. The idea is to rewrite the exponent of the probability distribution $P(D_{\mathrm{W}})$ as the sum of a $\mathrm{U}(n, n+\nu)$ invariant term $\mathrm{Tr} D_{\mathrm{W}}^2$ and a symmetry breaking term which is linear in D_{W}. This is achieved by introducing two Gaussian distributed Hermitian matrices S_{r} and S_{l} with

Joint work with M. Kieburg and J.J.M. Verbaarschot.

dimensions $n \times n$ and $(n+\nu) \times (n+\nu)$, respectively, i.e.

$$\begin{aligned} I[f] &= (2\pi\sqrt{1+a^2})^{-n^2-(n+\nu)^2} \left(-\frac{n}{2\pi}\right)^{n(n+\nu)} \exp\left[-\frac{a^2}{2}\left(\mu_{\mathrm{r}}^2 + \frac{n+\nu}{n}\mu_{\mathrm{l}}^2\right)\right] \\ &\quad \times \int d[D_{\mathrm{W}}] f(D_{\mathrm{W}}) \int d[S_{\mathrm{r}}, S_{\mathrm{l}}] \exp\left[\frac{n}{2}\mathrm{tr}\, D_{\mathrm{W}}^2 + \imath \mathrm{tr}\, D_{\mathrm{W}} \mathrm{diag}\,(S_{\mathrm{r}}, S_{\mathrm{l}})\right] \\ &\quad \times \exp\left[-\frac{a^2}{2n(1+a^2)}\left(\mathrm{tr}\,(S_{\mathrm{r}} + \imath\mu_{\mathrm{r}} \mathbb{1}_n)^2 + \mathrm{tr}\,(S_{\mathrm{l}} + \imath\mu_{\mathrm{l}} \mathbb{1}_{n+\nu})^2\right)\right]. \quad \text{(A.1)} \end{aligned}$$

The matrix $\mathrm{diag}(S_{\mathrm{r}}, S_{\mathrm{l}})$ is a block-diagonal matrix with S_{r} and S_{l} on the diagonal blocks. The measure for $S_{\mathrm{r}/\mathrm{l}}$ is

$$\begin{aligned} d[S_{\mathrm{r}}, S_{\mathrm{l}}] &= \prod_{j=1}^{n} dS_{jj}^{(\mathrm{r})} \prod_{1 \le i < j \le n} 2\, d\,\mathrm{Re}\, S_{ij}^{(\mathrm{r})} d\,\mathrm{Im}\, S_{ij}^{(\mathrm{r})} \\ &\quad \times \prod_{j=1}^{n+\nu} dS_{jj}^{(\mathrm{l})} \prod_{1 \le i < j \le n+\nu} 2\, d\,\mathrm{Re}\, S_{ij}^{(\mathrm{l})} d\,\mathrm{Im}\, S_{ij}^{(\mathrm{l})}. \quad \text{(A.2)} \end{aligned}$$

Then the non-compact unitary matrix diagonalizing D_{W} only appears quadratically in the exponent. Notice that we have to integrate first over the Hermitian matrices $S_{\mathrm{r}/\mathrm{l}}$ and have to be careful when interchanging integrals with integrals over D_{W}. Obviously the integrations over the eigenvalues of D_{W} are divergent without performing the $S_{\mathrm{r}/\mathrm{l}}$ integrals first and cannot be interchanged with these integrals. Also the coset integrals over $\mathbb{G}_l = \mathrm{U}(n, n+\nu)/[\mathrm{U}^{2n+\nu-l}(1) \times \mathrm{O}^{l}(1,1)]$, cf. Eq. (2.12), are not convergent. However we can understand them in a weak way and below, we will find Dirac delta functions resulting from the non-compact integrals.

Diagonalizing the matrices $D_l = U Z_l U^{-1}$ and $S_{\mathrm{r}/\mathrm{l}} = V_{\mathrm{r}/\mathrm{l}}\, s_{\mathrm{r}/\mathrm{l}}\, V_{\mathrm{r}/\mathrm{l}}^{\dagger}$ with $s_{\mathrm{r}} = \mathrm{diag}\,(s_1^{(\mathrm{r})}, \ldots, s_n^{(\mathrm{r})})$ and $s_{\mathrm{l}} = \mathrm{diag}\,(s_1^{(\mathrm{l})}, \ldots, s_{n+\nu}^{(\mathrm{l})})$ we can absorb the integrals

over V_r and V_l in the $U \in \mathbb{G}_l$ integral. Then we end up with the integral

$$\begin{aligned} I[f] &= \frac{C}{n!(n+\nu)!} \sum_{l=0}^{n} \frac{1}{2^l (n-l)!l!(n+\nu-l)!} \\ &\times \int\limits_{\mathbb{R}^{\nu+2(n-l)}\times\mathbb{C}^l} d[Z_l] |\Delta_{2n+\nu}(Z_l)|^2 \int\limits_{\mathbb{R}^{2n+\nu}} d[s_\mathrm{r}, s_\mathrm{l}] \Delta_n^2(s_\mathrm{r}) \Delta_{n+\nu}^2(s_\mathrm{l}) f(Z_l) \\ &\times \exp\left[\frac{n}{2}\mathrm{tr}\, Z_l^2 - \frac{a^2}{2n(1+a^2)} \left(\mathrm{tr}\,(s_\mathrm{r} + \imath\mu_\mathrm{r}\mathbb{1}_n)^2 + \mathrm{tr}\,(s_\mathrm{l} + \imath\mu_\mathrm{l}\mathbb{1}_{n+\nu})^2\right)\right] \\ &\times \int\limits_{\mathbb{G}_l} \exp\left[\imath \mathrm{tr}\, U Z_l U^{-1} \mathrm{diag}\,(s_\mathrm{r}, s_\mathrm{l})\right] d\mu_{\mathbb{G}_l}(U) \end{aligned} \tag{A.3}$$

and the normalization constant

$$C = \left(-\frac{n}{2\pi}\right)^{n(n+\nu)} \prod_{j=0}^{n-1} \frac{(2\pi)^j \exp\left[-a^2\mu_\mathrm{r}^2/2n\right]}{j!(2\pi\sqrt{1+a^2})^{2j+1}} \prod_{j=0}^{n+\nu-1} \frac{(2\pi)^j \exp\left[-a^2\mu_\mathrm{l}^2/2n\right]}{j!(2\pi\sqrt{1+a^2})^{2j+1}}. \tag{A.4}$$

See Sec. 2.2.2 for a discussion of the prefactors in the sum.

A.1.2 The Itzykson-Zuber integral over the non-compact coset $\mathbb{G}_l$

In the next step we calculate the integral

$$\mathcal{I}_l(Z_l, s) = \int\limits_{\mathbb{G}_l} \exp\left[\imath \mathrm{tr}\, U Z_l U^{-1} s\right] d\mu_{\mathbb{G}_l}(U). \tag{A.5}$$

with $s = \mathrm{diag}\,(s_\mathrm{r}, s_\mathrm{l})$. For $l = 0$ this integral was derived in Ref. [135].

We calculate this integral by determining a complete set of functions and expanding the integral for asymptotically large s in this set. In this limit it can be calculated by a stationary phase approximation. It turns out that this integral, as is the case with the usual Harish-Chandra-Itzykson-Zuber integral, is semi-classically exact.

Non-compact Harish-Chandra-Itzykson-Zuber Integral

Let us consider the non-compact integral

$$\mathcal{I}_l(Z_l, Z'_{l'}) \;=\; \int\limits_{\mathbb{G}_l} \exp\left[\imath \mathrm{tr}\, U Z_l U^{-1} Z'_{l'}\right] d\mu_{\mathbb{G}_l}(U) \tag{A.6}$$

in a bigger framework where $Z'_{l'}$ is a quasi-diagonal matrix with l' complex conjugate eigenvalue pairs. The integral is invariant under the Weyl group $\mathbf{S}(n-l)\times\mathbf{S}(l)\times\mathbf{S}(n+\nu-l)\times\mathbb{Z}_2^l$. To make the integral well-defined we have to assume that $l \geq l'$ otherwise the integral is divergent since the non-compact subgroup $\mathrm{O}^{l'-l}(1,1)\subset\mathbb{G}_l$ commutes with $Z'_{l'}$.

The integral (A.6) should be contrasted with the well-known compact Harish-Chandra-Itzykson-Zuber integral [136, 137]

$$\begin{aligned}\mathcal{I}^{\mathrm{com}}(X, X') \;&=\; \int\limits_{\mathrm{U}\,(2n+\nu)} \exp\left[\imath \mathrm{tr}\, U X U^{-1} X'\right] d\mu_{\mathrm{U}\,(2n+\nu)}(U) \\ &=\; \frac{(-2\pi\imath)^{\nu(\nu-1)/2}}{\Delta_\nu(x)\Delta_\nu(x')} \det\left[\exp\left(\imath x_i x'_j\right)\right]_{1\leq i,j\leq\nu}\end{aligned} \tag{A.7}$$

with Weyl group $\mathbf{S}(2n+\nu)$. Moreover, the compact case is symmetric when interchanging X with X'. This symmetry is broken in Z_l and $Z'_{l'}$ due to the coset $\mathbb{G}_l$.

For a γ_5-Hermitian matrix V with eigenvalues Z_l, we can rewrite the integral (A.6) as

$$\mathcal{I}_l(Z_l, Z'_{l'}) \;=\; \mathcal{I}_l(V, Z'_{l'}) = \int\limits_{\mathbb{G}_l} \exp\left[\imath \mathrm{tr}\, U V U^{-1} Z'_{l'}\right] d\mu_{\mathbb{G}_l}(U). \tag{A.8}$$

This trivially satisfies the Sekigushi-like differential equation [138, 139]

$$\det\left(\frac{\partial}{\partial V_{kl}} + u\mathbb{1}_{2n+\nu}\right)\mathcal{I}_l(V, Z'_{l'}) = \det\left(\imath Z'_{l'} + u\mathbb{1}_{2n+\nu}\right)\mathcal{I}_l(V, Z'_{l'}) \text{ for all } u\in\mathbb{C}. \tag{A.9}$$

This equation is written in terms of the independent matrix elements of V and hence, is independent of the fact to which sector l the matrix V can be quasi-diagonalized.

We would like to rewrite Eq. (A.9) in terms of derivatives with respect to the eigenvalues (Note that $\mathcal{I}_l(Z_l, Z'_{l'})$ does not depend on the unitary trans-

formation that diagonalizes V.). Because of the coefficients that enter after applying the chain rule when changing coordinates, the derivatives do not commute and a direct evaluation of the determinant is cumbersome. Therefore we will calculate $\mathcal{I}_l(Z_l, Z'_{l'})$ in an indirect way. We will do this by constructing a complete set of $\mathbf{S}(n-l) \times \mathbf{S}(l) \times \mathbf{S}(n+\nu-l) \times \mathbb{Z}_2^l$ symmetric functions in the space of the $\{Z_l\}$ with the $\{Z'_{l'}\}$ as quantum numbers which have to be $\mathbf{S}(n-l') \times \mathbf{S}(l') \times \mathbf{S}(n+\nu-l') \times \mathbb{Z}_2^{l'}$ symmetric. Then we expand $\mathcal{I}_l(Z_l, Z'_{l'})$ in this set of functions and determine the coefficients for asymptotically large $\{Z_l\}$ where the integral can be evaluated by a stationary phase approximation.

To determine the complete set of functions, we start from the usual Itzykson-Zuber integral over the compact group $\mathrm{U}(2n+\nu)$. This integral is well-known and satisfies the Sekigushi-like differential equation [138, 139] with

$$\begin{aligned} & \frac{1}{\Delta_{2n+\nu}(X)} \det\left(\frac{\partial}{\partial X} + u\mathbb{1}_{2n+\nu}\right) \Delta_{2n+\nu}(X)\mathcal{I}^{\mathrm{com}}(X, X') \\ = \; & \det\left(\imath X' + u\mathbb{1}_{2n+\nu}\right)\mathcal{I}^{\mathrm{com}}(X, X') \end{aligned} \tag{A.10}$$

in terms of the $(2n+\nu)$ real eigenvalues $X = \mathrm{diag}\,(x_1, \ldots, x_{2n+\nu})$ with

$$\det\left(\frac{\partial}{\partial X} + u\mathbb{1}_{2n+\nu}\right) = \prod_{j=1}^{2n+\nu}\left(\frac{\partial}{\partial x_j} + u\right). \tag{A.11}$$

The expansion in powers of u gives the complete set of $2n+\nu$ independent Casimir operators on the Cartan subspace of $\mathrm{U}(2n+\nu)$, so that the Sekigushi equation determines a complete set of functions $\mathcal{I}_l(Z_l, Z'_{l'})$ up to the Weyl group. Since the non-compact group $\mathrm{U}(n+\nu, n)$ shares the same complexified Lie algebra as $\mathrm{U}(2n+\nu)$ the Casimir operators are the same, i.e. the corresponding operator for $\mathrm{U}(n+\nu, n)$ to the one in Eq. (A.10) is

$$D_{Z_l}(u) \;=\; \frac{1}{\Delta_{2n+\nu}(Z_l)} \det\left(\frac{\partial}{\partial Z_l} + u\mathbb{1}_{2n+\nu}\right) \Delta_{2n+\nu}(Z_l) \tag{A.12}$$

with

$$\begin{aligned} & \det\left(\frac{\partial}{\partial Z_l} + u\mathbb{1}_{2n+\nu}\right) \\ = \; & \prod_{j=1}^{n-l}\left(\frac{\partial}{\partial x_j^{(1)}} + u\right) \prod_{j=1}^{l}\left(\frac{\partial}{\partial z_j^{(2)}} + u\right)\left(\frac{\partial}{\partial z_j^{(2)*}} + u\right) \prod_{j=1}^{n+\nu-l}\left(\frac{\partial}{\partial x_j^{(3)}} + u\right). \end{aligned} \tag{A.13}$$

Let f be an integrable test function on the Cartan-subset $\mathbb{R}^{2n+\nu-2l'} \times \mathbb{C}^{l'}$. Then

the solutions of the weak Sekigushi-like equation

$$\begin{aligned} & D_{Z_l}(u) \int\limits_{\mathbb{R}^{2(n-l')+\nu}\times\mathbb{C}^{l'}} d[Z'_{l'}] f(Z'_{l'}) \mathcal{I}_l(Z_l, Z'_{l'}) \\ = & \int\limits_{\mathbb{R}^{2(n-l')+\nu}\times\mathbb{C}^{l'}} d[Z'_{l'}] f(Z'_{l'}) \det\left(\imath Z'_{l'} + u \mathbb{1}_{2n+\nu}\right) \mathcal{I}_l(Z_l, Z'_{l'}) \end{aligned} \tag{A.14}$$

yield a complete set of functions for the non-compact case as well. The only difference is the corresponding Weyl group. This can be seen because we can generate any polynomial of order $k \in \mathbb{N}_0$ in $Z'_{l'}$ symmetric under $\mathbf{S}(n-l') \times \mathbf{S}(l') \times \mathbf{S}(n+\nu-l') \times \mathbb{Z}_2^{l'}$ via the differential operator $\prod_{j=1}^{k} D_{Z_l}(u_j)$. Since those polynomials are dense in the space of $\mathbf{S}(n-l') \times \mathbf{S}(l') \times \mathbf{S}(n+\nu-l') \times \mathbb{Z}_2^{l'}$ invariant functions, it immediately follows that if a function is in the kernel of $D_{Z_l}(u)$ it is zero, i.e.

$$D_{Z_l}(u) F(Z_l) = 0 \ \forall u \in \mathbb{C} \quad \Leftrightarrow \quad F(Z_l) = 0. \tag{A.15}$$

Therefore if we found a solution for Eq. (A.14) for an arbitrary test function f we found $\mathcal{I}_l(Z_l, Z'_{l'})$ up to the normalization which can be fixed in the large $\operatorname{tr} Z_l Z_l^\dagger$-limit.

Some important remarks about Eq. (A.14) are in order. The Vandermonde determinant $\Delta_{2n+\nu}(Z_l)$ enters in a trivial way in the operator $D_{Z_l}(u)$ and the remaining operator has plane waves as eigenfunctions which indeed build a complete set of functions. Thus a good ansatz of $\mathcal{I}_l(Z_l, Z'_{l'})$ is

$$\mathcal{I}_l(Z_l, Z'_{l'}) = \frac{1}{\Delta_{2n+\nu}(Z_l)} \prod_{j=1}^{l} \frac{y_j^{(2)}}{|y_j^{(2)}|} \sum_{\omega\in\mathbf{S}} c_\omega^{(ll')}(Z'_{l'}) \exp\left[\imath \operatorname{tr} \Pi_\omega Z_l \Pi_\omega^{-1} \widehat{Z}'_{l'}\right], \tag{A.16}$$

where the coefficients $c_\omega^{(ll')}(Z'_{l'})$ have to be determined. The factors $y_j^{(2)}/|y_j^{(2)}|$ guarantee the invariance under complex conjugation of each complex eigenvalue pair of Z_l. We sum over the permutation group ω and Π_ω is its standard representation in the $(2n+\nu) \times (2n+\nu)$ matrices. The $\mathbf{S}(n-l) \times \mathbf{S}(l) \times \mathbf{S}(n+\nu-l) \times \mathbb{Z}_2^l$ invariance in Z_l and the $\mathbf{S}(n-l') \times \mathbf{S}(l') \times \mathbf{S}(n+\nu-l') \times \mathbb{Z}_2^{l'}$ invariance in $Z'_{l'}$ carry over to the coefficients $c_\omega^{(ll')}(Z'_{l'})$. Hence, we can reduce

all coefficients to coefficients independent of ω,

$$\mathcal{I}_l(Z_l, Z'_{l'}) = \frac{1}{\Delta_{2n+\nu}(Z_l)} \sum_{\substack{\omega \in \mathbf{S}(n-l)\times\mathbf{S}(l)\times\mathbf{S}(n+\nu-l)\times\mathbf{Z}_2^l \\ \omega' \in \mathbf{S}(n-l')\times\mathbf{S}(l')\times\mathbf{S}(n+\nu-l')\times\mathbf{Z}_2^{l'}}} \operatorname{sign}\omega \; c^{(ll')}(Z'_{l'\omega'}) \exp\left[\imath \operatorname{tr} Z_{l\omega} Z'_{l'\omega'}\right] \tag{A.17}$$

where we employ the abbreviation

$$Z_{l\omega} = \Pi_\omega Z_l \Pi_\omega^{-1} \quad \text{and} \quad Z'_{l'\omega'} = \Pi_{\omega'} Z'_{l'} \Pi_{\omega'}^{-1}. \tag{A.18}$$

The sign of elements in the group $\mathbb{Z}_2$ generating the complex conjugation of single complex conjugated pairs is always $+1$. Moreover any element in the permutation group $\mathbf{S}(l)$ is an even permutation since it interchanges a complex conjugate pair with another one and thus, yields always a positive sign. Hence the sign of the permutation ω is the product of the sign of the permutations in $\mathbf{S}(n-l)$ and in $\mathbf{S}(n+\nu-l)$.

Solving the weak Sekigushi-like equation (A.14) for the general case $l \neq l'$ is quite complicated whereas for $l = l'$ the ansatz

$$\begin{aligned} \mathcal{I}_l(Z_l, Z'_l) \;=\; & \frac{(-2\pi\imath)^{(2n+\nu)(2n+\nu-1)/2}}{\Delta_{2n+\nu}(Z_l)\Delta_{2n+\nu}(Z'_l)} \det\left[\exp\left(\imath x_i^{(1)} x_j'^{(1)}\right)\right]_{1\le i,j\le n-l} \\ & \times \operatorname{perm}\left[\frac{y_i^{(2)} y_j'^{(2)}}{|y_i^{(2)} y_j'^{(2)}|}\left(\exp\left[2\imath \operatorname{Re}\, z_i^{(2)} z'^{(2)}_j\right] + \exp\left[2\imath \operatorname{Re}\, z_i^{(2)\,*} z'^{(2)}_j\right]\right)\right]_{1\le i,j\le l} \\ & \times \det\left[\exp\left(\imath x_i^{(3)} x_j'^{(3)}\right)\right]_{1\le i,j\le n+\nu-l}, \end{aligned} \tag{A.19}$$

i.e. $c^{(ll)}(Z'_{l\omega'}) \propto (\prod_{j=1}^{l'} y'^{(2)}_j / |y'^{(2)}_j|)/\Delta_{2n+\nu}(Z'_{l\omega'})$, does the job. Note that we have again the symmetry when interchanging Z_l with Z'_l since both matrices are in the Cartan subspace corresponding to $\mathbb{G}_l$. The constant can be fixed by a stationary phase approximation when taking $\operatorname{tr} Z_l Z_l^\dagger \to \infty$. The function "perm" is the permanent which is defined analogously to the determinant but without the sign-function in the sum over the permutations. It arises because the Vandermonde determinants are even under the interchange of a complex pair with another one, i.e. it is the $\mathbf{S}(l)$-invariance of the corresponding Weyl-group. It can be explicitly shown that the ansatz (A.19) satisfies the completeness relation in the space of functions on $\mathbb{R}^{\nu+2(n-l)} \times \mathbb{C}^l$ invariant under $\mathbf{S}(n-l)\times\mathbf{S}(l)\times\mathbf{S}(n+\nu-l)\times\mathbb{Z}_2^l$ and with the measure $|\Delta_{2n+\nu}(Z_l)|^2 d[Z_l]$,

i.e.

$$\begin{aligned}
&\int\limits_{\mathbb{R}^{\nu+2(n-l)}\times\mathbb{C}^l} \mathcal{I}_l(Z_l,Z_l')\mathcal{I}_l(Z_l'',Z_l)|\Delta_{2n+\nu}(Z_l)|^2 d[Z_l] \\
\propto\ & \frac{1}{\Delta_{2n+\nu}(Z_l')\Delta_{2n+\nu}(Z_l'')}\det\left[\delta\left(x_i'^{(1)}-x_j''^{(1)}\right)\right]_{1\le i,j\le n-l} \\
&\times\mathrm{perm}\left[\frac{y_i'^{(2)}y_j''^{(2)}}{|y_i'^{(2)}y_j''^{(2)}|}\delta\left(|y_i'^{(2)}|-|y_j''^{(2)}|\right)\delta\left(x_i'^{(2)}-x_j''^{(2)}\right)\right]_{1\le i,j\le l} \\
&\times\det\left[\delta\left(x_i'^{(3)}-x_j''^{(3)}\right)\right]_{1\le i,j\le n+\nu-l}. \qquad \text{(A.20)}
\end{aligned}$$

Therefore, the ansatz (A.19) is indeed the solution of the problem if $l = l'$. One has only to show that the global prefactor is correct, see A.1.2.

What happens in the general case $l \neq l'$? The ansatz (A.17) can only fulfill the Sekigushi-like differential equation (A.14) if we assume that the coefficient $c^{(ll')}(Z'_{l'\omega'})$ restricts the matrix $Z'_{l'}$ to a matrix in the sector with l complex conjugate eigenvalue pairs. This is only possible on the boundary of the Cartan subsets $\mathbb{R}^{2(n-l)+\nu}\times\mathbb{C}^l$ and $\mathbb{R}^{2(n-l')+\nu}\times\mathbb{C}^{l'}$, i.e. the coefficient has to be proportional to Dirac delta functions

$$c^{(ll')}(Z'_{l'\omega'}) \propto \prod_{j=1}^{l-l'}\delta\left(x'^{(1)}_{\omega'(n-l+j)}-x'^{(3)}_{\omega'(j)}\right). \qquad \text{(A.21)}$$

The reason for this originates from the fact that not all complex pairs of Z_l can couple with a complex eigenvalue pair in $Z'_{l'}$ and hence, $\mathrm{tr}\, Z_{l\omega}Z'_{l'\omega'}$ does not depend on the combinations $x'^{(1)}_{\omega'(n-l+j)}-x'^{(3)}_{\omega'(j)}$. Therefore we would miss it in the determinant $\det(Z'_{l'}+u\mathbb{1}_{2n+\nu})$ generated by the differential operator $D_{Z_l}(u)$. To cure this we have to understand $\mathcal{I}_l(Z_l,Z'_{l'})$ as a distribution where the Dirac delta functions set these missing terms to zero. In A.1.2 we show

that the promising ansatz

$$\begin{aligned}\mathcal{I}_l(Z_l, Z'_{l'}) &= \frac{c^{(ll')}}{\Delta_{2n+\nu}(Z_l)\Delta_{2n+\nu}(Z'_{l'})} \prod_{j=1}^{l} \frac{y_j^{(2)}}{|y_j^{(2)}|} \prod_{j=1}^{l'} \frac{y'^{(2)}_j}{|y'^{(2)}_j|} \\ &\times \sum_{\substack{\omega\in\mathbb{S}(n-l)\times\mathbb{S}(l)\times\mathbb{S}(n+\nu-l)\times\mathbb{Z}_2^l \\ \omega'\in\mathbb{S}(n-l')\times\mathbb{S}(l')\times\mathbb{S}(n+\nu-l')\times\mathbb{Z}_2^{l'}}} \operatorname{sign}\omega\omega' \exp\left(\imath \operatorname{tr} Z_{l\omega} Z'_{l'\omega'}\right) \\ &\times \prod_{j=1}^{|l-l'|} \left(x'^{(1)}_{\omega'(n-l+j)} - x'^{(3)}_{\omega'(j)}\right) \delta\left(x'^{(1)}_{\omega'(n-l+j)} - x'^{(3)}_{\omega'(j)}\right)\end{aligned} \tag{A.22}$$

is indeed the correct result.

Note that the ansatz (A.22) agrees with the solution (A.19) for the case $l = l'$. Furthermore one can easily verify that it also solves the weak Sekiguchi-like differential equation (A.14). Indeed, the ansatz is trivially invariant under the two Weyl groups $\mathbf{S}(n-l) \times \mathbf{S}(l) \times \mathbf{S}(n+\nu-l) \times \mathbb{Z}_2^l$ and $\mathbf{S}(n-l') \times \mathbf{S}(l') \times \mathbf{S}(n+\nu-l') \times \mathbb{Z}_2^{l'}$ due to the sum. The global prefactor $1/\Delta_{2n+\nu}(Z'_{l'})$ reflects the singularities when an eigenvalue in $x'^{(1)}$ agrees with one in $x'^{(3)}$ as well as a complex eigenvalue pair in $x'^{(2)}$ degenerates with another eigenvalue in $Z'_{l'}$, namely then $Z'_{l'}$ commutes with some non-compact subgroups in $\mathbb{G}_l$. Hereby the eigenvalues which have to degenerate via the Dirac delta functions are excluded.

In the next section we show that the chosen global coefficients in Eq. (A.22) are the correct ones. For this we consider the stationary phase approximation which fixes these coefficients.

The Stationary Phase Approximation of $\mathcal{I}_l(Z_l, Z'_{l'})$

Let us introduce a scalar parameter t as a small parameter in the integral $\mathcal{I}_l(t^{-1}Z_l, Z'_{l'})$ as a bookkeeping device for the expansion around the saddle-points. Taking $t \to 0$ the group integral (A.6) can be evaluated by a saddle point approximation. The saddlepoint equation is given by

$$\operatorname{tr} dUU^{-1}[UZ_lU^{-1}, Z'_{l'}]_- = 0. \tag{A.23}$$

If $l \neq l'$ this equation cannot be satisfied in all directions. The reason is that the quasi-diagonal matrix $Z'_{l'}$ will never commute with a γ_5-Hermitian matrix with exactly $l \neq l'$ complex conjugate eigenvalue pairs since UZ_lU^{-1} can be at most quasi-diagonalized by $\mathrm{U}(n, n+\nu)$ and generically $[Z_l, Z'_{l'}]_- \neq 0$. This means that we can only expand the sub-Lie-algebra $\mathrm{o}^{l-l'}(1/1)$ to the linear

order while the remaining massive modes are expanded to the second order. The extrema are given by

$$U_0 = \Pi' \Phi \Pi \in \mathbb{G}_l \tag{A.24}$$

where the permutations are

$$\begin{aligned} \Pi &\in \mathbf{S}(n-l) \times [\mathbf{S}(l)/[\mathbf{S}(l') \times \mathbf{S}(l-l')]] \times \mathbf{S}(n+\nu-l), \\ \Pi' &\in [\mathbf{S}(n-l')/\mathbf{S}(n-l)] \times \mathbf{S}(l') \times [\mathbf{S}(n+\nu-l')/\mathbf{S}(n+\nu-l)] \times \mathbb{Z}^{l'}, \end{aligned} \tag{A.25}$$

and a block-diagonal matrix

$$\Phi = \left[\begin{array}{c|c|c|c|c|c} \mathbb{1}_{n-l} & 0 & 0 & 0 & 0 & 0 \\ \hline 0 & \exp[\imath\widehat{\Phi}] & 0 & 0 & 0 & 0 \\ \hline 0 & 0 & \mathbb{1}_{l'} & 0 & 0 & 0 \\ \hline 0 & 0 & 0 & \mathbb{1}_{l'} & 0 & 0 \\ \hline 0 & 0 & 0 & 0 & \exp[-\imath\widehat{\Phi}] & 0 \\ \hline 0 & 0 & 0 & 0 & 0 & \mathbb{1}_{n+\nu-l} \end{array}\right], \tag{A.26}$$

where the diagonal matrix of angles is $\widehat{\Phi} = \mathrm{diag}\,(\varphi_1, \ldots, \varphi_{l-l'}) \in [0,\pi]^{l-l'}$. The matrix Φ describes the set $S_1^{l-l'}$ ($l-l'$ unit circles in the complex plane) which commutes with $Z'_{l'}$ and is a subgroup of $\mathbb{G}_l$. Note that other rotations commuting with $Z'_{l'}$ are already divided out in $\mathbb{G}_l$. The matrix of phases already comprises the complex conjugation of the complex eigenvalues represented by the finite group $\mathbb{Z}_2^{l-l'}$, choosing $\varphi_j = \pi/2$ switches the sign of the imaginary part y'_j. However we have to introduce the complex conjugation for those complex conjugated pairs in $Z'_{l'}$ which couple with pairs in Z_l, cf. the group $\mathbb{Z}^{l'}$ in Π'.

The expansion of U reads

$$U = \Pi' \Phi \left(\mathbb{1}_{2n+\nu} - tH_1 - \sqrt{t} H_2 + \frac{t}{2} H_2^2 \right) \Pi. \tag{A.27}$$

We employ the notation (A.18) for the action of $\omega \in \mathbf{S}(n-l) \times \mathbf{S}(l) \times \mathbf{S}(n+\nu-l) \times \mathbb{Z}^l$ and $\omega' \in \mathbf{S}(n-l') \times \mathbf{S}(l') \times \mathbf{S}(n+\nu-l') \times \mathbb{Z}^{l'}$ on the matrices $Z_{l\omega}$ and $Z'_{l'\omega'}$, respectively. Note that the matrix Φ commutes with $Z'_{l'\omega'}$ for any ω' and hence, only yields an overall prefactor $\pi^{l-l'}$. The matrix H_1 spans the

Lie algebra $\mathrm{o}^{l-l'}(1,1)$ and is embedded as

$$H_1 = \left(\begin{array}{c|c|c|c|c|c} 0 & 0 & 0 & 0 & 0 & 0 \\ \hline 0 & 0 & 0 & 0 & h & 0 \\ \hline 0 & 0 & 0 & 0 & 0 & 0 \\ \hline 0 & 0 & 0 & 0 & 0 & 0 \\ \hline 0 & h & 0 & 0 & 0 & 0 \\ \hline 0 & 0 & 0 & 0 & 0 & 0 \end{array}\right) \text{ with } h = \mathrm{diag}\,(h_1, \ldots, h_{l-l'}) \in \mathbb{R}^{l-l'}. \tag{A.28}$$

The matrix H_2 is in the tangent space of the coset $\mathbb{G}_l/[\mathrm{U}^{\,l-l'}(1) \times \mathrm{O}^{l-l'}(1,1)] = \mathrm{U}\,(n, n+\nu)/[\mathrm{U}^{\,2n+\nu-2l+l'}(1) \times \mathrm{O}^{l'}(1,1) \times \mathrm{U}^{\,l-l'}(1,1)]$ and has the form

$$H_2 = \left(\begin{array}{c|c||c|c|c||c} H_{11} & H_{12} & H_{13} & H_{14} & H_{15} & H_{16} \\ \hline\hline -H_{12}^\dagger & H_{22} & H_{23} & H_{24} & H_{25} & H_{26} \\ \hline -H_{13}^\dagger & -H_{23}^\dagger & H_{33} & H_{34} & H_{35} & H_{36} \\ H_{14}^\dagger & H_{24}^\dagger & H_{34}^\dagger & H_{44} & H_{45} & H_{46} \\ \hline H_{15}^\dagger & H_{25}^\dagger & H_{35}^\dagger & -H_{45}^\dagger & H_{55} & H_{56} \\ \hline\hline H_{16}^\dagger & H_{26}^\dagger & H_{36}^\dagger & -H_{46}^\dagger & -H_{56}^\dagger & H_{66} \end{array}\right), \tag{A.29}$$

where H_{11}, H_{22}, H_{55}, and H_{66} are anti-Hermitian matrices without diagonal elements since they are divided out in the coset $\mathbb{G}_l$ or are lost to Φ. The two matrices H_{33} and H_{44} are anti-Hermitian matrices whose diagonal elements are the same with opposite sign which is also because of the subgroup we divide in $\mathbb{G}_l$. The matrices H_{12}, H_{13}, H_{14}, H_{15}, H_{16}, H_{23}, H_{24}, H_{26}, H_{35}, H_{36}, H_{45}, H_{46}, and H_{56} are arbitrary complex matrices. Since we have to remove the degrees of freedom already included in H_1 and in the subgroups quotiened out in $\mathbb{G}_l$ the matrix H_{25} is a complex matrix with all $l - l'$ diagonal elements removed and H_{34} is a complex matrix whose diagonal entries are real. The sizes of the blocks of H_1 and H_2 correspond to the sizes shown in the diagonal matrix of phases Φ, see Eq. (A.26). The double lines in the matrix (A.29) shall show the decomposition of Z_l in its real and complex eigenvalues whereas the single lines represent the decomposition for $Z'_{l'}$.

The exponent in the coset integral (A.6) takes the form

$$\mathrm{tr}\, U Z_l U^{-1} Z'_{l'} = \mathrm{tr}\, Z_{l\omega} Z'_{l'\omega'} - t\mathrm{tr}\,[Z_{l\omega}, Z'_{l'\omega'}]_- H_1 - \frac{t}{2}\mathrm{tr}\,[Z_{l\omega}, H_2]_-[Z'_{l'\omega'}, H_2]_-. \tag{A.30}$$

The measure for H_1 and H_2 is the induced Haar measure, i.e.

$$\mathrm{tr}\,[U^{-1}dU, Z_{l\omega}]_-^2 = \mathrm{tr}\,[\Phi^\dagger d\Phi, Z_{l\omega}]_-^2 + t^2\mathrm{tr}\,[dH_1, Z_{l\omega}]_-^2 + t\mathrm{tr}\,[dH_2, Z_{l\omega}]_-^2 \tag{A.31}$$

which gives

$$\begin{aligned} d\mu_{\mathbb{G}}(U) &= t^{(2n+\nu)(2n+\nu-1)/2} d[H_1] d[\Phi] d[H_2] \\ &= (-1)^{n(n+\nu)} \left(\frac{2}{\imath}\right)^{l'} \prod_{j=1}^{l-l'} \frac{4t}{\imath} d\varphi_j dh_j \prod_{j,i} 2t\, d\mathrm{Re}\,(H_2)_{ij} d\mathrm{Im}\,(H_2)_{ij}. \end{aligned} \tag{A.32}$$

The product over the two indices i and j is over all independent matrix elements of H_2.

We emphasize again that the integrand in $\mathcal{I}_l(t^{-1}Z_l, Z'_{l'})$ does not depend on Φ making this integration trivial and yielding the prefactor $\pi^{l-l'}$. The integral over H_1 yields the $l-l'$ Dirac delta functions mentioned in Eq. (A.21), i.e. it yields

$$(2\pi)^{l-l'} \prod_{j=1}^{l-l'} \delta\left(2y^{(2)}_{\omega(j)}\left[x'^{(1)}_{\omega'(n-l+j)} - x'^{(3)}_{\omega'(j)}\right]\right) = \prod_{j=1}^{l-l'} \frac{\pi\delta\left(x'^{(1)}_{\omega'(n-l+j)} - x'^{(3)}_{\omega'(j)}\right)}{|y^{(2)}_{\omega(j)}|}. \tag{A.33}$$

The integrals over H_2 are simple Gaussian integrals resulting in the main result of this section,

$$\begin{aligned} \mathcal{I}_l(t^{-1}Z_l, Z'_{l'}) &= \frac{(-2\pi\imath)^{l-l'}}{l'!(l-l')!(n-l)!(n+\nu-l)!2^l} \\ &\times \frac{(-2\pi\imath)^{(2n+\nu)(2n+\nu-1)/2}}{\Delta_{2n+\nu}(t^{-1}Z_l)\Delta_{2n+\nu}(Z'_{l'})} \prod_{j=1}^{l} \frac{y^{(2)}_j}{|y^{(2)}_j|} \prod_{j=1}^{l'} \frac{y'^{(2)}_j}{|y'^{(2)}_j|} \\ &\times \sum_{\substack{\omega\in\mathbb{S}(n-l)\times\mathbb{S}(l)\times\mathbb{S}(n+\nu-l)\times\mathbb{Z}_2^l \\ \omega'\in\mathbb{S}(n-l')\times\mathbb{S}(l')\times\mathbb{S}(n+\nu-l')\times\mathbb{Z}_2^{l'}}} \mathrm{sign}\,\omega\omega' \exp\left(\frac{\imath}{t}\mathrm{tr}\, Z_{l\omega}Z'_{l'\omega'}\right) \\ &\times \prod_{j=1}^{|l-l'|} \left(x'^{(1)}_{\omega'(n-l+j)} - x'^{(3)}_{\omega'(j)}\right) \delta\left(x'^{(1)}_{\omega'(n-l+j)} - x'^{(3)}_{\omega'(j)}\right). \end{aligned} \tag{A.34}$$

The overall coefficient $c^{(ll')}$ in Eq. (A.22) can be easily read off. Thereby the numerator of the first factor results from the integral over H_1 and is related

to the $l-l'$ Dirac delta functions. The denominator is the volume of the finite group $\mathbf{S}(n-l)\times\mathbf{S}(l')\times\mathbf{S}(l-l')\times\mathbf{S}(n+\nu-l)\times\mathbb{Z}^l$ which we extend to summing over the full Weyl groups for Z_l and $Z'_{l'}$. We recall that the sum over permutations in $\mathbf{S}(l)$ and $\mathbf{S}(l')$ describe the interchange of complex pairs which are even permutations because we interchange both z_k and z_k^* with another pair. The numerator of the term with the Vandermonde determinants essentially results from the Gaussian integrals and always appear independent of how many complex pairs Z_l and $Z'_{l'}$ have. The factors of t^{-1} appear as prefactors of Z_l and can be omitted again since they have done their job as bookkeeping device.

Let us summarize what we have found. Comparing the result (A.34) with the Z_l dependence of the ansatz $\mathcal{I}(Z_l, Z'_l)$ given in Eq. (A.22), we observe that they are exactly the same. This implies that the asymptotically large Z_l result for the integral (A.6) is actually equal to the exact result. We conclude that the non-compact Harish-Chandra-Itzykson-Zuber integral is semi-classically exact and seems to fulfill the conditions of the Duistermaat-Heckman theorem [134].

Let us consider two particular cases. For $l=l'$ we sum over all permutation in $\mathbf{S}(l)$ which yields the permanent in Eq. (A.20), whereas the sum over permutations in $\mathbf{S}(n+\nu-l)$ and $\mathbf{S}(n-l)$ gives determinants and thus, agrees. The special case $n=0$ yields the original Harish-Chandra-Itzykson-Zuber integral [136, 137], see Eq. (A.7).

The joint probability density

We explicitly write out Z_l and apply Eq. (A.34) for $Z'_{l'}=s$. Then, we find for our original non-compact group integral

$$\begin{aligned}\mathcal{I}_l(Z_l,s) \;=\; & \frac{(-2\pi\imath)^{(2n+\nu)(2n+\nu-1)/2}}{(n-l)!l!(n+\nu-l)!}\frac{(-2\pi\imath)^l}{\Delta_{2n+\nu}(Z_l)\Delta_{2n+\nu}(s)} \\ & \times\sum_{\substack{\omega'\in\mathbf{S}(n-l)\times\mathbf{S}(l)\times\mathbf{S}(n+\nu-l)\\ \omega\in\mathbf{S}(n)\times\mathbf{S}(n+\nu)}}\operatorname{sign}(\omega\omega')\prod_{j=1}^{n-l}\exp\left(\imath x^{(1)}_{\omega'(j)}s^{(\mathrm{r})}_{\omega(j)}\right) \\ & \times\prod_{j=1}^{n+\nu-l}\exp\left(\imath x^{(3)}_{\omega'(j)}s^{(\mathrm{l})}_{\omega(l+j)}\right)\prod_{j=1}^{l}\frac{y^{(2)}_{\omega'(j)}}{|y^{(2)}_{\omega'(j)}|}\left(s^{(\mathrm{r})}_{\omega(n-l+j)}-s^{(\mathrm{l})}_{\omega(j)}\right) \\ & \times\delta\left(s^{(\mathrm{r})}_{\omega(n-l+j)}-s^{(\mathrm{l})}_{\omega(j)}\right)\exp\left(\imath x^{(2)}_{\omega'(j)}\left(s^{(\mathrm{r})}_{\omega(n-l+j)}+s^{(\mathrm{l})}_{\omega(j)}\right)\right).\end{aligned} \tag{A.35}$$

Now we are ready to integrate over s.

We plug Eq. (A.35) into the integral (A.3). The sum over the permutations

can be absorbed by the integral due to relabeling resulting in

$$
\begin{aligned}
I[f] = \quad & C \sum_{l=0}^{n} \frac{(-2\pi\imath)^{(2n+\nu)(2n+\nu-1)/2+l}}{2^l (n-l)!\, l!\, (n+\nu-l)!} \int\limits_{\mathbb{R}^{\nu+2(n-l)}\times\mathbb{C}^l} d[Z_l]\, \Delta_{2n+\nu}(Z_l^*) \qquad \text{(A.36)} \\
& \times f(Z_l) \prod_{j=1}^{l} \frac{y_j^{(2)}}{|y_j^{(2)}|} \int\limits_{\mathbb{R}^{2n+\nu}} d[s_{\mathrm{r}}, s_{\mathrm{l}}] \frac{\Delta_n^2(s_{\mathrm{r}})\, \Delta_{n+\nu}^2(s_{\mathrm{l}})}{\Delta_{2n+\nu}(s)} \\
& \times \prod_{j=1}^{n-l} \exp\left[\frac{n}{2} (x_j^{(1)})^2 + \imath x_j^{(1)} s_j^{(\mathrm{r})} - \frac{a^2}{2n(1+a^2)} (s_j^{(\mathrm{r})} + \imath\mu_{\mathrm{r}})^2 \right] \\
& \times \prod_{j=1}^{n+\nu-l} \exp\left[\frac{n}{2} (x_j^{(3)})^2 + \imath x_j^{(3)} s_{l+j}^{(\mathrm{l})} - \frac{a^2}{2n(1+a^2)} (s_{l+j}^{(\mathrm{l})} + \imath\mu_{\mathrm{l}})^2 \right] \\
& \times \prod_{j=1}^{l} \left(s_{n-l+j}^{(\mathrm{r})} - s_j^{(\mathrm{l})} \right) \delta\left(s_{n-l+j}^{(\mathrm{r})} - s_j^{(\mathrm{l})} \right) \exp\left[\frac{a^2}{4n(1+a^2)} (\mu_{\mathrm{r}} - \mu_{\mathrm{l}})^2 \right] \\
& \times \exp\left[n((x_j^{(2)})^2 - (y_j^{(2)})^2) + 2\imath x_j^{(2)} s_j^{(\mathrm{l})} - \frac{a^2}{n(1+a^2)} \left(s_j^{(\mathrm{l})} + \imath \frac{\mu_{\mathrm{r}} + \mu_{\mathrm{l}}}{2} \right)^2 \right].
\end{aligned}
$$

The quotient of the Vandermonde determinants is

$$
\frac{\Delta_n^2(s_{\mathrm{r}})\, \Delta_{n+\nu}^2(s_{\mathrm{l}})}{\Delta_{2n+\nu}(s)} = (-1)^{n(n-1)/2+\nu(\nu-1)/2} \det \begin{bmatrix} \left\{ \dfrac{1}{s_i^{(\mathrm{r})} - s_j^{(\mathrm{l})}} \right\}_{\substack{1\le i\le n \\ 1\le j\le n+\nu}} \\ \left\{ (s_j^{(\mathrm{l})})^{i-1} \right\}_{\substack{1\le i\le \nu \\ 1\le j\le n+\nu}} \end{bmatrix} \qquad \text{(A.37)}
$$

This determinant also appears in the supersymmetry method of RMT [139–141] and is a square root of a Berezinian (the supersymmetric analogue of the Jacobian).

Expanding the determinant (A.37) in the last l columns not all terms will survive. Only those terms which cancel the prefactor of the Dirac delta functions do not vanish. The integration over diag $(s_{n-l+1}^{(\mathrm{r})}, \ldots, s_{n-l+1}^{(\mathrm{r})}, s_1^{(\mathrm{l})}, \ldots, s_l^{(\mathrm{l})})$

yields

$$
\begin{aligned}
I[f] \;=\; & C\sum_{l=0}^{n}\frac{(-2\pi\imath)^{(2n+\nu)(2n+\nu-1)/2+l}(-1)^{n(n-1)/2+\nu(\nu-1)/2+(n+l)l}}{2^l(n-l)!l!(n+\nu-l)!} \qquad \text{(A.38)}\\
& \times \int\limits_{\mathbb{R}^{\nu+2(n-l)}\times\mathbb{C}^l} d[Z_l]\Delta_{2n+\nu}(Z_l^*)f(Z_l) \int\limits_{\mathbb{R}^{\nu+2(n-l)}} d[s_{\mathrm{r}}\,,s_{\mathrm{l}}]\\
& \times \det\begin{bmatrix} \left\{\dfrac{1}{s_i^{(\mathrm{r})}-s_j^{(\mathrm{l})}}\right\}_{\substack{1\le i\le n-l\\ 1\le j\le n+\nu-l}} \\ \left\{(s_j^{(\mathrm{l})})^{i-1}\right\}_{\substack{1\le i\le \nu\\ 1\le j\le n+\nu-l}} \end{bmatrix}\\
& \times \prod_{j=1}^{n-l}\exp\left[\frac{n}{2}(x_j^{(1)})^2+\imath x_j^{(1)}s_j^{(\mathrm{r})}-\frac{a^2}{2n(1+a^2)}(s_j^{(\mathrm{r})}+\imath\mu_{\mathrm{r}})^2\right]\\
& \times \prod_{j=1}^{n+\nu-l}\exp\left[\frac{n}{2}(x_j^{(3)})^2+\imath x_j^{(3)}s_{l+j}^{(\mathrm{l})}-\frac{a^2}{2n(1+a^2)}(s_{l+j}^{(\mathrm{l})}+\imath\mu_{\mathrm{l}})^2\right]\\
& \times \prod_{j=1}^{l}\sqrt{\frac{n\pi(1+a^2)}{a^2}}\frac{y_j^{(2)}}{|y_j^{(2)}|}\exp\left[\frac{a^2}{4n(1+a^2)}(\mu_{\mathrm{r}}-\mu_{\mathrm{l}})^2\right]\\
& \times \exp\left[-\frac{n}{a^2}(x_j^{(2)})^2-n(y_j^{(2)})^2+x_j^{(2)}(\mu_{\mathrm{r}}+\mu_{\mathrm{l}})\right].
\end{aligned}
$$

The other exponential functions as well as the remaining integrations over s_{r} and s_{l} can be pulled into the determinant. The integrals in the ν bottom rows yield harmonic oscillator wave function. These can be reordered into

monomials times a Gaussian. This results in

$$
\begin{aligned}
I[f] &= C\sum_{l=0}^{n}\frac{(-2\pi\imath)^{(2n+\nu)(2n+\nu-1)/2+l}(-1)^{n(n-1)/2+\nu(\nu-1)/2+(n+l)l}}{2^l(n-l)!l!(n+\nu-l)!} \qquad \text{(A.39)}\\
&\times(2\pi)^{\nu/2}\imath^{\nu(\nu-1)/2}\left(\frac{n(1+a^2)}{a^2}\right)^{\nu^2/2}\int\limits_{\mathbb{R}^{\nu+2(n-l)}\times\mathbb{C}^l} d[Z_l]\Delta_{2n+\nu}(Z_l^*)f(Z_l)\\
&\times\det\begin{bmatrix}\left\{\widetilde{G}(x_i^{(1)},x_j^{(3)})\right\}_{\substack{1\le i\le n-l\\1\le j\le n+\nu-l}}\\ \left\{(x_j^{(3)})^{i-1}\exp\left[-\frac{n}{2a^2}(x_j^{(3)})^2+\mu_{\rm l}x_j^{(3)}\right]\right\}_{\substack{1\le i\le \nu\\1\le j\le n+\nu-l}}\end{bmatrix}\\
&\times\prod_{j=1}^{l}\sqrt{\frac{n\pi(1+a^2)}{a^2}}\frac{y_j^{(2)}}{|y_j^{(2)}|}\exp\left[\frac{a^2}{4n(1+a^2)}(\mu_{\rm r}-\mu_{\rm l})^2\right]\\
&\times\exp\left[-\frac{n}{a^2}(x_j^{(2)})^2-n(y_j^{(2)})^2+x_j^{(2)}(\mu_{\rm r}+\mu_{\rm l})\right].
\end{aligned}
$$

What remains is to simplify the function

$$
\begin{aligned}
\widetilde{G}(x_i^{(1)},x_j^{(3)}) &= \int\limits_{\mathbb{R}^2} ds_{\rm r}\,ds_{\rm l}\,\frac{\exp\left[x_i^{(1)}\mu_{\rm r}+x_j^{(3)}\mu_{\rm l}\right]}{s_{\rm r}-s_{\rm l}+\imath n(1+a^2)(x_i^{(1)}-x_j^{(3)})/a^2} \qquad \text{(A.40)}\\
\times\exp&\left[-\frac{n}{2a^2}\left((x_i^{(1)})^2+(x_j^{(3)})^2\right)-\frac{a^2}{2n(1+a^2)}\left((s_{\rm r}+\imath\mu_{\rm r})^2+(s_{\rm l}+\imath\mu_{\rm l})^2\right)\right].
\end{aligned}
$$

We use the difference $x_i^{(1)}-x_j^{(3)}$ as a regularization of the integral. This works because generically this difference is not equal to zero. Then we can express the denominator as an exponential function. Let $\beta=(x_i^{(1)}-x_j^{(3)})/|x_i^{(1)}-x_j^{(3)}|$

be the sign of this difference. The integral (A.40) can be written as

$$\begin{aligned}
\widetilde{G}(x_i^{(1)}, x_j^{(3)}) &= \frac{\beta}{\imath} \exp\left[x_i^{(1)}\mu_{\mathrm{r}} + x_j^{(3)}\mu_{\mathrm{l}} - \frac{n}{2a^2}\left((x_i^{(1)})^2 + (x_j^{(3)})^2\right)\right] \\
&\quad \times \int_0^\infty dt \int_{\mathbb{R}^2} ds_{\mathrm{r}}\, ds_{\mathrm{l}} \exp\left[-\frac{n(1+a^2)}{a^2}|x_i^{(1)} - x_j^{(3)}|t + \imath\beta(s_{\mathrm{r}} - s_{\mathrm{l}})t\right] \\
&\quad \times \exp\left[-\frac{a^2}{2n(1+a^2)}\left((s_{\mathrm{r}} + \imath\mu_{\mathrm{r}})^2 + (s_{\mathrm{l}} + \imath\mu_{\mathrm{l}})^2\right)\right] \\
&= \frac{-2\pi\imath n(1+a^2)}{a^2}\beta \exp\left[x_i^{(1)}\mu_{\mathrm{r}} + x_j^{(3)}\mu_{\mathrm{l}} - \frac{n}{2a^2}\left((x_i^{(1)})^2 + (x_j^{(3)})^2\right)\right] \\
&\quad \times \int_0^\infty \exp\left[-\frac{n(1+a^2)}{a^2}t^2 + \left(\beta(\mu_{\mathrm{r}} - \mu_{\mathrm{l}}) - \frac{n(1+a^2)}{a^2}|x_i^{(1)} - x_j^{(3)}|\right)t\right] dt \\
&= -\pi\imath\sqrt{\frac{\pi n(1+a^2)}{a^2}}\beta \exp\left[-\frac{n}{4a^2}\left(x_i^{(1)} + x_j^{(3)}\right)^2 + \frac{n}{4}\left(x_i^{(1)} - x_j^{(3)}\right)^2\right] \\
&\quad \times \exp\left[\frac{1}{2}\left(x_i^{(1)} + x_j^{(3)}\right)(\mu_{\mathrm{r}} + \mu_{\mathrm{l}}) + \frac{a^2}{4n(1+a^2)}(\mu_{\mathrm{r}} - \mu_{\mathrm{l}})^2\right] \\
&\quad \times \mathrm{erfc}\left[\sqrt{\frac{n(1+a^2)}{4a^2}}|x_i^{(1)} - x_j^{(3)}| - \beta\sqrt{\frac{a^2}{4n(1+a^2)}}(\mu_{\mathrm{r}} - \mu_{\mathrm{l}})\right]. \qquad \text{(A.41)}
\end{aligned}$$

Plugging this result into Eq. (A.39) we get the joint probability density for a fixed number of real eigenvalues given in Eq. (2.25). Moreover one can perform the sum over l to find the joint probability density of all eigenvalues given in Eq. (2.18).

Appendix B

Two useful integral identities

In this appendix we evaluate two integrals that have been used to simplify the expression for ρ_{r} and ρ_{c}.

B.1 Two useful integral identities

B.1.1 Convolution of a Gaussian with an error function

Let $\mathrm{Re}\,\gamma^2 > -1$. We consider the integral

$$I(\alpha,\gamma) = \int_{\mathbb{R}} \exp[-(x+\alpha)^2]\mathrm{erf}(\gamma x)dx. \tag{B.1}$$

The solution can be obtained by constructing an initial value problem. Since the Gaussian is symmetric and the error function anti-symmetric around the origin we have

$$I(0,\gamma) = 0. \tag{B.2}$$

Joint work with M. Kieburg and J.J.M. Verbaarschot.

The derivative is

$$\begin{aligned}\partial_\alpha I(\alpha,\gamma) &= \int_{\mathbb{R}} \mathrm{erf}(\gamma x)\partial_x \exp[-(x+\alpha)^2]dx \\ &= -\frac{2\gamma}{\sqrt{\pi}}\int_{\mathbb{R}} \exp[-(x+\alpha)^2-\gamma^2x^2]dx \\ &= -\frac{2\gamma}{\sqrt{\gamma^2+1}}\exp\left[-\frac{\gamma^2\alpha^2}{\gamma^2+1}\right]. \end{aligned} \tag{B.3}$$

Integrating the derivative from 0 to α we find the desired result

$$\int_{\mathbb{R}} \exp[-(x+\alpha)^2]\mathrm{erf}(\gamma x)dx = -\sqrt{\pi}\,\mathrm{erf}\left(\frac{\gamma\alpha}{\sqrt{\gamma^2+1}}\right). \tag{B.4}$$

This integral is needed to simplify the term (2.44).

Another integral identity which is used for the derivation of the level density of the real eigenvalues with positive chirality is given by

$$\begin{aligned}&\int_{\mathbb{R}^2} \exp(-\alpha_1x_1^2-\alpha_2x_2^2+\beta_1x_1+\beta_2x_2)\mathrm{erf}\left(\frac{x_1+\delta x_2}{\gamma}+\epsilon\right)dx_1dx_2 \\ =\ &\frac{\pi}{\sqrt{\alpha_1\alpha_2}}\exp\left[\frac{1}{4}\left(\frac{\beta_1^2}{\alpha_1}+\frac{\beta_2^2}{\alpha_2}\right)\right]\mathrm{erf}\left(\frac{\alpha_2\gamma\beta_1+\alpha_1\gamma\delta\beta_2+2\alpha_1\alpha_2\gamma^2\epsilon}{2\sqrt{\alpha_1\alpha_2\gamma^2(\alpha_1\alpha_2\gamma^2+\alpha_1\delta^2+\alpha_2)}}\right). \end{aligned} \tag{B.5}$$

This identity is a direct consequence of the identity (B.4). The constants α_i (with $\mathrm{Re}\,\alpha_i > 0$), β_i, $\gamma \neq 0$, δ and ϵ are arbitrary.

B.1.2 Convolution of a Gaussian with a *sinus cardinalis*

The second integral enters in the simplification of the asymptotic behavior of ρ_c. It is the convolution integral

$$\widetilde{I}(\alpha,\gamma) = \int_{\mathbb{R}} dx \exp[-(x+\alpha)^2]\mathrm{sinc}(\gamma x). \tag{B.6}$$

To evaluate this integral we introduce an auxiliary integral to obtain a Fourier transform of a Gaussian, i.e.

$$\widetilde{I}(\alpha,\gamma) \;=\; \frac{1}{\gamma}\int_0^{\gamma} d\widetilde{\gamma}\int_{\mathbb{R}} dx\,\exp[-(x+\alpha)^2]\cos(\widetilde{\gamma}x). \tag{B.7}$$

First we integrate over x and then over $\widetilde{\gamma}$ to obtain an expression in terms of error functions,

$$\widetilde{I}(\alpha,\gamma) \;=\; \frac{\pi}{\gamma}\exp(-\alpha^2)\mathrm{Re}\ \mathrm{erf}\left(\frac{\gamma}{2}+\imath\alpha\right). \tag{B.8}$$

Appendix C

The $Z_{1/1}$ partition function

In this appendix we evaluate the partition function $Z^{\nu}_{1/1}$ which enters in the expression for the distribution of the chiralities over the real eigenvalues of $D_{\rm W}$. The derivation below is along the lines given in Ref. [102].

C.1 The $Z_{1/1}$ partition function

We employ the parametrization (2.53) to evaluate

$$\lim_{\varepsilon\to 0}\mathrm{Im}\int\frac{\det(D_{\rm W}-z_1\mathbb{1}_{2n+\nu})}{\det(D_{\rm W}-x_2\mathbb{1}_{2n+\nu}\mp\imath\varepsilon\gamma_5)}P(D_{\rm W})d[D_{\rm W}] \tag{C.1}$$

$$\stackrel{n\gg 1}{=}-\lim_{\varepsilon\to 0}\mathrm{Im}\int\frac{de^{\imath\varphi}}{2\pi\imath}de^{\vartheta}d\eta d\eta^{*}\mathrm{Sdet}^{\,\nu}U\exp[-\widehat{a}_8^2\mathrm{Str}\,(U^2+U^{-2})]$$

$$\times\exp\left[\pm\frac{\imath}{2}\mathrm{Str}\,\mathrm{diag}\,(\widehat{x}_2-\widehat{m}_6,\widehat{z}_1-\widehat{m}_6)(U-U^{-1})-\left(\varepsilon\pm\frac{\imath\widehat{\lambda}_7}{2}\right)\mathrm{Str}\,(U+U^{-1})\right].$$

We employ the same trick as in Ref. [102] to linearize the exponent in U and U^{-1} by introducing an auxiliary Gaussian integral over a supermatrix, i.e.

$$\exp[-\widehat{a}_8^2\mathrm{Str}\,(U^2+U^{-2})]=\int d[\sigma]\exp\left[-\frac{1}{16\widehat{a}_8^2}\mathrm{Str}\,\sigma^2\pm\frac{\imath}{2}\mathrm{Str}\,\sigma(U-U^{-1})\right] \tag{C.2}$$

with

$$\sigma=\begin{bmatrix}\sigma_1 & \eta_\sigma\\ \eta_\sigma^{*} & \imath\sigma_2\end{bmatrix}\ \text{and}\ d[\sigma]=d\sigma_1 d\sigma_2 d\eta_\sigma d\eta_\sigma^{*}. \tag{C.3}$$

Joint work with M. Kieburg and J.J.M. Verbaarschot.

After plugging Eq. (C.2) in Eq. (C.1) we diagonalize $\sigma = V\mathrm{diag}\,(s_1, s_2)V^\dagger$ and integrate over $V \in \mathrm{U}\,(1/1)$. We obtain

$$\begin{aligned}
&\lim_{\varepsilon\to 0}\mathrm{Im}\int \frac{\det(D_{\mathrm{W}} - z_1\mathbb{1}_{2n+\nu})}{\det(D_{\mathrm{W}} - x_2\mathbb{1}_{2n+\nu} \mp \imath\varepsilon\gamma_5)} P(D_{\mathrm{W}})d[D_{\mathrm{W}}] \qquad \text{(C.4)}\\
&\overset{n\gg 1}{=} \frac{1}{16\pi\widehat{a}_8^2}(\widehat{z}_1 - \widehat{x}_2)\lim_{\varepsilon\to 0}\mathrm{Im}\int \frac{ds_1 ds_2}{s_1 - \imath s_2}\left(\frac{s_1 - \widehat{\lambda}_7 \pm \imath\varepsilon}{s_1 + \widehat{\lambda}_7 \mp \imath\varepsilon}\frac{\imath s_2 + \widehat{\lambda}_7 \mp \imath\varepsilon}{\imath s_2 - \widehat{\lambda}_7 \pm \imath\varepsilon}\right)^{\nu/2}\\
&\quad\times \exp\left[-\frac{1}{16\widehat{a}_8^2}\left((s_1 - \widehat{x}_2 + \widehat{m}_6)^2 - (s_2 + \imath\widehat{z}_1 - \imath\widehat{m}_6)^2\right)\right]\\
&\quad\times Z^\nu_{1/1}\left(\sqrt{s_1^2 - (\widehat{\lambda}_7 \mp \imath\varepsilon)^2}, \imath\sqrt{s_2^2 + (\widehat{\lambda}_7 \mp \imath\varepsilon)^2}; \widehat{a} = 0\right),
\end{aligned}$$

which expresses the partition function at non-zero lattice spacing in terms of an integral over the partition function with one bosonic and one fermionic flavor at zero lattice spacing (2.56).

The resolvent $G_{1/1}$ is given by the derivative with respect to $\widehat{z}_1$, see Eq. (2.50). To obtain a non-zero result we necessarily have to differentiate the prefactor $(\widehat{z}_1 - \widehat{x}_2)$. The distribution of the chiralities of the real eigenvalues of D_{W} follows from the imaginary part of the resolvent. The Efetov-Wegner term [142, 143] appearing after diagonalizing σ is the normalization $Z^\nu_{1/1}(1,1) = 1$ and vanishes when taking the imaginary part.

Two terms contribute to the imaginary part of the resolvent. First, the imaginary part of

$$\frac{1}{\pi}\lim_{\varepsilon\to 0}\mathrm{Im}\left[\frac{1}{(s_1 + \widehat{\lambda}_7 - \imath\varepsilon)^\nu}\right] = \frac{(-1)^{\nu-1}}{(\nu-1)!}\delta^{(\nu)}(s_1 + \widehat{\lambda}_7), \qquad \text{(C.5)}$$

is the ν-th derivative of the Dirac delta-function. Second, when $|s_1| < |\widehat{\lambda}_7|$, the imaginary part arising from the logarithmic contribution of $K_\nu(z)$, i.e.

$$K_\nu(z) = (-1)^{\nu+1}I_\nu(z)\log z + \frac{1}{z^\nu}\sum_{k=0}^{\infty} a_k z^k. \qquad \text{(C.6)}$$

The Bessel functions of the imaginary part of $Z^\nu_{1/1}(x_1, x_2, \widehat{a} = 0)$ combine into the two flavor partition function $Z^\nu_{2/0}(x_1, x_2, \widehat{a} = 0)$. Adding both contributions

we arrive at the result

$$\begin{aligned}
&\lim_{\varepsilon\to 0}\mathrm{Im}\int\frac{\det(D_{\mathrm{W}}-z_1\mathbb{1}_{2n+\nu})}{\det(D_{\mathrm{W}}-x_2\mathbb{1}_{2n+\nu}\mp\imath\varepsilon\gamma_5)}P(D_{\mathrm{W}})d[D_{\mathrm{W}}] \qquad \text{(C.7)}\\
&\overset{n\gg 1}{=}\ \frac{1}{16\pi\widehat{a}_8^2}(\widehat{z}_1-\widehat{x}_2)\mathrm{Im}\int\frac{ds_1ds_2}{s_1-\imath s_2}(\imath s_2+\widehat{\lambda}_7)^\nu(s_1+\widehat{\lambda}_7)^\nu\\
&\quad\times\exp\left[-\frac{1}{16\widehat{a}_8^2}\left((s_1-\widehat{x}_2+\widehat{m}_6)^2-(s_2+\imath\widehat{z}_1-\imath\widehat{m}_6)^2\right)\right]\\
&\times\left[\frac{\delta^{(\nu-1)}(s_1+\widehat{\lambda}_7)}{(\nu-1)!(s_1-\widehat{\lambda}_7)^\nu}\left(\frac{s_1^2-\widehat{\lambda}_7^2}{s_2^2+\widehat{\lambda}_7^2}\right)^{\nu/2}Z^\nu_{1/1}\left(\sqrt{s_1^2-\widehat{\lambda}_7^2},\imath\sqrt{s_2^2+\widehat{\lambda}_7^2};\widehat{a}=0\right)\right.\\
&\left.-\mathrm{sign}(\widehat{\lambda}_7)\Theta(|\widehat{\lambda}_7|-|s_1|)\left(s_1^2+s_2^2\right)\frac{Z^\nu_{2/0}\left(\sqrt{s_1^2-\widehat{\lambda}_7^2},\imath\sqrt{s_2^2+\widehat{\lambda}_7^2};\widehat{a}=0\right)}{[(s_1^2-\widehat{\lambda}_7^2)(s_2^2+\widehat{\lambda}_7^2)]^{\nu/2}}\right].
\end{aligned}$$

Appendix D

Derivations of the asymptotic results given in Sec. 2.4

The derivation of asymptotic limits of the spectral density can be quite nontrivial because of cancellations of the leading contributions so that a naive saddle point approximation cannot be used.

D.1 Derivations of the asymptotic results given in Sec. 2.4

In the subsections below, we derive asymptotic expressions for the average number of additional real modes (D.1.1), the level density of the right handed modes (D.1.2) and the level density of the complex modes (D.1.3). In D.1.4 we consider the distribution of chirality over the real modes.

D.1.1 The average number of additional real modes

The limit of small lattice spacing is obvious and will not be discussed here. At large lattice spacing we rewrite Eq. (2.74) as

$$N_{\text{add}} = \int\limits_{[0,2\pi]^2} \frac{d\Phi d\varphi}{8\pi^2} \cos[2\nu\Phi] \frac{1-\exp\left[-8(\widehat{a}_8^2 \sin^2\varphi + 2\widehat{a}_7^2 \cos^2\varphi)\sin^2\Phi\right]}{\sin^2\Phi}. \quad \text{(D.1)}$$

Joint work with M. Kieburg and J.J.M. Verbaarschot.

Since $\widehat{a}_{7/8}$ are large we expand the angle Φ around the origin, in particular

$$\Phi = \frac{\delta\Phi}{\sqrt{\widehat{a}_8^2 \sin^2\varphi + 2\widehat{a}_7^2 \cos^2\varphi}} \ll 1. \tag{D.2}$$

Note that we have two equivalent saddlepoints at 0 and at π. We thus have

$$N_{\text{add}} = \int\limits_{\mathbb{R}\times[0,2\pi]} \frac{d\delta\Phi d\varphi}{4\pi^2} \frac{1-\exp\left[-8\delta\Phi^2\right]}{\delta\Phi^2} \sqrt{\widehat{a}_8^2 \sin^2\varphi + 2\widehat{a}_7^2 \cos^2\varphi}. \tag{D.3}$$

The integral over $\delta\Phi$ is equal to $\sqrt{32\pi}$, and the integral over φ is the elliptic integral of the second kind. Hence we obtain the result (2.75).

D.1.2 The distribution of the additional real modes

We have two different cases for the behavior of ρ_{r} at large lattice spacing. To derive the large $\widehat{a}$ asymptotics in the case $\widehat{a}_8^2 = 0$ we rewrite Eq. (2.70) as a group integral, i.e.

$$\begin{aligned}
\rho_{\text{r}}(\widehat{x}) \;=\; & \frac{1}{2^{15/2}\pi\widehat{a}_7\sqrt{\widehat{a}_8^2+2\widehat{a}_6^2}} \int\limits_{\mathbb{R}^2} d\widehat{\lambda}_7 d\widetilde{x} \int\limits_{\text{U}(2)} d\mu(U) \det{}^{\nu} U \exp\left[-\frac{\widehat{\lambda}_7^2}{16\widehat{a}_7^2}\right] \\
& \times \left[\text{sign}(\widetilde{x}-\widehat{x}) - \text{erf}\left(\frac{\widetilde{x}-\widehat{x}+2\widehat{\lambda}_7}{\sqrt{32\widehat{a}_8^2}}\right)\right](\widetilde{x}-\widehat{x}) \\
& \times \exp\left[-\widehat{a}_8^2 \text{tr}\left(U+U^{-1}-\frac{\widetilde{x}+\widehat{x}}{8\widehat{a}_8{}^2}\mathbb{1}_2\right)^2\right] \\
& \times \exp\left[\frac{\widehat{a}_6^2\widehat{a}_8^2}{\widehat{a}_8^2+2\widehat{a}_6^2}\text{tr}^{\,2}\left(U+U^{-1}-\frac{\widetilde{x}+\widehat{x}}{8\widehat{a}_8{}^2}\mathbb{1}_2\right)\right] \\
& \times \exp\left[\frac{\widetilde{x}-\widehat{x}}{4}\text{tr}\,\text{diag}\,(1,-1)(U+U^{-1}) + \frac{\widehat{\lambda}_7}{2}\text{tr}\,(U-U^{-1})\right]
\end{aligned} \tag{D.4}$$

For $\widehat{a}_8^2 = 0$ Eq. (D.4) simplifies to

$$\begin{aligned}
\rho_{\mathrm{r}}(\widehat{x}) &= \frac{1}{256\pi\widehat{a}_7\widehat{a}_6}\int\limits_{\mathbb{R}^2} d\widehat{\lambda}_7 d\widetilde{x} \int\limits_{\mathrm{U}\,(2)} d\mu(U)\det{}^{\nu}U \exp\left[-\frac{\widehat{\lambda}_7^2}{16\widehat{a}_7^2}\right] \\
&\quad \times \left[\mathrm{sign}(\widetilde{x}-\widehat{x}) - \mathrm{sign}(\widetilde{x}-\widehat{x}+2\widehat{\lambda}_7)\right](\widetilde{x}-\widehat{x}) \exp\left[-\frac{(\widetilde{x}+\widehat{x})^2}{64\widehat{a}_6^2}\right] \\
&\quad \times \exp\left[\frac{\widetilde{x}-\widehat{x}}{4}\mathrm{tr}\,\mathrm{diag}\,(1,-1)(U+U^{-1}) + \frac{\widehat{\lambda}_7}{2}\mathrm{tr}\,(U-U^{-1})\right] \\
&= \frac{1}{32\pi\widehat{a}_7\widehat{a}_6}\int\limits_{\mathbb{R}} d\widetilde{x}\left(\Theta(\widetilde{x})\int\limits_{-\infty}^{-\widetilde{x}} - \Theta(-\widetilde{x})\int\limits_{-\widetilde{x}}^{\infty}\right) d\widehat{\lambda}_7 \int\limits_{\mathrm{U}\,(2)} d\mu(U)\det{}^{\nu}U \\
&\quad \times\widetilde{x}\exp\left[-\frac{\widehat{\lambda}_7^2}{16\widehat{a}_7^2} - \frac{(\widetilde{x}+\widehat{x})^2}{16\widehat{a}_6^2} - \frac{\sqrt{\widehat{\lambda}_7^2-\widetilde{x}^2}}{2}\mathrm{tr}\,(U-U^{-1})\right]. \qquad \text{(D.5)}
\end{aligned}$$

For the second equality we substituted $\widetilde{x} \to 2\widetilde{x}+\widehat{x}$ and replaced the sign functions by the integration domains of $\widehat{\lambda}_7$. Moreover we used the fact that the group integral only depends on $\sqrt{\widehat{\lambda}_7^2-\widetilde{x}^2}$.

The saddlepoint equation of the U integral in Eq. (D.5) gives four saddle points,

$$U = \pm\imath\mathbb{1}_2, \text{ and } U = \pm\imath\mathrm{diag}\,(1,-1). \qquad \text{(D.6)}$$

The saddlepoints which are proportional to unity are algebraically suppressed while the contribution of the other two saddle points is the same. We thus find

$$\rho_{\mathrm{r}}(\widehat{x}) = \frac{1}{8\pi^2\widehat{a}_7\widehat{a}_6}\int\limits_0^{\infty} d\widetilde{x}\int\limits_{\widetilde{x}}^{\infty} d\widehat{\lambda}_7 \frac{\widetilde{x}}{\sqrt{\widehat{\lambda}_7^2-\widetilde{x}^2}}\cosh\left(\frac{\widetilde{x}\widehat{x}}{8\widehat{a}_6^2}\right)\exp\left[-\frac{\widehat{\lambda}_7^2}{16\widehat{a}_7^2} - \frac{\widetilde{x}^2+\widehat{x}^2}{16\widehat{a}_6^2}\right]. \qquad \text{(D.7)}$$

After substituting $\widehat{\lambda}_7 \to \widetilde{x}\cosh\vartheta$ the integral over ϑ yields the first case of Eq. (2.79).

For $\widehat{a}_8 \neq 0$ we start with Eqs. (2.70). The integration over the two error functions, see Eq. (2.71), makes it difficult to evaluate the result directly, particularly when $\widehat{a}_7 \neq 0$. As long as $\widehat{a}_7$ is finite, the second error function does not yield anything apart from giving a Gaussian cut-off to the integral. The

imaginary part of the argument of the second error function shows strong oscillations resulting in cancellations. These oscillations also impede a numerical evaluation of the integrals for large lattice spacing.

Let $\widehat{a}_6 = 0$ to begin with. A non-zero value of $\widehat{a}_6$ can be introduced later by a convolution with a Gaussian in $\widehat{x}$. To obtain the correct contribution from the first term we consider a slight modification of ρ_{r},

$$I(X,\alpha) = \int\limits_{[0,2\pi]^2} d\varphi_1 d\varphi_2 \sin^2\left[\frac{\varphi_1-\varphi_2}{2}\right] e^{\imath\nu(\varphi_1+\varphi_2)} \frac{\widehat{k}(X,\varphi_1,\varphi_2)-\widehat{k}(X,\varphi_2,\varphi_1)}{\cos\varphi_2-\cos\varphi_1} \tag{D.8}$$

with

$$\begin{aligned}\widehat{k}(X,\varphi_1,\varphi_2) &= \exp\left[4\widehat{a}_8^2\left(\cos\varphi_1-X\right)^2-4\widehat{a}_8^2\left(\cos\varphi_2-X\right)^2\right] \\ &\quad\times\exp\left[-4\widehat{a}_7^2(\sin\varphi_1+\sin\varphi_2)^2\right] \\ &\quad\times\left[\mathrm{erf}\left[\sqrt{8}\widehat{a}_8(X-\cos\varphi_1)\right]+\mathrm{erf}\left[2\widehat{a}_8\alpha(\cos\varphi_1-X)\right]\right].\end{aligned} \tag{D.9}$$

The variable X plays the role of $\widehat{x}/(8\widehat{a}_8^2)$. The error function with the constant α replaces the second error function in Eq. (2.71) and is of order one in the limit $\widetilde{a}\to\infty$. It regularizes the integral and its contribution will be removed at the end. However it has to fulfill some constraints to guarantee the existence of the saddlepoints

$$\varphi_1^{(0)},\varphi_2^{(0)} \in \{\pm\arccos X\} \text{ with } X\in[-1,1]. \tag{D.10}$$

Nevertheless these saddlepoints are independent of α. The saddle point $\varphi_1^{(0)} = \varphi_2^{(0)}$ is algebraically suppressed in comparison to $\varphi_1^{(0)} = -\varphi_2^{(0)}$ due to the $\sin^2$ factor in the measure. Expanding about the saddlepoints yields

$$\begin{aligned}I(X,\alpha) &\propto \frac{\Theta(1-|X|)}{\widehat{a}_8}\int\limits_{\mathbb{R}^2}\frac{d\delta\varphi_1 d\delta\varphi_2}{\delta\varphi_1+\delta\varphi_2}\exp\left[-\frac{\widehat{a}_7^2}{\widehat{a}_8^2}\gamma^2(\delta\varphi_1+\delta\varphi_2)^2\right] \\ &\quad\times\Big[\exp(\delta\varphi_1^2-\delta\varphi_2^2)\left(\mathrm{erf}(\sqrt{2}\delta\varphi_1)-\mathrm{erf}(\alpha\delta\varphi_1)\right) \\ &\quad+\exp(\delta\varphi_2^2-\delta\varphi_1^2)\left(\mathrm{erf}(\sqrt{2}\delta\varphi_2)-\mathrm{erf}(\alpha\delta\varphi_2)\right)\Big]\end{aligned} \tag{D.11}$$

with

$$\gamma = \frac{X}{\sqrt{1-X^2}}. \tag{D.12}$$

In the next step we change the coordinates to center-of-mass-relative coordinates, i.e. $\Phi = \delta\varphi_1 + \delta\varphi_2$ and $\Delta\varphi = \delta\varphi_1 - \delta\varphi_2$, and find

$$\begin{aligned} I(X,\alpha) \;\propto\; & \frac{\Theta(1-|X|)}{\widehat{a}_8} \int\limits_{\mathbb{R}^2} \frac{d\Phi d\Delta\varphi}{\Phi} \exp\left[-\frac{\widehat{a}_7^2}{\widehat{a}_8^2}\gamma^2\Phi^2\right] \\ & \times \left[\exp(\Phi\Delta\varphi)\left(\operatorname{erf}\left(\frac{\Phi+\Delta\varphi}{\sqrt{2}}\right) - \operatorname{erf}\left(\frac{\alpha}{2}(\Phi+\Delta\varphi)\right)\right)\right. \\ & \left. + \exp(-\Phi\Delta\varphi)\left(\operatorname{erf}\left(\frac{\Phi-\Delta\varphi}{\sqrt{2}}\right) - \operatorname{erf}\left(\frac{\alpha}{2}(\Phi-\Delta\varphi)\right)\right)\right]. \end{aligned} \tag{D.13}$$

We perform an integration by parts in $\Delta\varphi$ yielding Gaussian integrals in $\Delta\varphi$ which evaluate to

$$\begin{aligned} I(X,\alpha) \;\propto\; & \frac{\Theta(1-|X|)}{\widehat{a}_8} \int\limits_{\mathbb{R}} \frac{d\Phi}{\Phi^2} \exp\left[-\frac{\widehat{a}_7^2}{\widehat{a}_8^2}\gamma^2\Phi^2\right]. \\ & \times \left[\exp\left(-\frac{\Phi^2}{2}\right) - \exp\left(-\frac{1+\alpha^2}{\alpha^2}\Phi^2\right)\right] \end{aligned} \tag{D.14}$$

The $1/\Phi^2$ term can be exponentiated by introducing an auxiliary integral and the resulting Gaussian over Φ can be performed. We obtain

$$\begin{aligned} I(X,\alpha) \;\propto\; & \Theta(1-|X|) \int\limits_{(1+\alpha^2)/\alpha^2}^{1/2} \frac{dt}{\sqrt{\widehat{a}_7^2\gamma^2 + \widehat{a}_8^2 t}} \\ \propto\; & \frac{\Theta(1-|X|)}{\widehat{a}_8^2}\left(\sqrt{\widehat{a}_7^2\gamma^2 + \frac{\widehat{a}_8^2}{2}} - \sqrt{\widehat{a}_7^2\gamma^2 + \frac{1+\alpha^2}{\alpha^2}\widehat{a}_8^2}\right). \end{aligned} \tag{D.15}$$

The contribution of the artificial term depending on α can be readily read off, but it fixes the integral only up to an additive constant. This constant can be determined by integrating the result over $\widehat{x}$ which has to agree with the large $\widehat{a}$ limit of N_{add}, cf. Eq. (2.75). It turns out that this constant is equal to zero. The overall constant is also obtained by comparing to N_{add}.

The convolution with the Gaussian distribution generating $\widehat{a}_6$ does not give something new in the limit of large lattice spacing. The width of this Gaussian scales with $\widehat{a}$ while the distribution ρ_{r} has support on $\widehat{a}^2$, so that it becomes a Dirac delta-function in the large $\widehat{a}$ limit.

D.1.3 The distribution of the complex eigenvalues

Let $\widehat{a}_8 > 0$ and $\widehat{a} \gg 1$. Then we perform a saddlepoint approximation of Eq. (2.80) in the integration variables $\varphi_{1/2}$. The saddlepoints are given by

$$\varphi_1^{(0)} = -\varphi_2^{(0)} = \pm \arccos\left(\frac{\widehat{x}}{8\widehat{a}_8^2}\right) \quad \text{with} \quad \widehat{x} \in [-8\widehat{a}_8^2, 8\widehat{a}_8^2]. \tag{D.16}$$

We have also the saddlepoints $\varphi_1^{(0)} = \varphi_2^{(0)}$ if $\widehat{a}_7 = 0$. However they are algebraically suppressed due to the Haar measure. Notice the two saddlepoints in Eq. (D.16) yield the same contribution. After the integration over the massive modes about the saddlepoint we find the first case of Eq. (2.83). In the calculation we used the convolution integral derived in B.1.2.

Let us now look at the case with $\widehat{a}_8 = 0$. Then we have

$$\begin{aligned}\rho_{\mathrm{c}}(\widehat{z}) \overset{\widehat{a}\gg 1}{=} & \frac{|\widehat{y}|}{4\pi^2\sqrt{16\pi\widehat{a}_6^2}\sqrt{16\pi\widehat{a}_7^2}} \exp\left[-\frac{x^2}{16\widehat{a}_6^2}\right] \int\limits_{\mathbb{R}} d\widehat{\lambda}_7 \exp\left[-\frac{\widehat{\lambda}_7^2}{16\widehat{a}_7^2}\right] \\ & \times \int\limits_{[0,2\pi]^2} d\varphi_1 d\varphi_2 \sin^2\left[\frac{\varphi_1-\varphi_2}{2}\right] \cos[\nu(\varphi_1+\varphi_2)] \\ & \times \mathrm{sinc}\left[\widehat{y}(\cos\varphi_1 - \cos\varphi_2)\right] \exp\left[\imath\widehat{\lambda}_7(\sin\varphi_1 + \sin\varphi_2)\right].\end{aligned} \tag{D.17}$$

The integrals over the angles can be rewritten as a group integral over $\mathrm{U}(2)$,

$$\begin{aligned}&\int\limits_{[0,2\pi]^2} d\varphi_1 d\varphi_2 \sin^2\left[\frac{\varphi_1-\varphi_2}{2}\right] e^{\nu\imath(\varphi_1+\varphi_2)} \mathrm{sinc}\left[\widehat{y}(\cos\varphi_1 - \cos\varphi_2)\right] \\ &\exp\left[\imath\widehat{\lambda}_7(\sin\varphi_1 + \sin\varphi_2)\right] = 2\pi^2 \int\limits_{\mathrm{U}(2)} d\mu(U) \det{}^{\nu} U \exp\left[\frac{1}{2}\mathrm{tr}\left(\Lambda U - \Lambda^* U^\dagger\right)\right]\end{aligned} \tag{D.18}$$

with $\Lambda = \mathrm{diag}\left(\widehat{\lambda}_7 + \imath\widehat{y}, \widehat{\lambda}_7 - \imath\widehat{y}\right)$. This integral only depends on the quantity $\sqrt{\widehat{\lambda}_7^2 + \widehat{y}^2}$ because the angle of the combined complex variable $\widehat{\lambda} + \imath\widehat{y}$ can be

absorbed into U, i.e.

$$\int\limits_{\mathrm{U}(2)} d\mu(U)\det{}^{\nu}U\exp\left[\frac{1}{2}\mathrm{tr}\,(\Lambda U-\Lambda^{*}U^{\dagger})\right] \tag{D.19}$$
$$=\int\limits_{\mathrm{U}(2)} d\mu(U)\det{}^{\nu}U\exp\left[\frac{\sqrt{\widehat{\lambda}_7^2+\widehat{y}^2}}{2}\mathrm{tr}\,(U-U^{\dagger})\right].$$

The variable $\widehat{y}$ as well as the integration variable $\widehat{\lambda}_7$ are of the order $\widehat{a}$. Therefore we can perform a saddlepoint approximation and end up with

$$\rho_{\mathrm{c}}(\widehat{z})\overset{\widehat{a}\gg 1}{=}\frac{|\widehat{y}|}{\pi\sqrt{16\pi\widehat{a}_6^2}\sqrt{16\pi\widehat{a}_7^2}}\exp\left[-\frac{x^2}{16\widehat{a}_6^2}\right]\int\limits_{\mathbb{R}}d\widehat{\lambda}_7\frac{\exp\left[-\widehat{\lambda}_7^2/(16\widehat{a}_7^2)\right]}{\sqrt{\widehat{\lambda}_7^2+\widehat{y}^2}}. \tag{D.20}$$

resulting in the second case of Eq. (2.83).

D.1.4 The distribution of chirality over the real eigenvalues

In this Appendix we derive the large $\widehat{a}$ limit of $\rho_\chi(x)$ for $\widehat{a}_8>0$ given in Eq. (2.94). The case $\widehat{a}_8=0$ reduces the result (2.60) and will not be discussed in this section. We set $\widehat{a}_{6/7}=0$ to begin with and introduce them later on.

The best way to obtain the asymptotics for large lattice spacing is to start with Eq. (C.1) with $\widehat{m}_6=\widehat{\lambda}_7=\varepsilon=0$. The integral does not need a regularization since the $\widehat{a}_8$-term guarantees the convergence. We also omit the sign in front of the linear trace terms in the Lagrangian because we can change $U\to -U$.

In the first step we substitute $\eta\to e^{\imath\varphi}\eta$ and $\eta^*\to e^{\vartheta}\eta^*$. Then the measure is $d\varphi d\vartheta d\eta d\eta^*$ and the parameterization of U is given by

$$U=\begin{bmatrix} e^{\vartheta} & 0\\ 0 & e^{\imath\varphi}\end{bmatrix}\begin{bmatrix} 1 & \eta^*\\ \eta & 1\end{bmatrix},\ U^{-1}=\begin{bmatrix} 1+\eta^*\eta & -\eta^*\\ -\eta & 1-\eta^*\eta\end{bmatrix}\begin{bmatrix} e^{-\vartheta} & 0\\ 0 & e^{-\imath\varphi}\end{bmatrix} \tag{D.21}$$

There are two saddlepoints in the variables ϑ and φ, i.e.

$$e^{\vartheta_0}=-\frac{\imath\widehat{x}_2}{8\widehat{a}_8^2}+\sqrt{1-\left(\frac{\widehat{x}_2}{8\widehat{a}_8^2}\right)^2},\quad e^{\imath\varphi_0}=-\frac{\imath\widehat{z}_1}{8\widehat{a}_8^2}+L\sqrt{1-\left(\frac{\widehat{z}_1}{8\widehat{a}_8^2}\right)^2} \tag{D.22}$$

with $L\in\pm 1$. Moreover, the variables $\widehat{z}_1,\widehat{x}_2$ have to be in the interval

$[-8\widehat{a}_8^2, 8\widehat{a}_8^2]$ else the contributions will be exponentially suppressed. We have no second saddlepoint for the variable ϑ since the real part of the exponential has to be positive definite. Other saddlepoints which can be reached by shifting φ and ϑ by $2\pi\imath$ independently are forbidden since they are not accessible in the limit $\widehat{a}_8 \to \infty$. Notice that the saddlepoint solutions (D.22) are phases, i.e. $|e^{\vartheta_0}| = |e^{\imath\varphi_0}| = 1$.

In the second step we expand the integration variables

$$e^{\vartheta} = e^{\vartheta_0}\left(1 + \frac{\delta\vartheta}{\sqrt{(8\widehat{a}_8^2)^2 - \widehat{x}_2^2}}\right), \quad e^{\imath\varphi} = e^{\imath\varphi_0}\left(1 + \frac{\imath\delta\varphi}{\sqrt{(8\widehat{a}_8^2)^2 - \widehat{z}_1^2}}\right). \tag{D.23}$$

All terms in front of the exponential as well as of the Grassmann variables are replaced by the saddlepoint solutions ϑ_0 and φ_0. The resulting Gaussian integrals over the variables $\delta\vartheta$ and $\delta\varphi$ yield

$$\begin{aligned}
&\mathrm{Im}\int d\mu(U)\mathrm{Sdet}^{\,\nu}U\exp\left[-\widehat{a}_8^2\mathrm{Str}\,(U-U^{-1})^2 + \frac{\imath}{2}\mathrm{Str}\,\mathrm{diag}\,(\widehat{x}_2,\widehat{z}_1)(U-U^{-1})\right] \\
&\quad\propto \sum_{L\in\{\pm1\}} \mathrm{Im}\,\frac{\exp[\nu(\vartheta_0 - \imath\varphi_0)]}{\sqrt{(8\widehat{a}_8^2)^2 - \widehat{x}_2^2}\sqrt{(8\widehat{a}_8^2)^2 - \widehat{z}_1^2}}\exp\left[-\frac{\widehat{x}_2^2 - \widehat{z}_1^2}{16\widehat{a}_8^2}\right] \\
&\qquad\times\int d\eta d\eta^*(1-\eta^*\eta)^{\nu}\exp[-2\widehat{a}_8^2(e^{\vartheta_0} + e^{-\imath\varphi_0})(e^{-\vartheta_0} + e^{\imath\varphi_0})\eta^*\eta].
\end{aligned} \tag{D.24}$$

After the integration over the Grassmann variables we have two terms one is of order one and the other one of order $\widehat{a}_8^2$ which exceeds the first term for $\widehat{a}_8 \gg 1$. Hence we end up with

$$\begin{aligned}
&\mathrm{Im}\int d\mu(U)\mathrm{Sdet}^{\,\nu}U\exp\left[-\widehat{a}_8^2\mathrm{Str}\,(U-U^{-1})^2 + \frac{\imath}{2}\mathrm{Str}\,\mathrm{diag}\,(\widehat{x}_2,\widehat{z}_1)(U-U^{-1})\right] \\
&\propto\sum_{L\in\{\pm1\}} \mathrm{Im}\,\frac{1}{\sqrt{(8\widehat{a}_8^2)^2 - \widehat{x}_2^2}\sqrt{(8\widehat{a}_8^2)^2 - \widehat{z}_1^2}}\left(\frac{-\imath\widehat{x}_2 + \sqrt{(8\widehat{a}_8^2)^2 - \widehat{x}_2^2}}{-\imath\widehat{z}_1 + L\sqrt{(8\widehat{a}_8^2)^2 - \widehat{z}_1^2}}\right)^{\nu} \\
&\times\left[\left(\frac{\widehat{z}_1 - \widehat{x}_2}{8\widehat{a}_8^2}\right)^2 + \left(\sqrt{1 - \left(\frac{\widehat{x}_2}{8\widehat{a}_8^2}\right)^2} + L\sqrt{1 - \left(\frac{\widehat{z}_1}{8\widehat{a}_8^2}\right)^2}\right)^2\right]\exp\left[-\frac{\widehat{x}_2^2 - \widehat{z}_1^2}{16\widehat{a}_8^2}\right].
\end{aligned} \tag{D.25}$$

Notice that both saddlepoints, $L \in \{\pm1\}$, give a contribution for independent variables $\widehat{z}_1$ and $\widehat{x}_2$. To obtain the resolvent we differentiate this expression with respect to z_1 and put $z_1 = x_1$ afterwards. The first term between the large brackets and the second term for $L = -1$ are quadratic in $z_1 - x_2$ and

do not contribute to the resolvent. For $L = +1$ we obtain

$$\begin{aligned}
&\mathrm{Im}\,\partial_{\widehat{z}_1}|_{\widehat{z}_1=\widehat{x}_2}\int d\mu(U)\mathrm{Sdet}^{\,\nu}U\exp\left[-\widehat{a}_8^2\mathrm{Str}\,(U-U^{-1})^2+\frac{\imath}{2}\mathrm{Str}\,\mathrm{diag}\,(\widehat{x}_2,\widehat{z}_1)(U-U^{-1})\right]\\
&\quad\propto\quad \nu\frac{\theta(8\widehat{a}_8^2-|x_2|)}{2\widehat{a}_8^2\sqrt{64\widehat{a}_8^4-x_2^2}}
\end{aligned}\tag{D.26}$$

This limit yields the square root singularity. The normalization of ρ_χ to ν yields an overall normalization constant of $1/4\widehat{a}^2$.

The effect of $\widehat{a}_6$ is introduced by the integral

$$\begin{aligned}
&\frac{1}{4\widehat{a}_6\sqrt{\pi}}\int\limits_{\mathbb{R}}\exp\left[-\frac{\widehat{m}_6^2}{16\widehat{a}_6^2}\right]\frac{\Theta(8\widehat{a}_8^2-|\widehat{x}-\widehat{m}_6|)}{8\widehat{a}_8^4\sqrt{(8\widehat{a}_8^2)^2-(\widehat{x}-\widehat{m}_6)^2}}d\widehat{m}_6\\
&\propto\int\limits_0^{2\pi}\exp\left[-\frac{4\widehat{a}_8^4}{\widehat{a}_6^2}\left(\cos\varphi+\frac{\widehat{x}}{8\widehat{a}_8^2}\right)\right]d\varphi.
\end{aligned}\tag{D.27}$$

In the large $\widehat{a}$ limit this evaluates to

$$\nu\frac{\theta(8\widehat{a}_8^2-|x_2|)}{8\widehat{a}_8^4\sqrt{64\widehat{a}_8^4-x_2^2}},\tag{D.28}$$

which is exactly the same Heaviside distribution with the square root singularities in the interval $[-8\widehat{a}_8^2, 8\widehat{a}_8^2]$ of Eq. (D.27). The introduction of $\widehat{a}_7$ follows from Eq. (2.88). We have to replace $\widehat{a}_6^2 \to \widehat{a}_6^2+\widehat{a}_7^2$ and sum the result over the index j with the prefactor $\exp(-8\widehat{a}_7^2)[I_{j-\nu}(8\widehat{a}_7^2) - I_{j-\nu}(8\widehat{a}_7^2)]$. Since the result for $\widehat{a}_7 = 0$ is linear in the index, the sum over j can be performed according to

$$\sum_{j=1}^{\infty} j\left(I_{j-\nu}(8\widehat{a}_7^2) - I_{j+\nu}(8\widehat{a}_7^2)\right) = \nu\exp(8\widehat{a}_7^2)\tag{D.29}$$

resulting in the asymptotic result (2.94).

Appendix E

Superbosonization

In this appendix we will state the superbosonization formula for all values of the Dyson index β [144].

E.1 The superbosonization formula

Consider the integral of the integrable and analytical superfunction F over the "invariants"

$$I_{pq} = \int D\eta\, D\Phi\; F\begin{pmatrix} \eta^\dagger\eta & \eta^\dagger\Phi \\ \Phi^\dagger\eta & \Phi^\dagger\Phi \end{pmatrix}. \tag{E.1}$$

Here η is a $N \times p$ matrix (p even) of Grassmann variables, while Φ are commuting variables cast in a $N \times q$ matrix.

We will employ an identity to transform to an integration over the supermatrix Q.

$$Q = \begin{pmatrix} A & \sigma^\dagger \\ \sigma & B \end{pmatrix}, \tag{E.2}$$

with A, B being commuting variables and Grassmann variables σ, $\sigma^\dagger$. The advantage of this manipulation is the drastic reduction of integration variables. This is of great help when one studies the large N-limit of these integrals in order to employ a saddle point approximation.

After applying the superbosonization formula the integral E.1 will be cast in the superbosonized form

$$I_{pq} \propto \int DQ \mathrm{Sdet}^{\,M} F(Q), \tag{E.3}$$

where the measure $DQ = DADBD\sigma D\sigma^\dagger \mathrm{Sdet}^{\,\kappa}(Q)$.

For $\beta = 1$ $\kappa = (p-q-1)/2$ and $M = (N+p-q-1)/2$. The unitary

matrix A is antisymmetric and therefore belongs to the Circular Symplectic Ensemble (CSE) and B is real symmetric and positive. For $\beta = 2$ $\kappa = p - q$ and $M = N + p - q$. The unitary matrix A belongs to the Circular Unitary Ensemble and B is a positive hermitian matrix. For $\beta = 4$ $\kappa = (p - q + 1)/2$ and $M = (N + p + q + 1)/2$. The unitary matrix A is anti-self dual and unitary. The corresponding ensemble is the Circular Orthogonal Ensemble (COE), while the matrix B is hermitian, self-dual and positive.

E.2 A tentative proof for the case of bosonic variables

Consider $p = 0$, only commuting variables. Integrating [144, 145] $F(\Phi^\dagger\Phi)$

$$\begin{aligned} \int D\Phi F(\Phi^\dagger\Phi) &= \int DBD\Phi\ \delta(B - \Phi^\dagger\Phi)F(B) \\ &\propto \int DB\, F(B)(\det B)^M. \end{aligned} \tag{E.4}$$

To calculate the integral over Φ one needs to rescale the integration variables by a factor $\sqrt{B}$ and by employing dimensional arguments regarding the scaling dimension of the Hermitian matrix $\Phi^\dagger\Phi$ as well as of the measure, one obtains the correct expression for the power of the determinant. We will refer the reader for a more rigorous proof to the article by Fyodorov [145].

Bibliography

[1] F.C. Hansen and H. Leutwyler. Charge correlations and topological susceptibility in QCD. *Nucl.Phys.*, B350:201–227, 1991. doi: 10.1016/0550-3213(91)90259-Z.

[2] O. Bohigas, M.J. Giannoni, and C. Schmit. Characterization of chaotic quantum spectra and universality of level fluctuation laws. *Phys.Rev.Lett.*, 52:1–4, 1984. doi: 10.1103/PhysRevLett.52.1.

[3] Mario Kieburg, Jacobus J.M. Verbaarschot, and Savvas Zafeiropoulos. Eigenvalue Density of the non-Hermitian Wilson Dirac Operator. *Phys.Rev.Lett.*, 108:022001, 2012. doi: 10.1103/PhysRevLett.108.022001.

[4] Mario Kieburg, Jacobus J.M. Verbaarschot, and Savvas Zafeiropoulos. Random Matrix Models for Dirac Operators at finite Lattice Spacing. *PoS*, LATTICE2011:312, 2011.

[5] G. Akemann, P.H. Damgaard, K. Splittorff, and J.J.M. Verbaarschot. Spectrum of the Wilson Dirac Operator at Finite Lattice Spacings. *Phys.Rev.*, D83:085014, 2011. doi: 10.1103/PhysRevD.83.085014.

[6] J. Stehr and P.H. Weisz. Note on gauge fixing in lattice QCD. *Lett.Nuovo Cim.*, 37:173–177, 1983.

[7] K. Symanzik. Continuum Limit and Improved Action in Lattice Theories. 1. Principles and ϕ^4 Theory. *Nucl.Phys.*, B226:187, 1983. doi: 10.1016/0550-3213(83)90468-6.

[8] K. Symanzik. Continuum Limit and Improved Action in Lattice Theories. 2. O(N) Nonlinear Sigma Model in Perturbation Theory. *Nucl.Phys.*, B226:205, 1983. doi: 10.1016/0550-3213(83)90469-8.

[9] John D. Stack, Steven D. Neiman, and Roy J. Wensley. String tension from monopoles in SU(2) lattice gauge theory. *Phys.Rev.*, D50:3399–3405, 1994. doi: 10.1103/PhysRevD.50.3399.

[10] K.G. Wilson. New Phenomena In Subnuclear Physics. Part A. *Proceedings of the First Half of the 1975 International School of Subnuclear Physics. Ed. A. Zichichi, Plenum Press, New York*.

[11] Holger Bech Nielsen and M. Ninomiya. No Go Theorem for Regularizing Chiral Fermions. *Phys.Lett.*, B105:219, 1981. doi: 10.1016/0370-2693(81)91026-1.

[12] Holger Bech Nielsen and M. Ninomiya. Absence of Neutrinos on a Lattice. 1. Proof by Homotopy Theory. *Nucl.Phys.*, B185:20, 1981. doi: 10.1016/0550-3213(81)90361-8.

[13] Holger Bech Nielsen and M. Ninomiya. Absence of Neutrinos on a Lattice. 2. Intuitive Topological Proof. *Nucl.Phys.*, B193:173, 1981. doi: 10.1016/0550-3213(81)90524-1.

[14] John B. Kogut and Leonard Susskind. Hamiltonian Formulation of Wilson's Lattice Gauge Theories. *Phys.Rev.*, D11:395, 1975. doi: 10.1103/PhysRevD.11.395.

[15] N. Kawamoto and J. Smit. Effective Lagrangian and Dynamical Symmetry Breaking in Strongly Coupled Lattice QCD. *Nucl.Phys.*, B192:100, 1981. doi: 10.1016/0550-3213(81)90196-6.

[16] Michael Creutz. The 't Hooft vertex revisited. *Annals Phys.*, 323:2349–2365, 2008. doi: 10.1016/j.aop.2007.12.008.

[17] Claude Bernard, Maarten Golterman, Yigal Shamir, and Stephen R. Sharpe. 't Hooft vertices, partial quenching, and rooted staggered QCD. *Phys.Rev.*, D77:114504, 2008. doi: 10.1103/PhysRevD.77.114504.

[18] Stephen R. Sharpe. Rooted staggered fermions: Good, bad or ugly? *PoS*, LAT2006:022, 2006.

[19] Michael Creutz. The Saga of rooted staggered quarks. 2008.

[20] H. Kluberg-Stern, A. Morel, O. Napoly, and B. Petersson. Flavors of Lagrangian Susskind Fermions. *Nucl.Phys.*, B220:447, 1983. doi: 10.1016/0550-3213(83)90501-1.

[21] Paul H. Ginsparg and Kenneth G. Wilson. A Remnant of Chiral Symmetry on the Lattice. *Phys.Rev.*, D25:2649, 1982. doi: 10.1103/PhysRevD.25.2649.

[22] Herbert Neuberger. Exactly massless quarks on the lattice. *Phys.Lett.*, B417:141–144, 1998. doi: 10.1016/S0370-2693(97)01368-3.

[23] David B. Kaplan. A Method for simulating chiral fermions on the lattice. *Phys.Lett.*, B288:342–347, 1992. doi: 10.1016/0370-2693(92)91112-M.

[24] P. Lepage and C. Davies. High precision lattice QCD meets experiment. *Int.J.Mod.Phys.*, A19:877–886, 2004. doi: 10.1142/S0217751X04018841.

[25] Steven Weinberg. Phenomenological Lagrangians. *Physica*, A96:327, 1979.

[26] J. Gasser and H. Leutwyler. Chiral Perturbation Theory to One Loop. *Annals Phys.*, 158:142, 1984. doi: 10.1016/0003-4916(84)90242-2.

[27] J. Gasser and H. Leutwyler. Chiral Perturbation Theory: Expansions in the Mass of the Strange Quark. *Nucl.Phys.*, B250:465, 1985. doi: 10.1016/0550-3213(85)90492-4.

[28] J. Gasser and H. Leutwyler. Light Quarks at Low Temperatures. *Phys.Lett.*, B184:83, 1987. doi: 10.1016/0370-2693(87)90492-8.

[29] Maarten Golterman. Applications of chiral perturbation theory to lattice QCD. pages 423–515, 2009.

[30] Cumrun Vafa and Edward Witten. Eigenvalue inequalities for fermions in gauge theories. *Commun.Math.Phys.*, 95:257, 1984. doi: 10.1007/BF01212397.

[31] Murray Gell-Mann, R.J. Oakes, and B. Renner. Behavior of current divergences under $SU(3) \times SU(3)$. *Phys.Rev.*, 175:2195–2199, 1968. doi: 10.1103/PhysRev.175.2195.

[32] Susumu Okubo. Note on unitary symmetry in strong interactions. *Prog.Theor.Phys.*, 27:949–966, 1962. doi: 10.1143/PTP.27.949.

[33] J. Wess and B. Zumino. Consequences of anomalous Ward identities. *Phys.Lett.*, B37:95, 1971. doi: 10.1016/0370-2693(71)90582-X.

[34] Wolfgang Bietenholz, T. Chiarappa, K. Jansen, K.I. Nagai, and S. Shcheredin. Axial correlation functions in the epsilon regime: A Numerical study with overlap fermions. *JHEP*, 0402:023, 2004. doi: 10.1088/1126-6708/2004/02/023.

[35] Leonardo Giusti, P. Hernandez, M. Laine, P. Weisz, and H. Wittig. Low-energy couplings of QCD from current correlators near the chiral limit. *JHEP*, 0404:013, 2004. doi: 10.1088/1126-6708/2004/04/013.

[36] Anna Hasenfratz, Roland Hoffmann, and Stefan Schaefer. Low energy chiral constants from epsilon-regime simulations with improved Wilson fermions. *Phys.Rev.*, D78:054511, 2008. doi: 10.1103/PhysRevD.78.054511.

[37] Stephen R. Sharpe and Robert L. Singleton. Spontaneous flavor and parity breaking with Wilson fermions. *Phys.Rev.*, D58:074501, 1998. doi: 10.1103/PhysRevD.58.074501.

[38] Oliver Bar, Gautam Rupak, and Noam Shoresh. Simulations with different lattice Dirac operators for valence and sea quarks. *Phys.Rev.*, D67:114505, 2003. doi: 10.1103/PhysRevD.67.114505.

[39] Oliver Bar, Silvia Necco, and Stefan Schaefer. The Epsilon regime with Wilson fermions. *JHEP*, 0903:006, 2009. doi: 10.1088/1126-6708/2009/03/006.

[40] Stephen R. Sharpe. Discretization errors in the spectrum of the Hermitian Wilson-Dirac operator. *Phys.Rev.*, D74:014512, 2006. doi: 10.1103/PhysRevD.74.014512.

[41] E. Wigner. Characteristic Vectors of Bordered Matrices with Infinite Dimensions. *Ann.Math.*, 62:548564.

[42] P. Di Francesco, Paul H. Ginsparg, and Jean Zinn-Justin. 2-D Gravity and random matrices. *Phys.Rept.*, 254:1–133, 1995. doi: 10.1016/0370-1573(94)00084-G.

[43] M. Mehta. Random Matrices. *Academic Press, San Diego.*

[44] Thomas Guhr, Axel Muller-Groeling, and Hans A. Weidenmuller. Random matrix theories in quantum physics: Common concepts. *Phys.Rept.*, 299:189–425, 1998. doi: 10.1016/S0370-1573(97)00088-4.

[45] Martin R. Zirnbauer. Riemannian symmetric superspaces and their origin in random-matrix theory. *J.Math.Phys.*, 37:4986–5018, 1996.

[46] F. Dyson. Statistical Theory of the Energy Levels of Complex Systems. *Mathematical Physics*, 3:140156.

[47] Edward V. Shuryak and J.J.M. Verbaarschot. Random matrix theory and spectral sum rules for the Dirac operator in QCD. *Nucl.Phys.*, A560: 306–320, 1993. doi: 10.1016/0375-9474(93)90098-I.

[48] Alexander Altland and Martin R. Zirnbauer. Nonstandard symmetry classes in mesoscopic normal-superconducting hybrid structures. *Phys.Rev.*, B55:1142–1161, 1997. doi: 10.1103/PhysRevB.55.1142.

[49] Tom Banks and A. Casher. Chiral Symmetry Breaking in Confining Theories. *Nucl.Phys.*, B169:103, 1980. doi: 10.1016/0550-3213(80)90255-2.

[50] H. Leutwyler and Andrei V. Smilga. Spectrum of Dirac operator and role of winding number in QCD. *Phys.Rev.*, D46:5607–5632, 1992. doi: 10.1103/PhysRevD.46.5607.

[51] K.B. Efetov. Supersymmetry in disorder and chaos. *Cambridge University Press*.

[52] J.J.M. Verbaarschot, H.A. Weidenmuller, and M.R. Zirnbauer. Grassmann Integration in Stochastic Quantum Physics: The Case of Compound Nucleus Scattering. *Phys.Rept.*, 129:367–438, 1985. doi: 10.1016/0370-1573(85)90070-5.

[53] J.J.M. Verbaarschot and I. Zahed. Spectral density of the QCD Dirac operator near zero virtuality. *Phys.Rev.Lett.*, 70:3852–3855, 1993. doi: 10.1103/PhysRevLett.70.3852.

[54] Y. Makeenko. Methods of Contemporary Gauge Theory. *Cambridge University Press*.

[55] Marcos Marino. Les Houches lectures on matrix models and topological strings. *NATO Advanced Study Institute: Marie Curie Training Course: Applications of Random Matrices in Physics*, 2004.

[56] Claude W. Bernard and Maarten F.L. Golterman. Chiral perturbation theory for the quenched approximation of QCD. *Phys.Rev.*, D46:853–857, 1992. doi: 10.1103/PhysRevD.46.853.

[57] P.H. Damgaard, J.C. Osborn, D. Toublan, and J.J.M. Verbaarschot. The microscopic spectral density of the QCD Dirac operator. *Nucl.Phys.*, B547:305–328, 1999. doi: 10.1016/S0550-3213(99)00094-2.

[58] J.C. Osborn, D. Toublan, and J.J.M. Verbaarschot. From chiral random matrix theory to chiral perturbation theory. *Nucl.Phys.*, B540:317–344, 1999. doi: 10.1016/S0550-3213(98)00716-0.

[59] Thomas Guhr. On the graded group U(1/1). *J.Math.Phys.*, 34:2541–2553, 1993. doi: 10.1063/1.530406.

[60] Silvia Necco and Andrea Shindler. Spectral density of the Hermitean Wilson Dirac operator: a NLO computation in chiral perturbation theory. *JHEP*, 1104:031, 2011. doi: 10.1007/JHEP04(2011)031.

[61] Christopher Michael and Carsten Urbach. Neutral mesons and disconnected diagrams in Twisted Mass QCD. *PoS*, LAT2007:122, 2007.

[62] Sinya Aoki and Oliver Bar. WChPT analysis of twisted mass lattice data. *Eur.Phys.J.*, A31:481, 2007. doi: 10.1140/epja/i2006-10202-x.

[63] Remi Baron et al. Light Meson Physics from Maximally Twisted Mass Lattice QCD. *JHEP*, 1008:097, 2010. doi: 10.1007/JHEP08(2010)097.

[64] Albert Deuzeman, Urs Wenger, and Jair Wuilloud. Spectral properties of the Wilson Dirac operator in the ϵ-regime. *JHEP*, 1112:109, 2011. doi: 10.1007/JHEP12(2011)109.

[65] P.H. Damgaard, U.M. Heller, and K. Splittorff. Finite-Volume Scaling of the Wilson-Dirac Operator Spectrum. *Phys.Rev.*, D85:014505, 2012. doi: 10.1103/PhysRevD.85.014505.

[66] P.H. Damgaard, U.M. Heller, and K. Splittorff. New Ways to Determine Low-Energy Constants with Wilson Fermions. *Phys.Rev.*, D86:094502, 2012. doi: 10.1103/PhysRevD.86.094502.

[67] Fabio Bernardoni, John Bulava, and Rainer Sommer. Determination of the Wilson ChPT low energy constant c_2. *PoS*, LATTICE2011:095, 2011.

[68] P.H. Damgaard, K. Splittorff, and J.J.M. Verbaarschot. Microscopic Spectrum of the Wilson Dirac Operator. *Phys.Rev.Lett.*, 105:162002, 2010. doi: 10.1103/PhysRevLett.105.162002.

[69] Gernot Akemann, Poul H. Damgaard, Kim Splittorff, and Jacobus Verbaarschot. Effects of dynamical quarks on the spectrum of the Wilson Dirac operator. *PoS*, LATTICE2010:079, 2010.

[70] Gernot Akemann, Poul H. Damgaard, Kim Splittorff, and Jacobus Verbaarschot. Wilson Fermions, Random Matrix Theory and the Aoki Phase. *PoS*, LATTICE2010:092, 2010.

[71] Maxwell T. Hansen and Stephen R. Sharpe. Constraint on the Low Energy Constants of Wilson Chiral Perturbation Theory. *Phys.Rev.*, D85:014503, 2012. doi: 10.1103/PhysRevD.85.014503.

[72] K. Splittorff and J.J.M. Verbaarschot. Progress on the Microscopic Spectrum of the Dirac Operator for QCD with Wilson Fermions. *PoS*, LATTICE2011:113, 2011.

[73] M. Kieburg, K. Splittorff, and J.J.M. Verbaarschot. The Realization of the Sharpe-Singleton Scenario. *Phys.Rev.*, D85:094011, 2012. doi: 10.1103/PhysRevD.85.094011.

[74] Sinya Aoki. New Phase Structure for Lattice QCD with Wilson Fermions. *Phys.Rev.*, D30:2653, 1984. doi: 10.1103/PhysRevD.30.2653.

[75] Jacobus J. M. Verbaarschot. The Spectrum of the QCD Dirac operator and chiral random matrix theory: The Threefold way. *Phys.Rev.Lett.*, 72:2531–2533, 1994. doi: 10.1103/PhysRevLett.72.2531.

[76] James C. Osborn. Staggered chiral random matrix theory. *Phys.Rev.*, D83:034505, 2011. doi: 10.1103/PhysRevD.83.034505.

[77] James C. Osborn. Chiral random matrix theory for staggered fermions. *PoS*, LATTICE2011:110, 2011.

[78] Gautam Rupak and Noam Shoresh. Chiral perturbation theory for the Wilson lattice action. *Phys.Rev.*, D66:054503, 2002. doi: 10.1103/PhysRevD.66.054503.

[79] Oliver Bar, Gautam Rupak, and Noam Shoresh. Chiral perturbation theory at $O(a^2)$ for lattice QCD. *Phys.Rev.*, D70:034508, 2004. doi: 10.1103/PhysRevD.70.034508.

[80] Sinya Aoki. Chiral perturbation theory with Wilson type fermions including a^2 effects: $N_f = 2$ degenerate case. *Phys.Rev.*, D68:054508, 2003. doi: 10.1103/PhysRevD.68.054508.

[81] Maarten Golterman, Stephen R. Sharpe, and Jr. Singleton, Robert L. Effective theory for quenched lattice QCD and the Aaoki phase. *Phys.Rev.*, D71:094503, 2005. doi: 10.1103/PhysRevD.71.094503.

[82] Andrea Shindler. Observations on the Wilson fermions in the epsilon regime. *Phys.Lett.*, B672:82–88, 2009. doi: 10.1016/j.physletb.2008.12.061.

[83] Gernot Akemann and Taro Nagao. Random Matrix Theory for the Hermitian Wilson Dirac Operator and the chGUE-GUE Transition. *JHEP*, 1110:060, 2011. doi: 10.1007/JHEP10(2011)060.

[84] Mario Kieburg. Surprising Pfaffian factorizations in Random Matrix Theory with Dyson index $\beta = 2$. *J.Phys.*, A45:095205, 2012. doi: 10.1088/1751-8113/45/9/095205.

[85] Mario Kieburg. Mixing of orthogonal and skew-orthogonal polynomials and its relation to Wilson RMT. *J.Phys.*, A45:205203, 2012. doi: 10.1088/1751-8113/45/20/205203.

[86] S. Aoki, A. Ukawa, and T. Umemura. Finite temperature phase structure of lattice QCD with Wilson quark action. *Phys.Rev.Lett.*, 76:873–876, 1996. doi: 10.1103/PhysRevLett.76.873.

[87] S. Aoki. Phase structure of lattice QCD with Wilson fermion at finite temperature. *Nucl.Phys.Proc.Suppl.*, 60A:206–219, 1998.

[88] Ernst-Michael Ilgenfritz, W. Kerler, M. Muller-Preussker, A. Sternbeck, and H. Stuben. A Numerical reinvestigation of the Aoki phase with N(f) = 2 Wilson fermions at zero temperature. *Phys.Rev.*, D69:074511, 2004. doi: 10.1103/PhysRevD.69.074511.

[89] L. Del Debbio, Leonardo Giusti, M. Luscher, R. Petronzio, and N. Tantalo. Stability of lattice QCD simulations and the thermodynamic limit. *JHEP*, 0602:011, 2006. doi: 10.1088/1126-6708/2006/02/011.

[90] L. Del Debbio, Leonardo Giusti, M. Luscher, R. Petronzio, and N. Tantalo. QCD with light Wilson quarks on fine lattices (I): First experiences and physics results. *JHEP*, 0702:056, 2007. doi: 10.1088/1126-6708/2007/02/056.

[91] L. Del Debbio, Leonardo Giusti, M. Luscher, R. Petronzio, and N. Tantalo. QCD with light Wilson quarks on fine lattices. II. DD-HMC simulations and data analysis. *JHEP*, 0702:082, 2007. doi: 10.1088/1126-6708/2007/02/082.

[92] S. Aoki et al. Bulk first-order phase transition in three-flavor lattice QCD with $O(a)$-improved Wilson fermion action at zero temperature. *Phys.Rev.*, D72:054510, 2005. doi: 10.1103/PhysRevD.72.054510.

[93] F. Farchioni, R. Frezzotti, K. Jansen, I. Montvay, G.C. Rossi, et al. Twisted mass quarks and the phase structure of lattice QCD. *Eur.Phys.J.*, C39:421–433, 2005. doi: 10.1140/epjc/s2004-02078-9.

[94] F. Farchioni, K. Jansen, I. Montvay, E. Scholz, L. Scorzato, et al. The Phase structure of lattice QCD with Wilson quarks and renormalization group improved gluons. *Eur.Phys.J.*, C42:73–87, 2005. doi: 10.1140/epjc/s2005-02262-5.

[95] F. Farchioni, K. Jansen, I. Montvay, E.E. Scholz, L. Scorzato, et al. Lattice spacing dependence of the first order phase transition for dynamical twisted mass fermions. *Phys.Lett.*, B624:324–333, 2005. doi: 10.1016/j.physletb.2005.08.018.

[96] Sinya Aoki and Andreas Gocksch. Spontaneous breaking of parity in quenched lattice QCD with Wilson fermions. *Phys.Lett.*, B231:449, 1989. doi: 10.1016/0370-2693(89)90692-8.

[97] Sinya Aoki and Andreas Gocksch. More on parity and Wison fermions: Quenched simulations in finite temperature QCD. *Phys.Lett.*, B243:409–412, 1990. doi: 10.1016/0370-2693(90)91405-Z.

[98] S. Aoki and A. Gocksch. Spontaneous breaking of flavor symmetry and parity in lattice QCD with Wilson fermions. *Phys.Rev.*, D45:3845–3853, 1992. doi: 10.1103/PhysRevD.45.3845.

[99] K. Jansen et al. Flavor breaking effects of Wilson twisted mass fermions. *Phys.Lett.*, B624:334–341, 2005. doi: 10.1016/j.physletb.2005.08.029.

[100] G. Akemann and A.C. Ipsen. Individual Eigenvalue Distributions for the Wilson Dirac Operator. *JHEP*, 1204:102, 2012. doi: 10.1007/JHEP04(2012)102.

[101] Rasmus Normann Larsen. Microscopic Spectral Density of the Wilson Dirac Operator for One Flavor. *Phys.Lett.*, B709:390–395, 2012. doi: 10.1016/j.physletb.2012.02.038.

[102] K. Splittorff and J.J.M. Verbaarschot. The Wilson Dirac Spectrum for QCD with Dynamical Quarks. *Phys.Rev.*, D84:065031, 2011. doi: 10.1103/PhysRevD.84.065031.

[103] J.J.M. Verbaarschot. Universal scaling of the valence quark mass dependence of the chiral condensate. *Phys.Lett.*, B368:137–142, 1996. doi: 10.1016/0370-2693(95)01492-6.

[104] J.C. Osborn and J.J.M. Verbaarschot. Thouless energy and correlations of QCD Dirac eigenvalues. *Phys.Rev.Lett.*, 81:268–271, 1998. doi: 10.1103/PhysRevLett.81.268.

[105] C. Aubin and C. Bernard. Pion and kaon masses in staggered chiral perturbation theory. *Phys.Rev.*, D68:034014, 2003. doi: 10.1103/PhysRevD.68.034014.

[106] Kari Rummukainen. QCD-like technicolor on the lattice. *AIP Conf.Proc.*, 1343:51–56, 2011. doi: 10.1063/1.3574941.

[107] Francesco Sannino. Dynamical Stabilization of the Fermi Scale: Phase Diagram of Strongly Coupled Theories for (Minimal) Walking Technicolor and Unparticles. *arXiv: hep-ph 0804.0182*, 2008.

[108] Francis Bursa, Luigi Del Debbio, Liam Keegan, Claudio Pica, and Thomas Pickup. Mass anomalous dimension in SU(2) with two adjoint fermions. *Phys.Rev.*, D81:014505, 2010. doi: 10.1103/PhysRevD.81.014505.

[109] S. Itoh, Y. Iwasaki, and T. Yoshie. The U(1) problem and topological excitations on a lattice. *Phys.Rev.*, D36:527, 1987. doi: 10.1103/PhysRevD.36.527.

[110] Adam Miklos Halasz and J.J.M. Verbaarschot. Effective Lagrangians and chiral random matrix theory. *Phys.Rev.*, D52:2563–2573, 1995. doi: 10.1103/PhysRevD.52.2563.

[111] Jacobus J.M. Verbaarschot. The Supersymmetric method in random matrix theory and applications to QCD. *AIP Conf.Proc.*, 744:277–362, 2005. doi: 10.1063/1.1853204.

[112] P. Littelmann, H.-J. Sommers, and M. R. Zirnbauer. Superbosonization of Invariant Random Matrix Ensembles. *Communications in Mathematical Physics*, 283:343–395, October 2008. doi: 10.1007/s00220-008-0535-0.

[113] M. Kieburg, H.-J. Sommers, and T. Guhr. A comparison of the superbosonization formula and the generalized Hubbard-Stratonovich transformation. *Journal of Physics A Mathematical General*, 42:275206, July 2009. doi: 10.1088/1751-8113/42/27/275206.

[114] Mario Kieburg, Heiner Kohler, and Thomas Guhr. Integration of Grassmann variables over invariant functions on flat superspaces. *J.Math.Phys.*, 50:013528, 2009. doi: 10.1063/1.3049630.

[115] Aleksey Cherman, Masanori Hanada, and Daniel Robles-Llana. Orbifold equivalence and the sign problem at finite baryon density. *Phys.Rev.Lett.*, 106:091603, 2011. doi: 10.1103/PhysRevLett.106.091603.

[116] Andrei V. Smilga and J.J.M. Verbaarschot. Spectral sum rules and finite volume partition function in gauge theories with real and pseudoreal fermions. *Phys.Rev.*, D51:829–837, 1995. doi: 10.1103/PhysRevD.51.829.

[117] J.J.M. Verbaarschot and I. Zahed. Random matrix theory and QCD in three-dimensions. *Phys.Rev.Lett.*, 73:2288–2291, 1994. doi: 10.1103/PhysRevLett.73.2288.

[118] M.E. Berbenni-Bitsch, S. Meyer, A. Schafer, J.J.M. Verbaarschot, and T. Wettig. Microscopic universality in the spectrum of the lattice Dirac operator. *Phys.Rev.Lett.*, 80:1146–1149, 1998. doi: 10.1103/PhysRevLett.80.1146.

[119] E. Follana, A. Hart, and C.T.H. Davies. The Index theorem and universality properties of the low-lying eigenvalues of improved staggered quarks. *Phys.Rev.Lett.*, 93:241601, 2004. doi: 10.1103/PhysRevLett.93.241601.

[120] Stephan Durr, Christian Hoelbling, and Urs Wenger. Staggered eigenvalue mimicry. *Phys.Rev.*, D70:094502, 2004. doi: 10.1103/PhysRevD.70.094502.

[121] Eduardo Follana, Alistair Hart, and Christine T.H. Davies. The Index theorem and random matrix theory for improved staggered quarks. *PoS*, LAT2005:298, 2006.

[122] Falk Bruckmann, Stefan Keppeler, Marco Panero, and Tilo Wettig. Polyakov loops and SU(2) staggered Dirac spectra. *PoS*, LAT2007:274, 2007.

[123] Falk Bruckmann, Stefan Keppeler, Marco Panero, and Tilo Wettig. Polyakov loops and spectral properties of the staggered Dirac operator. *Phys.Rev.*, D78:034503, 2008. doi: 10.1103/PhysRevD.78.034503.

[124] J.C. Osborn and J.J.M. Verbaarschot. Thouless energy and correlations of QCD Dirac eigenvalues. *Nucl.Phys.*, B525:738–752, 1998. doi: 10.1016/S0550-3213(98)00424-6.

[125] Jacobus J. M. Verbaarschot. The Spectrum of the Dirac operator near zero virtuality for $N_c = 2$ and chiral random matrix theory. *Nucl.Phys.*, B426:559–574, 1994. doi: 10.1016/0550-3213(94)90021-3.

[126] T. Nagao and P.J. Forrester. Asymptotic correlations at the spectrum edge of random matrices. *Nucl.Phys.*, B435:401–420, 1995. doi: 10.1016/0550-3213(94)00545-P.

[127] P. Littelmann, H.-J. Sommers, and Zirnbauer M. R. Superbosonization of invariant random matrix ensembles. *Comm. Math. Phys.*, 283:343–395, 2008. doi: 10.1016/0550-3213(80)90255-2.

[128] M. R. Zirnbauer. Symmetry Classes. *ArXiv e-prints: math-ph 1001.0722*, January 2010.

[129] Ulrika Magnea. The Orthogonal ensemble of random matrices and QCD in three-dimensions. *Phys.Rev.*, D61:056005, 2000. doi: 10.1103/PhysRevD.61.056005.

[130] P.H. Damgaard, Urs M. Heller, R. Niclasen, and K. Rummukainen. Eigenvalue distributions of the QCD Dirac operator. *Phys.Lett.*, B495:263–270, 2000. doi: 10.1016/S0370-2693(00)01191-6.

[131] Ulrika Magnea. Three-dimensional QCD in the adjoint representation and random matrix theory. *Phys.Rev.*, D62:016005, 2000. doi: 10.1103/PhysRevD.62.016005.

[132] Shinsei Ryu, Andreas P. Schnyder, Akira Furusaki, and Andreas W.W. Ludwig. Topological insulators and superconductors: Tenfold way and dimensional hierarchy. *New J.Phys.*, 12:065010, 2010. doi: 10.1088/1367-2630/12/6/065010.

[133] Richard DeJonghe, Kimberly Frey, and Tom Imbo. Bott Periodicity and Realizations of Chiral Symmetry in Arbitrary Dimensions. *Phys.Lett.*, B718:603–609, 2012. doi: 10.1016/j.physletb.2012.10.043.

[134] J.J. Duistermaat and G.J. Heckman. On the Variation in the cohomology of the symplectic form of the reduced phase space. *Invent.Math.*, 69:259–268, 1982. doi: 10.1007/BF01399506.

[135] Yan V. Fyodorov and Eugene Strahov. Characteristic polynomials of random Hermitian matrices and Duistermaat-Heckman localization on noncompact Kahler manifolds. *Nucl.Phys.*, B630:453–491, 2002. doi: 10.1016/S0550-3213(02)00185-2.

[136] Harish-Chandra. Differential operators on a semisimple Lie algebra. *Am. J. Math.*, 79:87, 1957.

[137] C. Itzykson and J.B. Zuber. The Planar Approximation. 2. *J.Math.Phys.*, 21:411, 1980. doi: 10.1063/1.524438.

[138] A. Okounkov and G. Olshanski. Shifted Jack polynomials, binomial formula, and applications. page 8020, August 1996.

[139] M. Kieburg, J. Groenqvist, and T. Guhr. Arbitrary rotation invariant random matrix ensembles and supersymmetry: orthogonal and unitary-symplectic case. *Journal of Physics A Mathematical General*, 42(26): 275205, July 2009. doi: 10.1088/1751-8113/42/27/275205.

[140] Mario Kieburg and Thomas Guhr. A New approach to derive Pfaffian structures for random matrix ensembles. *J.Phys.*, A43:135204, 2010. doi: 10.1088/1751-8113/43/13/135204.

[141] Mario Kieburg and Thomas Guhr. Derivation of determinantal structures for random matrix ensembles in a new way. *J.Phys.*, A43:075201, 2010. doi: 10.1088/1751-8113/43/7/075201.

[142] F. Wegner. private communication. 1983.

[143] K.B Efetov. Supersymmetry and theory of disordered metals. *Adv.Phys.*, 32:53–127, 1983. doi: 10.1080/00018738300101531.

[144] H.-J. Sommers. Superbosonization. *Acta Physica Polonica B*, 38:4105, December 2007.

[145] Y. V. Fyodorov. Negative moments of characteristic polynomials of random matrices: Ingham-Siegel integral as an alternative to Hubbard-Stratonovich transformation. *Nuclear Physics B*, 621:643–674, January 2002. doi: 10.1016/S0550-3213(01)00508-9.